TOJSAT
The Online Journal of Science and Technology

ISSN 2146-7390

The Online Journal of Science and Technology

Volume 9 Issue 2
April 2019

www.tojsat.net
April 2019

Published in TURKEY

Contact Address:

Prof. Dr. Mustafa Şahin Dündar - TOJSAT, Editor Sakarya-Turkey

Message from the Editor-in-Chief

Dear Colleagues,

TOJSAT welcomes you. TOJSAT would like to thank you for your online journal interest. The online journal system has been diffused very fast for almost ten years. We are delighted that almost 185,000 educators, teachers, parents, and students from around the world have visited. It means that TOJSAT has continued to diffuse new trends in science and technology to all over the world since January, 2011. We hope that the volume 9, issue 2 will also successfully accomplish our global science and technology goal.

TOJSAT is confident that readers will learn and get different aspects on science and technology. Any views expressed in this publication are the views of the authors and are not the views of the Editor and TOJSAT.

TOJSAT thanks and appreciate the editorial board who have acted as reviewers for one or more submissions of this issue for their valuable contributions.

TOJSAT will organize ISTEC - 2019 - International Science & Technology Conference (www.iste-c.net) between July 03-05, 2019 in Prague, Czech Republic. This conference is now a well-known science and technology event. It promotes the development and dissemination of theoretical knowledge, conceptual research, and professional knowledge through conference activities. Its focus is to create and disseminate knowledge about science and technology. ISTEC-2018 conference book has been published at **http://www.iste-c.net/istecpubs**

For any suggestions and comments on the international online journal TOJSAT, please do not hesitate to fill out the comments & suggestion form.

Call for Papers

TOJSAT invites you article contributions. Submitted articles should be about all aspects of science and technology. The articles should be original, unpublished, and not in consideration for publication elsewhere at the time of submission to TOJSAT. Manuscripts must be submitted in English.

TOJSAT is guided by it's editors, guest editors and advisory boards. If you are interested in contributing to TOJSAT as an author, guest editor or reviewer, please send your cv to editor.

April 01, 2019
Prof. Dr. Aytekin ISMAN
Sakarya University

Message from the Editor

Dear Readers,

This is the volume 9, issue 2 of the Journal of Science and Technology which covers the whole areas of Science and Technology all over the World. Studies either applied or social sciences that are used to fill in the gap between science and technology. Globally, this century scientific and technological developments are going very fast and importance of the journal will be most useful for the papers.

The journal, which covers all scientific and technological subjects, is published 4 times a year. Selected papers are accepted from the science and developing technologies which is published in the journal.

Prof.Dr. M. Şahin Dündar

Editor

Table of Contents

AN ARCHITECTURAL EVALUATION OF KONYA CITY

Fatih SEMERCİ, Hakan Taha ÇETİN

Necmettin Erbakan University, Department of Architecture, Konya-TURKEY
fsemerci@gmail.com

Abstract: Konya is an important city that has been home to different civilizations throughout history, has been used as a capital by the Seljuk State for a long time and extending to the neolithic turn of the past. The foundation of the historical city center of Konya started around the mound settlement known today as Alâeddin Hill. This area has been used centrally by different civilizations for many years and the most magnificent time of this area was the Seljuk period. The development of the historical city center was realized between Alâeddin Hill and Mevlana Tomb. The rich architectural content of different civilizations is clearly seen on this powerful axis. It contains many different artifacts belonging to the Seljuk, Ottoman and Republican era, where the architectural values that can be accepted as our cultural heritage of different periods are together and serve as a whole. This axis, which contributes to the rich architectural content of the city today, still maintains its vitality. With this study, the daily contribution of the historical city center was examined through the buildings. Alaeddin Hill - Mevlana Museum, which are contain many qualified building, has been accepted as an area study. The three qualified samples which are identified on the axis were analyzed in terms of historical, urban and structural, and the influence of these structures on the area was determined. The effects of urban and cultural heritage of architectural values are revealed in the analyzes made. As a result of these analyzes; It has been reached that the buildings give an identity to the center of the city and its surroundings, that it is an important factor in the perception of the places it is in, its reading and that it creates a focus reflecting character of the its period.

Keywords: Konya, Architectural Space, Historical City, Historical Buildings

Introduction

Anatolia has been regarded as the whole of architectural values that reflect the architectural values of our country in the best and clearest way. Anatolia has also prosperous architectural content which is exhibiting the history of the past for us. Different civilizations, cultures and way of lives with the existing architecture have shed light on our age. Existing architectural structures have traces of different periods and all together have determined social, cultural, economic and artistic values. The architectural texture, which is a major factor in the formation of the region or the city, is a focal point for tourists and visitors. With its strong past, strong culture and spatial relation, the attraction power of the region for the users is also high. Thus, this has increased the value and quality of the city/region. In this way, all the qualified architectural values of the city have been seen as a gain.

Konya is a city that has preserved its significance thanks to its geographical features and position on the caravan routes in Anatolia and the significance as the capital of the Seljuk Sultanate of Rum for many years. Hence, Konya has been called as “Dârü’l- Mülk” (capital city) and become one of the most important centres of Turkish-Islamic culture and art in Anatolia (Baykara, 2002).

Historically, Konya has developed as a single-centred city. The central business areas of the city are Alaeddin Hill and its surroundings. The historical city center is located on Mevlana Street, which is the most significant transportation artery of the city, and mainly south side between Alaeddin Hill and Mevlana Külliyesi. The historical city center located between Alaeddin Tepesi and Mevlana Külliyesi is the area with the highest accessibility in the city (Ter and Özbek, 2005).

Mevlana Road has a significant texture among the architectural sides of the city. This texture has been destroyed several times in the last 100-150 years and has been subjected to reconstruction studies. In this study, the main aim is to examine and analyse the losses and gains experienced in terms of street and building scale throughout the historical process. It has been aimed at searching the current situation of the area and its positive and negative aspects. In this context, the development of the axis of Alaeddin Hill and Mevlana Tomb has been researched. In the area, three buildings which have functionally, structurally and spatially interesting historical process have been selected as sample. These buildings: Konya Governorship Building, İplikçi Mosque, the Central Bank Building.

Materials and Methods

The architectural transformation and transformation of the city center was discussed at Konya Governorship Building, Iplikci Mosque, Central Bank Building and it has been determined how the city entered into a process of changing during different periods. The historical, urban, structural and spatial values of the area were analyzed in the sample building. In the light of the researches and evaluations, the impact of architectural values on the city and cultural heritage has been revealed. The contribution of the sample building to the field has been determined in the historical process and the interaction of the area with the building has been analyzed. In this context, the existing architectural works of the area and its richness have been revealed. The values of the buildings belonging to different periods ensure that the field has rich content. The coexistence of different cultures in the field ensures the architectural quality. Therefore, user and visitor density increases in this area as a normal result.

Historical Development Process of Konya City Center

Konya with its geographical location, its historical and cultural wealth has always preserved its significance as a settlement. Konya was the capital of the Seljuks and important architectural works were brought to the city during this era (Baykara, 2002).

The development of the city from the Seljuks to our age has been organized around Alaeddin Hill which is an old tumulus. This hill has been dominating over 750 years and has provided control. The Phrygians, Lydians, Persians and Romans used this area as a settlement in the past (Bala, 2002). The city remained as a province of the Roman Empire until 395 AD. In Byzantium era, it became a Byzantine city aftermath of fragmentation/dissolution of the Roman Empire. The “Iconium” (the country of icons) in the Byzantium encountered Islamic raids and was compressed into Alaeddin Hill (Karpuz, 1998). The Turks, after 1071, have regarded this region as homeland. Because, the region familiar to Central Asia in terms of their natural and climatic conditions. This area surrounded by grazing lands suitable for horses and livestock is easy to defend in the Turkish war tactics and to be evacuated when necessary and it is appropriate for being a capital with a hill which is appropriate/suitable for the ruler-army-headquarters. Alaeddin Hill has important architectural content because it has been housed in the entire history from the Phrygian period to the Seljuks as the first place where Konya was founded (Kuştepe, 2011).

The first settlement area of Konya (Ikonion), a Roman colony city, has been Alaeddin Hill and the south side of the hill. In the Byzantine period, the locals established settlements in the areas of Alaeddin Hill and the southern areas. In the 13th century, the settlement texture of the city concentrated around the Alaeddin Hill. The Seljuk period constituted the best period of history in terms of both the social structure and political life of Konya, as well as transformation on physical texture. Alaeddin Keykubat brought Rumi (Mevlana Jelaleddin Rumi) and his father Bahaeddin Veled to Konya in 1229. Their immigration has increased the attractiveness of the city. Meanwhile, the scientists and intellectuals of the era began to come to Konya. After Rumi came to the city, the city overflowed from the city walls. It can be stated that the reason behind this overflow Rumi settled down outside of the city walls. Thus, apart from the baileys, free textured, enclosed streets and neighbourhoods that are integrated with garden and rich interior architecture began to be formed. After the death of Rumi, the city started to become a visited place and a social center which has commercial functions. As a capital, Konya was organized with an artistic, aesthetic architecture and understanding of a system that befitted Seljuks’ dignity in their era. In 1308, the city was under the dominance of different principals with the collapse of the Seljuks. It was under the Ilkhanids’ dominance and then it ruled by Karamanid and finally it was under the suzerainty of the Ottoman Empire. The city, which had been under Ottoman rule in 1465, became a provincial state where princes became the governor of the Ottoman Empire, the army camped in for the military expeditions towards the East. As a result, with the Ottomans, reconstruction activities in Konya began to decline. However, after the death of Rumi, the activities continued in the dervish lodge (dergah) which was founded for the name of Rumi. At the same time Rumi’s thoughts have continued to pervade around the dervish lodge. Thus, the dervish lodge has become a center of visitation and social center and has continued to contribute to its neighbourhood. In addition, thanks to its significance, the region has had functionality for trade. It has been known that in addition to these riches, the number of the houses has intensified in this area. With the beginning of the construction of the Mevlana Tomb, the Mevlevi people began to gather around the dervish lodge. Therefore, new residential areas began to form outside the city walls. As shown by the large cemetery area behind the dervish lodge, the understanding of being close to the tomb of Rumi became widely seen after the death (Konyalı, 1997). This condensation, which emerged around the dervish lodge, also affected roads of the city. During the Middle Ages and the following period, the city consisted of the center of a circle around Alaeddin Hill where the inner castle is located, and the radial roads leading to that centre (Kuştepe, 2011).

Due to the authority provided by a central empire in the Ottoman era, the walls lost their former significance. However, the entrance points of the roads to the city were again the fortifications. The perimeter of each door has become an art and trade district, and shops have been opened and bazaars have been formed around them. These

city walls, which were connected to the city roads, have influenced the formation of the urban road system (Ter and Özbek, 2005).
It was the period when the Ottoman Empire suffered economic difficulties from 1880 to 1900. In this period, there was no maintenance of historical monuments. The visuals of Konya in the early 19th century has proven this situation (Kuştepe, 2011).

The fire that started in 1867 and continued for three days became one of the important events that affected the physical structure of the city. After the fire, slow but continuous construction/zoning activity was seen in the city. These activities gained momentum in 1898-1902, and streets and roads which were crossing each other in the city center were opened. The most important of these streets is Mevlana Road which stretches between Alaeddin Hill and Mevlana Külliyesi, which still have been preserved its significance today (Kuştepe, 2011).

In the 19th and 20th century, Mevlana Külliyesi and its surroundings became the prestigious settlement area of the city, and buildings that have 2 or 3 floors have started to be built in Mevlana Road where houses of wealthy merchants and civil servants of the city were located. For the signalizing the borders of the old city center, the restrictive order of old transportation spine which can be defined as an embedded channels system played an active role. Historically, Konya has developed as a single-centered city. The business areas in the center of the city are located around Alaeddin Hill and its vicinity (Kuştepe, 2011).

The beginning of the 1900-1923, the early times of the 19th century, the First World War period when the Ottoman Empire participated and defeated. In this period, many architectural works on Mevlana Road demolished due to wrong policies. 9 madrasahs and 2 mosques between Alaeddin Hill and Governorship Building were ruined and disappeared and Mevlana Road was also built during this period (Kuştepe, 2011).

The process of development and change of the axis have caused the current situation of the city. Many civilizations, cultural and architectural values have combined and formed the city center of Konya as a whole. Each structure and space has had a separate value and contribution to the axis. The buildings belonging to different periods and different styles have fulfilled functions of our age and provide the opportunity to utilize facilities of the city. A few of these structures are Konya Governorship Building, İplikçi Mosque, Central Bank Building, which have been located on the axis in different periods. All have reflected the best of their era and provide a rich architectural content to the region. These constructions, which existed during the development process of the axis and continued to be carried to our age, are the cultural components that connect the past and the future (Semerci, 2017).

Iplikci Mosque

The Iplikçi Mosque is a building which was built on the southern side of the main road extending from Alaeddin Hill (from the citadel) to the east. The front entrance gate of the building which was built on Alaeddin Road, a central place in the city, is opened into the main road. The date of construction of the building is 1201 (Figure 1). It has been thought that the mosque was constructed since there was a necessity for Friday prayers. It has been known that there was a madrasah (Altunaba) in the vicinity of the building which does not exist today.

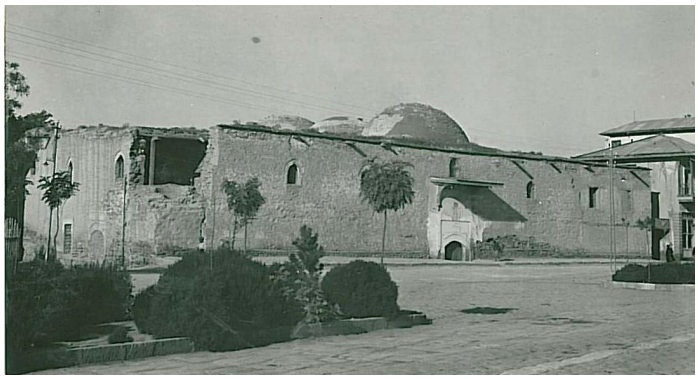

Figure 1. An old photograph of the building (Karpuz, 2009).

The dome in front of the mosque's niche is from the Friday prayer masjids (Mescid-i Cuma) of the Great Seljuks. The building has been considered as one of the first examples of the system adopted in Seljuk mosque in terms of plan, in the 13th century (Figure 2). It is one of the two examples in Anatolia where bricks are used as building material (Kustepe, 2011), (Figure 3). It has been known that the mosque has been restored many times during

different periods in the past. As a result of these restorations, the mosque has constantly changed. But it has never lost its original identity.

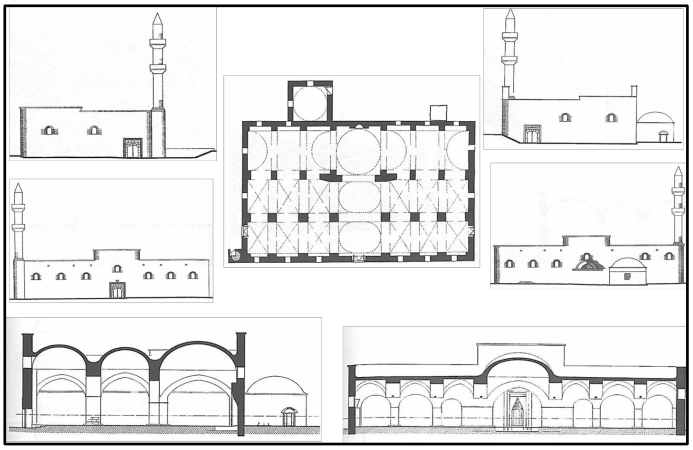

Figure 2. Building's plan, sections and views (Aygör, 2010).

Figure 3. Today's photo of the building.

The Mosque which reflects the Seljuk period on the axis in the best way, has added a distinctive value to the area. The building, which has enriched the functional and historical influence of the area, has been continuing to transmit the architectural value of its period.

Konya Governorship Building

The Governorship Building, also known as the Government Building, was built with using regular stones of the outer fortress walls of Konya in 1885-1886 during the period of Said Pasha of the Pre-Republican Governors of Konya (Figure 4). It has the architectural style of the 1st National Architecture Period. The building has a rectangular plan, courtyard and 3 floors (Duran, 2006).

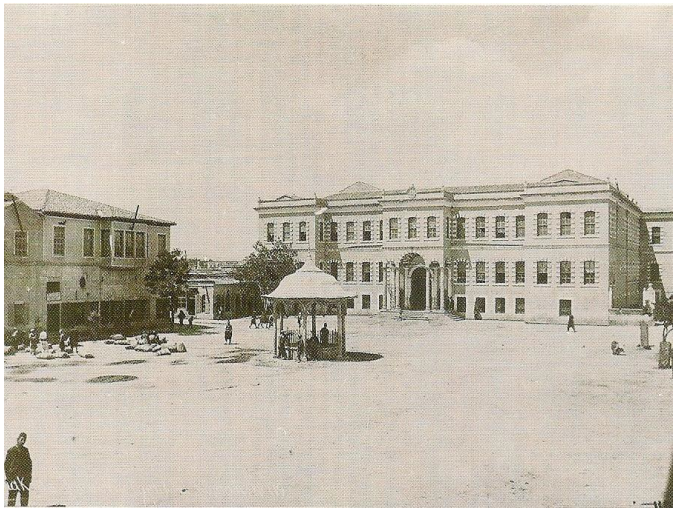

Figure 4. An old photograph of the building (Karpuz, 1998).

Governorship Building is one of the administrative structures that were ordered to be built in the provinces by Abdul Hamid II within the framework of the strengthening policies of the Ottoman provincial organization. The governorship building is a public building that has been directed to the square and to the Mevlana Museum and which has been continues to pursue its function located in the exact center of the Alaaddin-Mevlana axis. It is a building that we can figure out the features of the period (1st National Architecture) with looking its façade and plan and it distinguishes itself in silhouette and its gabarite is in tune with the buildings in surrounding. It has quadrangular form, so that we can easily perceive symmetry and rhythm. It is a masonry building which was constructed by using cutting stone (Karpuz, 2009), (Figure 5).

Figure 5. Today's photo of the building.

Central Bank Building

The Central Bank of Konya was built in 1975-1976. The building is located on the historical axis between the Alaeddin Hill and the Mevlana Tomb (Mevlana Road) in Konya city centre (Kapuz, 2003). It can be stated that Konya Branch of the Central Bank draws attention as a good example of modern republican structures (Figure 6-7).

Figure 6. A photo of the building (Mimarlık s.76).

Figure 7. A photo of the building (Mimarlık s.76).

The Central Bank, where the different functions are appeared together as planning is unique for also distinctive details on its façade. In order to provide natural lighting of mezzanine which is above the ground floor, liveliness has been provided on the façade.

The liveliness that provides uniqueness in modern lines of the building has shown itself within the elevation differences (Mimarlık p.76).

Konya Branch of the Central Bank Building is one of the prominent examples of modern buildings during the Republican Period. The building, which is one of the rare examples of modern buildings in the city of Konya and the Central Anatolia, appropriately summarizes the architectural movement that it has (Karpuz, 2003). This structure also is a pioneer work for other modern constructions of the city. Building has gained unique condition, since construction of the building was determined as a result of a project competition and it has modern identity. Having been registered as an example of modern building, the Central Bank has maintained its presence and function since its establishment with its strong identity.

Conclusion

Mevlana Road has been an economic, educational, religious, administrative, social and cultural center throughout history. This center has needed to be perceived well as the connection between the past and the present. Therefore, the history of the area and the process of spatial change should be appropriately analysed. The axis has witnessed different transformation and transformation processes in different periods and has functional diversity by incorporating different spaces. On the axle, changes have taken place in different scales during the process. As it can be figured out from the historical process of the area, structures belonging to different civilizations were destroyed while structures belonging to other civilizations (cultural) were found in the region. A typical example of this situation is the İş Bank Building. After finding a place in a different position on the axis, it has maintained its continuity functionally with a different architectural style in a different position afterwards. As we have pointed out here, the function of architectural understanding, position, characteristic and quality of structures have constantly

changed. It is interesting to protect the function within the strong central character of the area. As a result, structures, architects, spaces and functions in the historical city centres are constantly undergoing a change. In parallel, the city center reflects different cultures, civilizations and understandings as a whole. The important thing to note here is that the richness of the urban center, enriched by architectural diversity, can be included in this concept. This is because every building (architecture) that has taken place in the past and actively participated in the period has constant value that the area possesses and still contributes to the richness of the area.

References

Aygör, E., (2010). *Konya İl Merkezi Taşınmaz Kültür ve Tabiat Varlıkları Envanteri*, Konya B.Ş.B., Konya.

Baykara, T. (2002). *Türkiye Selçuklu Döneminde Toplum ve Ekonomi,* Yeni Türkiye Yayınları, Ankara.

Bala, H.A.,(2002). Plan Yapma ve Ona Sadık Kalarak Uygulama Geleneğine Sahip Bir Kent:Konya, *Yeni İpek Yolu Konya Ticaret Odası Dergisi,* Konya Kitabı V, 365-376.

Duran, R. (2006). *Konya'daki Geç Dönem Osmanlı Yapıları,*

Karpuz, H.,(1998). *Fotoğraflarla Geçmişte Konya,* İstanbul, 22-169.

Karpuz, H., 2003, "*Konya'nın Tarihi Yapılarına Toplu Bakış*", Tarih ve Kültür Başkenti Konya, Konya.

Karpuz, H., (2009). *Türk Kültür Varlıkları Envanteri Konya Cilt I,* Türk Tarih Kurumu, Ankara.

Konya Karatay Belediyesi Arşivi, (1967).

Konya Koyunoğlu Müzesi, Fotoğraf Arşivi, Konya.

Koyuncu, A., (2013). "*Kimliğin İnşaasında Kent: Konya Örneği*", Akademik İncelemeler Dergisi, Cilt:8, Sayı:2, s:169. Mimarlık Dergisi, Sayı:76, s. 100-103.

Kustepe, A., (2011). *Mevlana Caddesi Tarihi Dokunun Analizive SüreçİçindeDeğişimi,* Yüksek Lisans Tezi, Selçuk Üni., F.B.E., Konya.

Odabası, A.S., (1998). *20. Yüzyıl Başlarında Konya'nın Görünümü,* Konya, 13-149.

Önder, M., (1962). *Mevlâna Şehri Konya (Tarihi Kılavuz),* Yeni Kitap Basımevi, Konya.

Sharp, D. (2000). *Registering the Diaspora of Modern Architecture*, in: Sharp, D. ve Cooke, C. (Editörler) The Modern Movement in Architecture: Selections from the DOCOMOMO Registers Rotterdam: 010 publishers, s. 11-15.

Semerci, F., Alagöz, M., (2017). *Kentsel Sergileme Senaryolari: Konya Kenti Örneği,* İnönü Üni., Sanat ve Tasarım Dergisi, Cilt 7, sayı 16. DOI: 10.16950/iujad.311029

Sözen, M., (1984). *Cumhuriyet Dönemi Türk Mimarlığı*, Türkiye İş Bankası Kültür Yayınları, Tisa Matbaası, Ankara.

Tekeli, D., (2012). *Mimarlık:Zor Sanat:Anı,* Yapı Kredi Yayınları, İstanbul.

Ter, Ü., Özbek, O., (2005). *Kent Merkezlerinin Oluşumunda Alansal Gömülülük: Konya Tarihi Kent Merkezi,* Gazi Üniv. Müh. Mim. Fak. Derg. Cilt 20, No:4, 2005.

Uz, M. A., (2010). *Belgelerle Adım Adım Eski Konya, Eski Belediye Binası ile Hükümet Binası Arasındaki Bölge,* Merhaba Gazetesi Akademik Sayfalar, Cilt 10, Sayı 17, 257-260.

CASE STUDY OF THE IMPACT OF USING TECHNOLOGY IN SAUDI ARABIA PRIMARY SCHOOL IN SUPPORT OF TEACHING AND LEARNING WITH REGARD TO THE ENGLISH CURRICULUM

Mayada Abdulaziz Al Alharbi

School of Education, University of Lincoln, United Kingdom
e-mail: saudi6006@gmail.com

Abstract: This paper reports on an experimental case study that aimed to explore the impact of the use of technologies in the teaching of English in a primary school in Saudi Arabia. In this study, the researcher applied various technologies such as an iPad, a computer, and a projector when teaching English language to the groups of Primary children. These groups comprised of three different classes, while the traditional method of teaching, lecture style input was applied to control groups also made up of three age matched classes in the same school. The aim of using an experimental research approach was to determine the effectiveness of the technology when the teacher applied them in their English classes in a Saudi setting, and the effectiveness of using such technology in terms of the students' achievements particularly when technology is not traditionally used to support teaching in this context. The analysis included both qualitative and quantitative. The results drawn from this study demonstrates evidence that the different technological devices do support English language learning in some students.

Keywords: Primary School, English Curriculum, Case Study, Saudi Arabia

Literature Review

According to Riasati, Allahyar and Tan (2012), technology helps to increase student motivation such as when fun and games are brought into the classroom. Furthermore, it is proposed that the students' experience of new technologies in the learning environment can improve their engagement and motivation with regard to performing tasks. The authors also note that when used in the classroom as a tool for learning, technology encourages collaboration and communication during the performance of learning activities. For example, using technology such as an iPad, computer and projector, enables students to gather information and interact with resources such as songs, videos, presentations and images. According to Riasati, Allahyar and Tan (2012), another major advantage of using technology in the classroom is that it helps lower learners' anxiety levels, increase learner autonomy and encourage the development of particular language skills.

Moreover, Almutairi (2008) suggests that, as far as teaching English in Saudi classrooms is concerned the traditional method of teaching is that of lecture style, students only sit and listen to what the teachers says, while the teacher spends a lot of time explaining basic things to the students. While this technique makes it easier for the learners to achieve grammatical proficiency, it does not sufficiently implement new teaching techniques such as using technology in the classroom to support the teaching process. It could also be proposed that this lecture style approach does not enable students to practice their skills as effectively and does not support full mastery of the language. The research highlighted some of the problems with learning English in Saudi schools such as the large numbers of students in the class, limited English lessons, and the poor availability of technology in the classroom. As a result of this research, a number of recommendations are made in order to improve future practice and prevent these problems. In this paper, the researcher will present a case study of the impact of using technology in a Saudi primary school to support teaching and learning with regard to the English curriculum.

Learning English Technology to support types of Technology

A number of different technologies can be used in order to support learning in classroom, the focus for this study is on a number of readily available devices that could be applied in the classroom in Saudi Arabia, these include the computer and iPads. The computer and iPad applied by the researcher in teaching two different classes in the sampled school each fall within the umbrella of a computing device or a computer technology (Pearsoned Education, 2002). A computing device in this regard is an electronic device controlled by a processor and that can accept many software programmes for performing different functions (Emory University, 2017). A projector in itself is not a computing device but rather is an electronic device that is used to display images from a computer, film or images as noted by National Council For Teacher Education (2016).

The use of tablets or iPads and other devices such as mobile phones, and smartphones in teaching and learning has remained a subject of great controversy (Chartrand, 2016). For example: mobile devices have also been associated

with hardware and software failures and smaller screens which make reading of content and input of text difficult (Chartrand, 2016). However, there is a view that such technologies bring a wealth of creative options to the learning environment and, therefore, enhance the learning experience (Chartrand, 2016; Pellowe et al., 2014).

Many educational experts have noted the importance of computers and related technology in education (Simmons & Markwell 2001; Saba 2009). On their part, Simmons and Markwell (2001) note that technology can enhance education and is becoming more and more essential to learning. Saba (2009) is quick to note that mounting evidence indicates that technology helps improve student achievement both in terms of overall performance and in core subject areas. In addition, computers and mobile devices allow access to resources such as the Internet and YouTube, which may present new and exciting learning opportunities especially for students (Chartrand, 2016). Chartrand (2016) goes further to note that language teachers have found mobile devices useful in accessing online content, music and videos, all of which support the learning of new languages. Moreover, Saba (2009) notes that computers do not only have a potential impact on quantitative assessment performance in subjects but also leads to qualitative improvements compared to traditional teaching and learning methods. Studies also indicate that students with special needs and those who are low achievers tend to improve even more than high achievers and average students when they learn using computers as opposed to when they learn using traditional instructional methods (Saba, 2009).

On the other hand, projectors have been used to display images, notes and book content to the entire class and also to display course material to engage learners in games, songs, videos, presentations, simulations and quizzes among other activities (Klopfer et al. 2009). In both cases, the projectors have replaced or complemented whiteboards in the classroom, reducing the need for teachers and students to write notes on whiteboards (National Centre for Technology in Education, 2008). Also, Harrison (2008) notes that projectors when used to display presentations and electronic books enable the teacher to present well organised notes and make it easier for students to take better notes as they have the ability to discern the most useful information that the teacher displays to them. At the same time, the projector allows the easy and convenient display of previous information whenever there is need to revisit important content. One other main advantage of projectors is that they can be used to display information to an entire class rather than having to display information to each student individually such as through individual computers as noted by the National Centre for Technology in Education (2008). Furthermore, projects enable better use of time as the teacher does not necessarily need to write on the board and erase it when it is full. Instead, a simple click of the mouse leads to the display of new information, which effectively frees time for the teacher who would otherwise have to write and rewrite information (National Centre for Technology in Education, 2008).

Another benefit of using a projector in education relates to its capacity to reach students with multiple approaches. In this regard, learners enjoy seeing, hearing and interacting with technology as opposed to simply listening to the teacher or reading a textbook (Harrison 2008; National Centre for Technology in Education 2008). Learners can also take part in interactive and real time activities, which can help to promote the development of critical thinking skills. The projector can be used as a tool to effectively display or illustrate events or concepts in a way that may not be possible using the whiteboard according to the National Centre for Technology in Education (2008). National Centre for Technology in Education (2008) notes that when a projector is used in teaching and learning, the teacher and students can still maintain eye contact and can benefit from verbal and non-verbal communication as well.

The aim of this study is to explore the impact of technologies such as the iPad, computer and projector in support language learning in a primary school in Saudi Arabia. One of the research questions was: What is the impact of technology on student achievement and on making good progress in the English language?

The researcher used the assessment process to measure the learning outcomes. The assessment process was completed by the main English teacher. In the section below, the researcher explains the assessment methods, experimental design, and the experimental results to answer the research question.

Participants

This research focused on applying a single case study for understanding how technology enhances the English language learning in Saudi Arabian primary schools. In Saudi primary schools English lessons are started from grade four. These English language classes comprise grades four (A&B), five (A&B) and six (A&B) where students of ages 10, 11, and 12, in that order are enrolled. Each grade has two classes with a minimum of 30 students each. These grades have two teachers of English who teach English twice a week for each class in a 45 minutes long session. In this part of the study, the researcher applied various technologies such as an iPad for grade four B, a computer for grade five B, and a projector for grade six B when teaching English language to the

experimental groups. These comprised three different classes, while the traditional method of teaching was applied to control groups made up of three different classes: grade four A, grade five A, and grade six A. The researcher then used the assessment process to measure the learning outcomes. The assessment scale in this experiment is as follows: Excellent, Very Good, Good and Fail and was consistent with the form typically used in the school. The assessment process was completed by the main English teacher. The aim of using an experimental research approach was to determine the effectiveness of the technology when the teacher applied them in their teaching in English classes, and the effectiveness of using technology in terms of the students' achievements.

Methodology

Experimental Design

It is a challenge to conduct true experimental research within real life scenarios since it is difficult to derive perfectly aligned groups in relation to multiple variables including aspects of age, gender, income or work grade (Gray, 2004). In the current researcher's experiment, pupils were randomly assigned to either an experimental or a control group. In the current research, the researcher also explored the fluency in the language in terms of the ability of the students to read, write, comprehend, and speak English through assessment as accessed. In this assessment, the researcher follow the English curriculum but made change to the presentation aids. This approach enabled the researcher to explore if and how technology can be employed to support English language learning. The use of an experimental research design could be considered in the context of the wider research around the use of technological aids in the classroom. Associated technological aids are utilised towards evaluating 'treatment groups' in the context of action research. Such processes entail a significant degree of cooperation amongst both researchers and participants, which emphasises bringing around noticeable changes within the overall organisation (Gray, 2004). The emphasis of the initiative is to bring about changes within the attitudes and perspectives of participants within the field so that the data could be compiled in the context of both qualitative and quantitative methodologies (Gray, 2004).

The experimental group was provided with treatment – the introduction of iPads, computers, and projectors – while the control group experienced teaching in the normal way. The current study draws upon multiple methodologies to ensure the overall credibility and integrity of the study conducted.

Assessment Method

In the researcher's current experiment, pupils were randomly assigned to either an experimental group receiving intervention, or a control group receiving normal tuition. All of these groups are age matched. Learner assessments are some of the most important drivers of student learning, for example, computerised tests. Assessments aim to measure achievement of learning outcomes, and grading or classifying student achievement as noted by Winston-Salem State University (2016). In this study, the assessment method applied was exam testing. The assessment scale in this experiment is as follows: excellent, very good, good and fail. The results of the study revealed that learners in lower grades tended to show a dislike for taking exams possibly because of their inexperience and lack of confidence in using English language. However, experts note that written exams as an assessment method is advantageous in that it is economical and is a valuable source of information on student achievement, offers equal opportunities to learners and is less subject to plagiarism (Murphy, 2009). Also, Murphy (2009) mentioned that it is a fact that different teachers differ in their grading practices and policies which is another major limitation of exams as an assessment method.

Technology and Motivation

Qualitative Results

The qualitative results of this study have been collected by the current researcher from both controlled and experimental groups. So far, the results have demonstrated that, when the researcher used technology in the experimental groups, the students in classes who used technologies, seemed to be more motivated to learn than their counterparts in the traditional classes. This finding is consistent with several studies that indicate a relationship between technology use and learner motivation. Saba (2009) notes that technology is effective in improving attitudes towards learning. Many research studies have shown that most learners prefer to learn by using technology which subsequently leads to confidence boost and a better attitude towards education. Some experts are of the view that technology provides the opportunity for individualised learning as stated by Saba (2009). For example, when students take control of the rate at which they learn as they use technology which helps them avoid embarrassments that may come with making mistakes publicly. Another main advantage of learning using technology is that it provides immediate feedback with resultant reduction in learning time. This in effect makes learners feel more confident, develop a sense of accomplishment, and leads them also to develop a positive attitude towards learning (Erdamar & Melek 2008; Riasati, Allahyar and Tan, 2012). However, the use of different technologies in education is a subject that's has received significant attention among educational researchers.

According to Brown (2011), the use of different technologies can lead to higher levels of productivity, unprecedented flow of ideas and the avoidance of boredom. This rationale supported the researcher's use of different technologies during lessons with an aim of that specific technologies may not be rich in all aspects and therefore may need to be used together with other technologies or methods to meet the diverse needs and learning styles of learners.

Experimental Results

The results revealed that in grade 4A, 25 (58%) out of 43 students in the class in which the traditional teaching method was used scored Excellent grade in the English test. The remaining 18 (41%) students in the same class scored very good grade, with no student having a good or fail grade as evidenced by (Table 1). In grade 4B where technology was used to teach (iPad), 31 (72%) out of the 43 students in the class got excellent grade while the rest 12 (27%) of the students got very good grade as evidenced by (Table 2). No student got a good or fail grade as evidenced by (Fig. 1).

Table 1: The number of children achieving each grade when using traditional methods

Grade four A (Traditional methods)

Students	Percentage
Excellent 25	58%
Very good 18	41%
Good 0	0%
Failed 0	0%

Table 2: The number of children achieving each grade when using iPad

Grade four B (IPad)

Students	Percentage
Excellent 31	72%
Very good 12	27%
Good 0	0%
Failed 0	0%

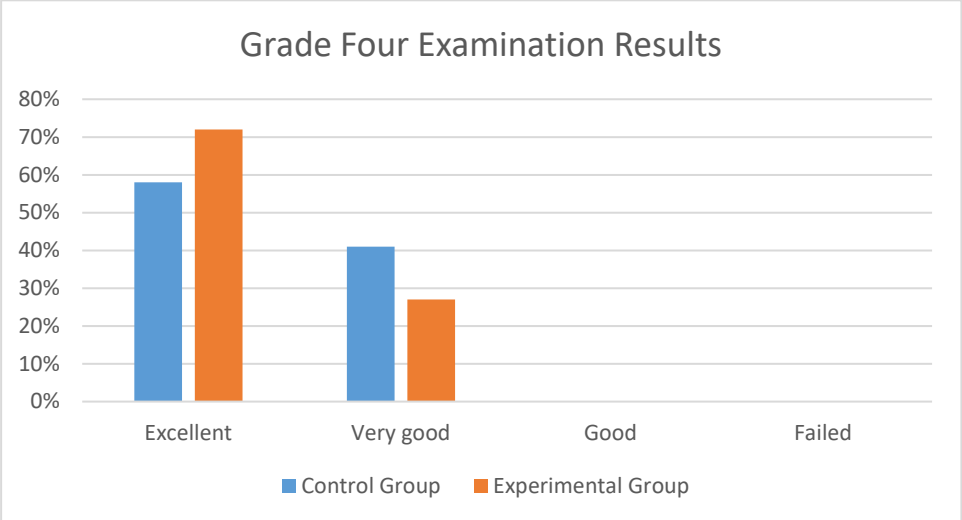

Figure 1: Summaries the test results as scored by grade 4A (the control group) and grade 4B (the experimental group) students.

The results demonstrate that these children in both the experimental and the control group were of similar ability, allowing the researcher to make comparisons easily. These results indicate that the use of an IPad appears to support learning in some children.

In grade 5A, in which the traditional method of teaching was used, 8 students out of 41 (20% of the class) obtained an excellent grade in the English test. Also, 24 students obtained a very good grade, accounting 59% of the class,

8 students were graded as good, accounting for 20% of the class while, and a student (2%) was graded Fail as evidenced by (Table 3). In grade 5B, in which technology was applied in teaching in the form of computers, 19 out of 40 students (48%) were given an excellent grade. Also, 17 students (43%) in the same class got a very good grade, and 4 got a good grade (10%) as evidenced by (Table 4). None of the students in the class was given a fail grade as evidenced by (Fig.2).

Table 3: The number of children achieving each grade when using traditional methods

Grade five A (Traditional methods)

Students	Percentage
Excellent 8	20%
Very good 24	59%
Good 8	20%
Failed 1	2%

Table 4: The number of children achieving each grade when using computer

Grade five B (Computer)

Students	Percentage
Excellent 19	48%
Very good 17	43%
Good 4	10%
Failed 0	0%

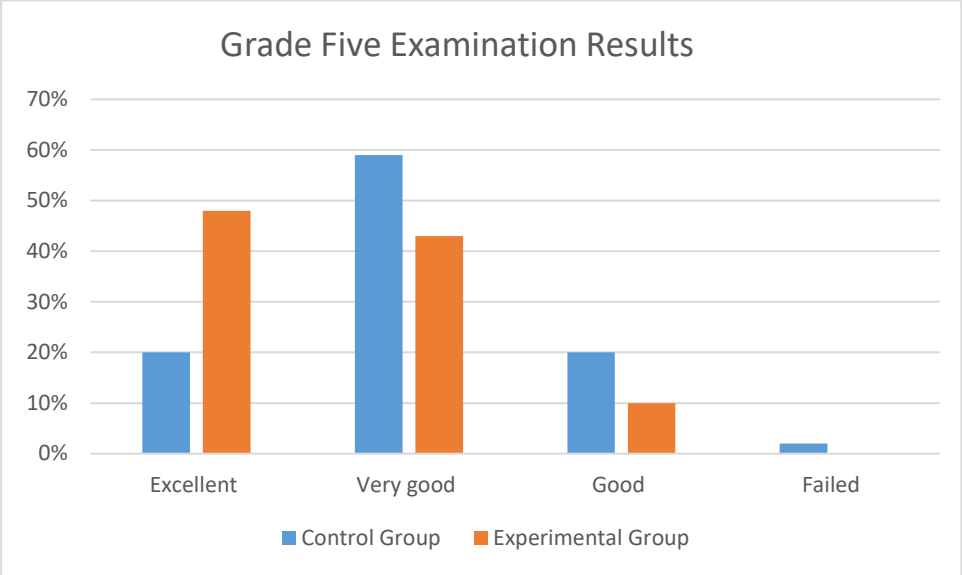

Figure 2: presents a summary of the test results for grade 5A (the control group) and grade 5B (the experimental group).

These results show that these children in the experimental and control groups were of similar ability. Consequently, it made comparisons easy. These results suggest that the use of computers appear to support learning in some children. However, it would appear that a much higher proportion passed the exam with an excellent grade when using a computer to support their learning. In addition, there were no failed students in the experimental group.

In grade 6A where the traditional method of teaching was applied, 17 (41%) out of the 41 students got excellent grade in the English test. Those who got very Good grades were 22 (54%) and good 2 students (5%) respectively. No student got a fail grade in the test as evidenced by (Table 5). On the other hand, 19 students (46%) out of 41 students in grade 6B, in which technology was applied in teaching (Projector), got excellent grade. Those who got very good grade were 22, representing (54%) of the class population as evidenced by (Table 6). None of the students in the class got good or fail grade as evidenced by (Fig.3).

Table 5: The number of children achieving each grade when using traditional methods

Grade six A (Traditional methods)

Students	Percentage
Excellent 17	41%
Very good 22	54%
Good 2	5%
Failed 0	0%

Table 6: The number of children achieving each grade when using projector

Grade six B (Projector)

Students	Percentage
Excellent 19	46%
Very good 22	54%
Good 0	0%
Failed 0	0%

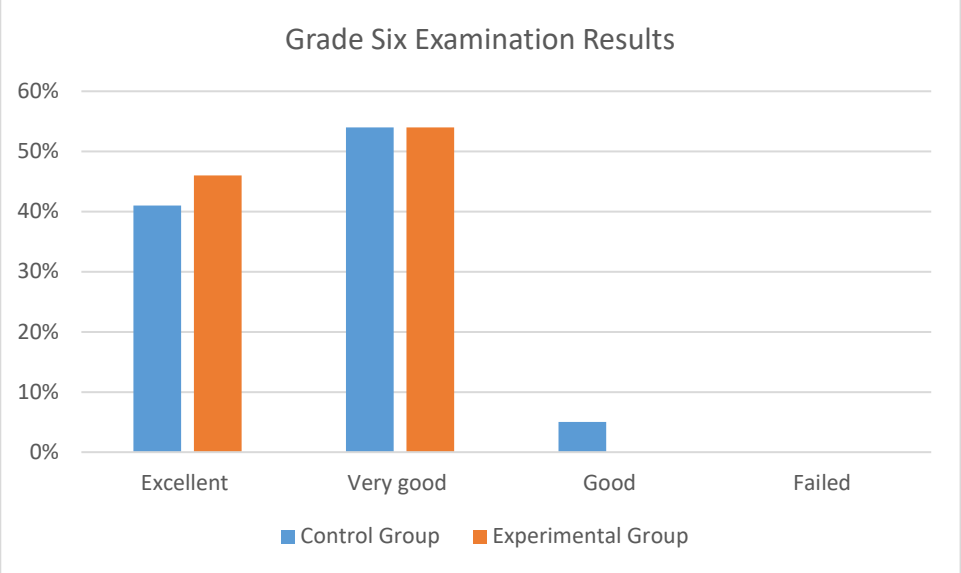

Figure 3: presents a summary of the results of the test for grade 6A (the control group) and grade 6B (the experimental group).

These results show that the children in both the experimental and control group were of similar ability. These results suggest that the use of a projector appears to support learning in some children. However, it would appear that a higher proportion of children passed the exam with an Excellent grade when using projector to support their learning and both groups more or less stayed obtained the same very good grade. Also, there were no good or fail students in this experimental group. This means that the use of the projector improved the students' achievement in the experimental group in that there were more excellent and good results.

It is evident from the test results that in each of the three grades, the experimental group showed better performance compared to the control group. On average, the experimental group had 16% higher number of students with excellent grades than the control group. The experimental groups also generally had a lower number of students with fail and good grades compared to the control groups in each grade as evidenced by (Fig.4).

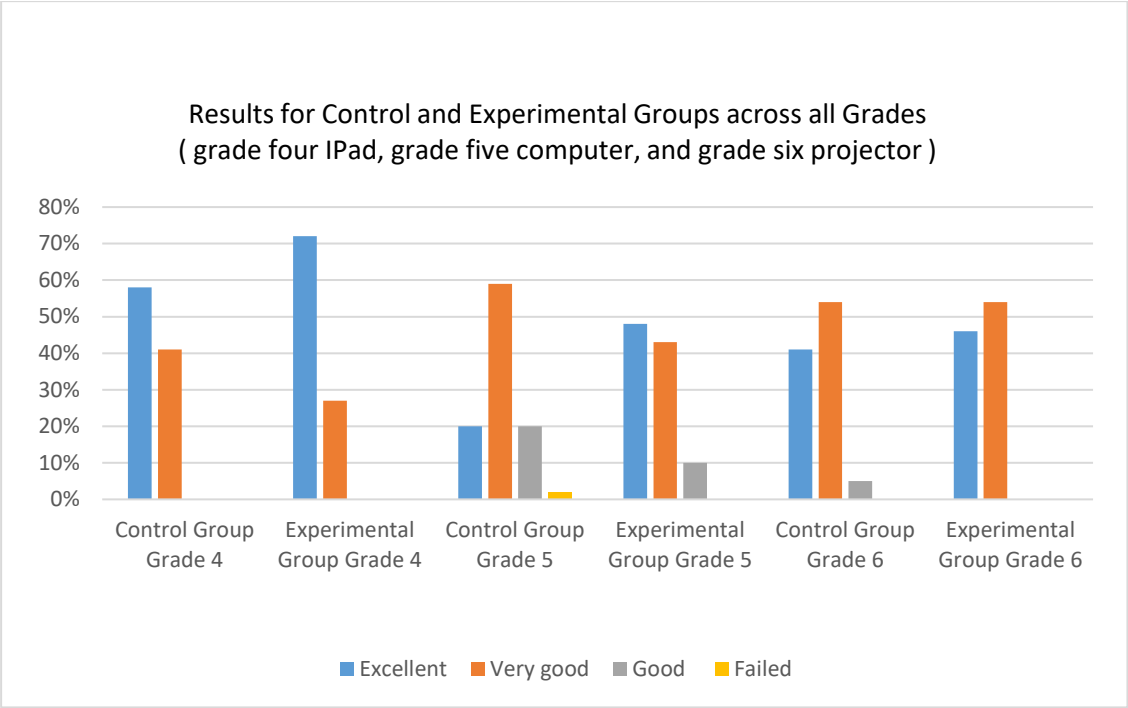

Figure 4: results for control and experimental groups across all grades

Table 4 shows the results of the assessment data across all the grades and conditions in the study. For example, the experimental groups in all grades had a higher number of students in the excellent category, and no students obtained a fail grade. It appears that in all cases, regardless of the type of technology used, its inclusion had a positive impact on learning compared to that of traditional classes which is the control groups.

The Key findings:

This paper presents the evidence from a single site case study in order to demonstrate the potential effectiveness of using technology in order to support student performance and motivation for English language learning in a primary school in Saudi Arabia. Various technologies, including a tablet (IPad), a computer and a projector were used when teaching the English language to the experimental groups. It has been discovered that the use of these devices supported learning in some students. At the same time, a much higher proportion of children passed the exam with an 'Excellent' grade when using the mentioned devices to support their learning. Also, Saba (2009) mentioned that technology contributed to higher levels of students' academic achievement. One key finding from the experimental study that group work was more beneficial to individual students' success and performance compared to working alone.

It is relevant to conclude that Saudi schools should more actively invest in technology in order to equip their teachers and students with the necessary tools and resources. The analysis outcomes have demonstrated that the use of technology such as tablets (IPad), computers, and projectors facilities the development of students' proficiency in the English language and add to their overall academic performance. At the same time, it is important to ensure that Saudi teachers are ready and willing to integrate technologies in the learning process and use these technologies in an effective manner (Abukhattala, 2016). So that they are able to capitalise on possible learning experience and advantages of using technology.

However, the Ministry of Education in Saudi Arabia said that the education will be transferred from the curriculum taught through the use of books, to electronic-based education, and the Ministry of Education stated that electronic-based education will cost 1.6 billion Riyals for the next three years. He said that electronic-based education will be available in 150 schools in the coming year, then 1,500 schools the year after, and it will be available to all schools in the third year. Moreover, as a result, he mentioned that this electronic-based education will be a very important event that would be available in every Saudi Arabian school by 2020 (Algamdi, 2017). As a result of the Ministry of Education's statement, this study into the impact of technology on English language learning and teaching, will support the introduction of electronic-based education. This development to more technology-based education highlights the timeliness of this study. However, this study has positively impacted on the use of the

technology which can be used for other aspects of the curriculum in Saudi Arabia schools. This study will also supports the transfer of education from the use of books to electronic-based education by 2020.

According to Shar (2018) at the second session of the fifth Professional Development meeting held at the Ministry of Education in Saudi Arabia on 31 January 2018, Dr. Al-Juhani pointed out that electronic learning is a form of informal education, but over time the general idea of informal education will change. It will become as important as formal education, especially with regard to the increased use of distance learning and the increase around the world of the interest of people in technology. In addition, Dr. Al-Juhani explained that electronic learning is based on the use of modern technology as a means of providing an educational curriculum that differs from what is offered within the traditional classroom. It can also take an interactive form as educational programs on the Internet. Dr. Al-Juhani reviewed some statistics and figures indicating the increasing reliance on technology and the use of the Internet. He pointed out that by mid-2017, is equivalent every 10 children have six children using the Internet, many of whom participate in called electronic learning, even if they do not realise it (Shar, 2018). This research supported the impact of the use of technology in primary school in Saudi Arabia.

References

Abukhattala, I., (2016) The Use of Technology in Language Classrooms in Libya. *International Journal of Social Science and Humanity*, 6 (4) 262.

Algamdi, A. (2017) *Stopping printing any books in the Tree years later in the schools.* Available from http://www.okaz.com.sa/article/ [accessed 15 January, 2018].

ALMutairy, N. (2008) *The influence of educational and sociocultural factors in the learning styles and strategies of female students in Saudi Arabia.* Ph.D. University of Leicester.

Blakstad, O. (2008) *Experimental research - A guide to scientific experiments*. Available from https://explorable.com/experimental-research [accessed 24 November 2016].

Chartrand, R. (2016) *Advantages and Disadvantages of Using Mobile Devices in a University Language Classroom.* Available from www.repository.kurume-u.ac.jp/dspace/bitstream/11316/445/1/gaiken23_1-13.pdf [accessed 8 September, 2017].

Emory University (2017) *Introduction to programmable computing devices,* available from www.mathcs.emory.edu/~dsavenk/courses/cs170/lectures/lecture-1.pdf [accessed 24 September, 2017]

Erdamar, G. & Melek D. (2008) Effects of constructivist learning approach on affective and cognitive learning outcomes. *Turkish Educational Sciences*, 6 (4) 629-661.

Gray, D.E. (2004) *Doing research in the real world*. London: Sage Publications.

Gulek, J. and Demirtas, H. (2005) "Learning with technology: The impact of laptop use on student achievement", *Journal of Technology, Learning, and Assessment*, 3 (2) 1-38.

Harrison, F. (2008) *Using Learning Resources to Enhance Teaching and Learning, Centre for Educational Development*. Imperial College London: London.

Klopfer E., Osterweil S., Groff J. & Haas J. (2009) *Using the technology of today, in the classroom today*. The Education Arcade Massachusetts Institute of Technology: Massachusetts.

Murphy, F. (2009) *UCD Teaching and Learning/ Resources*, UCD, Dublin.

National Centre for Technology in Education (2008) *NCTE Advice Sheet – Digital Projectors*, National Centre for Technology in Education, London.

National Council For Teacher Education (2016) *NCTE Advice Sheet – Digital Projectors.* Available from www.ncte.ie/media/15DigitalProjectorsAug09.pdf [accessed 20 September, 2017].

Pearsoned Education (2002) Chapter 5: Portable Computing Devices. Available from *catalogue.pearsoned.co.uk/samplechapter/0130091162.pdf* [accessed 24 September, 2017].

Pellowe, W., Holster, T., & Lake, J. (2014) *Peer assessment in the classroom using mobile devices, Paper presented at the EUROCALL Conference*. Groningen: The Netherlands.

Riasati M., Allahyar N. & Tan K. (2012) Technology in Language Education: Benefits and Barriers, *Journal of Education and Practice*, 3 (5) 25-31.

Saba, A. (2009) *Benefits of Technology Integration in Education*, Boise State University: Boise.

Shar, A. (2018) *Academic: e-learning will become of formal importance and will utilize communication platforms*. Available from https://sabq.org/Zw6dc2 [accessed 31 January, 2018].

Simmons E. & Markwell R. (2001) *Advantages of Educational Technology*, California State University: Sacramento.

Winston-Salem State University (2016) *Assessment Methods.* Available from: https://www.wssu.edu/about/assessment-and-research/.../assessmentmethods.pdf [accessed 24 September, 2017].

DEFINING CLOUD COMPUTING

Mustafa OF
Kocaeli University, Kocaeli Vocational School, Kocaeli, Turkey
mustafaof@kocaeli.edu.tr

Burak Çakır
Kocaeli University, Kocaeli Vocational School, Kocaeli, Turkey
burak@kocaeli.edu.tr

Abstract: With the development of computing technologies that have been at many points in our lives, cloud computing technology has begun to be used in a wide range of environments from a portable computer to a server computer. Accessibility is easy, cloud computing is at the top of the reasons for preference. Big companies in information technology (Microsoft, Google etc.) are leading the cloud computing services. It is thought that the installation of the cloud computing system is a big financial budget. However, a cloud computing system can be installed even in our home or office computers.

Accessibility is easy, cloud computing is at the top of the reasons for preference. Cloud computing facilitate access to data greatly. However, it should be known that the data are collected on the servers of the cloud computing service provider. In terms of importance, more or less important data are stored in cloud computing servers. It is important not to forget that in the event of a corruption of trust relations it will have serious results.

The aim of this work is to explain the installation steps of our own cloud computing server and client system on a virtual or real server system. It is to explain that a cloud computing system is easily installable. A cloud computing system can be set up in short steps and at low cost. In this way, contributed to the growth of national software works. The data is stored in cloud computing servers, one or more national and reliable institutions.

Keywords: Cloud Computing, Server, Linux Operating System, Open Source Software, OwnCloud, Cyber Security

Introduction

Cloud Computing System

While it is not known exactly when the term cloud computing is known (Estimated 1950s), this concept is the most generic name given to the Internet-based information services that can be shared among users by using the server computers and similar devices connected to the Internet. It is about the provision of services to be taken by using software at minimum level without the need for service infrastructure by the user. Cloud computing provides services based on three basic models. These are Software as a Service, Platform as a Service, Infrastracture as a Service.

With cloud computing, data, applications and many other information services are stored in the server systems of the provider or organization. Ease of use is one of the great benefits. Google Drive, Microsoft OneDrive, cloud services are the obvious. With mobile, tablet, laptop or desktop computer access, data can be accessed continuously wherever an Internet connection is available. While cloud computing has good sides, it also has bad sides. The presence of data in a server system that is unaware of the user can lead to unpredictable results if the trust agreement is compromised. For example, cloud computing is one of the bad results that the country has cut off its support on a country or company basis. In terms of security, countries must have their own cloud computing server systems.

Advantages;
Variable cost instead of capital investment: Instead of making large investments in data centers and servers that you don't know how to use, you can only pay for the resources it uses and the time you use it.

Benefit from the advantages of large-scale use: You can benefit from low usage costs that you cannot reach yourself by using cloud computing. With hundreds of thousands of customers in the cloud, large service providers can reach more affordable costs on large scales, which reduces pay as you go.
Stop capacity estimation: Stop anticipating the capacity needs of your infrastructure. If you determine the capacity before you distribute the application, you may have to pay high wages for the resources you have paid, or you may

have to manage with insufficient capacity. Cloud computing eliminates these problems. You can access the desired size of resources and increase or decrease the scale as required by just a few minutes in advance.

Get faster and more agile: In the cloud computing environment, new IT resources are just a click away. This allows you to reduce the time it takes to deliver these resources to software developers from a few weeks to a few minutes. This significantly increases the agility of the organization as it pulls down the costs and time required for testing and development.

Stop running data centers and spending money on maintenance: Focus on projects that will make a difference for your business, not infrastructure. With cloud computing, you can focus on your customers rather than server staging, editing, and infrastructure provisioning.

Turn to the world in minutes: Deploy your app to different regions around the world in just a few clicks. This allows you to easily and cost-effectively reduce latency and offer a better experience to your customers.

Disadvantages;
Security: Cloud companies are becoming an open target for attackers because many companies or customers receive service. The cloud computing firm must maximize its security level.

Privacy: The firm or customers receiving services from the Cloud Computing Company register their data on the server computers. These data should not be available to unauthorized persons.

Continuity: The service provided by the cloud computing company should be continuous. Any interruption in service will affect the workflow of all customers.

Cloud Computing Server Installation
We can turn a Linux-based computer into a cloud computing server. A cloud computing system can be prepared with ownCloud, which is open source and free. Official site is www.owncloud.org. ownCloud is the most simple way to file or document share data. With ownCloud all your data is where ever you are; accessible desktop or mobile devices, any time. You can install ownCloud Community edition.

ownCloud required one of them Linux distributions.

- Centos Linux 6 and 7
- Debian 7 and 8
- Fedora 27 and 28
- Red Hat Enterprise Linux 6 and 7
- SUSE Linux Enterprise Server 12 with SP1, SP2 and SP3
- openSUSE Tumbleweed and Leap 15.0, 42.3
- Ubuntu 16.04 and 18.04

It required Apache 2.4 Web server and Php 5.6 or above. Database can be one of them;

- MySQL or MariaDB 5.5+
- Oracle 11g
- PostgreSQL
- SQLite

We will use Ubuntu 16.04 Linux to install ownCloud.

ownCloud installation steps on Ubuntu 16.04 are below;

Step 1: Apache2 Install (Web Server)

sudo apt install apache2

After Apache2 installation run this command

sudo sed -i "s/Options Indexes FollowSymLinks/Options FollowSymLinks/" /etc/apache2/apache2.conf

Next run commands

sudo systemctl stop apache2.service
sudo systemctl start apache2.service
sudo systemctl enable apache2.service

Step 2: MariaDB Install (Database)

ownCloud requires a database server software.
Run this command

sudo apt-get install mariadb-server mariadb-client

After MariaDB installation run this command

sudo systemctl stop mysql.service
sudo systemctl start mysql.service
sudo systemctl enable mysql.service

After that, run the commands below to give security information of MariaDB server.

sudo mysql_secure_installation

Give database password and other informations.

Run with this command to start database server

sudo systemctl restart mysql.service

Step 3: Php and related modules install

PHP 7.1 isn't available on Ubuntu default repositories. In order to install it, you will have to get it from third-party repositories.

Run the commands below to add the below third-party repository to upgrade to PHP 7.1

sudo apt-get install software-properties-common
sudo add-apt-repository ppa:ondrej/php

Then current Php upgrade to PHP 7.1
sudo apt update

Run these commands install PHP 7.1 and related modules.

sudo apt install php7.1 libapache2-mod-php7.1 php7.1-common libapache2-mod-php7.1 php7.1-mbstring php7.1-xmlrpc php7.1-soap php7.1-apcu php7.1-smbclient php7.1-ldap php7.1-redis php7.1-gd php7.1-xml php7.1-intl php7.1-json php7.1-imagick php7.1-mysql php7.1-cli php7.1-mcrypt php7.1-ldap php7.1-zip php7.1-curl

After install Php 7.1 edit config file with nano

sudo nano /etc/php/7.1/apache2/php.ini

Then make the change the following lines below in the file and save.

file_uploads = On
allow_url_fopen = On
memory_limit = 256M
upload_max_filesize = 64M
max_execution_time = 360

Step 4: Create your OwnCloud Database

Now that you've install all the packages that are required, continue below to start configuring the servers. First run the commands below to create OwnCloud database.

Run the commands below to logon to the database server. When prompted for a password, type the root password you created above. You will open MariaDB command console.

sudo mysql -u root -p

Then create "owncloud" database. Database name is owncloud

CREATE DATABASE owncloud;

Create a database user called "owncloud user" with new password. Example : own12345

CREATE USER 'owncloud user'@'localhost' IDENTIFIED BY ' own12345*';*

Then grant the user full access to the database.

GRANT ALL ON owncloud. TO 'owncloud user'@'localhost' IDENTIFIED BY 'own12345' WITH GRANT OPTION;*

Save your changes and exit

FLUSH PRIVILEGES;
EXIT;

Step 5: Download OwnCloud Latest version

Download OwnCloud free copy latest release from site to /tmp folder. The community edition will be download. It may take some time according to your internet speed.

cd /tmp && wget https://download.owncloud.org/community/owncloud-10.0.3.zip

Unzip downloaded zip file. If unzip command not found then install unzip. (sudo apt-get install unzip)

unzip owncloud-10.0.3.zip

Move folder new location

sudo mv owncloud /var/www/html/owncloud/

Then run these commands below to set the correct permissions for OwnCloud to function.

sudo chown -R www-data:www-data /var/www/html/owncloud/
sudo chmod -R 755 /var/www/html/owncloud/

Conclusions

With the ownCloud system, small or medium sized companies can install their own cloud systems. It is enough to install the public version on their servers. In this way, they can share their files securely. Files can only be accessed from their network. The philosophy of general public license (GPL) responds to many needs without paying any price. ownCloud system is one of them. There is always no need to pay a large amount for a good information system. Sometimes a free software can do a lot more work. In a few steps as described above, we were able to establish our own cloud computing system.

References

Seyrek, İ.H. (2011). Cloud Computing: Opportunities and Challenges for Businesses. Gaziantep Journal of Social Sciences
https://azure.microsoft.com/tr-tr/overview/what-is-paas (Access Date: 16.07.2018)
https://aws.amazon.com/tr/what-is-cloud-computing/ (Access Date: 22.08.2018)
https://owncloud.org/features/ (Access Date: 23.09.2018)
https://www.digitalocean.com/community/tutorials/how-to-install-and-configure-owncloud-on-ubuntu-16-04 (Access Date: 14.09.2018)
https://websiteforstudents.com/install-owncloud-on-ubuntu-16-04-lts-with-apache2-mariadb-and-php-7-1-support/ (Access Date: 18.09.2018)

DETERMINATION OF PHYSICAL AND MECHANICAL PROPERTIES OF POLYPROPYLENE FIBRE CONCRETE

Hakan SARIKAYA, Gülşah SUSURLUK

Faculty of Engineering, Civil Engineering Department, Usak University, Usak, Turkey

Associate's Degree Vocational School, Textile Technology Department, Beykent University, Istanbul, Turkey

hakan.sarikaya@usak.edu.tr
gulsahsusurluk@beykent.edu.tr

Abstract: In this study, it is aimed to investigate the physical and mechanical properties of concretes obtained by using polypropylene fibers at different ratios by keeping amount of cement constant in the concrete mixtures. According to experimental results, it was seen that the increasing fiber dosage in the concrete mixtures, flexural strength and ultrasonic velocity was increased by addition of fibers to concrete, compressive strength and slump was decreased.

Keywords: fiber concrete**,** polypropylene fiber, mechanical strengths.

Introduction

Since the existence of humankind the second basic necessity has been the sheltering after the necessity of eating and drinking, In this way the building sector has always remained on the agenda and has continued to work on developing practical methods. In today's world, as in all areas, the basic goal is to reach the solution at the earliest with minimal expenditure. Various special properties have been developed or some special concrete with different production and application techniques are widely used due to emerging needs in today's use. It is very important to design and economical production of concrete for the purpose of use. (Sarıkaya, 2014). Due to the increase in the world population, complex and multi-storey buildings have been widespread in recent years instead of simple and single storey buildings. As the building height and number of floors increase, the quality of the material used becomes important (Erdem vd., 1997). In multi-storey buildings, concrete performance is of great importance in order to reduce the structural security and the effect of the earthquake (Neville, 1981).

Concrete; is a composite material consisting of mortar phase and aggregate which is obtained by mixing cement, water, aggregate and additives if necessary (mineral, chemical, fiber etc.) in certain conditions and ratios and which is in plastic form at the beginning and gains resistance by hardening by developing chemical reaction (hydration) over time between cement and water (Özel, 2007). When concrete has just been mixed, it takes the name of fresh concrete and when it hardens it becomes hardened concrete (Neville, 1993). In concrete, when the materials entering the composition are specifically rated, the mixture can be poured anyplace and brings a plastic mass that can take the shape of the mold and the size (Baradan, 1997).

Cement based materials such as concrete, tensile strength and tensile unit deformation capacity are materials with very low brittle construction. Conventional concrete is typically; it shows poor performance in terms of fatigue strength, cavitation and abrasion resistance, tensile strength, deformation capacity, shear strength, load carrying strength after cracking and toughness. Where these properties of concrete are obviously required, the addition of high-tech fibers produced from different materials within the concrete improves the above weaknesses of the concrete, thereby increasing the interest in materials such as concrete. The result of the addition of technical properties high fiber, produced from different materials in concrete, improves the poor features of the concrete above, causing to increase the interest in materials such as concrete. Thus, polypropylene fiber, carbon fiber, plastic-glass based fibers and steel fibers have begun to be used in concrete. In terms of advantages in the field of Civil Engineering, the importance of fiber reinforced concrete is increasing rapidly and important steps have been taken to improve the properties of composites (Yardımcı, 2007).

The polypropylene fiber used in this study is a very light polymer that is contained within the thermoplastics as material. It forms almost half of the raw materials used in daily life. From this point of view, it is also possible to say that production is a cheap plastic. The most important effect of polypropylene fiber concrete in concrete or plaster is to check cracks due to plastic shrinkage within the first few hours after pouring concrete into the mold. In the first phase of concrete hardening, the velocity of formation of concrete strength is slower than the rate of formation of tensile stresses due to shrinkage. This plastic shrinkage is essentially a natural consequence of

chemical reaction and evaporation starting between water and cement (Arazsu, 2012). Polypropylene fibers increase the mechanical strength of concrete compared to steel fibers and are not very effective. Yet, at a minimum, they give to concrete energy absorbing capability the plastic shrinkage with the feature is also very effective. Especially polypropylene fibers are preferred against very strong shrinkage. The function of polypropylene fibers, while the concrete is limited to soft, plastic phase, the strength-increasing effect of steel fibers, after taking the concrete setting and hardening it will continue to be noticeable. In the plastic phase of the concrete there is a preventive and limiting effect of the cracks of steel fibers. However, it is weaker than the effect of polypropylene fibers dispersed perfectly in concrete (Figure 1). However, with the reduction of cracks due to long-term drying shrinkage of hardened concrete, steel fibers significantly increase the strength of the concrete by giving a certain durability and toughness to the material (Bekaert, 1998).

Figure 1. Polypropylene Fiber

Material and Methods

In this study, 15 cement samples were produced at 10 cm x 10 cm x 10 cm sizes using 1%, 2% and 3% (polypropylene fiber) of cement weight, keeping amount of cement constant for C 30 concrete**.** The chemical properties of cement, normal aggregate and polypropylene fiber used are shown in Table 1 and the chemical and physical properties of the polypropylene fiber are shown in Table 2.

Table 1. Chemical Properties of Cement, Aggregate and Polypropylene Fiber Used in Concrete Mixtures

Composition	**CEM I 42,5 R (%)**	**Normal Aggregate (%)**	**Polypropylene Fiber (%)**
SiO_2	20.02	2.75	0.38
Fe_2O_3	3.52	1.29	0.06
Al_2O_3	5.16	-	-
CaO	63.46	0.2	53.85
MgO	1.03	2.8	0.34
SO_3	2.74	-	-
Loss of ignition	2.35	-	-

Table 2. Chemical and Physical Properties of Polypropylene Fibre

Appearance	Natural White Fibers
Purity	% 100 Pure
Specific Gravity	0.91 g/cm^3
Module of Elasticity	3000-3500 N/mm^2 (MPa)
Tensile Strength	450/700 N/mm^2 (MPa)
Melting Point	162 ˚C
Ignition Point	593 ˚C
Length	6mm - 12 mm – 19 mm
Profile &Diameter	Circular 18µm - 40 µm

Production of concrete samples, physical and mechanical properties tests were carried out in the Construction Laboratory of Civil Engineering Department of Uşak University. In this study, concrete was produced in 4 different mixing ratios. The amount of cement and fiber dosage was kept constant in all mixtures. Mixing ratios of the produced samples are shown in Table 3. Natural spring water was used for mixing water. The concrete mixing process was carried out with the help of a vertical axis mixer. In order to determine the consistency of the samples, slump with abrams cone concrete temperatures and spesific bulk densitys were measured. For use in various experiments, the mortar was placed in three stages, 100 mm × 100 mm × 100 mm size cube molds on vibratory table unit. At each stage, the mortar was vibration by the vibratory table tool for 10 seconds. For each series, 15 cube samples were produced. The samples were left in mold for 24 hours. At the end of this period, the samples were removed from the mold with the aid of rubber wedges. The samples were kept in the curing pool until the day of the experiment.

Table 3. Mixture ratios of the produced samples

Mix	Cement (% wt)	Polypropylene Fiber (%)
NB	100	-
NL1	99	1
NL2	98	2
NL3	97	3

ASTM C143 (2000) and TS EN 12350-2 (2002) standards have been adopted in many countries. In this experiment also called Abrams Cone; As shown in Figure 2, the top of a 100 mm diameter, 200 mm lower diameter and 300 mm height is cut into three equal layers into a truncated conical metal mold and each layer is freshly squeezed 25 times with a special rod (diameter 16 mm, length 600 mm) concrete filled.

Then the filled concrete was pulled up through the truncated cone mold before it was vibrating. The concrete has collapsed with its own weight and the slump value was measured (Özel 2007).

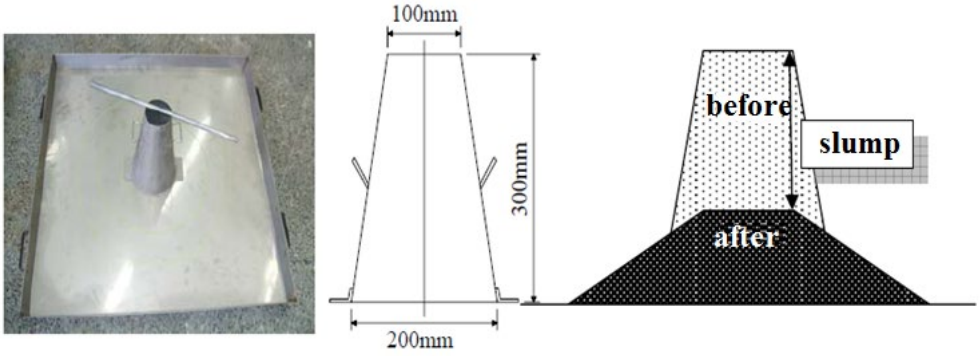

Figure 2. Tools used in the slump test and experimental procedure (Özel, 2007)

In the destructive test method, uniaxial pressure test and flexure test were performed. To measure ultrasonic pulse velocity, ultrasonic measuring instrument in the Construction Laboratory of Civil Engineering Department of Uşak University was used (Fiure 3). The ultrasonic velocity measurement was performed with a 12-volt accumulator-equipped with a digital indicator ultrasonic measuring instrument. The instrument was first set to zero, then calibrated. By spraying grease on both sides of the samples, gaps between the probes and the sample were prevented. By the experiment on the cube samples, the times of passing sound waves were measured.

In evaluating ultrasound velocity test results, the ultrasonic pulse velocity time values (micro second) were calculated in terms of km/s in ultrasonic velocity, calculated by Equation 1.

$$V = \frac{L}{t} \quad (1)$$

V: Ultrasonic velocity (km/s),
L: Sample size (km),
t: Ultrasonic pulse velocity time (s)

Figure 3. Ultrasonic measuring instrument

Results and Discussions

The test results of concrete samples produced within the scope of this study are shown in Table 4. The results of polypropylene fiber added concrete are given in Figure 4-7.

Table 4. Physical and mechanical properties of polypropylene fiber added concrete samples

Mix	Dry Unit Weight (kg/m^3)	Slump (mm)	Ultrasonic Velocity (km/sn)	28 Days Compressive Strength (MPa)	28 Days Flexural Strength (MPa)
NB	2.419	170	19.50	49.76	9.68
NL1	2.395	45	20.10	45.88	9.78
NL2	2.375	30	20.70	45.17	10.15
NL3	2.365	20	21.10	44.19	10.45

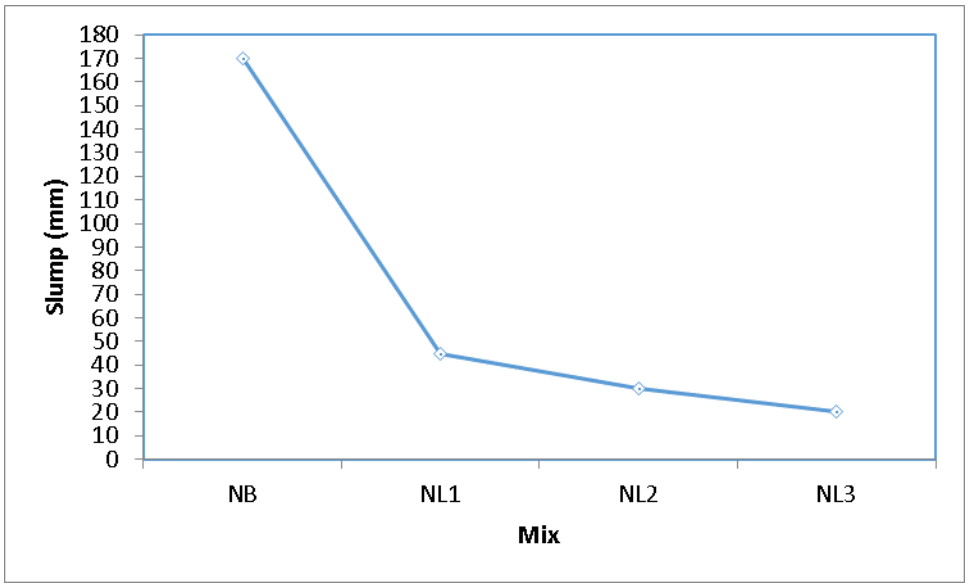

Figure 4. Slump Test Results of Polypropylene Fiber Added Concrete Samples

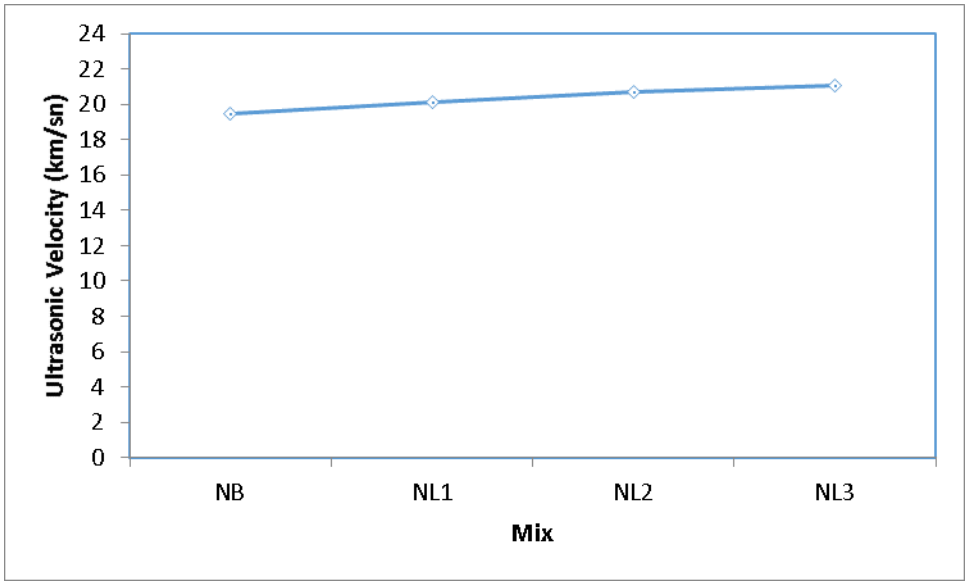

Figure 5. Ultrasonic Velocity Test Results of Polypropylene Fiber Added Concretes Samples

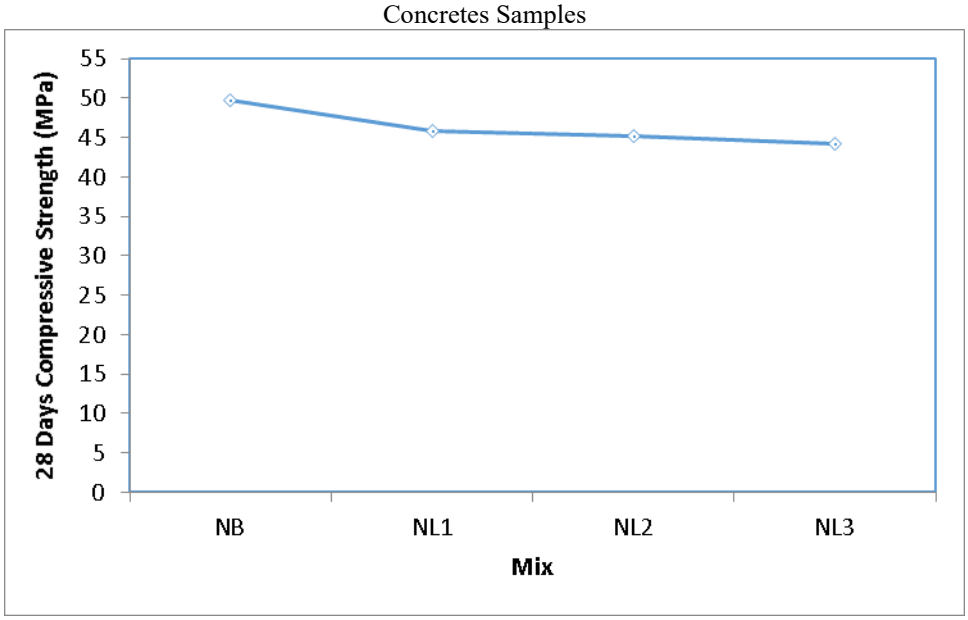

Figure 6. Compressive Strenght Test Results of Polypropylene Fiber Added Concretes Samples

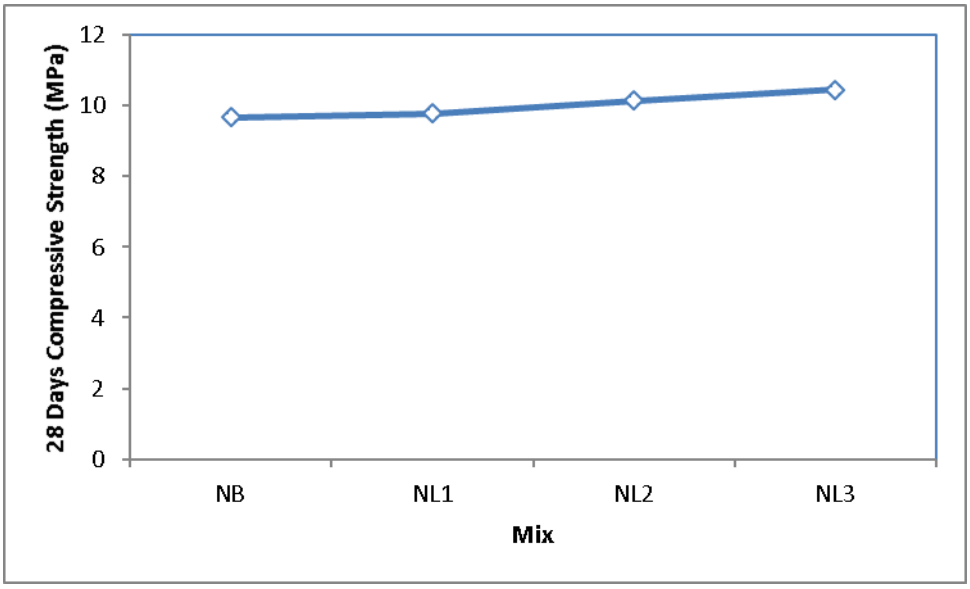

Figure 7. Flexural Strenght Test Results of Polypropylene Fiber Added Concretes Samples

Conclusion

- Increasing fiber dosage in fluid concrete brings about a decrease slump. This is an important feature in terms of cohesion of fresh concrete, even though workability may seem like a negative effect.
- Increasing fiber dosage brings about a decrease in 28 days compresssive strengt results.
- Increasing fiber dosage brings about a increase in 28 days flexural strengt results.
- As the fiber dosage increases, ultrasonic velocity increase.

Reference

Arazsu, U. (2012). Polipropilen Lifli Betonların Taze ve Sertleşmiş Beton Özellikleri. Fırat Üniversitesi Fen Bilimleri Enstitüsü, Yüksek lisans tezi, 63s., Elazığ.

Bekaert, 1998. Duomix Hakkında Genel Bilgiler Kılavuzu. Bekaert, Belgium.

Baradan, B., (1997). Yapı Malzemesi II Dokuz Eylül Üniversitesi Mühendislik Fakültesi Yayınları, İzmir.

Erdem, E., Donat, R., Çetişli, H., 1997. Hydration and Mechanical Properties of Cement Containing Zeolite, 1. International Symposium on Mineral Admixtures in Cement, 6-9 November 1997, 216-220, İstanbul, Türkiye.

Neville, A.M., (1981). Properties of Concrete, Longman Scientific, New York, 843 pp.

Neville, A.M., (1993). Properties of Concrete, ISBN 0-582-23070-5, 3rd edition, London.

Özel, C., (2007). Katkılı Betonların Reolojik Özeliklerinin Taze Beton Deney Yöntemlerine Göre Belirlenmesi, Süleyman Demirel Üniversitesi, Fen Bilimleri Enstitüsü, İnşaat Mühendisliği, Doktora Tezi, Isparta.

Sarıkaya, H., (2014). Bor Katkılı Özellikli Beton Üretimi, Süleyman Demirel Üniversitesi, Fen Bilimleri Enstitüsü, Maden Mühendisliği, Doktora Tezi, Isparta.

TS EN 802, Beton Karışım Hesapları, Türk Standartları Enstitüsü, Ankara.

TS EN 932-1, Beton Agregalarından Numune Alma ve Deney Numunesi Hazırlama Yöntemi, Türk Standartları Enstitüsü, Ankara, Aralık.

TS EN 12350-2 (2002). Beton – Taze Beton Deneyleri – Bölüm 2: Çökme (Slump) Deneyi. Türk Standartları Enstitüsü, Ankara, Turkey.

TS EN 12390-4, 2002. Basınç Mukavemeti Tayini, Türk Standartları Enstitüsü, Ankara, Aralık.

Ünlüer Ö., 2001. Alçı Kalıplar ve Alçı Kalıplarda Mikroyapı Dizaynı, Anadolu Üniversitesi, Fen Bilimleri Enstitüsü, Seramik Mühendisliği Anabilim dalı, Yüksek Lisans Tezi, Eskişehir.

Yardımcı, M.Y. (2007). Çelik Lifli Kendiliğinden Yerleşen Betonların Reolojik, Mekanik, Kırılma Parametrelerinin Araştırılması Ve Optimum Tasarımı. Dokuz Eylül Üniversitesi, Fen Bilimleri Enstitüsü, Doktora Tezi, İzmir.

DEVELOPMENT OF MESH-STRUCTURE APPLIED GUM METAL ARTIFICIAL MEDICAL PRODUCTS

Jianmei HE

Kogakuin University, 1-24-2, Nishi-shinjuku, Shinjuku-ku, Tokyo, 163-8677 Japan
e-mail: at13148@ns.kogakuin.ac.jp

Abstract: It is interested in this study to develope mesh-structure applied Gum Metal (one kind of titanium alloy, also called Gum Titanium) plates with high biocompatibility, elastic deformability and comparatively lower elastic modulus for implant applications. Meshed gum metal plates with excellent 3-demensional flexibility and light-weight performance compared to usual metal plate implants are designed parametrically using 3D CAD tools for different bone graft applications. Mechanical properties like tensile/compression and bending stiffness and volume densities of sample meshed gum metal plates are experimentally and analytically evaluated with respect to different design parameters like basic mesh shapes, mesh line width etc.

Keywords: Meshed Gum Metal plates, High flexibility, Mechanical property, Experiment, FEM analysis

Introduction

It is interested in this study to develop mesh-structure applied Gum Metal (one kind of titanium alloy, also called Gum Titanium) plates with high biocompatibility, elastic deformability and comparatively lower elastic modulus for implant applications. Table1 shows the mechanical properties of Gum Metal material under different working types. Sample meshed GUM METAL plate specimens with excellent 3-demensional flexibility and light-weight performance compared to usual metal-alloy plate implants are designed parametrically using 3D CAD tools for different medical devices applications. Mechanical properties like tensile/compression and bending stiffness and volume densities of sample meshed Gum Metal plates are fabricated using laser cutting processes for experimental and analytical evaluations with respect to different design parameters like basic mesh shapes, mesh line width etc. as shown in Fig. 1.

Table 1. Material property of gum metal plates based from different working process.

Type of Working	Cold Working	Hot Working
Yong's Modulus (GPa)	30～60	85～95
0.2% Proof Strength (MPa)	900～1100	1400～1700
Tensile Strength (MPa)	1000～1200	1500～1800
Density (g/cm^3)	5.6	

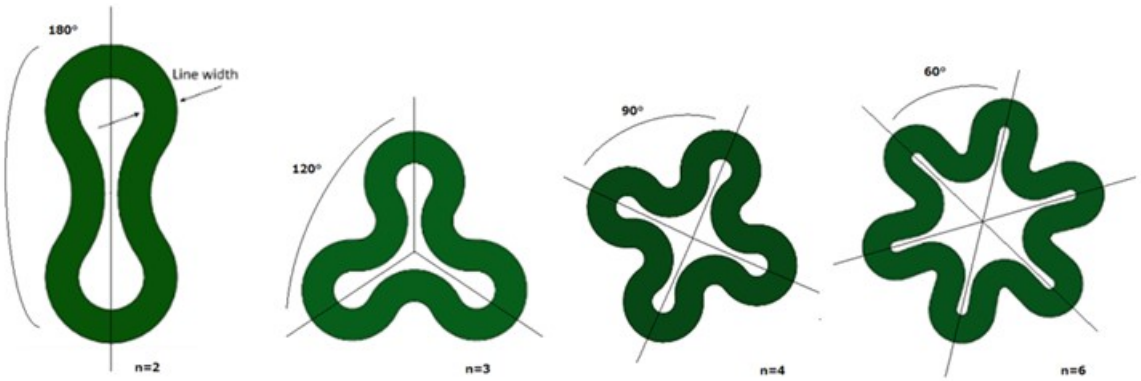

(a)180° axisymmetric shape (b)120° axisymmetric shape (c)90° axisymmetric shape (d)60° axisymmetric shape

Fig. 1. Four Samples of basic mesh shapes designed for experimental evaluations.

3D models designed for meshed Gum Metal plate specimens

Three dimensional models for sample meshed GUM METAL plate specimens with higher flexibility and light-weight performance are designed parametrically using CAD software Solidworks. Fig. 2 shows the meshed plate shape models for tensile property evaluations with 0.8 mm mesh line width. Fig.3 shows four types of meshed plate shape models for compressive and bending property evaluations with 1.0 mm mesh line width.

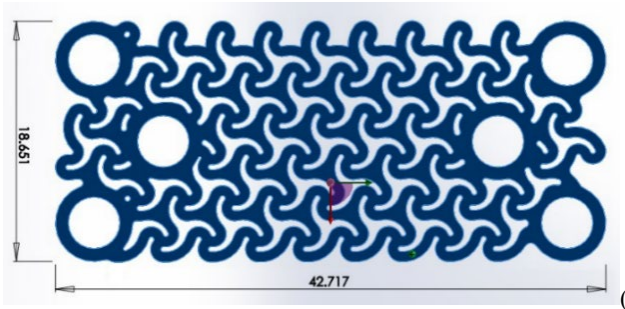

(a) 120° axisymmetric specimen (0.8mm)

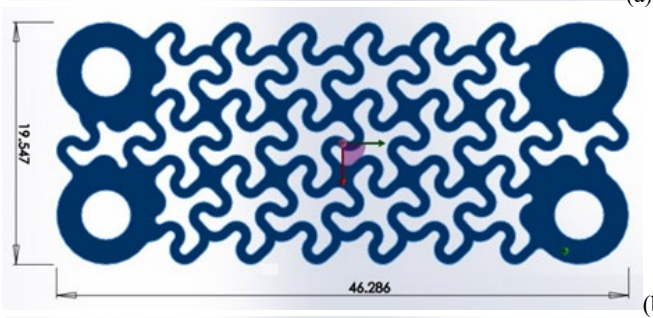

(b) 90° axisymmetric specimen (0.8mm)

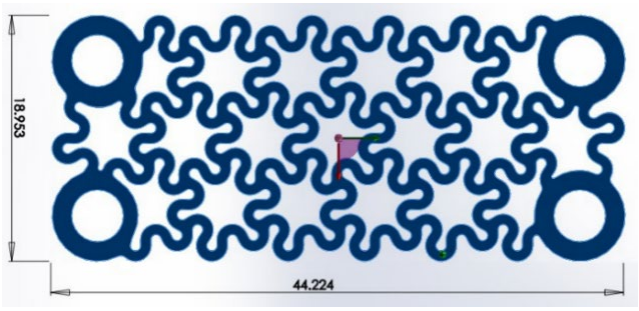

(c) 60° axisymmetric specimen (0.8mm)

Fig. 2 Meshed plate shape models for sample specimen evaluations (Tensile specimens)

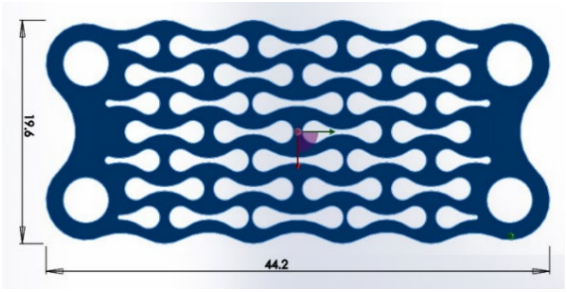

(d) 180° axisymmetric specimen (1.0mm)

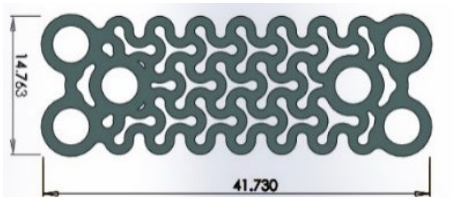

(e) 120° axisymmetric specimen (1.0mm)

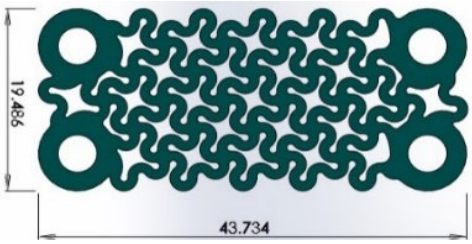

(f) 90° axisymmetric specimen (1.0mm)

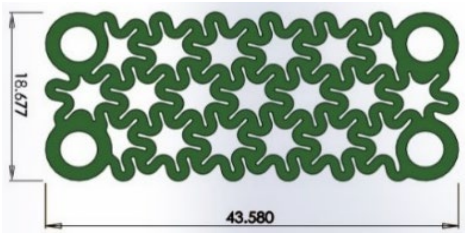

(g) 60° axisymmetric specimen (1.0mm)

Fig. 3. Meshed plate shape models for sample specimen evaluations (Compressional and bending specimens)

Evaluation on mechanical properties of sample meshed Gum Metal plate specimens

Experimental evaluation

Sample meshed Gum Metal plate specimens are fabricated using laser cutting process and shown in Fig. 4. Fig.5 shows the examined volume densities of different sample meshed Gum Metal plate specimens compared with original Gum Metal material. One can see that sample meshed Gum Metal plate specimens with different basic mesh shapes are resulted in light-weight structures compared with original Gum Metal plates.

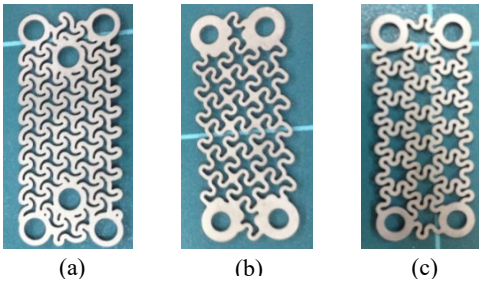

Fig.4. Meshed gum metal plate specimens for mechanical property evaluation

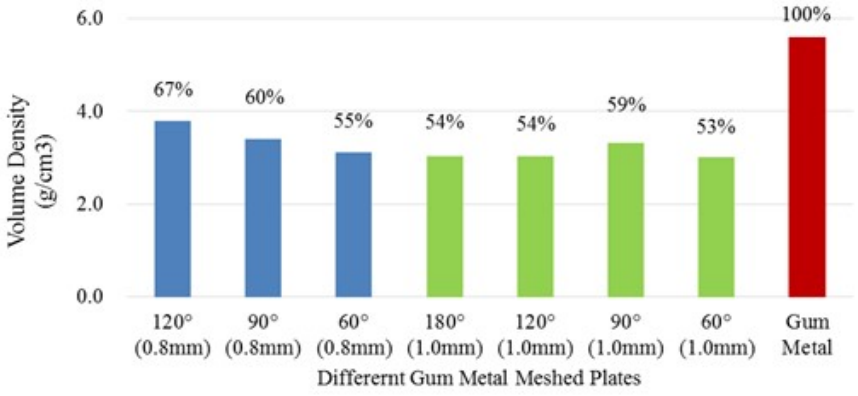

Fig. 5. Volume density of sample meshed gum metal plate specimens

Analytical evaluation

Based on the three dimensional models for sample meshed GUM METAL plate specimens shown in Fig. 2, analytical evaluation on tensile, compressional and 3-point bending experiments on those sample meshed Gum Metal plate specimens are executed for comparison with experimental results. Fig. 6 shows the analytical models for three experiments of meshed Gum Metal plate specimens and Fig.7 shows the sample image of finite element mesh for compressive analysis of meshed gum titanium plates. Table 2 shows the material properties of Gum Metal for analytical inputs.

Table2. Material property of Gum Metal for analytical approach

Density (kg/m^3)	5600
Young's Modulus (GPa)	40.0
Poison's Ratio	0.32

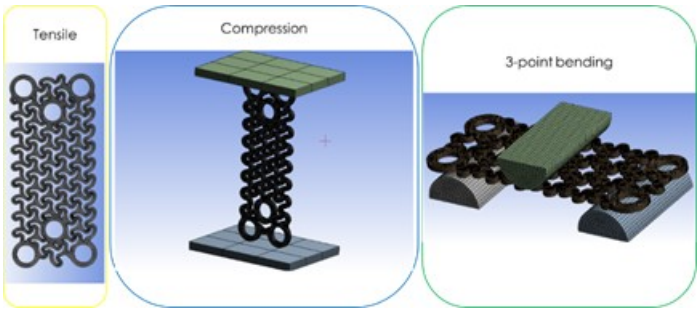

Fig. 6. Analytical approaches on mechanical properties of meshed Gum Metal plates

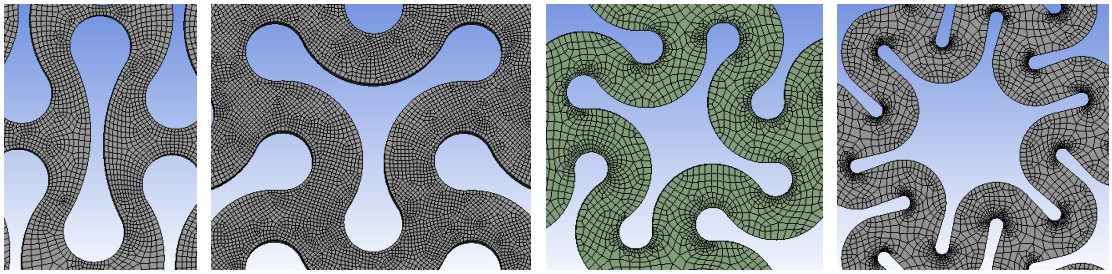

180° 120° 90° 60°

Fig.7. Image of finite element mesh for compressive analysis of meshed gum titanium plates

Results and Discussion

Fig. 8 shows the typical loading-displacement results obtained from tensile, compression and 3-point bending experiments of sample meshed Gum Metal plate specimens based on different JIS standards. Fig. 9 shows the comparison on quasi- tensional and compressional elastic modulus of sample meshed gum titanium plates. From these results, quasi- tensile, compressional and bending elastic moduli are evaluated and the radar chart of mechanical properties of sample meshed Gum Metal plate specimens are shown in Fig. 10. From these experimental results, sample meshed Gum Metal plate specimens introduced here with different basic mesh shapes are resulted in tensile, compressive and bending flexible plate structures.

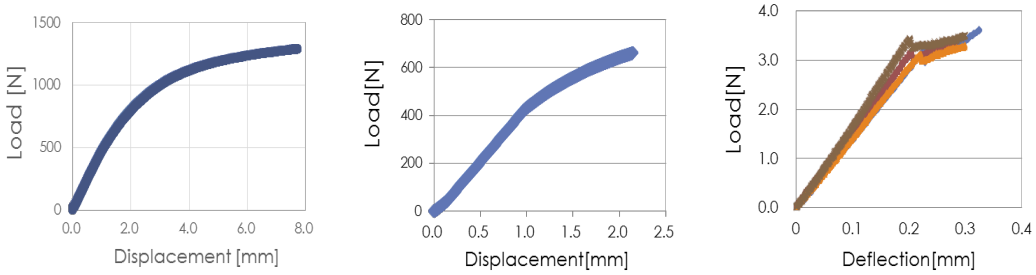

(1) Tensile (2) Compression (3) Bending

Fig. 8. Typical experiment results for mechanical property evaluation of meshed Gum Metal plate specimens

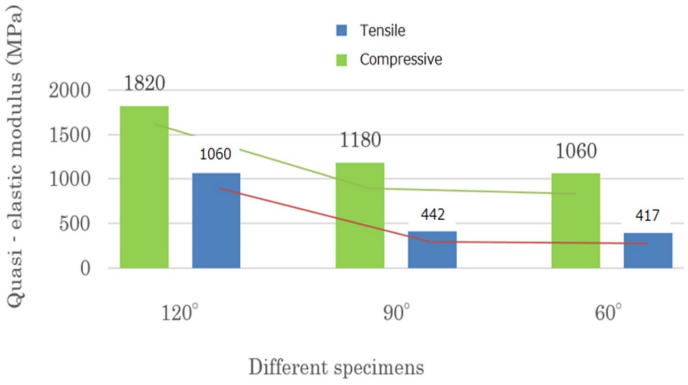

Fig. 9. Comparison on tensile and compressive properties of meshed Gum Metal plate specimens

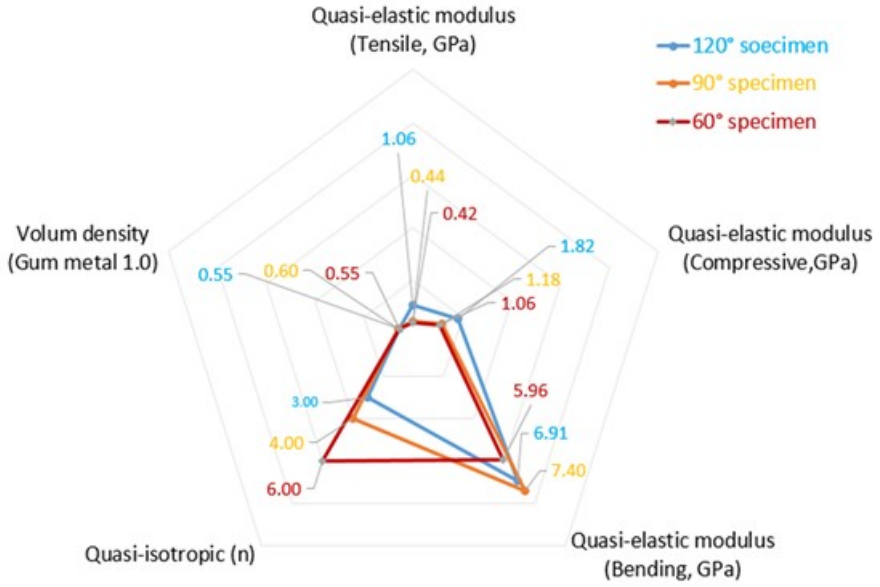

Fig. 10. Radar chart on mechanical properties of sample meshed Gum Metal plate specimens

Fig. 11 shows typical analytical Von Mises stress result obtained for tensile experiment of meshed Gum Metal plate specimens. From these analytical results, comparison between analytical and experimental tensile, compressive quasi-elastic modulus and bending deflections are shown in Fig. 12 to Fig. 14. These comparison on analytically obtained pseudo-tensile elastic modulus, pseudo-compression elastic modulus and bending rigidity of meshed Gum Metal plate specimens with experimental results validate the analytical approach method adopted in this study.

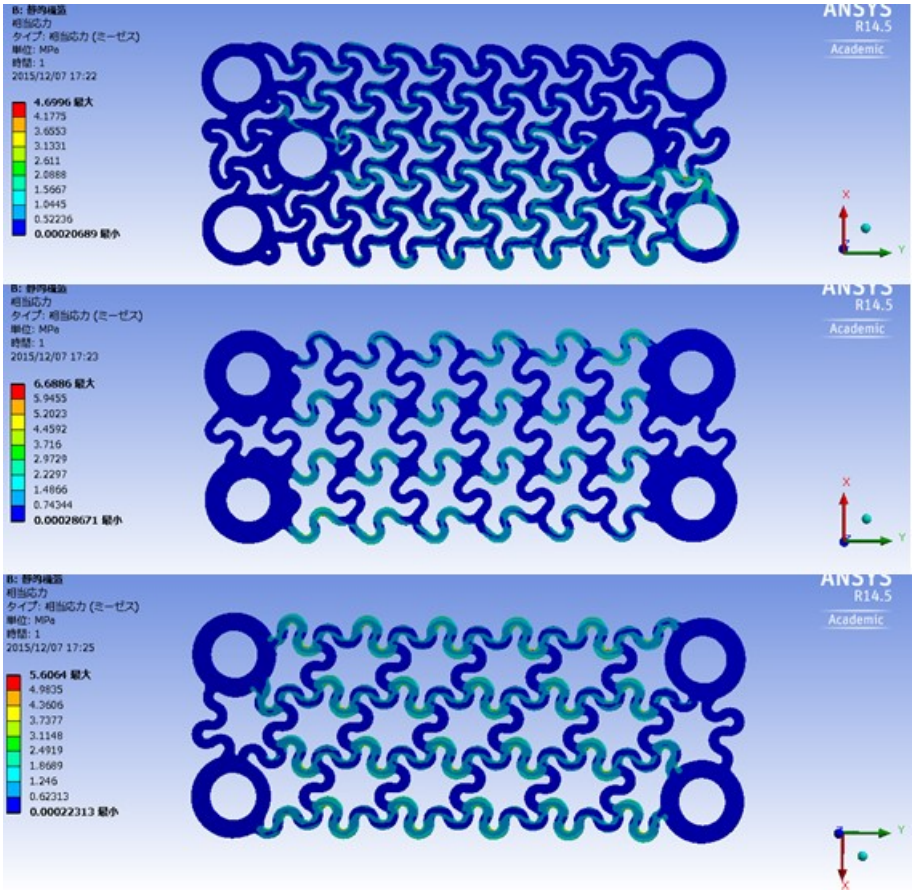

Fig. 11. Analytical results of tensile meshed gum titanium plate specimens (Von Mises Stress).

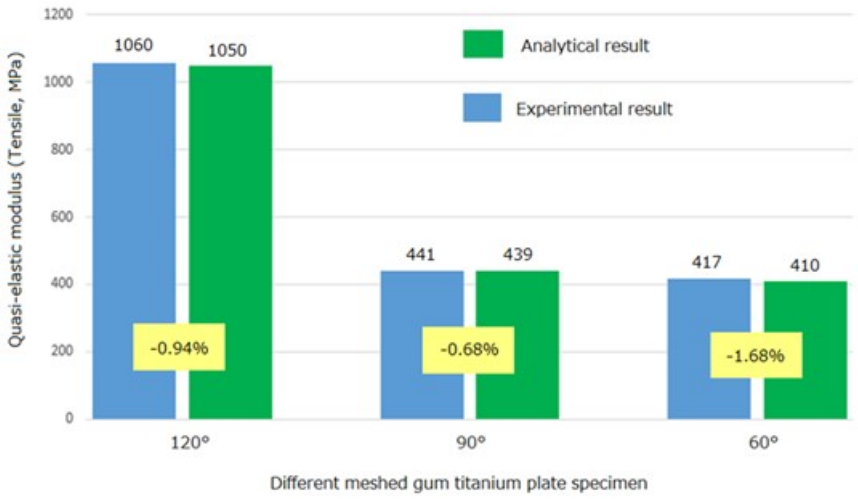

Fig. 12. Comparison between experimental and analytical results of tensile quasi-elastic modulus

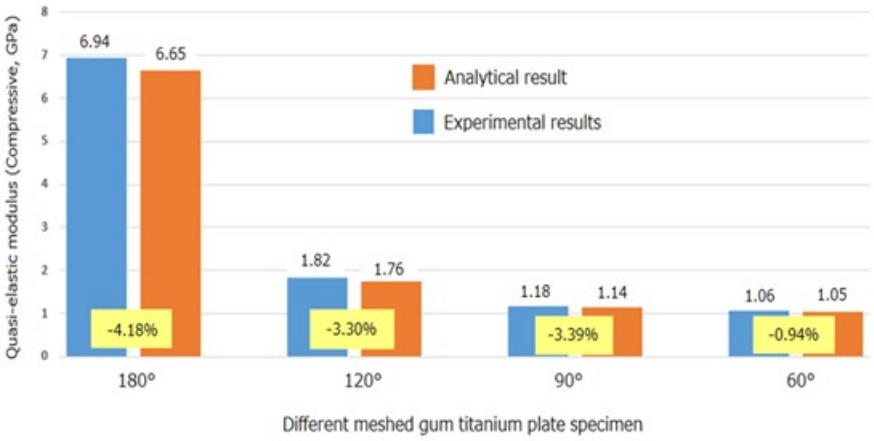

Fig. 13. Comparison between experimental and analytical results of compressive quasi-elastic modulus

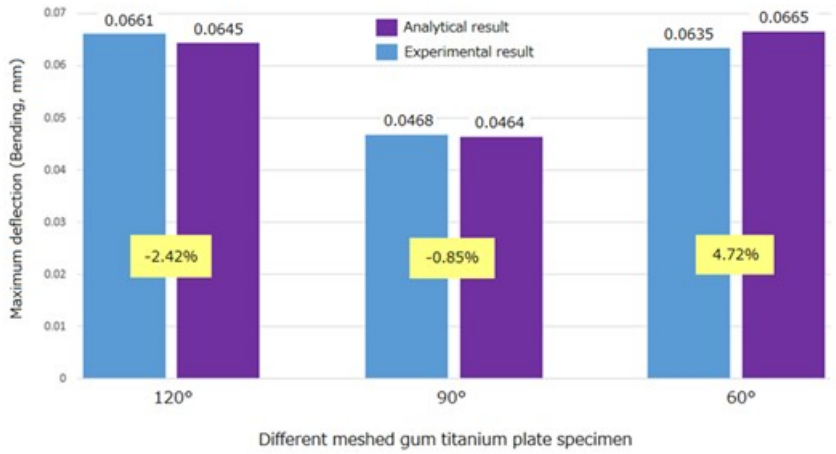

Fig. 14. Comparison between experimental and analytical results of bending deflection

Conclusion

Mechanical properties of meshed Gum Metal plates designed for medical devices applications were experimentally and analytically evaluated and the following points were clarified.

(1) Sample meshed Gum Metal plate specimens with different basic mesh shapes are fabricated through laser cutting process, resulting in light-weight and flexible plate structures
(2) In order to improve the structural flexibility of meshed Gum Metal plates, it is considered better to design the basic mesh shape with higher priority.
(3) It is considered that the in-plane pseudo-tensile elastic modulus and the in-plane pseudo-compressive elastic modulus of meshed Gum Metal plates are greatly affected by pseudo-isotropy (rotational axis-symmetry) due to the basic mesh shapes.
(4) For out-of-plane bending rigidity and pseudo-bending modulus, the influence of pseudo-isotropy due to due to the basic mesh shapes is considered to be small.
(5) Comparison on analytically obtained pseudo-tensile elastic modulus, pseudo-compression elastic modulus and bending rigidity of meshed Gum Metal plate specimens with experimental results validate the analytical approach method adopted in this study.

Parametrical investigations on mechanical properties of meshed plate models can be carried outies analytically due to different design variables to develop databases dealing with different medical devices applications.

References

Nissei Corporation, Introduction of Gum Metal, available from <http://www.nissey-sabae.co.jp/wp/wp-content/uploads/gummetal.pdf>, (Reference date: June 10, 2016).

R. Abiko, K. Zama, T. Sinoda, S. Suzuki and J. He, A Primary Study on the Titanium mesh plate Structures for Reinforcement of Tricalcium Phosphate Bone Implants, International Conference on Advanced Technology in Experimental Mechanics 2011 (ATEM'11, 2011), Kobe, Japan.

S. Suzuki, J. He, U. Chung and N. Sasaki, Three-dimensionally moldable lattice structure, Japan Patent No. 533997 (2012).

J. He, S. Suzuki and U. Chung, Developments of 3D free form titanium mesh plates for implantation (Design of mesh structures for titanium mesh plates), Transactions of the JSME (in Japanese), Vol.80, No.809(2014), DOI:10.1299/transjsme.2014smm0003.

DIFFERENTIATION OF BUILDING WITH THE COMMUNITY CONCEPT FROM EXISTING MODELS, AND ITS IMPLEMENTATION IN PROJECTS IN AFRICA

Hakan Taha Çetin[1], Fatih Semerci[2]

[1]Department of Architecture, Necmettin Erbakan University
e-mail: htcetin@konya.edu.tr

[2]Department of Architecture, Necmettin Erbakan University
e-mail: fsemerci@konya.edu.tr

Abstract: Building with the community, which is starting to construction with training of labors to construct their vernacular in larger scale, became a trend in 80s and 90s in Africa in order to not only to construct building but also to develop society and it drew apart a different path from existing models. This research examines the rationale of this architectural trend by focusing on mostly projects which won Aga Khan Architectural Award (AKAA) like Halawa House by Abdel Wahed El-Wakil, Yaama Mosque by El Hadji Falke Barmou and Gando Primary School Francis Diebedo Kere and socio-economic and cultural backgrounds of their locations. The preliminary results of the research show that this technic gave chance to society both to survive in such a bad condition by gaining necessary skills and to implement these skills in other buildings forms like schools and hospitals which have a great importance for the development of the society with low-cost solutions. The conclusion can also be drawn that how the way of implementing architecture helps communities in the form of sociological, psychological and economical aspects.

Keywords: Building with the community, Traditional African Architecture, Aga Khan Award for Architecture, Diebedo Francis Kere, local materials

Introduction

For centuries, communities had played an important role in terms of shaping their environment by inventing new techniques or implementing the old ones. This role of communities has been forgotten for a while. With the emergence of co-design concept communities started to find part by their ideas in creating or rearranging the environment. In Africa, this implementation moved one step further by involvement of community to every stage of building life cycle because of the distinctive features of Africa. Many architects have tried this method for providing necessary artificial environment. Furthermore, building with community makes great contribution of well-being of community and its economy. It also provides competitive advantages to architect to gain prestige via awarding by prestigious foundations. In this paper, firstly differentiation of building with the community from existing models will be indicated. After that, implementation on some buildings will mention. Lastly, its benefits and effects on winning prestigious awards will be explained.

Differentiation of Building with The Community Concept (Commin-Arch) from Existing Models

Designing for users

Traditional method of design is about disintegration of professionals who focus only their professions. In this type, design team takes all responsibility of design and makes all design decisions considering the needs and expectations of end-users. Ideas of end-users cannot take part in the design process. After the completion of design, other professions like stakeholders and construction teams practice their duties and building become ready for end-users. Considering only the needs and expectations of end-users give rise to some problems especially in public buildings. Inferences of design team is more likely to fail to correspond changing needs and expectations of societies. This possibility leads to think different about the role of end-users in design process. Direct relations of users to design can prevent some problems which traditional method fails to prevent. These processes make way for designing with users also called as co-design or participatory design.

Designing with users

Participatory design is a methodology which aims to bring together all participants of building life cycle such as employees, partners, customers, citizens and end-users in design process. Origin of participatory design arise from advanced technological developments. Especially in public building design contribution of users are substantial

resource for designer (Kanga, Choob, & Watters, 2015). Instead of relying on the personal creativity of designers to puzzle out design problems in an identified context, the collective generativity of stakeholder is a main source of a participatory design process. In other words, it develops thoughts and imaginings by the collective ability of stakeholders. It can be revealed by designers that the tacit needs of users which are the needs that are indicated but not virtually pointed out by examining what users create with generative toolkits (Joon & Kun, 2008).

Figure 1. Meeting with users (Amstel, 2012)

Figure 2. Co-design activities (AIGA Chicago, 2011)

Building with the community (Commin-arch)

Commin-arch, which is starting to construction with training of labors to construct their vernacular in larger scale, became a trend in 80s and 90s in Africa in order to not only to construct building but also to develop society. Community can find part almost during every stage of building life cycle. Training of labors is not the only thing about commin-arch. Usage of local materials and traditional construction techniques make contribution to these type of buildings. Commin-arch differs greatly from participatory design and traditional method in terms of participation of the community which is only contribution of idea in co-design.

There are numerous reasons such as poverty and high unemployment rate why this concept has developed in Africa. This technic gave chance to society both to survive in such a bad condition by gaining necessary skills and to implement these skills in other buildings forms like schools and hospitals which have a great importance for the development of the society with low-cost solutions.

Three Buildings in Africa with Constructed with Commin-Arch

Halawa House by Abdel Wahed El-Wakil

Halawa House was built in Tahoua, Niger according to traditional Islamic or Egyptian prototypes by involving the courtyard and its fountain. The house has a loggia, a wind catch, alcoves, masonry benches and a belvedere. Most of the labor except for the master mason, plasterer and carpenter, who were skilled craftsmen, was local unskilled Bedouins that trained before construction. Selection of materials and construction techniques reflect sociocultural structure of community.

All materials used in construction is local, and there are no imported materials used in. The basic wall structures are of undressed local limestone and cement mortar. Burnt red bricks and mud mortar are used for all arches, vaults and domes and for the claustra work. All renderings, inside and out, consist of three coats of traditional sand-lime-cement plaster which is called as Alexandrine plastering. Other finishing materials are; sandstone paving from

Muqattam, near Cairo, for courtyard, stairs and backyard, Egyptian marble, from Aswan, for living areas, locally made tiles in other rooms, and zân wood joinery for doors and windows including mashrabiyya which is the Arabic term given to a type of projecting oriel window enclosed with carved wood latticework located on the second storey of a building or higher, often lined with stained glass. The project was awarded by Aga Khan Trust for Culture in 1978-1980 cycle.

Figure 3. View from the secondary court to the domed living room and loggia (AKTC)

Figure 4. Using mud brick construction techniques, a mason builds an inclined barrel vault (AKTC)

Yaama Mosque by El Hadji Falke Barmou

Yaama Mosque is Friday Mosque nearby Tahoua, Niger. Idea of building Friday Mosque came from the elderly people of community. They assigned the role of building to Mr. Falke Barmou who is a local architect-mason. The major characteristics of the mosque were defined by also village elders, mainly by giving an indication of the dimensions and by discussing models which were or were not to be used as example. After several discussions mud brick structure with local characteristics but in larger scale was agreed on. Mud brick structures require cyclical maintenance, alterations and repairs. For the Yaama Mosque this activity was from the beginning an act of religious devotion in which the entire community participates, and so it continues to be. Everyone contributes to the caretaking of the mosque in proportion to his or her ability to do so. Some make mud bricks; others carry them to the building site. Women carry water for brick and mortar production while others cut and gather wood. Structural materials are the sun-dried brick and wood. The wood is of all possible kinds because of being scarce. Mortar for renderings is made of mud into various agricultural and/or animal waste products are mixed for various purposes. The project was awarded by Aga Khan Trust for culture in 1984-1986 cycle.

Figure 5. Yaama Mosque and its surroundings (AKTC)

Figure 6. Front Façade of Yaama Mosque (AKTC)

Primary School by Diebedo Francis Kere

As a native of Burkina Faso, childhood of Francis Kere had many challenges and few resources. His primary school was 40 kilometers away from hometown in another village with poor lighting and ventilation. This experiences inspired him to become an architect and build primary school in his village with adequate psychical conditions. To do so, he established a foundation which named as Schulbausteine fuer Gando, Bricks for Gando, in university to collect funds to start the construction of his primary school. cost, climate, resource availability, and construction feasibility were main parameters for the design of Primary School. In this project, these parameters were not only negated but also embraced. Building with the clay is traditional construction technique for housing in Gando. For maximizing results with the minimal resources available and for being known by community, a clay/mud hybrid construction was primarily used. Natural ventilation was provided by pulling away the roof from learning space of interior and by using dry stacked brick ceiling. In turn, the ecological footprint of the school is vastly reduced by alleviating the need for air-conditioning (Archdaily, 2016).

Although Francis Kere is an architect of the project, the success of it can associated to the close involvement of the local villagers. Every members of community made contribution according to their skills and capability. Traditionally, members of a whole village community work together to build and repair homes in rural Burkina Faso. In keeping with this cultural practice, low-tech and sustainable techniques were developed and improved so that the Gando villagers could participate in the process. Children gathered stones for the school foundation and women brought water for the brick manufacturing. In this way, traditional building techniques were utilized alongside modern engineering methods in order to produce the best quality building solution while simplifying construction and maintenance for the workers. The Primary School was completed in 2001 and received the Aga Khan Award for Architecture in 2004. More importantly, however, the Primary School became a landmark of community pride and collectivity. As the collective knowledge of construction began to spread and inspire Gando, new cultural and educational projects have since been introduced to further support sustainable development in the village (Archdaily, 2016).

Figure 7. Exterior view of Primary School, Photographer, Özgür Basak Alkan

Figure 8. Workers assembling roof trusses, Photographer, Özgür Basak Alkan

Conclusion

Commin-arch give community the benefits of gaining necessary skills to survive such a bad condition, and chance to build necessary infrastructures and educational, and cultural structures with low-budget, and chance to continue their vernacular in advanced ways. In terms of construction process, it provides acceleration by building with the labor knowing implementation of traditional techniques, usage of local materials, and surrounding environment, and available labor-force for all day long, and coalescence of labors. In the field of economy low-budget solution compared to skilled labor costs and reducing or eliminating transportation cost and spent time for it by using local materials can be gained.

Based on the research above, it seems building with the community in Africa helps community by enhancing the way of their life. Also, it has clearly distinguishable advantages in terms of construction process and economy. Furthermore, by the benefits of commin-arch concept architects can earn reputation and become famous.

References

The Aga Khan Award for Architecture. (1975). Halawa House Agamy, Egypt. Retrieved 4 Aug 2018 from http://www.akdn.org/sites/akdn/files/media/documents/AKAA%20press%20kits/1980%20AKAA/Halawa%20House%20-%20Egypt.pdf

The Aga Khan Award for Architecture. (1982). Yaama Mosque Yaama, Niger. Retrieved 4 Aug 2018 from http://www.akdn.org/sites/akdn/files/media/documents/AKAA%20press%20kits/1986%20AKAA/Yaama%20Mosque%20-%20Niger.pdf

AIGA Chicago. (2011). AIGA Chicago Co-Design Workshop. Retrieved 4 Aug 2018 from http://www.terriwada.com/case-studies-raquo/aiga-chicago-co-design-workshop

Amstel, F. (2012). When Participatory Design makes sense. Retrieved 4 Aug 2018 from http://fredvanamstel.com/blog/when-participatory-design-makes-sense

Archdaily. (2016). Primary School in Gando / Kéré Architecture. Retrieved 4 Aug 2018 from http://www.archdaily.com/785955/primary-school-in-gando-kere-architecture

Joon, S., & Kun, P. (2008). A participatory design approach to information architecture design for children. CoDesign, 4:3, 173. doi:10.1080/15710880802281026

Kanga, M., Choob, P., & Watters, C. E. (2015). Design for experiencing: participatory design approach with multidisciplinary perspectives. Procedia - Social and Behavioral Sciences 174, 831. doi:10.1016/j.sbspro.2015.01.676

DYNAMIC MIXING OF ADIPRENE® L-100

Matt Jackson, Emily Hunt, Benton Allen

West Texas A& M University, Stephanie Steelman, CNS Pantex Plant

mjackson@wtamu.edu

Abstract: This project used a dynamic mixing system purchased from BDTronics to investigate automatic mixing and dispensing of polyurethane formulations to replace archaic hand mixing techniques at Pantex Plant that resulted in poor quality parts and inability to have good repeatability between results on lots of material. Over the course of approximately 18 months several curing agents and secondary extenders were evaluated but Ethacure® 300 and 1,4 butandiol were found to be the most similar to the previous curatives. Room temperature and heat cured formulations were identified to meet the needs of Pantex Plant Plastics Shop. By varying the formulation using the plasticizer benzylbutylphthalate (BBP), Ethacure® 300, and 1,4 butanediol, and adjusting the curing time and temperature, to the final physical properties were adjusted to include compression, tear, hardness, and tensile strength. A modeling study evaluated molds using a software package called Moldflow®. Moldflow® software helped determine the best points to place injection holes, vent holes and identified if damming issues or void formations would occur. This study determined that the new formulations as well as new colorants identified would be a good replacement for the production tools used at Pantex Plant.

Keywords: Dynamic Mixing; Plastics; Moldflow

Introduction

This paper summarizes a joint endeavor between West Texas A & M University (WTAMU) Engineering and Computer Sciences Department and Pantex. The project establishes a process for dynamic mixing system purchased from BDTronics to include investigating formulations and automatic mixing of polyurethane formulations replacing archaic hand mixing techniques to increase quality, safety, and efficiency.

The focus of the project includes the development of formulations using liquid curing agents to replace the solid curing agents Cyanacure™ and trimethylolpropane (TMP). Cyanacure™ is an amine curing agent used with the pre-polymer Adiprene® L-100 in various hand mixed polyurethane formulations at Pantex Plant. TMP is a solid hydroxyl terminated curing agent that when coupled at various levels acts synergistically with Cyanacure™ to soften final products. To convert from hand mixing to dynamic mixing, two alternate liquid curing agents were evaluated. Ethacure® 300 (E300) and 1, 4 butandiol (BD) are both liquids at room temperature and have similar properties to TMP and Cyanacure™. The materials developed in the Pantex plastics shop is used for coatings, seals, cushions, tool covers, table covers, sealing rings, and many other applications.

As part of the conversion, Pantex requested formulations and curing parameters that meet the following expectations:

- Targeted hardness reached and stable within 24 hours
- Less voids, warping, shrinking and rework
- Repeatable and reproducible results between batches
- Ability to have Adiprene® formulations cured at room temperature for coating applications
- More flexibility in curing temperatures and times
- Better color differentiation between mixes
- Help with mold designs to minimize warping, void volumes and under filling

After a laboratory evaluation at the manufacturer's site, principle investigators determined that the Cyanacure™ and TMP would not work in a dynamic mixer due to the elevated temperatures needed to melt TMP and Cyanacure™.

Further investigation revealed that consideration of Ethacure® 300 as a possible replacement for the MBCA occurred before Cyanacure™ was adopted at Pantex Plant. Based on this information, investigators conducted a second laboratory trial where Ethacure® 300 worked as an alternative to Cyanacure™. The plasticizer BBP did not have synergy with E300 at the previous loading levels used with Cyanacure™ for creating soft polyurethane segments. Reformulation using the new mixer needed to encompass the entire range of hardnesses. Several plasticizers with similar functionality were evaluated to attempt to find L-100 based polymers with the same functionality and physical properties as the current mixes with increased tear. The Manufacturing Division agreed to purchase a dynamic mixer and requested development assistance to identify appropriate formulations, curing parameters, and develop the new colorant system.

The experimental design refined the composition of each formulation to achieve the hardness ranges. The second aspect of the experiment determined the proper curing parameters that result in a cured and post annealed sample where the hardness did not change over time. In some formulations, the change in cure parameter results in variations of the hardness by several points. Identifying formulations that meet each hardness range is accomplished by development of stoichiometric ratios to produce materials within a few points of the targeted hardness. Cure parameters are adjusted and if that does not result in a final hardness that meets the requirements, the mixture ratios are adjusted and then the material reformulated. A study at Pantex Plant in 2007 resulted in four formulations with colors identifying the ranges. This process entailed a hand mixing procedure and while the formulations worked well, the hand mixing process led to problems with batch to batch variations as well as issues with parts shrinking due to high temperature cures which occurs in in most unfilled polyurethanes cured at anything above room temperature. The higher the temperature the more shrinkage occurs (Szycher, 1999), voids form due to the introduction of air into the molds during filling, lengthy fill times are necessary, and locations of vents and injection are based on trial and error.

The experiments conducted during this research project with the new L-100 formulations examined the effects of curing with different ratios E300 and BD, as well as the effects of cure temperature and time on hardness. The use of the plasticizer BBP with Ethacure® 300 was used in formulation for the grey material. The project scope included:
Screening experiments

- Determining best temperature and time for curing in order to stop creep from occurring
- Physical and chemical reactivity testing of the new L-100 formulations with the best results
- Analysis of molds using Moldflow® software.

Methods, Assumptions and Procedures

Current Mixing Process

The Plastics Shop currently uses a blend of Adiprene® L-100 and the curatives Cyanacure and trimethylylpropanol (TMP), with BBP, a phthalate plasticizer, used to adjust hardness as needed. The current process works well if only the formulation contained two constituents. Currently all mixing is done using an antiquated process by hand in paper buckets that is lengthy and takes 2-3 hours to prepare materials and the mold. The first step includes reconstitution of the prepolymer to a pourable liquid. Paper buckets are weighed and the large bucket is marked for an approximate amount to add. Kits with the dyes, extenders, and curing agents are weighed based on the amount of L-100 required. The curing agents are heated in an oven. L-100 is placed in a steam kettle and degassed. L- 100 is removed, reweighed and the curatives are adjusted based on the amount of L-100 lost in transfer. The technician verifies the amounts in use before mixing. After hand mixing the final mixture is degassed again then injected into the mold and multiple injections may be needed depending on the mold size. The mold is then placed into a walk-in oven to cure.

Dynamic Mixer Overview

Dynamic mixing is used for dispensing multi-component formulation directly into molds and commonly referred to as a one shot method. Vacuum for degassing as well as mixing formulation is done by equipment. Mixing in the mix head does not introduce air. Dispensing is very accurate with variability measured in the hundredths of a gram. With the right curatives, extenders, and prepolymers a polyurethane elastomer is produced in a single step and dispensed directly into the mold. While many polyurethanes use a static mixing setup, a dynamic mixer allows for an unlimited pot life. This allows fast curing agents to be explored if desired. These dynamic mixing systems are common to the polyurethane industry but typically are two part mixers. When building a system like this, the formulation is already determined and the process is defined. Based on the chemistry of the components and the final mixture, the system is designed to create a repeatable, controlled and automated dispensing process. The machine design is based on expected stoichiometry in

the future mixes. In the dynamic mixer introduction of moisture or air is limited to transferring from the five gallon container into the Adiprene® tank. Employing an automatic pump system further minimizes moisture and air contamination. The material is then degassed under vacuum and placed under an inert nitrogen blanket. The material is pushed through the system using cavitation pumps and nitrogen gas for pressure. Design aspects include:

- vacuum degassing
- temperature control
- agitation
- controlled temperature conditions
- adjustable and precise dispensing

Figure 1: Forward View of the Dynamic Mixer

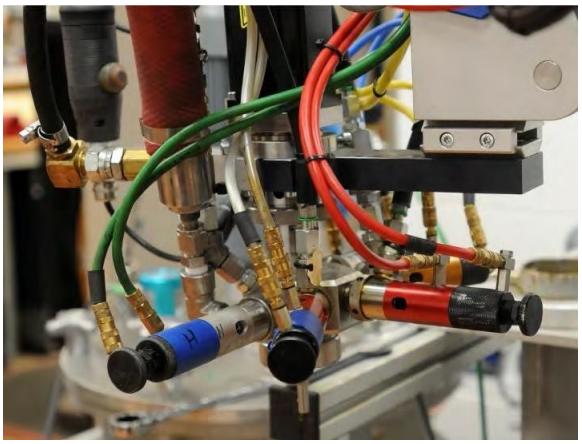

Figure 2: Dynamic mix head with valves

Positive displacement volumetric gear pumps achieve the desired dispensing mix ratios. The pumps and valves are readily changed if a change in formulation is desired. The dynamic mixing occurs at the dispensing head (Figure 2) to homogeneously mix components in the product it dispenses after a preset "wait" time. This results in an unlimited pot life during mixing. With the dispensing rate of 12 grams per second the largest mold at Pantex Plant fills in less than 5 minutes versus the previous 15-20 minutes.

System identification and system performance is based on the following: 3 shifts per day 7.5 hours per shift, 250 days per year. Original custom formulation was based on these starting criteria. Dispensing rate was at 15 grams per second capable of filling the largest mold in 6 minutes (5.44kg). The large Adiprene® tank is double jacketed with two discharge ports. It has an agitator and vacuum system and is heated. The equipment is controlled using a Beckhoff-CX PLU logic controller to regulate dispensing, heating, degassing. The controller contains digital I/Os, USB, Ethernet connection for internet, and flash memory. The software uses programmable logic control with Windows XP embedded security. The dynamic mix head is made of stainless steel which has five exchangeable dispensing valves for the Adiprene®, Ethacure®, plasticizers and cleaning solvent. The mix head is removable for cleaning as well as replacing with other size mixing heads. The dynamic mix head has an adjustable servomotor with the ability to run between 100-5000 rpms. The pumps are DC motor driven and each independently controls the dispensing flow rates for the curing agent and plasticizer. These are volumetric gear pumps. The original design used a progressive cavity metering pump for the Adiprene® L-100 that was changed to a gear pump after several pump failures due to the crimp and the stator covered in FKM. These failures will be discussed later. Six pressure transducers (from 0-40 bar) monitor the working pressure between the dispensing pump and valve. This provides online monitoring of the process and ensures the process is under control. Each of the extender tanks included a full set of tank, hoses, pressure sensor, pump motor and valve. This is an advantage because there is no waste material from changing hoses when a color change or hardness change is made since the components are directly dispensed into the mix head. Temperature regulation for the L-100 includes a fluid cooling unit with water circulation control pump and a distribution manifold to maintain constant temperature (tolerance of ±2 in range of 0 to 30°C) for the hoses and vessel for L-100 as well as the dynamic mix head.

The machine frame is made of tubular aluminum and is on casters and has a self-supported cantilever articulating arm. It is manually operated for free movement in the X, Y, and Z planes. It has a footprint of four foot wide by eight foot long and weighs 2800 pounds. The tubing on the valves and pumps is color coded to match the dispensed formulations to minimize possible mistakes. The large tank contains the Adiprene® the smaller tank to the left is for E300 and the

four tanks along the back are for the extenders BBP, BD which also contain the colorants.

As part of the project a comprehensive operating aid was created that includes startup, operation, shut down, troubleshooting, cleaning, and preventative maintenance processes to facilitate startup process at the plant. With the new dynamic mixer the PU flowing into the mold (assisted by pressure injection of the polymer) displaces the air inside the mold. Proper air vents placed in proper areas must be part of the mold design or voids will form within the molded part. Using complex geometric shapes with varying wall thickness exacerbates air entrapment. To overcome this obstacle, tall shapes or complex shapes containing thin and thick portions should be filled from the bottom, not from the top to ensure proper filling and air displacement. For these molds a delivery tube system reaching the bottom of the mold should be employed instead of using a small injection port at the top of the mold. As the mold is filled the tube is removed before the PU begins to set. (Clemitson, Castable Polyurethanes, 2008)

Equipment Difficulties

When evaluating equipment in an R & D process, challenges occur. For example, within the first week of operation the main pump delivering Adiprene® to the mixing chamber seized and ceased functioning. The pump was disassembled and failure of a crimp was determined to be the culprit. A new stator with FKM (a fluoroelastomer usually considered chemically inert) was installed. At the beginning of the experiment the manufacturer of L-100 said the typical mixing temperature for L-100 is 165°F. The material was stored at 145°F between mixes. During the next two months of the experiment no issues were experienced. After this time interval, pump failure occurred again with the failure caused by the pump type. Replacement of the pump did not solve the problem. Further consultation with a technical person at Chemtura determined prolonged heating of Adiprene® at the low temperature of 130°F affects the prepolymer causing crosslinking and gel formation that raise the viscosity of the material.

Inconsistencies in Adiprene® flow prompted viscosity testing. Based on the results this issue resulted from two possible scenarios. Either the material reacted with the air used to pressurize the tanks or dimerization occurred. The tank was emptied, cleaned and refilled with fresh material. A nitrogen blanketing system pressurized the tanks. Attempts to dispense the new Adiprene® failed when a clog between the pump and valve occurred. After the hose was cleaned and reassembled, L-100 dispensed with poor consistency resulting in high variations in the test weights. During viscosity tests, the L-100 flow slowed to a few grams per second versus the set point of 11 grams per second. The cause was found to be a clog in the L-100 hose between the storage tank and the pump. While attempting to clear the clog, a leak formed between the Adiprene® hose and the coolant sleeve. Since water acts as a blowing agent in polyurethanes, cured material formed in the hose. To address the ongoing issues, a less precise gear pump was ordered that still gave better precision than hand mixing processes.

Because of the elevated temperature for storage, two hoses clogged resulting in extended downtime waiting on new hoses to arrive. To overcome this setback a local manufacturer of high pressure hoses used the fittings from the clogged hose and fabricated a high pressure hose that worked with the current system. Another stator was ordered with polytetrafluoroethylene (PTFE) and installed, operations proceeded, and then maximum pressure errors occurred during dispensing. Due to schedule conflicts, the material sat in the mixer and aged at higher than expected temperatures. L-100 has active sites that react with other materials or with itself causing the formation of dimers and trimers. In both cases, an increased viscosity (doubled when measured at WTAMU) results. The specification for the high precision stator pump identified in the original design was not for higher viscosity material which caused one failure. The pump was disassembled where it was found that the crimp on the rotor (that had failed during the first week of operations) had failed again. A new rotor was purchased and installed with the pump operating as normal.

While cleaning the dynamic mix head, an attempt to remove the agitator resulted in a sheared shaft. Once the problems were corrected and the machine was operational, small black pieces of the stator sloughed off during dispensing into the molds. This was most likely a reaction between the TDI ends of the prepolymer and the stator. Liquid urethane prepolymers react with themselves through the isocynate and form allophanate branching. This occurs from excessive heat history. Even though the initial contact with Chemtura suggested storing at temperatures at or near 120°F, mixing at 160°F was thought to present any special obstacles; multiple problems with hoses suggested that even at 140°F within 40 days, the allophane reaction occurs. Testing with GPC verified a dimerization reaction occurred and a doubling to tripling of the molecular weight of the prepolymer while resident in the hose. Heat history is one of most common causes of substandard physical properties in polyurethane part production and explains why there was lot to lot variation in the hand mixing. This over heating or reheating results in the TDI levels decreasing, gelled material in the tank and is a cumulative process. Reheating the same tank of material causes irreversible damage. Containers of

the L-100 should be protected from excessive heat and kept tightly closed under dry nitrogen or dry air. At a temperature of 122°F about 2000 hours produce a loss of 5% NCO content. If raised to 175°F the prepolymer degrades after 82 hours; At 212°F, it fully degrades after 14 hours. Heat history shows itself in the dynamic mixer as increased pressure in the L-100 line and issues with consistent dispensing. The L-100 requires slow heat to get it into liquid form before adding to the dynamic mixer with dispensing at the lowest temperature possible. To dispense the correct amount of material requires the adjustment of pump speeds and the weight of the amount dispensed. To facilitate an easy way to identify correct pump speeds, an Excel pump speed calculation spreadsheet was created.

Dye Experiment

Dyes are added to the polyurethane formulations at Pantex Plant as a visual tool to differentiate between hardness ranges. The machine design includes four tanks dedicated to different plasticizers or an alternate curing agent where each tank uses a specific dye color. The following dye assignments define each hardness range:

80-90 black 65-80 grey 50-65 red 35-50 green

To determine the amount of dye, each were tested in their respective mixes via hand mixes. When evaluating the dyes, the resin was added last in appropriate amounts. To evaluate the effect of curing process on dye and color, two molds are filled with one curing at room temperature and the other at an elevated temperature. Initial tests indicate that the dye mixed much better with the curing agent or plasticizer rather than the prepolymer.

Table 1: Grams of Color in Extender

Color	g	Curative (1000g)
red	118.58	in BD
green	38.61	in BD
black	24.365	in E300
grey	0.327	in BBP

Initial testing indicated when using 2 and 4 parts of colorant, colors were so opaque they were difficult to distinguish between the green, grey, and black. Several other types of powder dyes proved ineffective in improving material results. Further tests conducted on the liquid dyes found that reducing the added amounts by a factor of ten resulted in the sample colors becoming translucent and distinguishable. The new level of colorant is in the range of 0.4 parts for every 100 parts of Adiprene®. The color levels result in a slight change in the shade of the color as parts become thicker or when the cure temperature changes. The red and green pigments used at Pantex are immiscible in the BD and formed micelles. Alternate colorants were found from Polytek. This pigment shows to easily dissolve in the BD and result in translucent polymers as well. Manufacturing personnel liked the produced translucent parts which allows for easy identification of voids.

Testing Procedures

Samples were tested using ASTM D-2240 Standard method of Test for Indentation Hardness of Rubber and Plastics by Means of a Durometer. This method uses a specific indentor forced into the material and is based on the penetration of the indentor under ambient conditions. This is an empirical test and was the screening test for the experiments. An Instron Shore Conveloader Shore A durometer tester was used. All samples were tested at room temperature. The samples were dispensed directly into preheated 6061 aluminum plaque molds with molded part dimensions of 2” x 2” x ¼”. The molds were then cured at various temperatures and times to evaluate the hardness of the test plaques at 1 day, 7 day and 30 days. A Thermal Production Solutions Blue M oven Series DC 146 with a temperature range of 15°C to 350°C and accuracy of ±0.1°C was used to cure the parts.

After meeting the hardness criteria, formulation samples were prepared for tensile, tear C and compression testing. Samples were tested in accordance with ASTM D-624 Standard Test Method for Tear Strength of Conventional Vulcanized Rubber and Thermoplastic Elastomers using the Die C geometry using five un-nicked samples punched from a slab of cured 1/8 inch thick PU and tested using a Model Sintech 10/D from MTS Systems Corporation at a crosshead speed of 20 inches per minute.

Four tensile testing samples were prepared and tested in accordance with ASTM D-412-06 Standard Test Methods for Vulcanized Rubber and Thermoplastic Elastomers-Tension using the dumbbell geometry. Five samples were punched

from the same slab used for tear testing then loaded into the Sintech machine using a crosshead speed of 20 inches per minute measuring the tensile strength (the maximum tensile stress applied in stretching a specimen to rupture) and peak load.

Compression testing is a historical test for Adiprene® at the Pantex Plant. Compression samples were cured and tested in accordance with ASTM D-575 Standard Test Methods for Rubber Properties in Compression using the 40% deflection test method. Five samples were cut from a ½ inch thick slab and tested in the Sintech machine. While this test method is good for polyurethane foams it is not a valid method when evaluating set occurring in the elastomeric material. The applicable test to use is the compression set. Additionally for the softer PU materials (grey, red, green) the samples should be molded instead of cut, with the softer material and high modulus cutting results in parts that do not meet the criteria set forth in the ASTM method.

Viscosity of a fluid is a measurement of the friction of a fluid when it moves in relation to another layer as measured through the shear stress and rate of shear. Viscosity is molecular weight and time dependent. Many of the formulations were tested for viscosity as a quality control tool and to determine physical values for use in the Moldflow® experiments. Viscosity testing was done on material dispensed from the dynamic mix head using a Brookfield viscometer following ASTM D2196 Standard Test Methods for Rheological Properties of Non- Newtonian Materials by Rotational (Brookfield type) Viscometer. The compounded formulation was dispensed into a 600 mL beaker and placed in the viscometer. The torque percentage is maintained between 10 – 100% until the temperature of the material reaches 40°C. The LV2 spindle was used for testing and the temperature was 120°F.

Results and Discussion

Formulation, Cure, and Hardness Results

Black

A formulation of 10.97 E300 showed the best hardness results for the black formulation with a range from 80-90 Shore A. At room temperature this formulation cures to the mid-range of the black formulation. A temperature of 93°C for two hours sufficiently cures this material without significant creep. All cure temperatures result in a final Shore A hardness of 84. If a harder material is needed, adjusting the amount of Cyanacure added gives a higher stoichiometric cure ratio resulting a Shore A hardness in the range of 88-92. Preparation of this formulation the A & B tanks on the dynamic mixer results in a clear formulation.

Grey

Grey formulations were varied and multiple formulations were identified for room temperature as well as heated cures. Room temperature cures experience creep in all formulations. With the multiple formulations available, if different physical properties are needed for the same hardness range there is flexibility based on end use. Testing of these formulations' physical properties determine if different grey formulations work better for specific applications. Since a BBP based formulation was picked for the heated cure, the most likely formulation for a room temperature cure is 8.9 parts E300 extended with 40 parts of BBP. This will result in a 75 Shore A hardness. Moisture affects room temperature cures, so humidity plays a role in consistency between batches if cured at room temperature. As expected, inconsistency increases with room temperature cures. When curing at 93°C, the two hour and four hour cure had identical results. When comparing all three curing times, the standard deviation is 0.57 with a 95% confidence range of 68 to 71 suggesting that these three cures are indistinguishable.

Red

Red formulations comprised the range from 50 to 65 Shore A and gave the most flexibility in formulation for both room temperature and heated cures. Many of the formulations targeted green but the results placed the formulations in the red range. While attempting to find a room temperature cure for green and red, several formulations worked with low levels of BD and 100% level of E300. Based on these formulations the 3BD provides the best solution for a room temperature cure. However, if better tear resistance is needed, the higher hardness formulations require evaluation.

Red formulations were evaluated at three different temperatures for a heated cure. These included 71, 80, 93 and 120°C. The BD was kept constant and the E300 was dropped to below 95% stoichiometric cure. The best blend in this situation was the 7 pbw E300 cured for six hours. When E300 was increased to 10.97 pbw and blended with 2.7 BD resulting in higher creep. The six hour cure showed the least amount of creep but also resulted in hardness at the high end of the red scale. When three parts of E300 were blended with 3 parts of BD and the temperature increased to 140°C to force the urethane cure, substantial creep of hardness was observed with a final targeted hardness between 60-62 for all cure

times. When varying the amount of BD used at 80°C, the result shifted the final hardness towards the upper limits of the red range. None of these were considered a target even though several of them are adequate for red at the upper end of the hardness range. When applying various formulations at 120°C, three of the formulations had very consistent start and finish hardness falling in the middle of the red range. Four parts of BD resulted in a higher amount ofcreep.

Green

Green formulations were the most difficult to obtain consistent results. The best formulations for heat cured green were determined by varying the E300 and keeping BD at 4 parts and curing at 140°C with the five hour and seven hour cures giving consistent with minimal creep experienced. Early in experimentation one of the molds evaluated produced an explosives vacuum lifting fixture. This part has the seal leak rate tested in the Plastics Shop so that vacuum decay does not exceed 2 inches of mercury over a minute period. Based on the new formulation with a hardness of 40 Shore A, it was determined the new formulation sealed better than the old formulation. When introducing irregularities into the surface of the test piece the seal held and formed better to the part with no decay for over two minutes. It is possible to get a green formulation but it is at the upper end of the green range (50 Shore A). One hour at 71°C showed a creep stop at 7 days. However the initial hardness started below the current material requirements at 24 hours.

Mechanical and chemical properties

Table 2: Final Formulation Hardness Results

Final Formulations (L-100/E300/Extender)	Color Code	Cure Temp and Time	1 Day Hardness	7 Day Hardness	30 Day Hardness
100/3.5/3 BD	R1	120°C 5H	59	60	60
100/8.88/50 BBP	Grey 1	93°C 4H	70	71	69
100/10.97/0	Black	93°C 4H	83	84	84
100/4/4 BD	Green 2	140°C 7H	40	40	40

Hardness results are shown in Table 2. The tear strength (resistance to tear) in units of pounds per linear inch is calculated from the maximum load divided by the thickness of the specimen (Table 3). Tear results were higher in all of the formulations except grey. Tensile strength is a measurement of the force required to break the specimen as it is pulled apart. It is expressed in pounds per square inch (psi). The tensile testing is summarized in Table 4 for the specimens tested. For many of the red specimens the elongation stretched beyond the maximum vertical travel of the UTM, so the highest value is reported and explains the 95% confidence for the red formulation. All tensile testing results were higher on the new formulations. Tensile testing is not a good measurement for the red formulation due to the high modulus of the material.

Table 3: Tear Results on Final Formulations

Color	Tear(1b/in)	S.D	95% Conf
Black	430	25	50
Grey	248	5	9
Red	122	2	5
Green	52	2	4

Table 4: Tensile Results on Final Formulations

Color	Tensile (psi)	S.D	95% Conf
Black	4388	249	487
Grey	963	67	131
Red	2320	862	1690
Green	211	5	9

Compression at a load deflection of 40% is a measurement of firmness in pounds per square inch giving the spring force of the rubber. It compares to squeezing a piece of rubber between the thumb and forefinger to determine if the rubber works in the application. It provides a better way of determining what elastomer to use in an application instead of a Shore A hardness since Shore A hardness is more of a surface test whereas compression testing is a measurement of the polymers ability to compress and resist compression. This helps identify materials that will be too rigid or may compress too much in a seal application.

Table 5: Compression Results of Final Formulations

	Compression	S.D.	95% Confidence
Black	2342	157	308
Grey	1084	27	24
Red	901	10	9
Green	275	6.8	6

The viscosity data are presented in Table 6. Viscosity results provided data into the Moldflow CAD analysis.

Table 6: Viscosity Testing of Formulated Compounds

Color	Material/Composition	Fluid Temp. (°C)	Viscosity (cP)	% Torque	RPM
Green	100/4/4BD	55.0	2768	92.3	10
Green	100/4/4BD	53.6	2738	91.3	10
Red	100/3/3BD	54.0	2783	92.8	10
Red	100/3/3BD	53.4	2615	87.2	10
Black	100/10.97/0	54.6	2888	96.3	10
Grey	100/8.88/55BBP	45.7	1141	76.1	20
Grey	100/8.88/55BBP	46.0	1089	72.6	20
Black	100/10.97/0	56.3	2840	94.7	10
Green	100/10/5BD	52.4	3371	89.9	8
Green	100/10/5BD	54.0	3086	82.3	8
Green	100/10/5BD	54.0	2954	78.8	8
Green	100/5/4BD	54.0	2872	76.6	8
Green	100/5/4BD	54.0	2962	79.0	8
Red	100/3.5/3BD	54.0	2932	78.2	8
Red	100/3.5/3BD	54.0	2969	79.2	8
Grey	100/8.88/50BBP	44.0	1386	92.4	20
Grey	100/8.88/50BBP	44.0	1342	89.5	20

Moldflow® Study

Autodesk Simulation Moldflow® is a software suite designed to simulate the plastic injection molding process and provides a quick, simple method to prepare, run and post-process analyze an injection mold. It also has fast, easy- to-use wizards for creating multiple cavities, runner systems and cooling circuits. Included with Autodesk Simulation Moldflow® is an extensive material database. Material creation tools exist to import, change/modify and create materials to be used for any analysis and a report generator to create reports to contain any of the results derived from the analysis. The reports can contain images of the part(s) analyzed, including animations. Moldflow® uses finite element analysis (FEA) and the finite element method (FEM) for understanding plastic injection molding. The computer simulation software predicts how material flows during the injection portion of the molding cycle by analyzing a mesh of the 3D part model. The program simulates flow by calculating the flow front growth from the first node to connecting node, starting at the injection node. The cycle continues until the flow front expands to fill the last node. There are several models used in the software, the following were included in this study, and a select few of these are detailed below:

- Nominal wall thickness
- Draft angle
- Under cut
- Molding window analysis
- Flow resistance
- Gate suitability
- Fill time
- Plastic flow

Autodesk Simulation Moldflow® requires accurate material-property data in order to generate the best predictions. It contains a materials database holding rheological information required to perform analysis for more than 8000 polymers. A personal database is used to store material-property information custom created by the user. The following is a brief sampling of some of the results obtained from Moldflow and utilized to refine mold designs.

The Design Advisor within Moldflow analysis is the initial experiment which provides feedback on the design of the part including: nominal thickness, draft angle and undercuts. The nominal wall thickness result calculates the nominal wall thickness of the part, and then displays the thicknesses in bands relative to the nominal wall (Figure 3). The wall thickness is expressed as a percentage of the nominal wall (colored legend left in Figure 3) or as values. Ideally the part thickness should be as uniform as possible. Lower variance from the nominal wall thickness reduces filling and packing problems to avoid warping or surface defects such as weld lines or voids. Variations in part thickness may cause flow variation such as race-tracking or hesitation and may also result in excessive part warping.

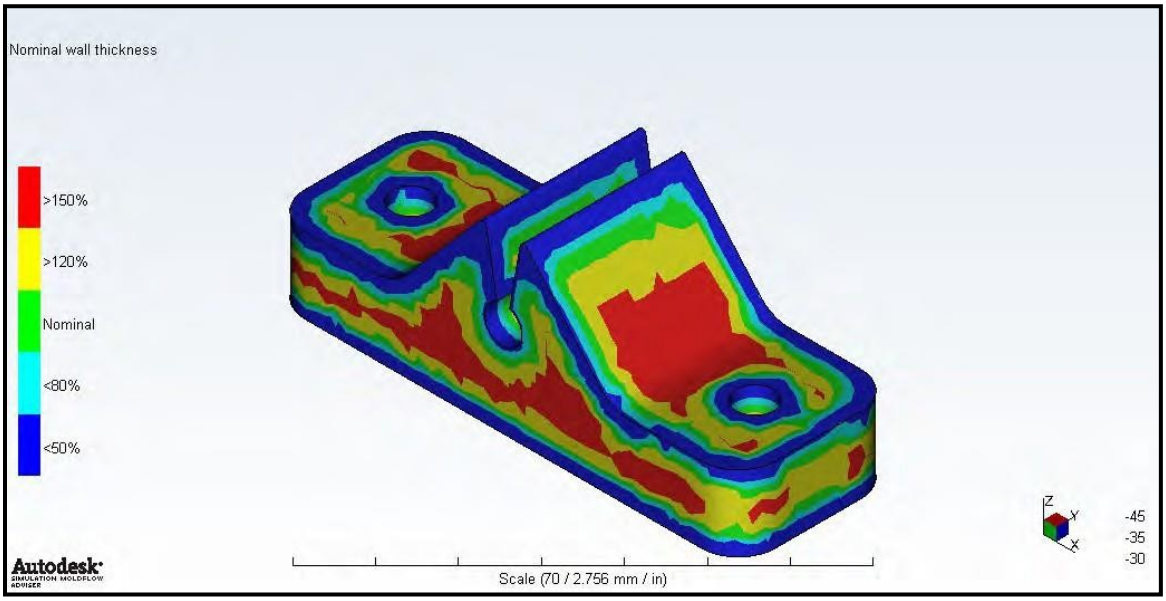

Figure 3: Nominal Wall Thickness

Autodesk Moldflow® Advisor has the capability to determine if a part will fill completely under specific processing conditions. If the plastic does not completely fill the cavity, then the part is short shot. A short shot occurs when the flow of plastic freezes off before all of the flow paths have filled. A part can short shot due to many different or combined factors such as flow restrictions due to long or complex flow paths, low melt and/or mold temperature, slow injection speed, or hesitation in thin sections, or fast curing.

Moldflow® Advisor helps determine what materials work best for the part with regards to mold filling such as pressure, shear stress, or temperature distribution. By using Moldflow® as an early evaluation tool in the design cycle of molds, the finalization of the mold design are accomplished quickly instead of by trial and error. Advisor helps narrow down processing conditions to mold a part. Suitable molding conditions are determined from a Molding Window analysis, and used, perhaps with slight modification, in subsequent filling analyses. In addition to optimizing the molding conditions, a Molding Window analysis is used as a quick initial analysis to compare materials or gate locations. Significant analysis time is saved by determining good processing conditions before running filling analyses.

Advisor has algorithms to determine where the gate (injection location) is located or if multiple gates are required. The Gating Suitability result is produced by the Gate Location analysis when the Advanced Gate Locator algorithm is used. The Advanced Gate Locator algorithm minimizes the flow resistance when determining the best gate position for the first and only injection location. The user can specify prohibited gate regions to block the solver from placing an injection location in the prohibited areas such as critical mating surfaces or surfaces requiring visual aesthetics. The Gate Location analysis produces a Flow resistance indicator plot and a Gating suitability plot. The Flow resistance indicator result (Figure 4) shows the resistance to the flow front from the gate(s). If the flow resistance is not evenly distributed from the injection location(s) to the end of the flow paths, defects or filling problems may arise.

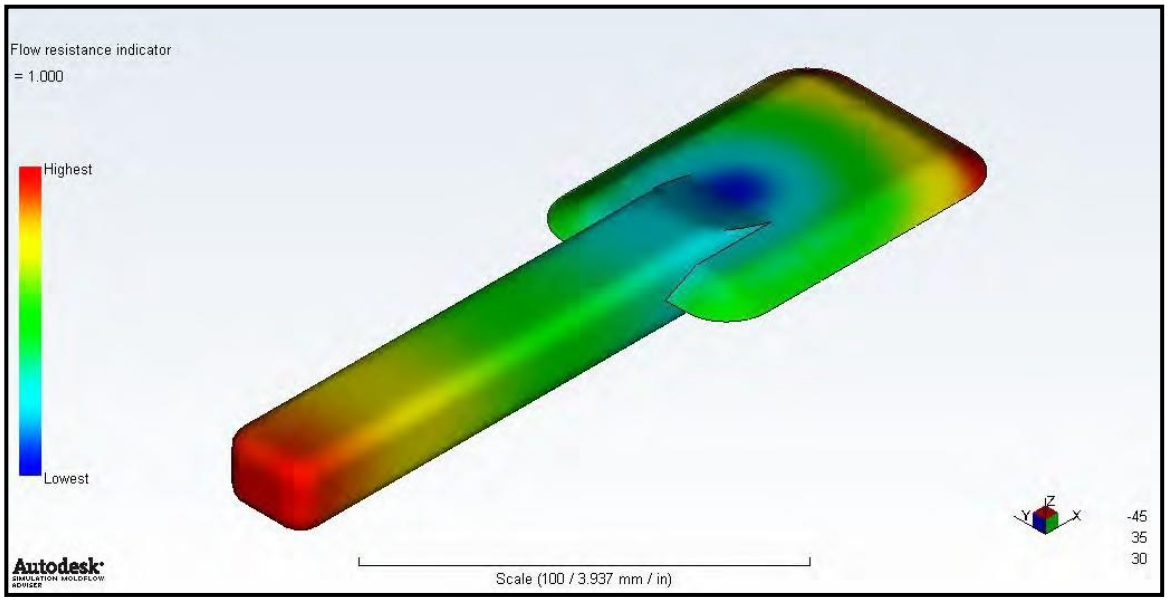

Figure 4: Flow Resistance Indicator

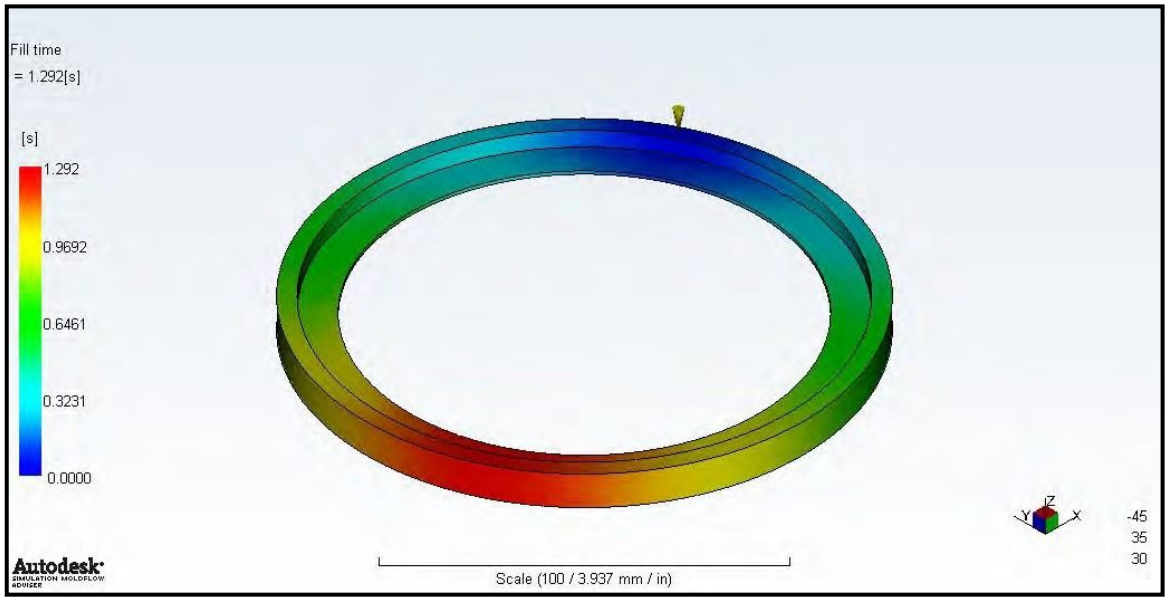

Figure 5: Fill time result.

The Gating Suitability analysis quantifies each place on the model for its suitability for an injection location. The suitable areas shown in this result are worth pursuing as potential injection locations. The best areas shown on the result do not necessarily represent a good solution for a high quality part or high confidence of fill, but rather the best one for the specific case at hand using the selected material.

Some of the most important and most used results are generated from a Fill analysis. The Fill analysis predicts the plastic polymer flow inside the mold in the filling phase. This analysis is often run as the first part of a Fill+Pack analysis sequence. A Fill analysis calculates the flow front growing through the part incrementally from the injection location, and continues until the velocity/pressure switch-over point has been reached. Results generated from a Fill analysis include the Confidence of Fill and Quality Prediction results, as well as Fill Time, Injection Pressure, Pressure Drop and Flow Front Temperature results. The Fill time result (Figure 5) shows the position of the flow front at regular intervals as the cavity fills. It also shows how the material will flow around part features which are the cause of weld lines and possible gas traps. By ensuring all extremities of the mold fill at the same time this minimizes issues with the end product.

The Fill analysis also generates a Plastic flow result plot. The plastic flow result is a different representation of the fill time result. The fill time and plastic flow results can be animated to visually show how the plastic flows from the injection location to the end of fill. The Confidence of Fill result displays the probability of plastic filling a region within the mold cavity under the conditions set for the analysis. This result derives from the pressure and temperature results. The Confidence of Fill result uses four colors (green, yellow, red and translucent) to indicate whether the part will definitely fill, may/will be difficult to fill or may have quality problems, or will not fill and results in a short shot. If the part is all green, the part is easily filled and part quality should be acceptable. If yellow is displayed, the part may be difficult to mold or quality may not be acceptable. As the percentage of yellow increases, the difficulty in molding the part increases and the part quality decreases. If yellow and red is displayed, the part is extremely difficult to fill or quality is more likely unacceptable. If the part displays any translucent, the part cannot be molded because a short shot will occur. The confidence of fill result is determined by both material melt temperature and injection pressure. A medium quality prediction may be caused by low or high flow front temperatures, cooling times, shear rates, or shear stresses. Autodesk Simulation Moldflow® Advisor contains features to help determine the cause of quality problems as well as suggestions and procedures on how to correct these problems.

The average temperature result (Figure 6) shows the velocity-weighted temperature average through the thickness of the part at the end of fill. Because of the velocity weighting, areas of low temperature have a very low velocity and areas of high temperature have a high velocity. If the average temperature is too low in a thin area, hesitation or a short shot may occur. If there is also a weld line in this area, the weld line will be more visually obvious. If the average temperature is too high, material degradation or surface defects may occur.

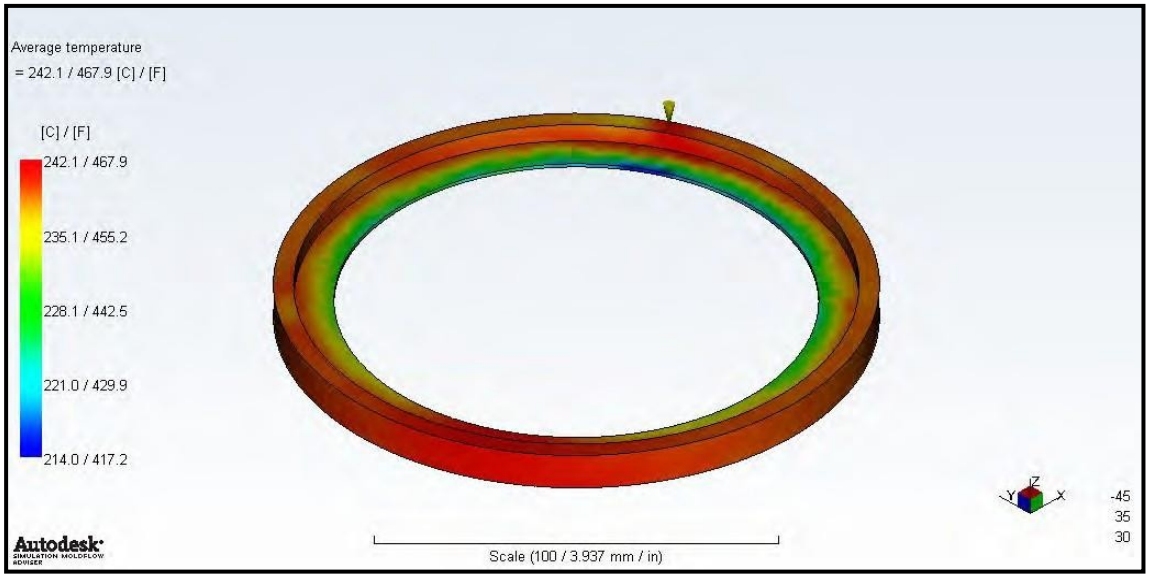

Figure 6: Average Temperature

The Temperature at flow front result shows the temperature of the polymer when the flow front reaches a specified point in the center of the plastic cross-section. The Temperature at flow front result uses a range of colors to indicate the region of lowest temperature (in blue) through to the region of highest temperature (in red). The flow front temperature should not drop more than 2°C to 5°C during the filling phase as a general rule. A large drop in flow front temperature indicates the injection time is too slow, or areas of hesitation exist in the mold design. When the confidence of fill result is poor, the temperature at flow front result determines whether the problems are caused by low melt temperatures.

Similar to the Air trap result, Moldflow® Advisor can predict the formation of weld lines. A weld line (which refers to either a weld or a meld line) is a weakness or visible flaw created when two or more flow paths meet during the filling process. A meld line is typically formed by parallel flows and weld lines are formed by flows meeting at higher angles, often head on. Weld lines can be caused by holes or inserts in the part, multiple injection gates, or variable wall thickness where hesitation or race tracking can occur. The quality of the weld line is dependent on the material type, the type and amount of fillers, and the pressure and temperature at the weld line. Weld lines should be moved to areas

where strength is of less importance and visual appearance less obvious. The Weld lines result displays the angle of convergence as two flow fronts meet.

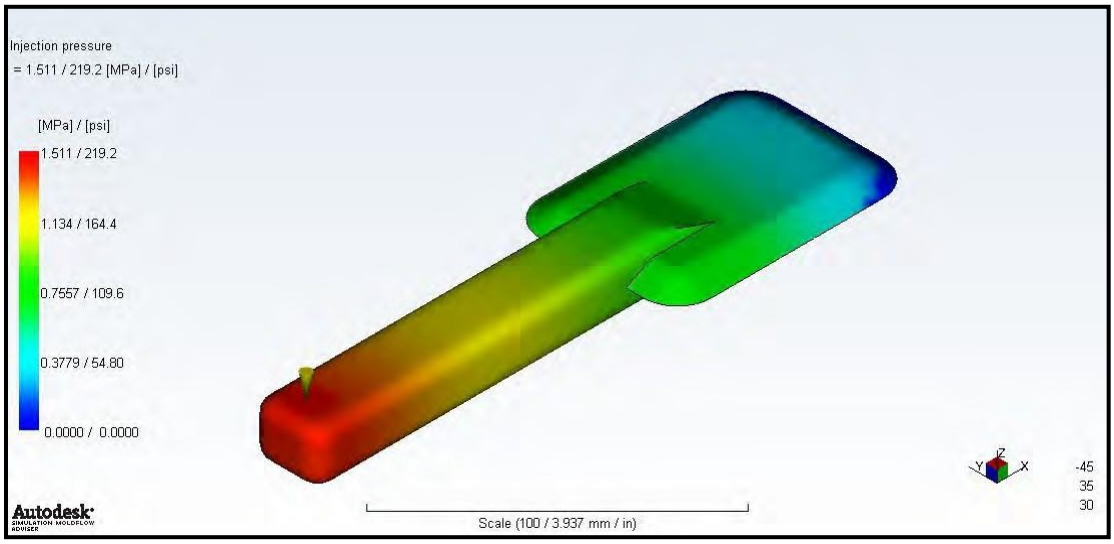

Figure 7: Injection Pressure

The Injection pressure result (Figure 7), is produced by the fill analysis and shows the maximum injection pressure value obtained before the velocity/pressure switch-over occurs during the filling phase. The pressure at a specific location starts to increase after the melt front reaches the location, and continues to increase as the melt front moves past, due to the increasing flow length between this specific location and the melt front. The pressure difference from one location to another is the force pushing the polymer melt to flow during filling. The maximum pressure occurs at the polymer injection locations and the minimum pressure occurs at the melt front during the filling stage. The magnitude of the pressure or pressure gradient depends on the resistance of the polymer in the mold. This is because a polymer with high viscosity requires more pressure to fill the cavity. Restricted areas in the mold, such as thin sections, small runners, and long flow lengths, also require a larger pressure gradient and, therefore, a higher pressure to fill.

The final two analyses from Autodesk Simulation Moldflow® Advisor are "fill+pack" analysis and warp analysis. The “fill+pack” analysis generates the fill analysis results and performs a packing analysis. This analysis is run as the second stage of a “fill+pack” analysis sequence. A pack analysis calculates flow front growing from the filled locations in the model when the velocity/pressure switch-over point was reached. This analysis simulates the stage of the injection molding cycle when pressure is applied to the polymer melt to compress the polymer and to force more material into the mold. This compensates for the shrinkage occurring as the polymer cools from the melt temperature to ambient temperature. A pack analysis generates a volumetric shrinkage at ejection result that shows the volumetric shrinkage for each area expressed as a percent of the original modeled volume. A warp analysis is used to diagnose the cause of warping and recommend a solution, such as gate location changes, design parameter changes, or reduction of wall thickness variations. The Warpage indicator, all effects result highlights those areas of the part where the out- of-plane deflections are approaching or exceeding the specific nominal maximum deflection (NMD) value. This result is based on a “best fit” technique where the original geometry and the deformed geometry are overlaid showing the original size and the warped part.

Health and Safety - Vertecbio™ Citrus 120 as a Replacement for Toluene

The Plastics Shop uses toluene for cleanup after polyurethane mixing. Steam vessels are cleaned with heated toluene and the technicians wear a respirator in order to protect themselves from toluene vapors as well as the isocyanates released from heating. The process takes approximately 240 ml of toluene for cleaning. The new system uses VertecBio™ Citrus 120. It removes the cured and uncured polyurethane faster, will require less solvent, and is derived from renewable resources (100% biodegradable and recyclable through distillation). Its flashpoint is 105°F with a boiling point of 226°F. It does not contain hazardous air pollutants (HAP) and is an Environmental Protection Agency approved SNAP solvent (alternate to aerosol type solvents no ozone depleting constituents). VertecBio™ Citrus 120 is a non-SARA (Superfund Amendment and Reauthorization Act) 313 reportable chemical and is approved for plant

site use. Toluene is considered a hazardous air pollutant (HAP) and is a SARA 313 chemical. The VertecBio™ Citrus solvent is also less expensive than toluene. The Plastics Shop uses toluene as the rate of 15.8 gallons emissions and 5 gallons of liquid toluene waste per year. None of this is recoverable. The new system uses a 5 second cleanout cycle. The system dispenses solvent at the rate of 25-30 ml/second with an average use of 125-140 ml per cleanout cycle. Table 7 compares the chemical and physical properties of the two solvents. The evaporation rate for the new solvent is substantially lower than toluene and will result in minimum emissions.

Table 7: Comparison of VertecBioTM Citrus 120 and Toluene

	VertecBio™ Citrus 120	Toluene
Flash Point (closed cup)	105°F ASTM D93	39.2°F
Vapor Pressure	4 mmHg@68°F	28.5@68°F
Specific Gravity	0.91 @ 77°F	0.867 @ 68°F
Evaporation Rate (compared to Ether)	0.3	4.5
Vapor Density	3	3.1
Boiling Point	226°F	231°F

Based on current practices and the rate at which parts are fabricated this would decrease air emissions 100% and, if the solvent was recycled, decrease liquid waste stream by five gallons. Even if the solvent is not recycled, it is biodegradable since it is based on ethyl lactate and the only waste associated with the system is the solid polymer caught in the solvent filter. The solvent filtrate system allows the same batch of the VertecBio™ Citrus solvent to be used for upwards of a month before a change in solvent is needed. There have not been any toxicological issues with this product.

According to the technical datasheet, Ethacure® 300 (DMTDA) has undergone toxicological testing. No mutagenic or carcinogenic risks are expected. It was found to be slightly toxic orally to rats (LD50 >2000 mg/kg) and nontoxic dermally to rabbits (LD50> 2000 mg/kg. Eye irritation was experienced in observations with rabbits (Albemare Corporation, 2000).

Efficiencies

The new system is more efficient and results in significant cost savings. Tables 8 through 11 document the expected cost and time benefits associated with switching to the new system. In Table 8 the overall cost is unknown due to the need to base estimates on the number of mixes for each color completed in a year.

Table 8: Colorant Change and Cost ($) per 100 grams dispensed

	Black	Grey	Red	Green
Old cost per mix	0.14	0.09	0.08	0.08
New cost per mix	0.03	0.01	0.05	0.05
Cost savings per 100 g	0.11	0.08	0.03	0.03

Table 9 documents the time and costs to currently hand mix the PU in the Plastics Shop based on the man hours used and a conservative estimate of rejected parts overall in the 30% range (it has been estimated on some parts rejection is as high as 80%). There is a possible cost savings of approximately $130k.

Table 9: Mix time and Costs ($)

	Hours	Cost per Mix (Burdened)	Cost per Mix with 30% rejection rate	Cost per year
Manual	2.5	$208.95	$271.6	$141,250
Dynamic	0.25	$20.90	$20.90	$10,868
Annual cost savings				$130,382

Current plastics mixing requires packaging as five gallon bulk kits. Approximately 22 bulk kits are prepared annually. Each time a kit is created, the Plastics Shop mixes the appropriate material and sends it for testing. Based on past consumption of kits and the new Adiprene® tank holds approximately the same amount of material in 3 Adiprene® kits testing is expected to decrease by approximately 66%. This would result in a cost savings of approximately $41k annually.

Table 10: Annual Packaging and Testing Costs($) All Colors

	Current Hours	Current Cost per Year	Expected Hours	Expected Cost per year
Packaging 22 five gallon kits	120	$10,029	0	0
Testing kits	528*	$44,130	156	$13,039
Total		$54,159		$13,039
Total Savings per year				$41,120

The final area savings area is from switching to a biodegradable solvent. Toluene is 5-½ times more expensive than the VertecBio™Citrus 120. This will result in approximately a $4k saving per year. However, cost savings from establishing a safer solvent alternative are hard to estimate.

Table 11: Solvent Cost ($) Savings

	VertecBio™ Citrus 120	Toluene
Cost per liter	$8.95	$49.25
Amount Used per year (liters)	55(expected)	$95
Annual Cost	$492.25	$4678.75
Cost Savings per year	$4186.5	

Conclusions

The new dynamic mixer was demonstrated successfully when formulation studies were conducted at West Texas A & M University. The project was successful in meeting the following objectives:

- targeted hardness reached and stable within a 24 hour time frame
- less voids, warping, shrinking and rework
- repeatable and reproducible results between batches
- ability to have Adiprene® formulations cured at room temperature for coating applications
- more flexibility in curing temperatures and times
- better color differentiation between mixes
- more efficient mold designs to minimize warping, void volumes and under filling

When compared to current production lot testing, an increase in physical testing values for all four heat cured formulations occurred except in tear resistance for the grey formulation. The experiment identified room temperature cure formulations that would work within each range as well.

The new dynamic mixer reduces cycle time: a 15 minute cycle versus a 2-3 hour cycle per mix. Cleanup is safer, costs less and no longer requires respirator or exposure to toluene. Total cost savings per year is estimated at approximately $176K annually.

References

Albemare Corporation. (2000). *ETHACURE(r) Curatives A Convenient Liquid for all Urethane Applications.* Baton Rouge: Albemare Corporation.

BDtronic Dispensing Process-competence. (n.d.). Retrieved May 23, 2014, from bdtronic: http://www.bdtronic.com/dispensing/process-competence/

Boyd, M. (1983). *Organic Chemistry. 4th Ed.* Boston: Allyn and Bacon.

Chemtura. (2011, September 29). *Adiprene L-100 A urethane elastomer.* Retrieved May 01, 2014, from www.chemtura.com:

Clemitson, I. (2008). Castable Polyurethane Elastomers. Boca Raton: CRC Press. Clemitson, I. (2008). Castable Polyurethanes. Boca Raton: CRC Press.

Epoxy Technology Inc. (2014). *Tech Tip 26.* Retrieved May 23, 2014, from Epotek: http://www.epotek.com/site/files/Techtips/pdfs/techtips_26_7.pdf

Flowers, G. (1982). *Cyanacure- An Adiprene L-100 Curative Replacement for MBCA (MOCA).* Amarillo: Mason and Hanger Pantex Plant.

Fuest, R. (2002, October). Castable Polyurethane Elastomers-Serving Demand Engineering Applications. *Rubber World*, pp. 39-58.

Guess, T. R. (1996). *Isothermal Aging of Three Polyurethane Elastomers.* Albuquerque: Sandia National Laboratories.

Huntsman International LLC, Polurethanes Business. (2010). *The Polyurethanes Book.* John Wiley and Sons.

Myers, L. (1980). *The Chemical Reactivity Test - A Compatibility Screening Test for Explosives.* Amsterdam: Elsevier Scientific .

Nagaraj, P., Laskowitz, I., Palinkas, R., Emanuel, R., & Nybakken, G. (n.d.). *Low Free MDI Prepolymers Cured with tris (4,4'-Diamino-Diphenyl Methane) Sodium Chloride.* Retrieved May 01, 2014.

Richardson, B. (2011). *High Explosive Compatibility Testing at the Pantex Plant.* Amarillo: B&W Pantex.

Rodin, W., Spence, R., Russell, B., Ashcraft, R., & Vincent, R. (2007). *Laboratory Formulation of Adiprene Thermoset Elastomers with Varying Hardnesses (U).* Amarillo: BWTX- Pantex Plant.

Rodin, W., Spence, R., Russell, B., Ashcraft, R., & Vincent, R. (2009). *Laboratory Formulation of Adiprene Thermoset Elastomers with Varying Hardnesses(U).* Amarillo: B&W Pantex.

Szycher, M. (1999). Szycher's Handbook of Polyurethanes. Boca Raton: CRC Press LLC.

TRI-ISO. (2013, 08 6).

Van Krevelen, D. (2012). *Properties of Polymers.* Amsterdam: Elsevier.

Vickers, L. (2003). *HE Skid Test Engineering Equivalency Analysis for Adiprene Covered Surfaces in the W78 Process (U).* Amarillo: BWXT Pantex.

Weigle, J. (2006). *Effects of Temperature and Humidity on Wilethane 44 Cure.* Los Alamos: Los Alamos National Laboratory.

Wilson, M.H. (1992). *Cyancure Replacement Study.* Kansas City : Kansas City Plant, KCP-613- 4948.

EFFECT OF PRANDLT NUMBER ON TURBULENT HEAT TRANSFER OF CORRUGATED TRAPEZOIDAL PLATE HEAT EXCHANGERS USING NANOFLUIDS

Elif Büyük Öğüt

Kocaeli University Hereke MYO, 41800 Hereke, Kocaeli
elif.ogut@kocaeli.edu.tr

Seda Dilki

Kocaeli University Institue of Science, Kocaeli
seda_dilki@hotmail.com

Abstract: In this study, fully developed turbulent flow and heat transfer behavior of water, ethylene glycol, mercury and propane based nanofluids in a corrugated trapezoidal plate heat exchanger have been numerically investigated. A constant heat flux was applied to the heat exchanger and the constant heat flux was chosen to be 6 kW / m^2, volume fractions ϕ=0%-4%, diameter d = 20 nm and Al_2O_3 was selected as nanoparticle.The Reynolds number varies from 6000 to 20000. Geometric parameters of the corrugated trapezoidal channel, trapezoidal height e=5mm, trapezoidal pitch Pe=12mm, width of the top trapezoidal channel w=3mm. Executive equations have been solved with Ansys Fluent programme. The velocity distribution,temperature contours,pressure drop, average Nu number and thermal-hydraulic performance have been analyzed and presented. The effects of nanofluids have been examined on heat and flow fields and it has been observed that the heat transfer increases together with the nanoparticle volume concentration. When the nanofluid is used in a forced convection, the amount of heat transfer increases as the Prandtl number increases. The highest value of the average Nusselt number was obtained in the ethylene glycol-based nanofluid, and the lowest value was obtained in the mercury-based nano-fluid.Results show that the use of nanofluid in the corrugated trapezoidal channel increases the thermal performance of systems and thus contributes to the design of more compact heat exchanger.

Key words: Heat exchanger, corrugated trapezoidal plate, nanofluid, Prandtl number, CFD

Introduction

Heat transfer by means of a fluid is used in many areas, such as heat exchangers, solar collectors, refrigerators, automobiles, cooling of electronic devices, power plants, and many other engineering fields.There is a need to develop advanced heat transfer fluids to improve compact and performance heat exchangers with high thermal conductivity and to meet needs of ındustry.However, since the base fluids such as air, water, oil, ethylene glycol used for convective heat transfer have very low thermal conductivity, they can not meet the desired properties in today's technology. One of the techniques used for increasing the heat transfer characteristics of heat transfer fluids is the addition of solid particles whose thermal conductivities are higher than base fluids. (Lee and Choi,1999). The discovery of nanofluids, a new type of suspension in which less than 100 nanometers of solid particles (metal, metal oxide, carbon nanotube) are concerned, have recently increased their use as heat transfer fluids as a result of recent work. The reason for this increase is that nanoparticles have high thermal conductivity values even at very small nanoparticle concentrations (Choi,1995). Copper, silver, copper oxide, titanium oxide and aluminum oxide are usually used as the nanoparticle. Keblinski at al. (2002) the significant increase in the heat transfer ability of nanofluids is due to factors such as the Brownian motion of the solid particles, the liquid layer at the molecular level at the liquid solid common surface, the nature of the heat transfer mechanism, and nanoparticle collapse. The most important parameter related to the heat transfer in nanofluids is heat conduction ability.

The use of corrugated plate can increase appropriately thermal performance and compactness.The use of a corrugated channel results in a more complex flow structure and improves heat transfer to two or three times that of a conventional straight channel. (Islamoğlu,2003). Many researchers have developed strategies to reduce the system size of traditional fluid passing through a various cross-section-shaped channel and to improve system performance. They pointed out that wave angle and channel height affect temperature distribution and flow rate significantly.Tanda (2007) has made an experimental study on forced convection in a rectangular channel and V-shaped broken ribbed and transverse rectangular channels. Kwon et al. (2008) have made experimental and numerical studies on various wave-angle rectangular wave pipes.When the performance factor (1.8) and Reynolds

number were 1000, the highest level was found at 100. Naphon (2009), has expressed that corrugated channel arrangements and channel geometries have improved heat transfer performance by increasing surface area and accelerating vortex formation in the flow.

There are many studies in the literature on the thermal performance of water-based nanofluids for plate heat (PHE) exchangers. Pantzali et al. (2009) studied experimentally the effects of 4% CuO nanofluids on the performance of commercial herring-one-type plate heat exchanger (PHE). The experimental data confirmed that besides the physical properties, the type of flowinside the heat exchanging equipment also affects the efficacy of a nanofluid as coolant. The fluid viscosity seems also to be a crucial factor for the heat exchanger performance. Heidary ve Kermani (2010) reported that the addition of 10% Cu-nanoparticles enhances the heat exchange by 25%. Suspension of solid particles in a traditional fluid is another effective passive technique because it effectively enhances the thermophysical properties of the fluid. For this reason, the effect of various types of nanofluids on the performance of different geometries has been tested experimentally and numerically compared to that of the base fluids. Ahmed et al. (2011), explored numerically the laminar forced convection of flow and heat transfer enhancement in a wavy and trapezoidal channel using a Cu–water nanofluid with nanoparticle volume fraction from 0% to 5%. The friction coefficient and Nusselt number increase as the amplitude of the wavy channel increases. As the nanoparticle volume fraction increases, the Nusselt number significantly increases along with a slight increase in the friction coefficient. It was found that the trapezoidal channel has the highest Nusselt number and followed by the sinusoidal, triangular and straight channel. Tiwari et al. (2014) studied numerically fluid flow characteristics of CeO_2-water and Al_2O_3-water nanofluids flowing in a chevron corrugated-plate heat exchanger (PHE). It was found that the use of nanofluid as alternate coolant reduces the pumping cost as it delivers more heat transfer for the same pressure drop as that in the case of water as coolant. Ahmed et al. (2014), convective heat transfer of SiO_2–water nanofluid flow in channels with different shapes is numerically and experimentally have studied over Reynolds number ranges of 400–4000, it is observed that the trapezoidal-corrugated channel has the highest average Nusselt number, pressure drop and heat transfer enhancement followed by the sinusoidal-corrugated channel and straight channel. Rostami (2015) numerically investigated the convective heat transfer of nanofluid flow in a sinusoidal-wavy channel under constant heat flux. Numerical results were obtained for Reynolds numbers range of 100– 250 and nanoparticle volume fraction range of 0–10%. The two types of the base fluids such as water and ethylene glycol with Al_2O_3 nanoparticles were considered. Nusselt number and friction factor increased with the increasing of Reynolds number and nanoparticles volume fraction. In addition, the Nusselt number and friction factor of Al_2O_3- ethylene glycol nanofluid were higher than those of the Al_2O_3-water nanofluid. Esmaeili et al. (2010) focused on the alumina nanofluid flow in sinusoidal wavy channel. In this study, the boundary condition was applied as a constant heat flux on the channel walls. The governing equations were solved using finite volume method. The results showed that the nanoparticles addition to the basefluid may significantly increase the heat transfer enhancement, but the wall shear stress also increased. It was also found that at a given nanoparticle fractions, the Nusselt number values at high Reynolds number was higher than those at low Reynolds number. Heidary and Kermani (2012) have studied the laminar flow and heat transfer of nanofluid in sinusoidal-wall channel using finite volume approach. The results indicated that the heat transfer is enhanced by 50% with the increasing of nanofluid volume concentrations of copper as compared to water. On other hand, there was a slight effect of nanoparticles suspension on the skin friction coefficient. Ozbolat and Sahin (2007) have studied the thermal flow of Al_2O_3 in eight wave channel. The wavelength and the amplitude of the wavy channel were 28 mm and 3.5 mm, respectively. The upper and the lower walls of the wavy channel were maintained at uniform wall temperature condition. Tanda (2010) investigated the effect of four differentpitch-to-height ratios (p/e) including 6.66, 10.0, 13.33, and 20.0, onheat transfer in a rectangular channel with one-ribbed wall and tworibbedwall. Results showed that p/e = 13.33 was slightly preferablefor the 1RW case (especially at the highest Re values) while a smallerp/e value (p/e=6.66–10) gave the best performance for the 2RWcase. Singh et al. carried out an investigation on the effectof flow-attack-angle (α) on thermo-hydraulic performance of rectangularducts roughened with a new configuration of 'V-down rib havinggap' on one wide wall. The results showed the best flow-attack-angle(α) was from 30° to 75°.

In this study, fully developed turbulent flow and heat transfer behavior of water, ethylene glycol, mercury and propane based nanofluids in a corrugated trapezoidal plate heat exchanger have been numerically investigated. The effects of Prandtl number on the turbulent flow and heat transfer of the effects of Al_2O_3 nanoparticles at different volume fractions (ϕ =0% - 4%) under constant heat flow (6 kW / m^2).

Physical Model

In this study, the two-dimensional geometry of the trapezoidal channel plate examined in the analyzes is shown in Fig 1. Selected geometric parameters; the channel height is H=12,5 mm, the channel length is L=95 mm, the floor height of trapeze channel is b=4 mm, trapezoidal height is e= 5 mm,trapezoidal pitch is Pe= 12 mm, width of the

top trapezoidal channel is w=Pe/4= 3 mm. To ensure a fully-developed flow, the length of each adiabatic wall section before and after the corrugated section is set to be 250 and 100 mm, respectively.In the analyzes, the nanoparticle and the fluid are assumed to be at the same velocity and thermodynamic equilibrium. Water, ethylene glycol, mercury and propane are used as the base fluid, and also Al_2O_3 is used as the nanoparticle. Nanofluid suspension was obtained by adding Al_2O_3 nanoparticles at 20 nm diameter and different volume fractions 0%, 1%, 2%, 3%, 4% in water, ethylene glycol, mercury and propane base fluids.The thermophysical properties of the base fluidsand nanoparticle are given in Table 1.

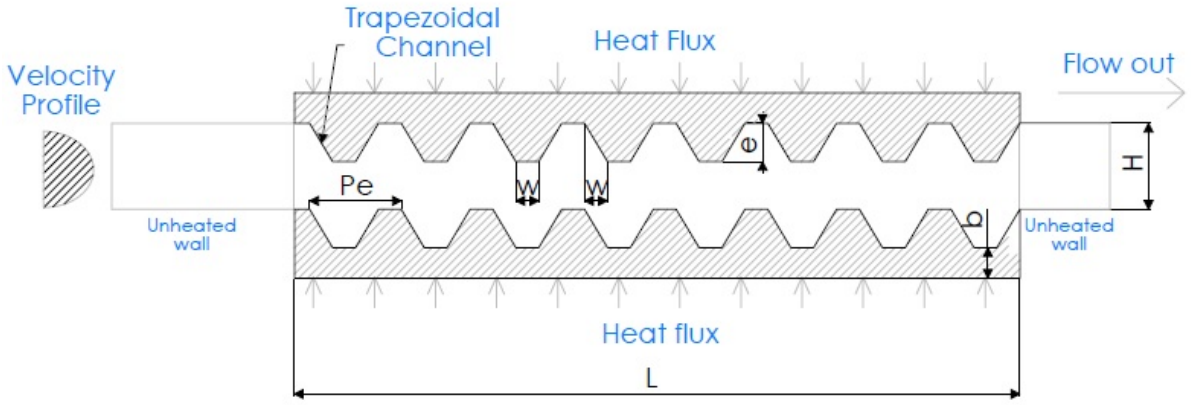

Fig.1. Schematic diagram of the corrugated trapezoidal channel.

Table 1. Thermophysical properties of base fluids and nanoparticle.

Properties	Mercury	Propane	Water	EG	Al_2O_3
ρ (kg/m^3)	13534	492,2	997,1	1132	3970
C_p (J/kgK)	139,4	2742	4180	2349	765
k (W/mK)	8,52	0,0928	0,613	0,258	40
μ kg/m.s)	0,00153	0,000097	0,000891	0,0151	--
β(1/K)	0,000181	0,00337	0,00021	0,00057	0,000024
Pr	0.0251	2.87	6.07	137.48	-

Mathematical Model

In this study,the single-phase and the k–ε standard turbulence model have been used to solve the turbulent heat transfer and flow characteristics. The executive equations can be written in the following form;

The continuity equation is;

$$\frac{\partial}{\partial x_i}(\rho u_i) = 0 \tag{1}$$

The momentum equation is;

$$\frac{\partial}{\partial x_j}(\rho u_i u_j) = -\frac{\partial p}{\partial x_i} + \frac{\partial}{\partial x_j}\left[\mu\left(\frac{\partial u_i}{\partial x_j} + \frac{\partial u_j}{\partial x_i} - \frac{2}{3}\delta_{ij}\frac{\partial u_i}{\partial x_j}\right)\right] + \frac{\partial}{\partial x_j}\left(-\rho\overline{u_i' u_j'}\right) \tag{2}$$

The energy equation is;

$$\frac{\partial}{\partial x_i}\left[u_i(\rho E+p)\right]=\frac{\partial}{\partial x_j}\left[\left(k+\frac{C_P\mu_t}{Pr_t}\right)\frac{\partial T}{\partial x_j}+u_i(\tau_{ij})_{eff}\right] \quad (3)$$

The symbols ρ, μ, u′, u_i, u_j, are fluid density,viscosity,fluctuated velocity , axial velocity and the velocity in vertical direction respectively.The term $\overline{\rho u_i' u_j'}$ is turbulent shear stress where Pr_t is the turbulent Prandtl number (0.85) ve $(\tau_{ij})_{eff}$ is the deviatoric stress tensor.

Boundary Conditions

The boundary conditions imposed at the external corrugated channel are no-slip, and with constant heat flux, whereas the flat walls are thermally insulated. The velocity boundary condition is applied at the inlet, whereas the pressure boundary condition is used at the outlet. The boundary conditions for a steady-state, 2D flow rate are as follows:

At the wall; $$u=0, v=0, q=q_{wall} \quad (4)$$

At the inlet; $$u=u_{in}, v=0, T=T_{in} \quad (5)$$

The average heat transfer coefficient along the corrugated trapezoidal channel h_c, can be calculated from the average heat transfer rate obtained from;

$$Q_{ave}=h_c A_c(\Delta T_{LMTD}) \quad (6)$$

$$\Delta T_{LMTD}=\left[\frac{(T_{s,ave}-T_{nf,ave,in})-(T_{s,ave}-T_{nf,ave,out})}{In(T_{s,ave}-T_{nf,ave,in}/T_{s,ave}-T_{nf,ave,out})}\right] \quad (7)$$

The average Nusselt number is; $$Nu_{ave}=\frac{h_c H\bar{x}}{kL_{corr}} \quad (8)$$

The inlet velocity and Reynolds number is; $$u_{in}=\frac{Re\mu}{\rho D_H}, \quad Re=\frac{\rho D_H u_{in}}{\mu} \quad (9)$$

The hydraulic diameter is; $$D_H=\frac{4A_{cross}}{P} \quad (10)$$

The Fanning friction factor is; $$C_{fx}=\frac{2\tau_s}{\rho u_{in}^2} \quad (11)$$

The Darcy friction factor is; $$f=4C_{fx} \quad (12)$$

The pressure drop is; $$\Delta p=f\frac{L\rho u_{in}^2}{2D_H} \quad (13)$$

The values used in analyzes are taken as A_c=0.278m^2, H=0.0125m, L_{corr}=0.095m, $\bar{x}$=0.05m, D_H=0.025m.

Models used for thermophysical properties of nanofluid

The proposed models for viscosity and thermal conductivity of the nanofluid are as follows. In these equations ϕ is the volumetric ratios of the solid particles, while the subindices nf, f and p represent the nanofluid, base fluid and solid nanoparticles, respectively.

The effective density is;

$$\rho_{nf} = (1-\phi)\rho_f + \phi\rho_p \quad (14)$$

The heat capacity is;

$$(\rho C_p)_{nf} = (1-\phi)(\rho C_p)_f + \phi(\rho C_p)_p \quad (15)$$

The effective thermal conductivity is;

$$\frac{k_{nf}}{k_f} = \frac{k_p + 2k_f + 2(k_p - k_f)(1+\eta)^3\phi}{k_p + 2k_f - (k_p - k_f)(1+\eta)^3} \quad (16)$$

The Yu and Choi model was used for the thermal conductivity of the nanofluid. Parameter value in the equation; the ratio of the thickness of the liquid layer to the radius is taken as η = 0.1.

The viscosity is;

$$\mu_{nf} = \frac{\mu_f}{(1-\phi)^{2.5}} \quad (17)$$

The Brinkman model was used to determine the viscosity of the nanofluid.

Numerical Solution Method

In this study, the continuity, momentum and energy equations are solved using ANSYS FLUENT CFD software, which is based on the finite volume method. The problem is considered as two-dimensional and the flow is accepted to be turbulent and the k-ε standard turbulant model is used. The finite volume method has been used to discretize the executive equations of flow, using the SIMPLEC algorithm to couple the pressure–velocity system. Second order upwind scheme and structure, uniform grid system have been employed to discretize the executive equation. The solutions are considered converged when the normalized residual values reach (10^{-5}) for all variables.

Compared with the results of the numerical and experimental study done by Abed et al. (2015). The comparison of the results of analysis of the present and reference study of Nusselt number with the different Re numbers of Al_2O_3-water nanofluid with solid volume ratio of ϕ= 0.04 is presented in Table 2. It has been found that there is a good fit between the results obtained.

Table 2. Comparison of present and literature results of average Nusselt value for different Reynolds numbers.

Re	6000	8000	12000	16000	20000
Mevcut	44.61	48.94	65.23	84.68	102.41
Abed vd. [15]	75.13	83.80	95.96	105.53	117.39

Results and Discussion

As working intervals in numerical analysis; the effects of Al_2O_3 nanoparticles with different base fluids (water, ethylene glycol, mercury and propane) and diameter d = 20 nm at different solid volume ratios (ϕ =0% - 4%) under constant heat flow (q = 6 kW / m^2).Geometric parameters of the trapezoidal channel; trapezoidal height is e = 5 mm, trapezoidal pitch is Pe = 12 mm, width of the top trapezoidal channel is w=Pe/4= 3 mm. The length of the heat source (w =L) and total width of channel was used as the non-diamensional distance D / L = 0.21 (D=20.5mm) of the heat source from the right and left adiabatic walls.

Fig.2 shows that velocity distributions on the left and isotherm contours on the right of the mercury based nanofluid at different Reynolds numbers and ϕ=0.04 volume fraction.As the number of Reynolds increases, the circulation increases and flow velocity profiles appear in the vortex appearance in the regions near the wall of the corrugated trapezoidal channel. As the Reynolds number and the solid volume ratios increase, the velocity increases. Accordingly, as the velocity increases, the circulation regions begin to grow laterally along the corrugated channel cavities, and flow structures is not disturbed by corrugated channel. In terms of isotherm countours, it increases

the flow temperature of the corrugated channel walls more because of the low velocity value due to the viscosity of the nanofluid. It is observed that the cold fluid is uniform at the lower boundary of the channel grooves in the central region. As the Reynolds number increases, thermal boundary layers develop near the walls. The nanofluid supports the mixing of the hot fluid near the thermal boundary layer and the cold fluid in the central region. The beginning and growth of the circulation flow allows mixing of the fluid in the central region with the hot fluid near the boundary layer.The flow is determined in a groove which forms a secondary circulation flow. As the Reynolds number increases, the thermal boundary layer thickness decrease. The reverse flow occurs in the groove near the upper and lower walls of the corrugated channel. As the Reynolds number increases, the velocity in the groove near the walls in the opposite direction of the main flow increases. The density of secondary flow increases for main flow and the size of the circulation region increases. Then, the circulation flow becomes even more turbulent. Temperature gradients increase with increasing Reynolds number due to the circulation flow occured near the corrugated wall.

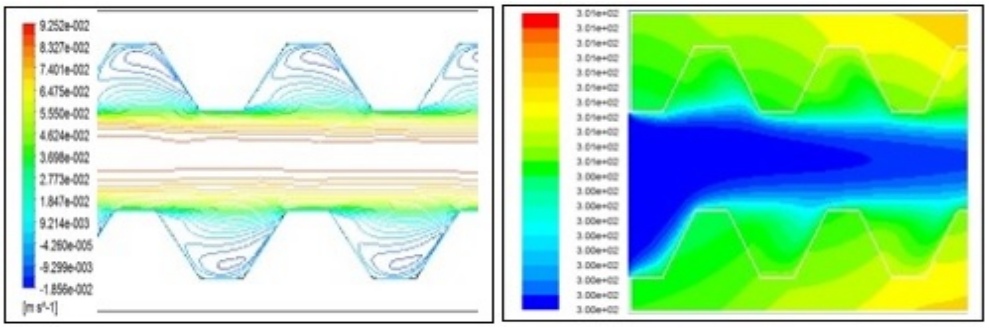

Re=6000

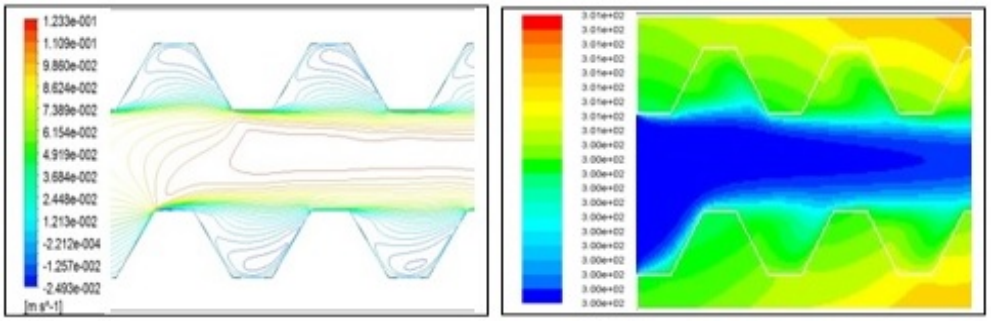

Re=8000

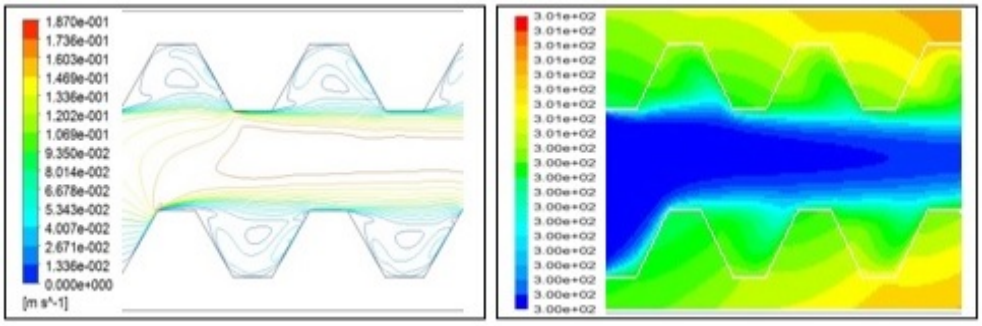

Re=12000

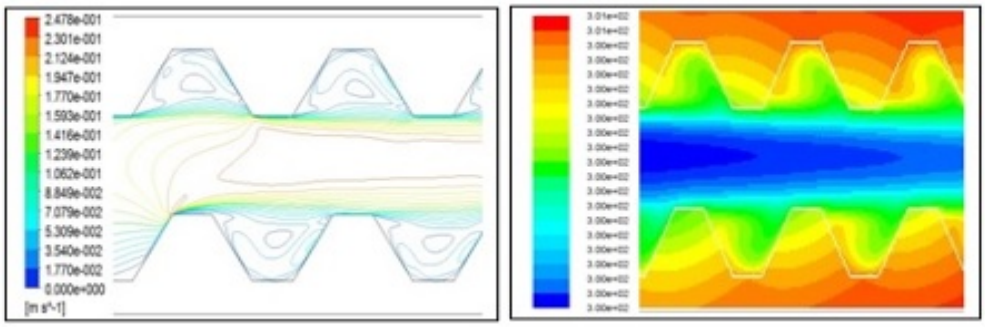

Re=16000

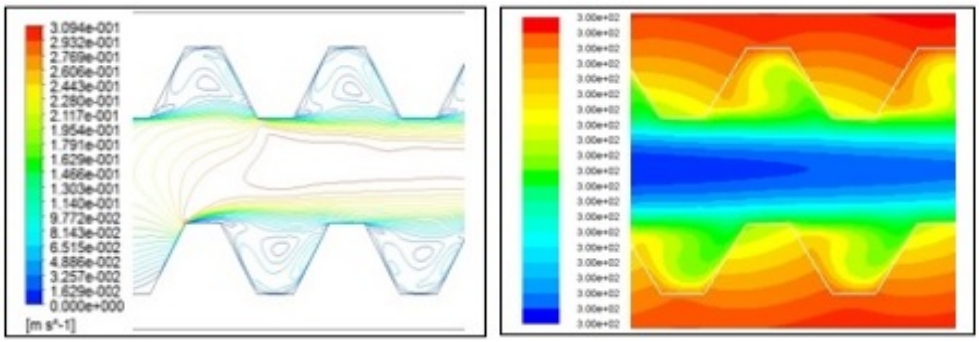

Re=20000

Fig. 2. Velocity distribution (left) and isotherms (right) contours of the mercury based nanofluid at different Reynolds numbers and volume fraction ϕ=0.04.

Fig.3 shows that velocity distribution on the left and isotherm contours on the right of the ethylene glycol based nanofluid at Re=12000 and different volume fractions. With the Brownian action, the rates of nanoparticles added to the base fluid ethylene glycol increase, increasing volume fraction. In terms of isotherm contours, the temperature gradient increases with the increase of volume fraction by the addition of nanoparticles having high thermal conductivity with respect to the base fluid. When the velocity distribution and isotherm contours are compared to ethylene glycol with a high Prandtl number and mercury with a lower Prandtl number;as the Prandtl number increases, the inlet velocities of the fluid increase, so the circulation increases and the thermal boundary layers become thinner.

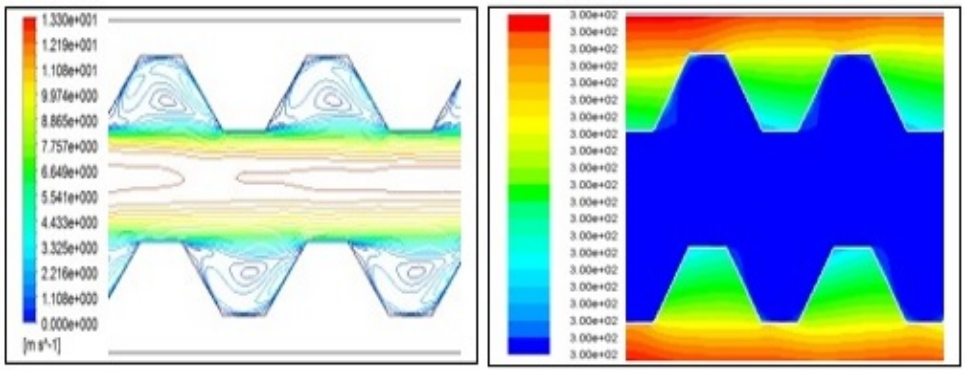

ϕ=0.00

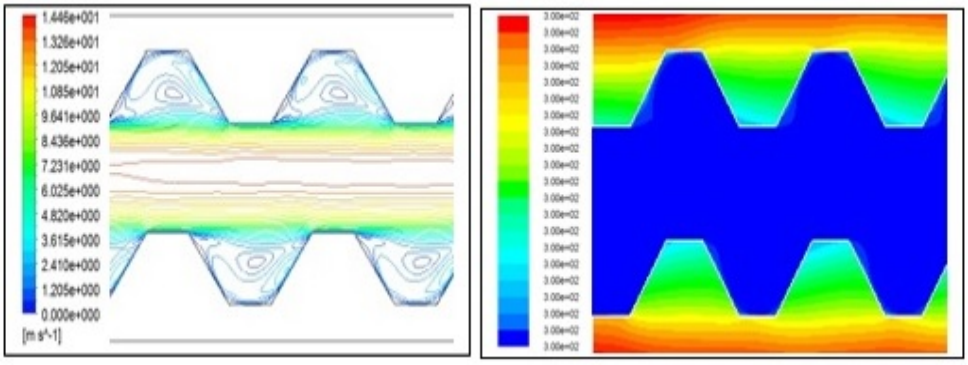

ϕ=0.01

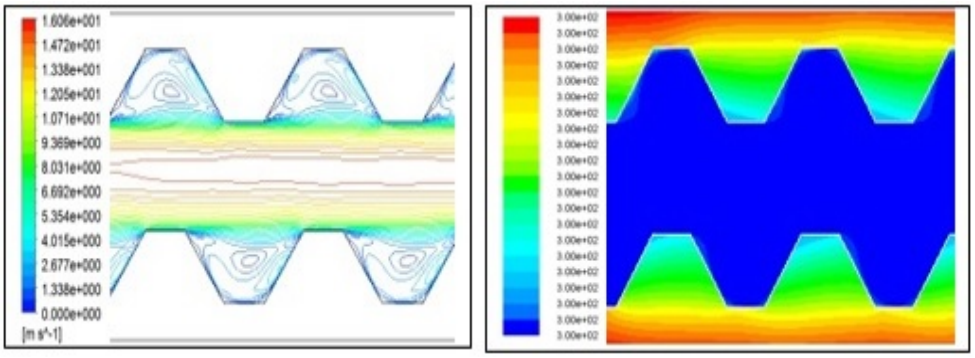

ϕ=0.02

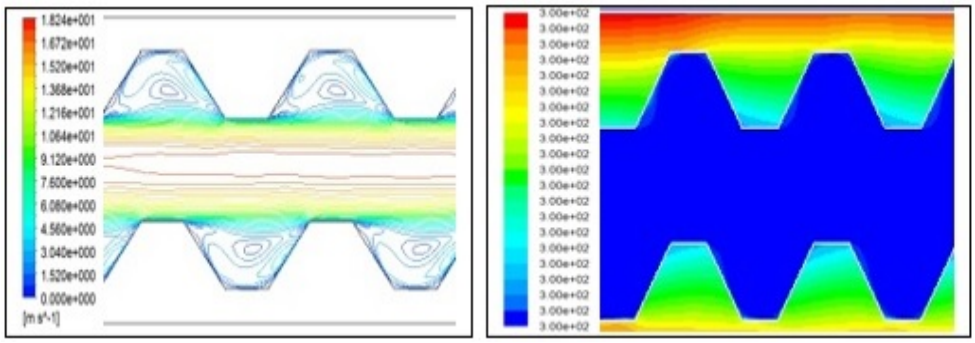

ϕ=0.03

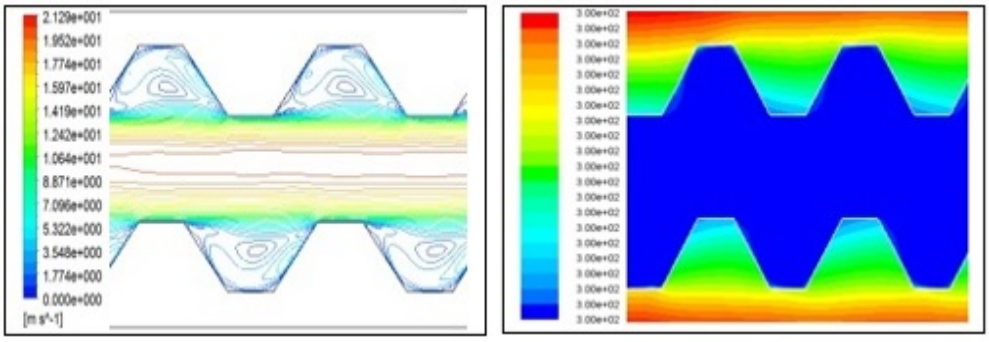

ϕ=0.04

Fig. 3. Velocity distribution (left) and isotherms (right) contours of the ethylene glycol based nanofluid at Re=12000 and different volume fractions.

Fig.4. shows that the average Nusselt number on the left and pressure drops on the right of water,ethylene glycol,mercury,propane based fluids at different Reynold numbers and volume fraction ϕ=0.04.Since the viscosity of the ethylene glycol based nanofluid is higher than water, mercury and propane based nanofluids, the velocity values and hence the temperature change are increasing. In this case, both the average Nu number and the pressure drops higher values were obtained.

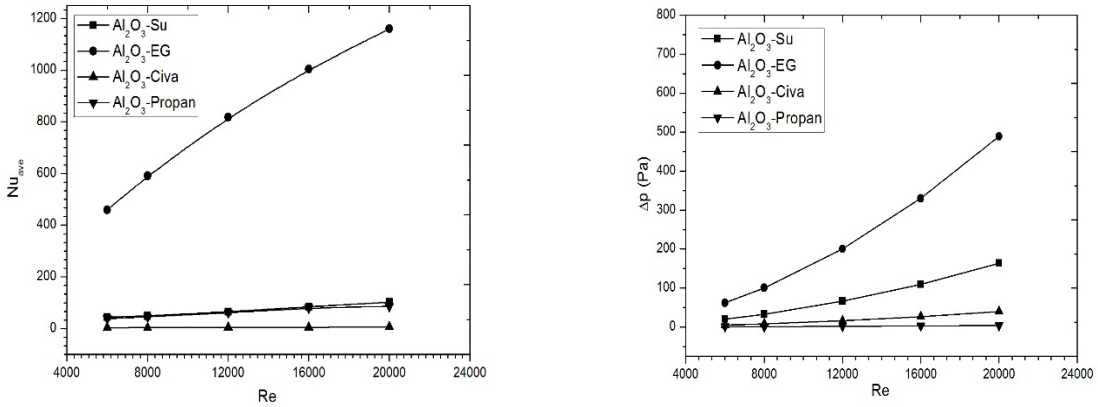

Fig. 4. Effect of various base fluids with different Reynolds numbers on the average Nusselt number (left) and the pressure drops (right) volume fraction ϕ=0.04.

Fig.5. shows that the average Nusselt number on the left and pressure drops on the right of Al_2O_3-water nanofluid at different Reynolds numbers and volume fractions. Accordingly, both the average Nusselt number and the pressure drop increase with increasing Reynolds number and volume fraction.

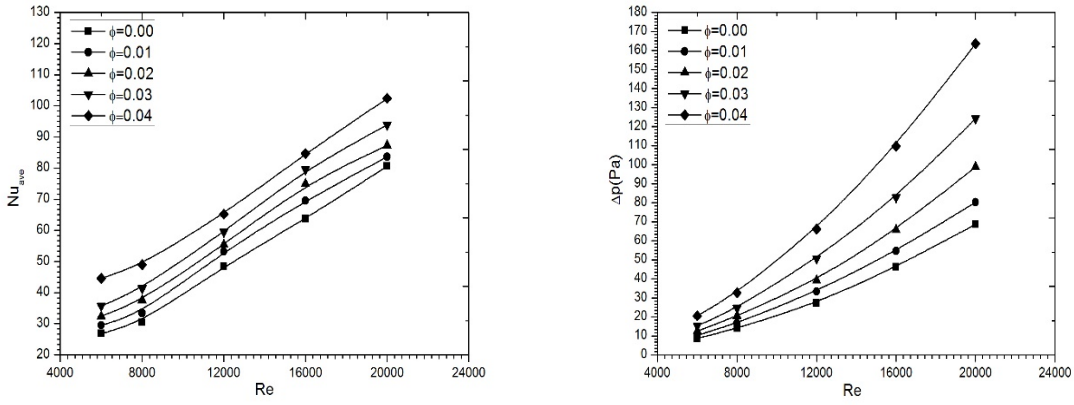

Fig. 5. Effect of Al_2O_3-water nanofluid on the average Nusselt number (left) and the pressure drops (right) at different Reynolds number and volume fractions

The average Nusselt values of the different base fluids and nanofluids with different volume fractions obtained from the studies in the numerical analyzes are presented in Table 3. Accordingly, the average Nusselt number, increases as the solid volume ratio of the nanoparticles increases. As a result of increasing Reynolds number, high velocity values are obtained and the average Nusselt values increase. The temperature difference from the analyzes affects the average h_c heat transfer coefficient along the corrugated trapezoidal channel.When different base fluid of nanofluids were compared, the highest average Nusselt value was obtained with ethylene glycol based nanofluid

and the lowest the average Nusselt value was obtained with mercury based nanofluid.The propane based nanofluid has been observed to be close to the water based nanofluid. That is, as Prandtl number increases, the average amount of heat transfer increases.

Table 3. Comparison of the average Nu numbers of different Reynolds numbers, Prandtl numbers and volume fractions

Re	ϕ	Al_2O_3-Mercury (Pr=0.0251)	Al_2O_3-Propane (Pr=2.87)	Al_2O_3-water (Pr=6.07)	Al_2O_3-EG (Pr=137.48)
6000	0.00	3.23	25.85	26.89	385.22
	0.01	3.26	27.57	29.52	393.93
	0.02	3.28	29.92	32.43	407.38
	0.03	3.33	31.32	35.71	429.72
	0.04	3.42	38.17	44.61	458.82
8000	0.00	3.37	26.68	30.45	492.76
	0.01	3.42	32.88	33.45	510.09
	0.02	3.50	36.74	37.47	527.30
	0.03	3.61	39.25	41.35	553.59
	0.04	3.77	45.71	48.95	590.86
12000	0.00	3.78	39.01	48.42	702.46
	0.01	3.90	40.03	53.18	716.15
	0.02	4.03	52.76	55.39	749.60
	0.03	4.23	54.61	59.47	771.33
	0.04	4.48	61.23	65.23	817.49
16000	0.00	4.23	50.26	63.72	873.65
	0.01	4.39	57.74	69.54	889.46
	0.02	4.59	63.12	74.96	915.14
	0.03	4.84	70.92	79.62	953.29
	0.04	5.16	79.65	84.69	1003.51
20000	0.00	4.69	69.20	80.61	1018.67
	0.01	4.87	77.57	83.64	1037.54
	0.02	5.09	78.63	87.24	1064.45
	0.03	5.40	84.95	93.88	1106.48
	0.04	5.80	86.92	102.41	1159.49

Conclusions

In this study, fully developed turbulent forced convective flow and heat transfer behavior of the nanofluid containing water, ethylene glycol, mercury and propane based Al_2O_3 nanoparticles in a two-dimensional corrugated trapezoidal plate heat exchanger have been numerically investigated.Corrugated trapezoidal channel constant heat flow boundary condition was applied. According to the results obtained; adding nanoparticles to base fluids increases heat transfer. It is also seen that the heat transfer is increased by increasing the volume fraction of the nanofluid. As the concentration of nanoparticles increases, the average Nusselt number and pressure drop increase. When the base fluids were compared, the highest average Nu and pressure drop were obtained with ethylene glycol based nanofluid and the lowest value with mercury based nanofluid.On the other hand, the increase of Prandtl number causes the heat to spread more slowly than the momentum.The heat transfer is significantly affected. Compared analyzes made with pure water as the base fluid, the increase in pressure loss in the case where volume fraction of the water-based nanofluid is 4% and the Reynolds number is 20000 is about 2.4 times as high. The average Nusselt number has improved by around 13%. It was observed that the water-based nanofluid is higher but close to the propane-based nanofluidic values. The following findings can be written:

- There is no study that has focused on convective heat transfer by nanofluid through corrugated trapezoidal channel step.
- The utilization of nanofluids in the corrugated channels has augmented the heat transfer with slight pressure drop.
- The enhancement of heat transfer potential of the base fluids in the corrugated trapzoidal channels will offer an opportunity for engineers to develop highly compact and effective heat transfer equipment for many industrial applications.
- The benefit of the utilization of nanofluids in the new channels is used in many applications including transportation, the electronic cooling systems, the chemical processes, the combustion chambers, the cooling of turbine blades, the environmental control systems and the high performance heat exchangers.
- It is necessary to study the development of correlations of friction factor and Nusselt number in the corrugated trapezoidal channels with nanofluids.

References

Abed,A.M., Alghoul,M.A., Sopian,K., Mohammed,H.A., Majdi,H. & Al-Shamani,A.N. (2015). Design characteristics of corrugated trapezoidal plate heat exchangers using nanofluids, *Chemical Engineering and Processing*,87 (pp.88–103).

Ahmed,M.A., Shuaib,N., Yusoff,M. & Al-Falahi,A. (2011). Numerical investigations of flow and heat transfer enhancement in a corrugated channel using nanofluid, *Int. Commun. Heat Mass Transfer*,38 (pp.1368–1375).

Ahmed,M.A., Yusoff,M.Z., Ng,K.C. & Shuaib,N.H. (2015). Numerical and experimental investigations on the heat transfer enhancement in corrugated channels using SiO2–water nanofluid, *Case Studies in Thermal Engineering 6* (pp.77–92).

Choi,S-S. (1995). Enhancing thermal conductivity of fluids with nanoparticles, *Develop. Appl. Non Newtonian Flows*(pp.99–106).

Esmaeili,M., Sadeghy,K. & Moghaddami,M. (2010). Heat transfer enhancement of wavy channels using Al2O3 nanoparticles. *J Enhancement Heat Transfer* ,17(2),(pp.139).

Heidary,H. & Kermani,M. (2010). Effect of nano-particles on forced convection in sinusoidal-wall channel, *Int. Commun. Heat Mass Transfer*,37 (pp.1520–1527).

Heidary,H. & Kermani,M. (2012). Heat transfer enhancement in a channel with block (s) effect and utilizing nano-fluid, *Int. J. Therm. Sci.*,57 (pp.163–171).

Islamoğlu,Y., & Parmaksızoğlu,C. (2003). The effect of channel height on the enhanced heat transfer characteristics in a corrugated heat exchanger channel, *Appl. Therm. Eng*.,23 (pp.979-987).

Keblinski, P., Phillpot, S.R., Choi,S-S., & Eastman, J.A. (2002). Mechanisms of Heat Flow in Suspensions of Nano- sized Particles (nanofluids), *Int. J. Heat Mass Transfer,*45 (pp.855–863).

Kwon,H.G., Hwang,S.D., Cho,H.H. (2008). Flow and heat/mass transfer in a wavy duct with various corrugation angles in two dimensional flow regimes, *Heat Mass Transfer*,45 (pp.157–165).

Lee,S., Choi,S-S., Li,S., & Eastman,J.A. (1999). Measuring thermal conductivity of fluids containing oxide nanoparticles, *ASME J. Heat Transfer*,121 (pp.280-289).

Mohammed,H., Abed,A.M., & Wahid,M. (2013). The effects of geometrical parameters of a corrugated channel with in out-of-phase arrangement, *Int. Commun. Heat Mass Transfer*,40 (pp.47-57).

Navaei,A.S., Mohammed,H.A., Munisamy,K.M., Yarmand,H. & Gharehkhani,S. (2015). Heat transfer enchancement of turbulent nanofluid flow over various types of internally corrugated channels, *Power Tecnology* (pp.332–341).

Naphon,P. (2007). Laminar convective heat transfer and pressure drop in the corrugated channels, *Int. Commun. Heat Mass Transfer*,34 (pp.62–71).

Naphon,P. (2009). Effect of wavy plate geometry configurations on the temperature and flow distributions, *Int. Commun. Heat Mass Transfer,*36 (pp.942–946).

Ozbolat ,V. & Sahin,B. (2013). Numerical investigations of heat transfer enhancement of water-based Al2O3 nanofluids in a sinusoidal-wall channel. *ASME International Mechanical Engineering Congress and Exposition*. *American Society of Mechanical Engineers*,(V08AT09A051-V08AT09A051).

Pantzali,M., Mouza,A. & Paras,S. (2009). Investigating the efficacy of nanofluids as coolants in plate heat exchangers (PHE), *Chem. Eng. Sci.*,64 (pp.3290–3300).

Rostami,J. (2007) Convective heat transfer in a wavy channel utilizing nanofluids. *J Enhancement Heat Transfer* (pp.14-52).

Tanda,G. (2007). Heat transfer in rectangular channels with transverse and V-shaped broken ribs, Int. J. Heat Mass Transfer,47 (pp.229–243).

Tiwari,A.K., Ghosh,P., Sarkar,J., Dahiya,H. & Parekh,J. (2014). Numerical investigation of heat transfer and fluid flow in plate heat exchanger using nanofluids, *Int. J. Therm. Sci.*,85 (pp.93–103).

EVALUATION OF OCCUPATIONAL SAFETY AND HEALTH IN THE GLOBAL FISHING SECTOR

Veysel TATAR

Artvin Coruh University, Department of Maritime and Port Management, Artvin-Turkey

vtatar@artvin.edu.tr

Abstract: Commercial fishing is one of the most hazardous occupations causing over 24,000 fatalities each year, the large majority of which occur aboard small fishing vessels. The International Maritime Organization (IMO), which is the United Nations body that has the primary responsibility for maritime safety and the protection of the marine environment, has taken on the responsibility of redressing the situation. Occupational Health and Safety (OHS) can simply be defined as providing secure working conditions for the employees. Employee safety issues are becoming more and more important every day, not only in working environments but also in every activity within the societies. Safety can be considered at both individual and institutional levels. The fishing industry (or fishing sector) is extraordinarily diverse. At one extreme are large, multinational joint ventures, utilizing large factory trawlers and numerous other vessels, employing thousands of workers on several oceans. At the other are small, wooden canoes and other boats used by individual fishermen' to catch sufficient food for their families and perhaps more to sell in their local communities. Most fishing operations fall somewhere between these extremes. The technology used can be simple and traditional, or it may be highly sophisticated, incorporating the most advanced electronic and other equipment. This paper analyses the role of OHS, occupational accidents, occupational diseases, risks and legislation are mentioned in the fishing industry.

Keywords: Fishing, Occupational Health and Safety, Maritime Legislation

Introduction

Occupational Safety and Health (OSH) is a discipline dealing with the prevention of work related injuries and diseases as well as the protection and promotion of the health of workers. It aims at the improvement of working conditions and environment. Occupational safety and health (OSH) is generally defined as the science of the anticipation, recognition, evaluation and control of hazards arising in or from the workplace that could impair the health and well-being of workers, taking into ac-count the possible impact on the surrounding communities and the general environment (Alli, 2008). According to ILO, every year, 2.2 million employees all around the world die beca-use of accidents and diseases related with work. 270 million employees have accidents, 160 million employees suffer from diseases related with work. Occupational health and safety imposes on enterprises an expected penalty that is positively related to the presence of unsafe working conditions for firms not in compliance with the standards (Viscusi, 1986). Hazard control and prevention strategies to as-sure every working man and woman safe, healthful workplace conditions regard training as anaxiomatic part of all such efforts (Cohen and Colligan, 1998). Some of the common features of these industries are improper workplace design, ill structured jobs, mismatch between worker abilities and job demands, adverse environment, poor human-machine system design and inappropriate management programs (Shikdar and Sawaqed, 2003). Occupational safety and health is an extensive multidisciplinary activities such as ergonomics, physics and chemistry (Holmes et al. 1999). The main elements of the OSH management system for the workplace,), are shown in figure 1. Occupational Health and Safety is based on:

> Hazard identification – The process of recognizing that a hazard exists (source or situation with the potential to cause harm in terms of human injury or ill-health)

> Risk assessment – The process of evaluating the risk arising from the hazard (combi-nation of the likelihood of a hazardous event or exposure and the severity of injury or ill health that can be caused by the event of exposure)

> Determination of applicable controls – Measures relevant to eliminate or reduce risk to an acceptable level.

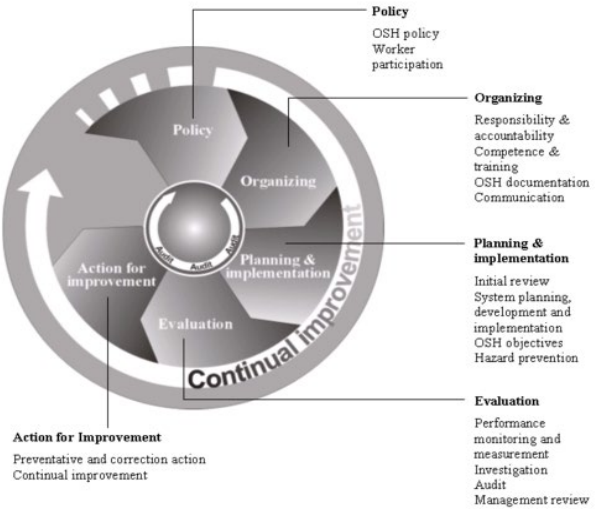

Figure 1. Main elements of the OSH management system (ILO, 2001)

The fishing industry (or fishing sector) is extraordinarily diverse. At one extreme are large, multinational joint ventures, utilizing large factory trawlers and numerous other vessels, employing thousands of workers on several oceans. At the other are small, wooden canoes and other boats used by individual fishermen' to catch sufficient food for their families and perhaps more to sell in their local communities. Most fishing operations fall somewhere between these extremes. The technology used can be simple and traditional, or it may be highly sophisticated, incorporating the most advanced electronic and other equipment. The International Maritime Organization has the primary responsibility for maritime safety and marine pollution prevention. The safety of fishing vessels had been a matter of concern to IMO since the Organization came into existence, but the great differences in design and operation between fishing vessels and other types of ships had always proved a major obstacle to their inclusion in the Conventions on Safety of Life at Sea (SOLAS) and Load Lines: while other vessels load cargo in port, fishing vessels must sail empty and load their cargo at sea. FAO and IMO have estimated that commercial fishing is one of the most hazardous occupations in the world with more than 24,000 fatalities per year, the large majority of which occur aboard small fishing vessels. Available statistics for countries with significant commercial fisheries indicate that fishing occupational fatalities and injuries occur at rates much higher than national averages for occupational fatalities and injuries, regardless of the level of industrialization (FAO, 2001). These high rates of fatalities and injuries can be partially attributed to the inherently dangerous working conditions involved in the industry. These include: an unpredictable and often hostile marine environment; unstable work platforms; resources that are mobile, variable, diverse, often dangerous (bites, poison, allergies) and often located in remote offshore areas; moveable and often heavy equipment, and a dependence on vessels for shelter and survival. Furthermore, shift work and the intense and prolonged working activity typically associated with fishing can cause fatigue, a common factor in many fishingrelated incidents (ILO, 1999).

The potential importance of interactivity among factors has been used to argue for social-ecological approaches to understanding health in fisheries (Dolan et al. 2005). The latest publication, jointly developed by the three organizations, is the FAO/ILO/IMO Safety Recommendations for Decked Fishing Vessels of Less than 12 metres in Length and Undecked Fishing Vessels which was recently published. This international instrument applies to more than 90% of the world fishing fleet and is therefore an important step in improving the safety of small fishing vessels and the crews serving on board those vessels. Among men, most exposure was reported in the sectors Mining and quarrying, Fishing, and Construction. Among women, most exposure was experienced in the sectors Agriculture, and Health and social work (Graph 1).

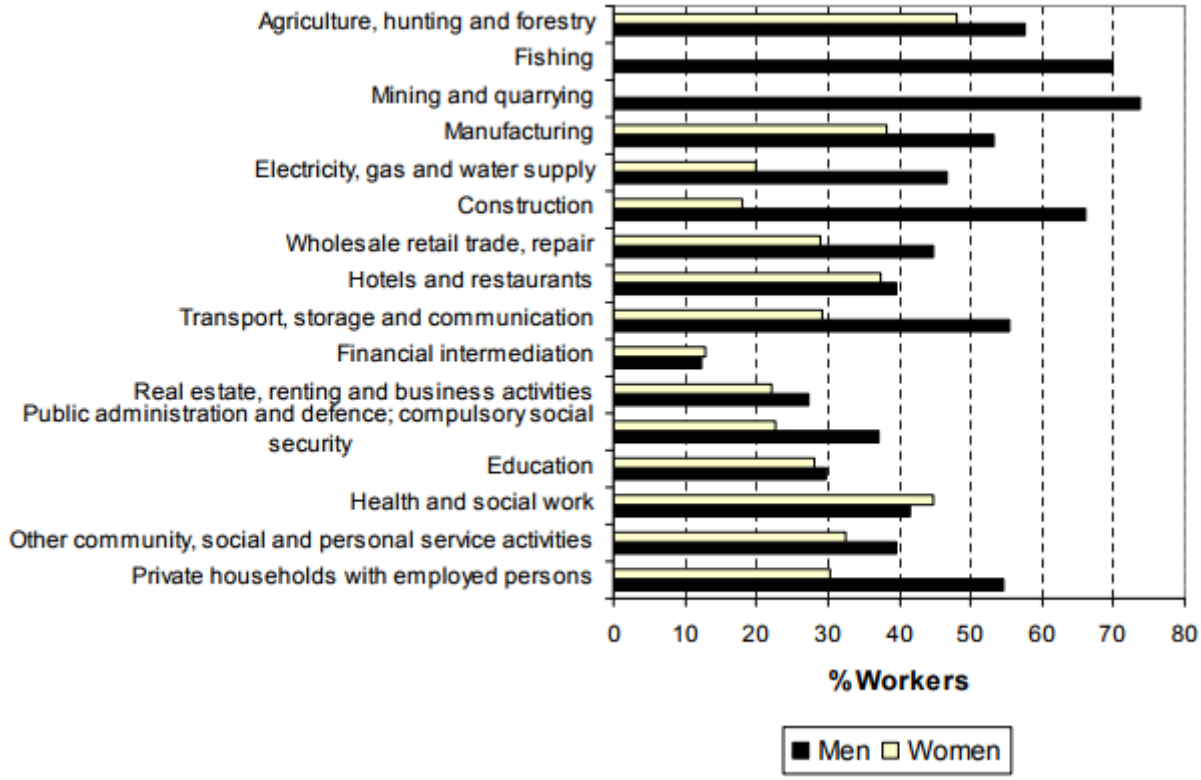

Graph 1. Workers exposed to one or more factors adversely affecting physical health in different sectors (Eurostat (Statistics in focus Contact: 63/2009)

Analysis Of The Global Fishing Industry

Global fish production1 peaked at about 171 million tonnes in 2016, with aquaculture representing 47 percent of the total and 53 percent if non-food uses (including reduction to fishmeal and fish oil) are excluded. The total first sale value of fisheries and aquaculture production in 2016 was estimated at USD 362 billion, of which USD 232 billion was from aquaculture production. With capture fishery production relatively static since the late 1980s, aquaculture has been responsible for the continuing impressive growth in the supply of fish for human consumption (Figure 2). Between 1961 and 2016, the average annual increase in global food fish consumption2 (3.2 percent) outpaced population growth (1.6 percent) (Figure 3) and exceeded that of meat from all terrestrial animals combined (2.8 percent). In per capita terms, food fish consumption grew from 9.0 kg in 1961 to 20.2 kg in 2015, at an average rate of about 1.5 percent per year. Preliminary estimates for 2016 and 2017 point to further growth to about 20.3 and 20.5 kg, respectively. The expansion in consumption has been driven not only by increased production, but also by other factors, including reduced wastage. In 2015, fish accounted for about 17 percent of animal protein consumed by the global population. Moreover, fish provided about 3.2 billion people with almost 20 percent of their average per capita intake of animal protein. Despite their relatively low levels of fish consumption, people in developing countries have a higher share of fish protein in their diets than those in developed countries. The highest per capita fish consumption, over 50 kg, is found in several small island developing States (SIDS), particularly in Oceania, while the lowest levels, just above 2 kg, are in Central Asia and some landlocked countries. Global capture fisheries production was 90.9 million tonnes in 2016, a small decrease in comparison to the two previous years (Table 1). Fisheries in marine and inland waters provided 87.2 and 12.8 percent of the global total, respectively (FAO, 2018).

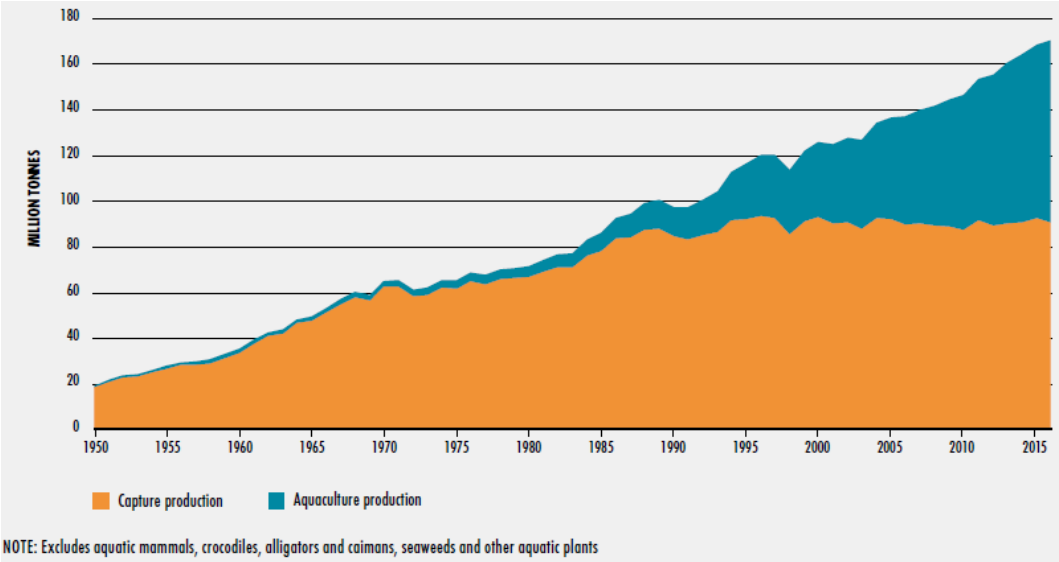

Figure 2. World capture fisheries and aquaculture production (FAO, 2018)

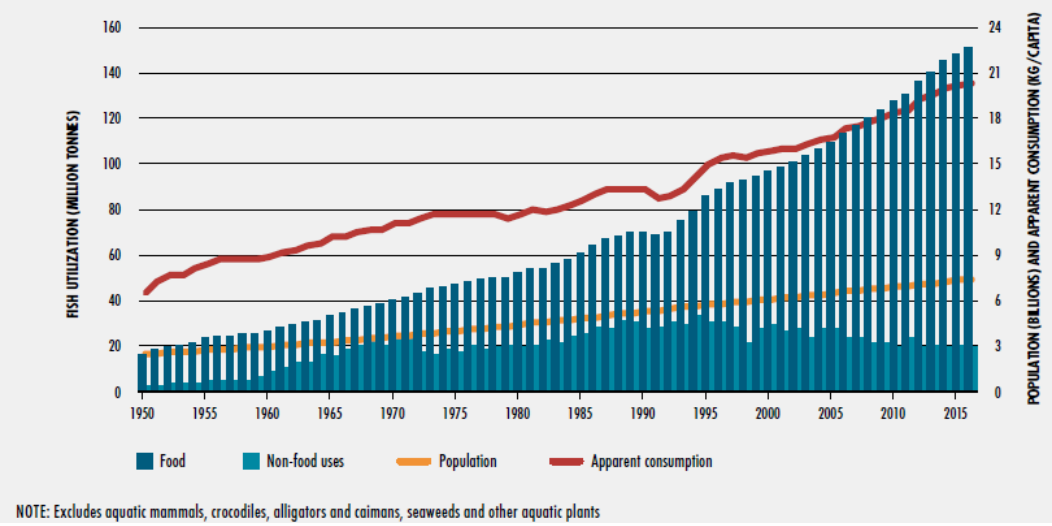

Figure 3. World fish utilization and apparent consumption (FAO, 2018)

Table 1. World fisheries and aquaculture production and utilization (million tonnes)[a] (FAO, 2018)

Category	2011	2012	2013	2014	2015	2016
Production						
Capture						
Inland	10.7	11.2	11.2	11.3	11.4	11.6
Marine	81.5	78.4	79.4	79.9	81.2	79.3
Total capture	**92.2**	**89.5**	**90.6**	**91.2**	**92.7**	**90.9**
Aquaculture						
Inland	38.6	42.0	44.8	46.9	48.6	51.4
Marine	23.2	24.4	25.4	26.8	27.5	28.7
Total aquaculture	**61.8**	**66.4**	**70.2**	**73.7**	**76.1**	**80.0**
Total world fisheries and aquaculture	**154.0**	**156.0**	**160.7**	**164.9**	**168.7**	**170.9**
Utilization[b]						
Human consumption	130.0	136.4	140.1	144.8	148.4	151.2
Non-food uses	24.0	19.6	20.6	20.0	20.3	19.7
Population (*billions*)[c]	7.0	7.1	7.2	7.3	7.3	7.4
Per capita apparent consumption (*kg*)	18.5	19.2	19.5	19.9	20.2	20.3

[a] Excludes aquatic mammals, crocodiles, alligators and caimans, seaweeds and other aquatic plants.
[b] Utilization data for 2014–2016 are provisional estimates.
[c] Source of population figures: UN, 2015e.

World total marine catch was 81.2 million tonnes in 2015 and 79.3 million tonnes in 2016, representing a decrease of almost 2 million tonnes. Catches of anchoveta (Engraulis ringens) by Peru and Chile, which are often substantial yet highly variable because of the inf luence of El Niño, accounted for 1.1 million tonnes of this decrease, with other major countries and species, particularly cephalopods, also showing reduced catches between 2015 and 2016 (Tables 2 and 3). Decreasing catches affected 64 percent of the 25 top producer countries, but only 37 percent of the remaining 170 countries.

Table 2. Marine capture production: major producer countries (FAO, 2018)

Country	Production (tonnes)			% Variation		Variation, 2015 to 2016 (tonnes)
	Average 2005–2014	2015	2016	2005–2014 (average) to 2016	2015 to 2016	
China	13 189 273	15 314 000	15 246 234	15.6	–0.4	–67 766
Indonesia	5 074 932	6 216 777	6 109 783	20.4	–1.7	–106 994
United States of America	4 757 179	5 019 399	4 897 322	2.9	–2.4	–122 077
Russian Federation	3 601 031	4 172 073	4 466 503	24.0	7.1	294 430
Peru Total	6 438 839	4 786 551	3 774 887	–41.4	–21.1	–1 011 664
Excluding anchoveta	989 918	1 016 631	919 847	–7.1	–9.5	–96 784
India	3 218 050	3 497 284	3 599 693	11.9	2.9	102 409
Japan[a]	3 992 458	3 423 099	3 167 610	–20.7	–7.5	–255 489
Viet Nam	2 081 551	2 607 214	2 678 406	28.7	2.7	71 192
Norway	2 348 154	2 293 462	2 033 560	–13.4	–11.3	–259 902
Philippines	2 155 951	1 948 101	1 865 213	–13.5	–4.3	–82 888
Malaysia	1 387 577	1 486 050	1 574 443	13.5	5.9	88 393
Chile Total	3 157 946	1 786 249	1 499 531	–52.5	–16.1	–286 718
Excluding anchoveta	2 109 785	1 246 154	1 162 095	–44.9	–6.7	–84 059
Morocco	1 074 063	1 349 937	1 431 518	33.3	6.0	81 581
Republic of Korea	1 746 579	1 640 669	1 377 343	–21.1	–16.0	–263 326
Thailand	1 830 315	1 317 217	1 343 283	–26.6	2.0	26 066
Mexico	1 401 294	1 315 851	1 311 089	–6.4	–0.4	–4 762
Myanmar[a]	1 159 708	1 107 020	1 185 610	2.2	7.1	78 590
Iceland	1 281 597	1 318 916	1 067 015	–16.7	–19.1	–251 901
Spain	939 384	967 240	905 638	–3.6	–6.4	–61 602
Canada	914 371	823 155	831 614	–9.1	1.0	8 459
Taiwan, Province of China	960 193	989 311	750 021	–21.9	–24.2	–239 290
Argentina	879 839	795 415	736 337	–16.3	–7.4	–59 078
Ecuador	493 858	643 176	715 357	44.9	11.2	72 181
United Kingdom	631 398	65 451 506	701 749	11.1	–0.4	–2 753
Denmark	735 966	868 892	670 207	–8.9	–22.9	–198 685
Total 25 major countries	**65 451 506**	**66 391 560**	**63 939 966**	**–2.3**	**–3.7**	**–2 451 594**
Total other 170 countries	**14 326 675**	**14 856 282**	**15 336 882**	**7.1**	**3.2**	**480 600**
World total	**79 778 181**	**81 247 842**	**79 276 848**	**–0.6**	**–2.4**	**–1 970 994**

Table 3. Marine capture production: major species and genera (FAO, 2018)

Scientific name	FAO English name	Production (tonnes)			% Variation		Variation, 2015 to 2016 (tonnes)
		Average 2005–2014	2015	2016	2005–2014 (average) to 2016	2015 to 2016	
Theragra chalcogramma	Alaska pollock (=walleye pollock)	2 952 134	3 372 752	3 476 149	17.8	3.1%	103 397
Engraulis ringens	Anchoveta (=Peruvian anchovy)	6 522 544	4 310 015	3 192 476	–51.1	–25.9%	–1 117 539
Katsuwonus pelamis	Skipjack tuna	2 638 124	2 809 954	2 829 929	7.3	0.7%	19 975
Sardinella spp.[a]	Sardinellas nei	2 281 285	2 238 903	2 289 830	0.4	2.3%	50 927
Trachurus spp.[a]	Jack and horse mackerels nei	2 463 428	1 738 352	1 743 917	–29.2	0.3%	5 565
Clupea harengus	Atlantic herring	2 111 101	1 512 174	1 639 760	–22.3	8.4%	127 586
Scomber japonicus	Pacific chub mackerel	1 454 794	1 484 780	1 598 950	9.9	7.7%	114 170
Thunnus albacares	Yellowfin tuna	1 219 326	1 356 883	1 462 540	19.9	7.8%	105 657
Gadus morhua	Atlantic cod	995 853	1 303 726	1 329 450	33.5	2.0%	25 724
Engraulis japonicus	Japanese anchovy	1 323 022	1 336 218	1 304 484	–1.4	–2.4%	–31 734
Decapterus spp.[a]	Scads nei	1 394 772	1 186 555	1 298 914	–6.9	9.5%	112 359
Sardina pilchardus	European pilchard (=sardine)	1 098 400	1 174 611	1 281 391	16.7	9.1%	106 780
Trichiurus lepturus	Largehead hairtail	1 315 337	1 269 525	1 280 214	–2.7	0.8%	10 689
Micromesistius poutassou	Blue whiting (=poutassou)	1 054 918	1 414 131	1 190 282	12.8	–15.8%	–223 849
Scomber scombrus	Atlantic mackerel	822 081	1 247 666	1 138 053	38.4	–8.8%	–109 613
Scomberomorus spp.[a]	Seerfishes nei	889 840	903 632	918 967	3.3	1.7%	15 335
Dosidicus gigas	Jumbo flying squid	855 602	1 003 774	747 010	–12.7	–25.6%	–256 764
Nemipterus spp.[a]	Threadfin breams nei	541 470	629 062	683 213	26.2	8.6%	54 151
Brevoortia patronus	Gulf menhaden	464 165	536 129	618 719	33.3	15.4%	82 590
Sprattus sprattus	European sprat	567 697	677 048	584 577	3.0	–13.7%	–92 471
Portunus trituberculatus	Gazami crab	414 034	560 831	557 728	34.7	–0.6%	–3 103
Acetes japonicus	Akiami paste shrimp	582 763	543 992	531 847	–8.7	–2.2%	–12 145
Sardinops melanostictus	Japanese pilchard	257 346	489 294	531 466	106.5	8.6%	42 172
Scomber colias	Atlantic chub mackerel	314 380	467 796	511 618	62.7	9.4%	43 822
Rastrelliger kanagurta	Indian mackerel	324 049	498 149	499 474	54.1	0.3%	1 325
Total 25 major species and genera		**34 858 465**	**34 065 952**	**33 240 958**	**–4.6%**	**–2.4**	**–824 994**
Total other 1 566 species items		**44 919 716**	**47 181 890**	**46 035 890**	**2.5%**	**–2.4**	**–1 146 000**
World total		**79 778 181**	**81 247 842**	**79 276 848**	**–0.6%**	**–2.4**	**–1 970 994**

Table 4 shows the top exporters and importers. China is the main fish producer and since 2002 has also been the largest exporter of fish and fish products, although they represent only 1 percent of its total merchandise trade. After exceptionally rapid gains through the 1990s and 2000s, the average annual increase in the value of Chinese exports of fish and fish products dropped from 14 percent in 2000–2008 to 9.1 percent in 2009–2017. In 2017, Chinese exports of fish and fish products reached USD 20.5 billion, with an increase of 2 percent relative to 2016 and of 4 percent relative to 2015.

Table 4. Top ten exporters and importers of fish and fish products (FAO, 2018)

Country	2006		2016		APR* (%)
	Value (million USD)	Share (%)	Value (million USD)	Share (%)	
Exporters					
China	8 968	10.4	20 131	14.1	8.4
Norway	5 503	6.4	10 770	7.6	6.9
Viet Nam	3 372	3.9	7 320	5.1	8.1
Thailand	5 267	6.1	5 893	4.1	1.1
United States of America	4 143	4.8	5 812	4.1	3.4
India	1 763	2.0	5 546	3.9	12.1
Chile	3 557	4.1	5 143	3.6	3.8
Canada	3 660	4.2	5 004	3.5	3.2
Denmark	3 987	4.6	4 696	3.3	1.7
Sweden	1 551	1.8	4 418	3.1	11.0
Top ten subtotal	**41 771**	**48.4**	**74 734**	**52.4**	**6.0**
Rest of world total	**44 523**	**51.6**	**67 796**	**47.6**	**4.3**
World total	**86 293**	**100.0**	**142 530**	**100.0**	**5.1**
Importers					
United States of America	14 058	15.5	20 547	15.1	3.9
Japan	13 971	15.4	13 878	10.2	-0.1
China	4 126	4.5	8 783	6.5	7.9
Spain	6 359	7.0	7 108	5.2	1.1
France	5 069	5.6	6 177	4.6	2.0
Germany	4 717	5.2	6 153	4.5	2.7
Italy	3 739	4.1	5 601	4.1	4.1
Sweden	2 028	2.2	5 187	3.8	9.8
Republic of Korea	2 753	3.0	4 604	3.4	5.3
United Kingdom	3 714	4.1	4 210	3.1	1.3
Top ten subtotal	**60 533**	**66.6**	**82 250**	**60.7**	**3.1**
Rest of world total	**30 338**	**33.4**	**52 787**	**39.3**	**5.7**
World total	**90 871**	**100.0**	**135 037**	**100.0**	**4.0**

* APR: average annual percentage growth rate for 2006–2016.

The total number of fishing vessels in the world in 2016 was estimated to be about 4.6 million, unchanged from 2014. The fleet in Asia was the largest, consisting of 3.5 million vessels, accounting for 75 percent of the global fleet. In Africa and North America the estimated number of vessels declined from 2014 by just over 30 000 and by nearly 5 000, respectively. For Asia, Latin America and the Caribbean and Oceania the numbers all increased, largely as a result of improvements in estimation procedures. Globally, the number of engine-powered vessels was estimated to be 2.8 million in 2016, remaining steady from 2014. Motorized vessels represented 61 percent of all fishing vessels in 2016, down from 64 percent in 2014, as the number of nonmotorized vessels increased, probably because of improved estimations. Generally, motorized vessels make up a much higher proportion in marineoperating vessels than in the inland water f leet. However, data reporting was not of sufficient qualit y to disaggregate marine and inland water f leets. The proportion of motorized and non-motorized vessels by region. The motorized fleet is distributed unevenly around the world with Asia having nearly 80 percent of the reported motorized fleet in 2016 (2.2 million vessels), followed by Africa with about 153 000 powered vessels. In Europe, the fleet capacity has continued to decline steadily since 2000 as a result of management measures to reduce the fleet capacity. This region has the highest percentage of motorized vessels in the overall fleet.

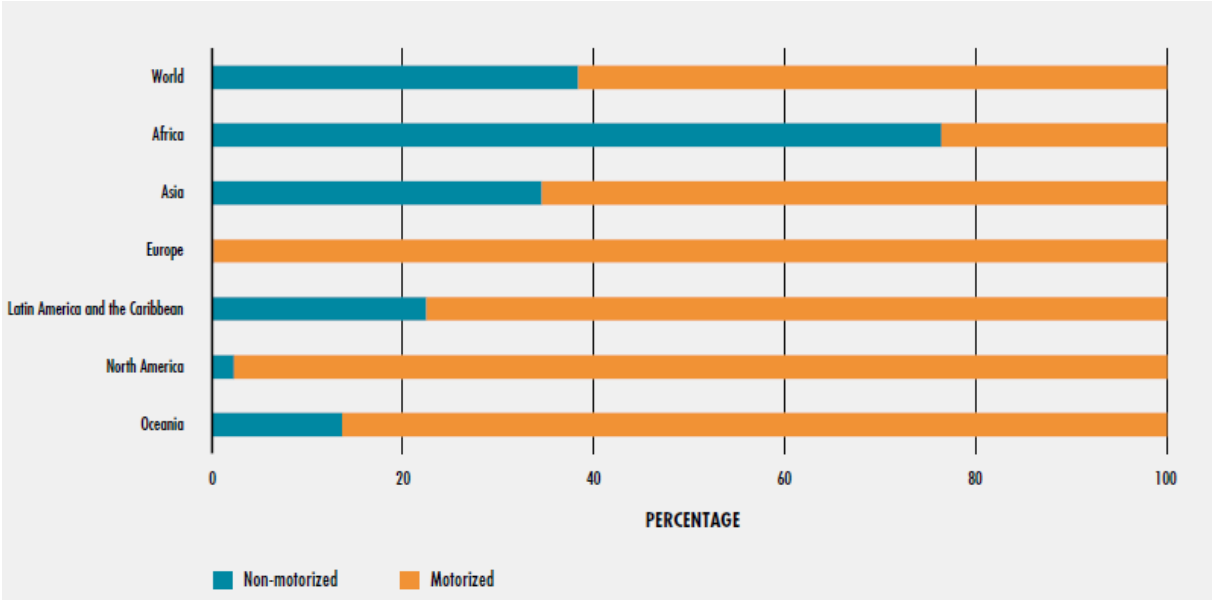

Figure 4. Distribution of motorized and non-motorized fishing vessels by region, 2016 (thousands) (FAO, 2018)

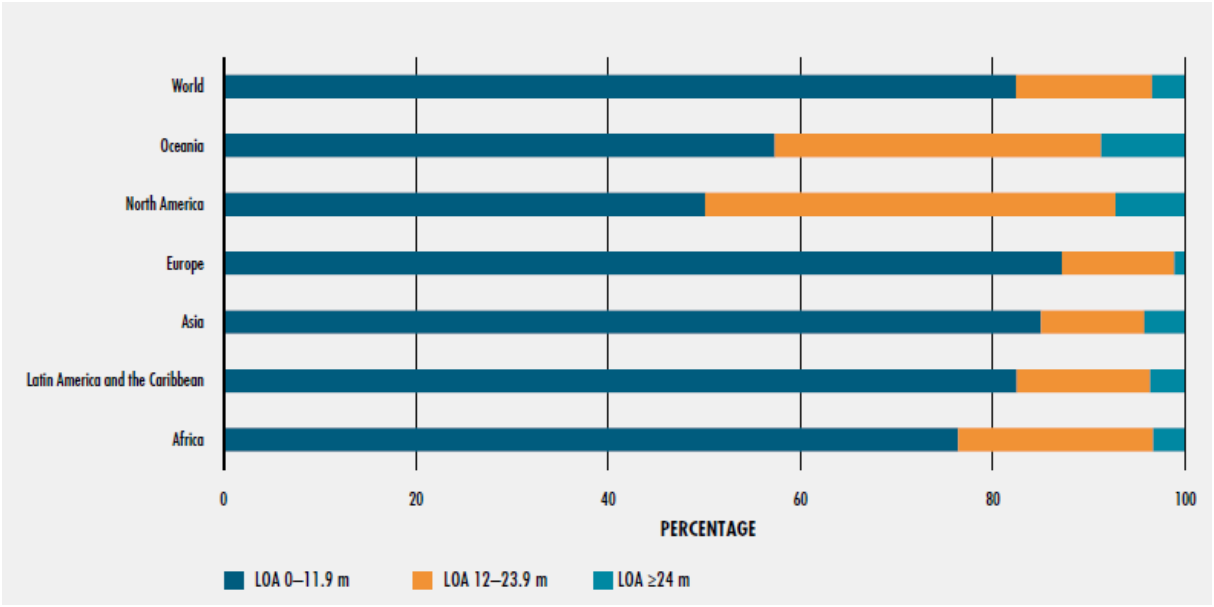

Figure 5. Size distribution of motorized fishing vessels by region, 2016 (FAO, 2018)

Safety And Health In The Fishing Industry

Internationally the sea fishing sector is recognised worldwide as the most hazardous industry to work in, accounting for significantly higher rates of fatal and/or serious accidents when compared to other sectors such as agriculture or construction (ILO, 1999). Sadly, each year within the industry the same accidents tend to reoccur often arising from fatigue, poor decision making, taking chances or not following basic precautions such as heeding weather forecasts, wearing Personal Flotation Devices or guarding and maintaining machinery. It is difficult to measure the degree of suffering and hardship that the victims of accidents and their families endure. Within fishing, hazards can be broadly classified into four categories.

1. Biological hazards, for example, risk of infection from handling dead fish or slime on live fish or an injury from fish bones, scales or fish hooks becoming infected.
2. Chemical hazards, for example exposure to poorly vented engine exhaust gases.
3. Physical hazards, for example, exposure to unguarded machinery.
4. Health (including psychosocial) hazards, for example, work related stress.

Fishing is a hazardous occupation when compared to other occupations. Sustained efforts are needed at all levels and by all parties to improve the safety and health of fishermen. The issue of safety and health must be considered

broadly in order to identify and mitigate – if not eliminate – the underlying causes of accidents and diseases in this sector. Consideration also needs to be given to the great diversity within the industry based on the size of the vessel, type of fishing and gear, area of operation, etc.

1.The areas of priority for improving occupational safety and health in the fishing industry are:

Implementing and improving safety and health training;

Enhancing social dialogue at all levels in the sector;

Extending social protection to cover fishermen where it does not exist;

Collecting and disseminating statistics, data and safety information;

Promoting appropriate international standards;

Providing international guidance for the safety and health of fishermen, particularly on vessels under 24 m in length;

2. International standards concerning the safety of fishing vessels should be ratified and fully implemented, in particular, the STCW-F Convention.

3. Safety and health improvements cannot be achieved solely through legislation. A safety culture should be promoted in the fishing industry, including the use of safety management systems appropriate to the enterprise and the dissemination of safety information. Governments, employers and workers' organizations should be involved in the development and implementation of such systems.

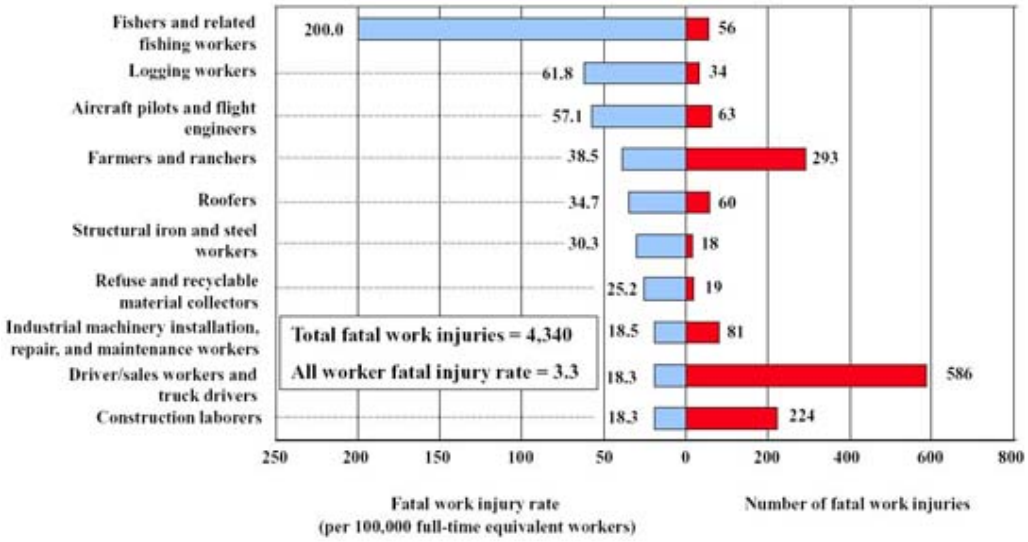

Graph 2. Fatal work injury rate U.S. 2009 (per 100.000 full time equivalent workers)(U.S. Bureau of Labor Statistics, U.S. Department of Labor, 2010)

Cuts, scratches, injuries, lashes and bruises are generally not even considered as accidents, but simply as part of the job. The risk of being involved in a non-fatal accident is 2.4 times greater in the fishing activity when compared with other industrial sectors. The scale of employment in the sector alone does not explain these results. According to research, almost 70% of the accidents happen at sea. In a 2009 survey, 69% of persons working in the sector reported that their most recent accident at work or in the course of the work resulted in sick leave in the past 12 months. Because of the seriousness of the accidents occurring in the sector, workers are normally absent longer than in other sectors. Out of 4,453 total non-fatal accidents in the sector, a large proportion led to 7 and more days of absence in 2012, whereas the proportion of accidents leading to less than 6 days of absence was relatively small. This leads to increased social security costs and reduced output for the employer.

Annually, around 13,000 workers in the Agriculture, forestry and fishing sector in Great Britain were suffering from an illness they believe was caused or made worse by their work. Around a third of these cases were new conditions which started during the year, while the remainder were long-standing conditions. Musculoskeletal disorders was the most common work-related ill-health condition in workers in the sector. Annually around 16,000 'Skilled agricultural and related trade' workers in Great Britain were suffering from an illness they believe was caused or made worse by their work (many of these employed in the agriculture, forestry and fishing sector but also in other sectors especially 'Landscape service activities) (Graph 3) (HSE, 2015).

Graph 3. Estimated annual number of cases of selfreported work-related illness in the agriculture, forestry and fishing sector (HSE, 2015)

An analysis of 24 Irish fatal fishing incidents which occurred over an 11 year period and resulted in 42 fishermen losing their lives, showed that the main cause of the incidents was the vessel taking on water or capsizing and then sinking. The next most common cause of fatalities was entanglement in nets or other gear and being dragged overboard. In many cases these fishermen were wearing no form of Personal Flotation Device (PFD). This made their recovery from the water slow and difficult for those involved with the search and rescue operations and in some cases impossible. In a quarter of the cases, no bodies were ever recovered (HSA, 2014).

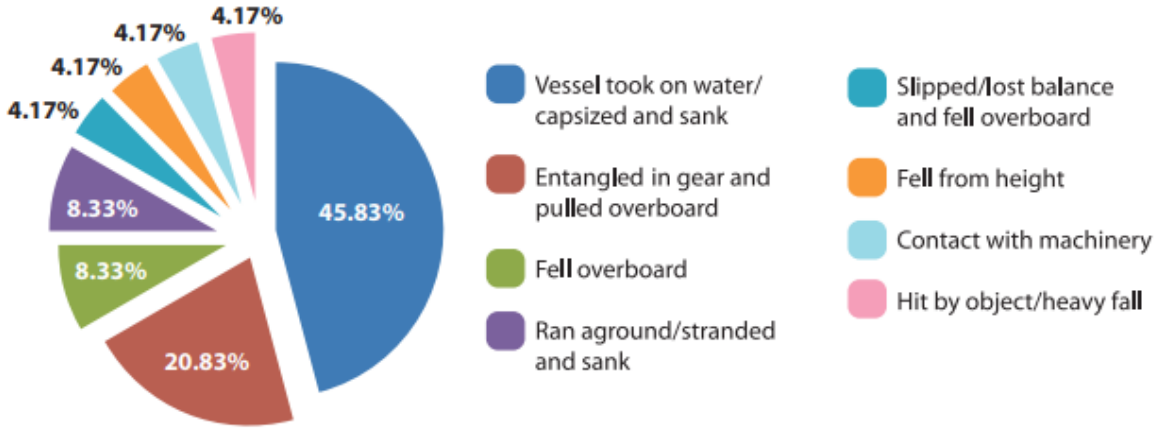

Graph 4. Main causes of fatalities (HSA, 2014)

The IMO has collected information from member States on the primary causes of casualties which led to the death of fishermen (Table 5) (IMO, 1999). The table divides primary causes into a number of categories covering both vessel and human factors. Human error, fishing gear incidents and adverse weather appear as important Primary causes in the accidents reported to the IMO. As will be seen later in this report, new investigation techniques are helping investigators obtain a better understanding of what causes accidents.

Table 5. Primary causes of fatalities of fishermen (IMO)

	1995			1996			1997			Total
	<12	12<<24	>24	<12	12<<24	>24	<12	12<<24	>24	
Human error	13	6	6	12	1	5	8	7	1	59
Steering gear failure										
Fishing gear incident	1	2	1	4	1	3	2	7	4	25
Other failure of vessel, its machinery or equipment	1	1	2					2	1	7
Adverse weather	11	6	2	9	1	3	7	6	1	46
Icing						1				1
Other	4	2	1	9	1	9	3	4		33
Unknown	50	11	14	23	12	5	29	13	15	172
Subtotal	80	28	26	57	16	26	49	39	22	
Total		**134**			**99**			**110**		**343**

Provisional figures show over 900 employer reported non-fatal injuries to employees in the Agriculture, forestry and fishing sector in 2014/15. Reported non-fatal injuries are categorised as either specified (a pre-defined list of certain injury types which includes for example fractures, amputations, serious burns5) or as resulting in over 7-days off work. Around 40% of the injury reports in 2014/15 were for specified injuries (Graph 5).

Graph 5. Employer-reported non-fatal injuries to employees in the agriculture, forestry and fishing sector (HSE, 2016)

Since 2001/02, the annual average rate of self-reported non-fatal injury has fluctuated between 3,840 and 5,830 per 100,000 workers (3.8% to 5.8%) with no overall clear trend (Graph 6).

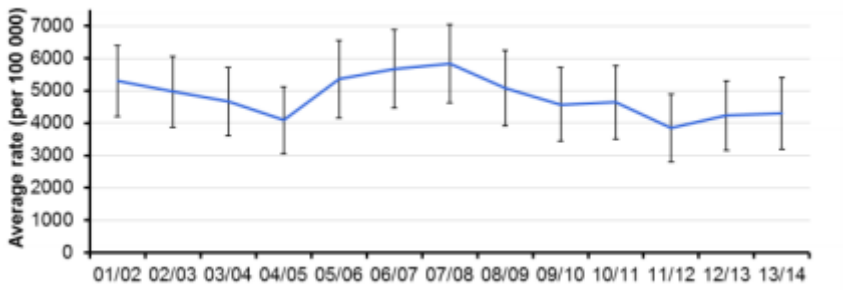

Graph 6. Incidence rate of all self-reported workplace injury in the agriculture, forestry and fishing sector (HSE, 2016)

There is a long-standing cooperation between IMO, ILO, and FAO in developing guidelines and standards on the safety of fishing vessels and fishermen. The first attempt to address the safety of fishing vessels and fishermen on an international level took place in the early 1960s when the three organizations entered into an agreement to co-operate, within their respective fields of experience. The agreement acknowledged that the respective areas of competence were (FAO, 2016, FAO/ILO/IMO, 2012):
FAO – fisheries in general (which includes areas such as safety in fishing operations and the relationship between fisheries management and safety at sea);
ILO – labour in the fishing industry; and
IMO – safety of life, vessels and equipment at sea. The voluntary instruments that have been jointly developed by IMO, ILO and FAO are the following:
• Code of Safety of Fishermen and Fishing Vessels, Parts A and B;
Voluntary Guidelines for the Design, Construction and Equipment of Small Fishing Vessels;
• Document for Guidance on Training and Certification of Fishing Vessel Personnel;
• Safety Recommendations for Decked Fishing Vessels of Less than 12 metres in Length and Undecked Fishing Vessels; and
• Guidelines to Assist Competent Authorities in the Implementation of Part B of the Code of Safety for Fishermen and Fishing Vessels, the Voluntary Guidelines for the Design, Construction and Equipment of Small Fishing Vessels, and the Safety Recommendations for Decked Fishing Vessels of Less than 12 metres in Length and Undecked Fishing Vessels (The Implementation Guidelines).

Conclusions

Fishermen accept the danger associated with their chosen occupation, but some may not take the danger as seriously as they should (Kaplan and Kite-Powell, 2000). Convention No. 188 and Recommendation No. 1999 replace five of the existing seven ILO instruments specific to the fishing sector. The adoption of this instrument is a very important step in improving the working and living conditions on board fishing vessels of all sizes everywhere in the world. It is envisaged that the Convention is likely to achieve widespread ratification and should, therefore, soon enter into force. Although fisheries management policies are enacted primarily to achieve fishery management goals, they may affect fishing safety indirectly. Other policies, undertaken for goals other than safety or fisheries management, may also affect fishing safety indirectly. Examples include marine liability laws, unemployment insurance laws, and economic development policies (Figure 6) (FAO, 2016). The International Maritime Organization (IMO), the ILO, and the Food and Agriculture Organization (FAO) to improve fishing OHS are important but more needs to bedone, at multiple levels, to monitor and promote fishing OHS, particularly in the smaller scale fisheries thatcomprise the bulk of the world fishing fleet (Windle et al. 2008). Results from this international comparison of northern countries and regions confirm that fishing-related workplace death is a major occupational safety and health problem in many northern nations. There are similar causes and circumstances responsible for fishermen's occupational traumatic injuries in each country, but close comparison is not always possible because categories may be different for each countries (i.e., capsize vs. foundering vs. sinking) (Abraham, 2001).

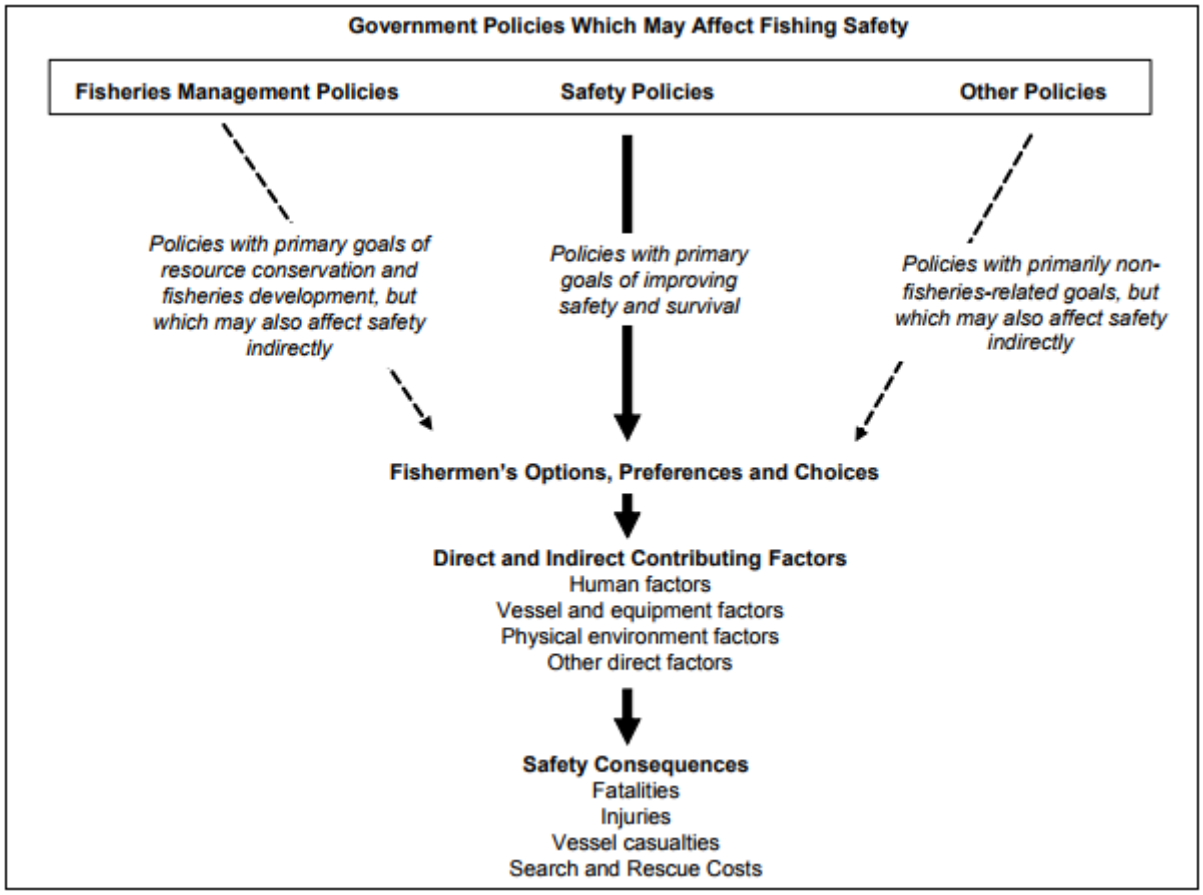

Figure 6. Pathways of how government policies affect fishing safety (FAO, 2016)

References

Abraham, P. P. (2001). International Comparison Of Occupational Injuries Among Commercial Fishers Of Selected Northern Countries And Regions. Barents Newsletter on Occupational Health and Safety 4: 24-28.

Alli, B.O. (2008). Fundamental Principles of Occupational Health and Safety, International Labour Office – Geneva ILO.

Cohen, A., Colligan, M. J. (1998). Assessing Occupational Safety and Health Training: A Literature Review, National Institute for Occupational Safety and Health, Cincinnati.

Dolan, AH., Taylor, M., Neis, B., Ommer R, Eyles J, Schneider D, et al. (2005). Restructuring And Health İn Canadian Coastal Communities. EcoHealth, 2:195–208.

European Commission (EC). EuroStat. Statistics in focus 63/2009. http://ec.europa.eu/eurostat/documents/3433488/5283817/KS-SF-09-063-EN.PDF/10b62d3b-e4dd-403f-b337-af6ffd3de8de

FAO/ILO/IMO. (2012). Safety Recommendations for Decked Fishing Vessels of Less than 12 metres in Length and Undecked Fishing Vessels. Rome, FAO. 254 pp. (http://www.fao.org/docrep/017/i3108e/i3108e.pdf)

Food and Agriculture Organization (FAO). (2001). Fisheries Circular N0. 966 FIIT/C966: Safety At Sea as an Integral Part of Fisheries Management.

Food and Agriculture Organization (FAO). (2016). Internatıonal Commercıal Fıshıng Management Regime Safety Study: Synthesıs Of Case Reports. Fisheries and Aquaculture Circular No. 1073. Rome.

Food and Agriculture Organization (FAO). (2016). The State of World Fisheries and Aquaculture 2016. Contributing to food security and nutrition for all. Rome. 200 pp. (also available at http://www.fao.org/3/a-i5555e.pdf).

Food and Agriculture Organization (FAO). (2018). The State of World Fisheries and Aquaculture 2018 - Meeting the sustainable development goals. Rome.

Health and Safety Authority (HSA). (2014). Managing Health and SafetyinFishing http://www.hsa.ie/eng/Publications_and_Forms/Publications/Fishing/Managing_Health_and_Safety_in_Fishing.html

Health and Safety Executive (HSE). (2015). Health And Safety In Agriculture, Forestry And Fishing In Great Britain, 2014/15. http://www.hse.gov.uk/statistics/industry/agriculture/agriculture.pdf
Health and Safety Executive (HSE). (2016). Kinds Of Accident In Great Britain. http://www.hse.gov.uk/statistics
Holmes, N., Lingard, H., Yesilyurt, Z., De Munk, F. (1999). An Exploratory Study Of Meanings Of Risk Control For Long Term And Acute Effect Occupational Health And Safety Risks In Small Business Construction Firms, Journal of Safety Research, 30(4), 251-261.
International Labour Organization (ILO). (1999). Safety and Health In the Fishing Industry. Report for discussion at the Tripartite Meeting on Safety and Health in the Fishing Industry. Geneva.
International Labour Organization (ILO). (1999). Safety And Health In The Fishing Industry. Geneva.
International Labour Organization (ILO). (2001). Guidelines On Occupational Safety And Health Management Systems, ILO-OSH 2001. (ISBN 92-2- 211634-8, Geneva.
International Maritime Organization (IMO). (1999). Collection And Analysis Of Casualty Statistics Of Fishing Vessels And Fishermen. Doc. FSI 7/6/2, 29 January.
Kaplan, I. M. and Kite-Powell, H. L., 2000. Safety At Sea And Fisheries Management: Fishermen's Attitudes And The Need For Co-Management. Marine Policy 24: 493-497.
Shikdar, A.A., Sawaqed, N.M. (2003). Worker Productivity, And Occupational Health And Safety Issues In Selected Industries, Computers & Industrial Engineering, 45(4): 563-572.
U.S. Bureau of Labor Statistics, U.S. Department of Labor. (2010).
Viscusi, W. K. (1986). The Impact of Occupational Safety and Health Regulation 1973-1983, The RAND Journal of Economics 17(4):567-58.
Windle, M.J.S. , Neis, B., Bornstein, S., Binkley, M., Navarro, P. (2008). Fishing Occupational Health And Safety: A Comparison Of Regulatory Regimes And Safety Outcomes In Six Countries. Marine Policy 32(4), pp.701–710. http://dx.doi.org/10.1016/j.marpol.200

EXPERIMENTAL INVESTIGATION OF MACHINABILITY PROPERTIES OF 5035 STEEL

Ayhan AYTAÇ
Milli Savunma Üniversitesi Kara Harp Okulu, Türkiye
aytac@kho.edu.tr

Muhammed İLİVAN
Dumlupınar Üniversitesi, Türkiye
muhammed.ilivan@dpu.edu.tr

Abstract: One of the main purposes in machining is to bring surface roughness to the top level. The stage where the most decisive work can be done in improving the product quality is the parameter design phase for both product and process design. In order to determine the most effective parameters and to evaluate the results more efficiently, the Taguchi experiment design technique is preferred to realize the experiments in a shorter time. This performed study was done by the aim of investigating the effect of change in terms of hardness, feed rate, and cutting tool of "Dual Phase" steel, which is a class of HSLA (High Strength Low Alloy) steels that increases usage and importance day by day, on surface quality in turning process in the pieces subjected to high forces in machine, device, car manufacturing. Experimental design In the Minitab statistical analysis program, Taguchi experiment design technique and 9 trials according to L9 orthogonal design. Experiments were performed in dry cutting conditions in CNC Turning Table that has 1.5 kW power and rotates with maximum 2000 rpm. Variance analysis and signal / noise ratio were used in the evaluation of the test results. . It was possible to achieve the intended results with only one third of the number of experiments required in full factorial design (9 experiments instead of 27). In the experiments, the cutting tool type (CBN, Ceramic and Carbide cutter), the feed rate (0,02, 0,04 and 0,06 mm/cycle) and the material hardness (Material with two different hardness values obtained by annealing at 745 and 760 degrees without heat treatment and obtained after heat treatment) were used as the independent variable (factor). The mean surface roughness value (Ra) as a dependent variable was determined from measurements taken at 6 different points in three trials. As a result, the most effective parameters on the surface quality are the feed rate, the material hardness (microstructure) and the cutting tool. The results obtained are interpreted together with the evaluations which have been entered into the literature before.

Keywords: Taguchi, Dual Phase, Surface Quality, Machinability.

Introduction

One of the main purposes in machining is to bring surface roughness to the top level. Being surface quality of material well has a positive effect on mechanical properties of material. It is required to choose cutting parameters the most suitable to get a good surface quality (Thomas and Ark., 1996).

Importance of heat treatment applied in the process of improving mechanical properties has gradually increased with growing technology. Heat treatment applied to steel plays an important role on defining machinability properties of steel (Uzkut and Ark., 2001., Çeviker, 1991., Demir and Ark., 2011). Material technology and cutting tool technology growing in recent years allows machinability of heat treated steels easily and quality (Elbestawi and Ark., 1996, Yaka and Ark., 2016). After heat treatment applied of steels, internal strains occur in material. This causes problems such as warping in workpiece, burning on surface, and micro crack. Arising these problems can be eliminated with various processes applied after heat treatment Çolak, 2006., Daghini and Nicolescu., 2007., Binali and Ark., 2018).

Dewes et al., processed AISI H13 material with 52 HRc hardness by using WC solid milling machine coated with TiCN. They observed that cutting speed increase temperature, temperature increases as directly proportional with cutting speed, and temperature in cutting area decreases with increasing tool radius. Asilturk and Akkus (2011), investigated effect of cutting speed, cutting depth, and feed rate on surface roughness in turning process of hardened AISI 4140 (51 HRC) with coated carbide. As a result of experimental studies, they showed that feed rate has the most significant effect on Ra and Rz.

Ren at al. (2014) investigated the study about optimization of cutting geometry in last milling process on Ti-5Al-5Mo-5V-1Cr-1Fe alloy with Taguchi method. They aimed at reaching combination to minimize cutting forces and surface roughness, and to optimize cutting speed by changing milling cutter geometry in the study. As a result, they found that multi performance characteristics can be improved with grey-Taguchi method. Zhao (2017), performed an experimental study to understand the effect of cutting edge radius on workpiece machining performance with regards to surface roughness and tool abrasion in AISI52100 steel. Three groups of cutter

(CBN) with 20, 30, 40 µm nominal edge radius were used in the study. Change in cutting edge radius was evaluated with an optical microscope. The effect of surface radius and tool abrasion on cutting edge radius was investigated in different machining conditions with different machining tests by designing three-leveled, two-factored experiments with Taguchi. Variations tends to lower with increasing nominal values of cutting radius, and also, it was resulted that cutting radius has an important effect on surface roughness and tool abrasion.

The situation defined above is an example of typical problem showing up machining tool that is appropriate to tolerance in engineering and research and development studies. It is required to improve surface quality which is a measurement of machinability, to make experiment to investigate effect of tool type, cutting speed and feed rate on performance, and make optimization by evaluating these experiments.

The purpose of this study is to make optimization and investigate effect of material and cutting parameters (feed rate and cutting tool type) on workpiece surface roughness that is an important machinability criterion by doing machinability experiments with turning method on steels used in machine production industry. In this study, dual-phased steel specimen obtained in three different hardness after heat treatment was performed to turning process with three different feed rate by using three different cutter type by evaluating factors affecting turning surface quality after literature review. Results obtained from Taguchi optimization were evaluated with regards to adaptation to literature.

Experimental Study

Used Material and Properties

5035 ERDEMIR quality numbered SAE 1035 Standard Tool produced as hot mill product in Eregli Iron and Steel Factories (ERDEMIR) T.A.S and given chemical composition in Table 1 was used by preparing 12 mm diameter, and hardness measurement was performed by doing heat treatment.

Table 1: Chemical Composition of 3936 quality steel

Quality	Standard	Chemical Composition (% Weight)					
		C	Mn	P	S	Si	Al
5035	SAE 1035	0.36	0.71	0.012	0.006	0.230	0.041

It was utilized from previous studies to define relevant annealing temperatures. Temperatures values in the study performed related to mechanical properties of materials having same chemical composition (Tayanç and Toktas, 2001).

It was given water in water to turning specimen annealed 30 minutes in 745, 760, and 775 C° temperatures on the purpose of obtaining three different hardness on same material in total. During preparation of specimen, it was waited to chill oven for two different temperatures to prevent different heat treatment conditions. Specimens were subjected to cooling in water after annealing process. Temperature-time diagram (T-t) belong to aforesaid heat treatment was shown in Figure 1.

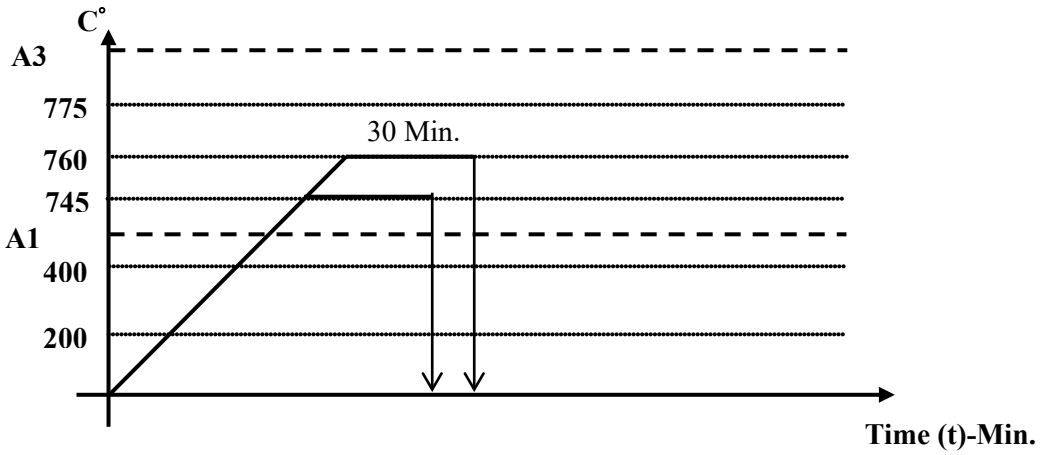

Figure 1. Temperature (T)-Time(t) diagram.

Microhardness Measurement

Hardness measurement of specimens were performed with micro Vickers method in Qness Q10 microhardness test equipment. HV 0,5 load and 10 seconds main loading values were defined as test parameters, and trace

image was taken by the help of 40X lens. Hardness measurements of materials were obtained as Vickers (HV) in Qness Q10 microhardness equipment. Results were given in Table 2.

Table 2: Micro Hardness Values

Material	Non-Processed	745◦	760◦
Measurement 1 (HV)	155	184	389
Measurement 2 (HV)	162	190	376
Average hardness (HV)	158,5	187	382,5

Surface Roughness Measurement

Surface roughness was measured with TIME TR200 surface roughness equipment. Three measurement trace to parallel and vertical to cutting direction were measured. The mean of three arithmetical average surface roughness measurement (Ra) in the direction and through cutting were used to show surface roughness of specimen.

Choosing Cutting Parameters and its Levels

Experimental studies within study were performed in CNC Turning Table that has 1.5 kW power and rotates with maximum 2000 rpm. Dual phase steels is a new class of high strenght-low alloy steels (HSLA). A cylindrical workpiece made from 5035 number steel having 0,36 % C ratio that is produced by ERDEMIR as special wheel steel was processed with Al_2O_3 coated Cementite Carbide, Ceramic, and CBN cutting tools by applying three different feed rate in dry cutting conditions in the study. Cutting area order is shown in Figure 2. Factors used in machining and its levels were defined with user experience and were specified in Table 3.

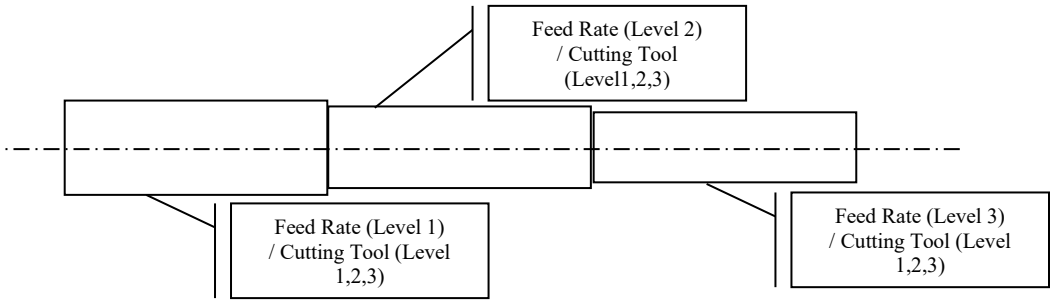

Figure 2: Cutting Area Order

Fishbone diagram is one of output in designing experiments. A fishbone diagram can be created to see relations defined factors to each other's exactly (Şirvancı, 1997). This diagram specifies all factors representing product or process quality and affecting measured values (Savaskan at al., 2004). It was decided variable and constant factors with the help of fishbone diagram. Factors affecting machinability are collected under four main categories (cutting parameters, rigidity, workpiece, cutting tool) as shown in Figure 3.

Values of variable parameters except factors that has to be constant and that cannot be controlled were taken as compatible with real working environment values as much as possible. Because cooling liquid usage will have positive effect to surface quality, experiments were planned in dry condition to keep experiment numbers in certain amount.

Table 3: Cutting Parameters

Factors	Unit	Symbol	Level 1	Level 2	Level 3
Cutting Tool	-	A	Carbide	Ceramic	CBN
Feed Rate	Mm/dev	B	0,02	0,04	0,06
Heat Treatment /Hardness	/Hv0.5	C	Non-Processed	745◦C	760◦C

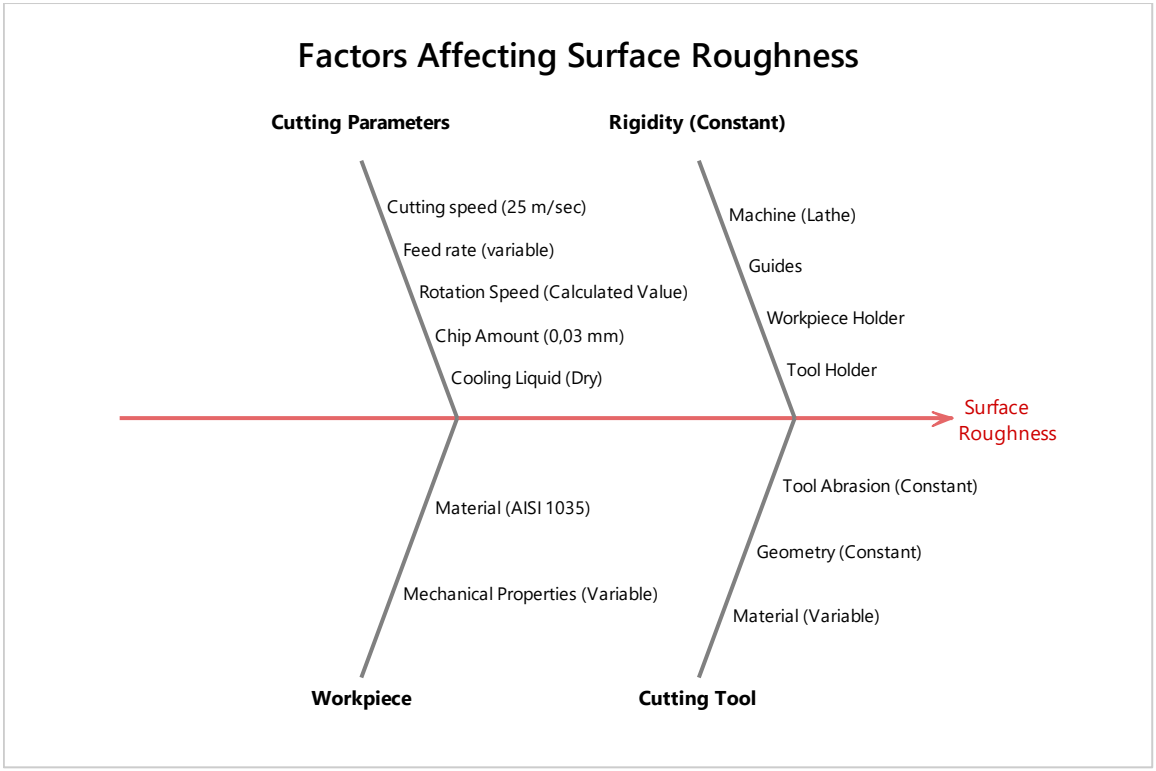

Figure 3. Evaluation of Factors Affecting Surface Roughness with Fishbone Diagram

Taguchi Experiment Design

Choosing optimum process conditions is an extremely important subject since it defines surface quality of produced pieces and dimensional sensitivity. Contact surfaces of machine elements working together are desired to finish with particular rough, especially in machine design. Sometimes, sensitive surfaces are required, and sometimes rough surfaces are suitable to work machine properly, as well. Therefore, it is important to define surface roughness in design step, and to control in production step. After, surfaces can be operated in desired roughness values (Karayel, 2009). It is needed to optimize surface quality and to define optimum cutting parameters on the purpose of machining machine pieces as suitable to environment they will work. For this purpose, feed rate, cutting tool, and material hardness was defined as parameters to use in this study. Machining experiments were performed by considering Taguchi one patterned (each factor was taken three levels) L9 orthogonal design. Experiment index was given in Table 4.

Table 4: Taguchi L9 experiment design

Experiment Nu.	Control Factors		
	Cutting Tool (A)	Feed Rate (B)	Hardness (C)
1	1	1	1
2	1	2	2
3	1	3	3
4	2	1	2
5	2	2	3
6	2	3	1
7	3	1	3
8	3	2	1
9	3	3	2

Analysis of S/N Ratios

Taguchi experiment design and analysis were performed in Minitab 16.1 package program, and basic leveled (three level) L_9 orthogonal index was used. "Smallest-the best" formula specified equation 1 was used to evaluate obtained Signal-Noise Ratios (S/N).

$$\frac{S}{N} = -10 * \log\left[\sum_{i=1}^{n} \frac{Y_i^2}{n}\right] \quad \text{Eq. (1)}$$

S/N ratios were calculated by using "smallest-the best" equation after obtained surface roughness ratios in machining experiments of ERDEMIR 5040 quality steel according to performed Taguchi L9 experiment design. Surface roughness values and S/N ratios obtained after machining were shown in Table 5.

Table 5: Surface roughness values and S/N ratios obtained after machining

Experiment Nu.	Control Factors			Average Surface Roughness Values (Ra) µm	S/N Ratios (dB)
	Cutting Tool	Feed Rate	Hardness		
1	1	1	1	5,255	-14,4115
2	1	2	2	2,456	-7,8046
3	1	3	3	4,890	-13,7862
4	2	1	2	0,430	7,3306
5	2	2	3	0,352	9,0691
6	2	3	1	0,632	3,9857
7	3	1	3	2,622	-8,3727
8	3	2	1	1,514	-3,6025
9	3	3	2	1,517	-3,6197

Effect of control factors on surface roughness values was analyzed by using S/N response table. S/N response table was given in Table 6 for surface roughness. This table, which is created with Taguchi method to get optimum surface roughness value, shows optimum levels besides factor effect range. S/N values of control factors for surface roughness were shown in Figure 4.

Table 6: S/N response table for surface roughness

Level	**Cutting Tool**	**Feed Rate**	**Hardness**
1	-12,0007	-5,1512	-4,6761
2	6,7951	-0,7793	-1,3645
3	-5,1983	-4,4734	-4,3632
Delta	18,7959	4,3718	3,3116
Effect Range	1	2	3

Optimum levels of control factors for surface roughness for A cutting tool (Ceramic-Level 2), B feed rate (0,04 mm/cyc-Level 2), C Hardness (745 C° Heat Treatment, Level 2) was specified. However, this result couldn't be measured in L9 Taguchi experiment design. These levels didn't take place in eliminated experiments because experiments number was reduced from 27 in total factorial to 9.

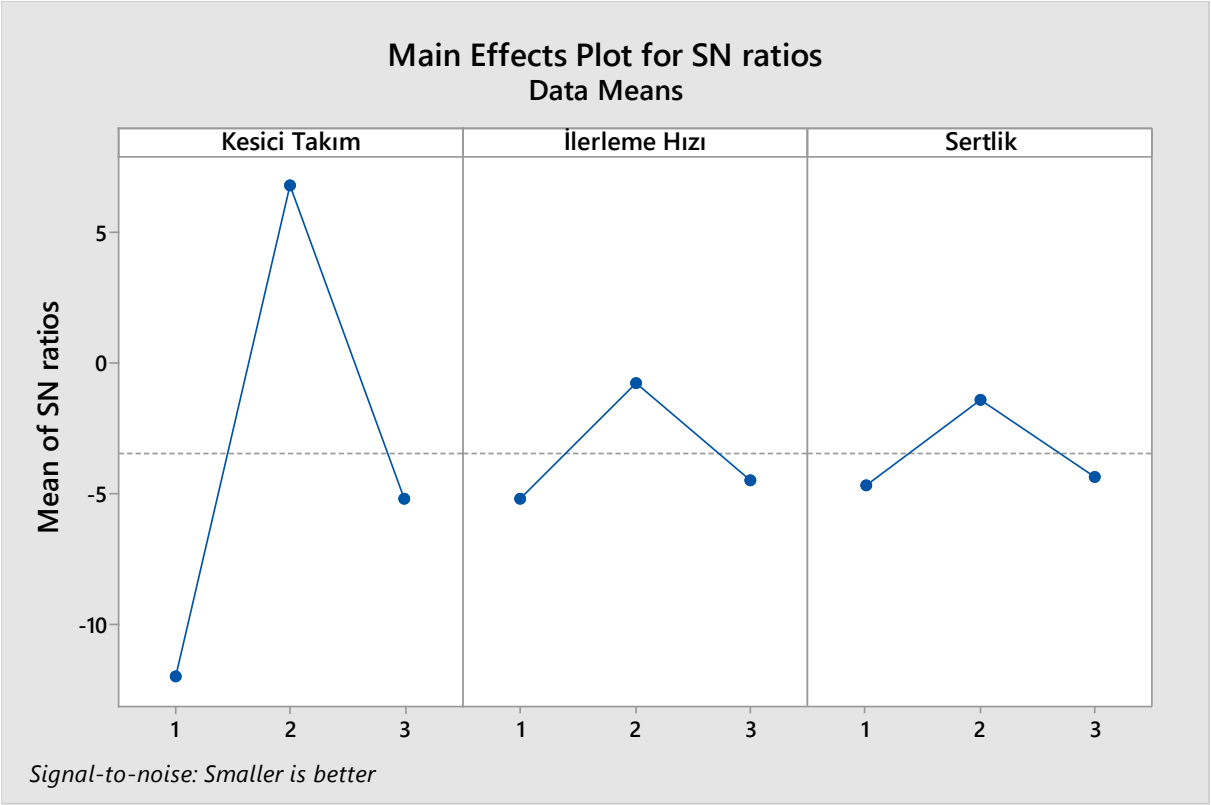

Figure 4. S/N values of control factors for surface roughness

Evaluation of Experiment Results

Change in surface roughness depending on cutting team and feed rate were explained in Figure 5 in turning ERDEMIR 5040 quality steel. When the graph is investigated, a decrease in surface roughness are seen with an increase of feed rate in CBN cutter, and the best surface roughness value was observed in 0,04 mm/cyc feed rate for every three cutter. Also, the best surface roughness value in medium steel materials was obtained from ceramic tool as seen in graph.

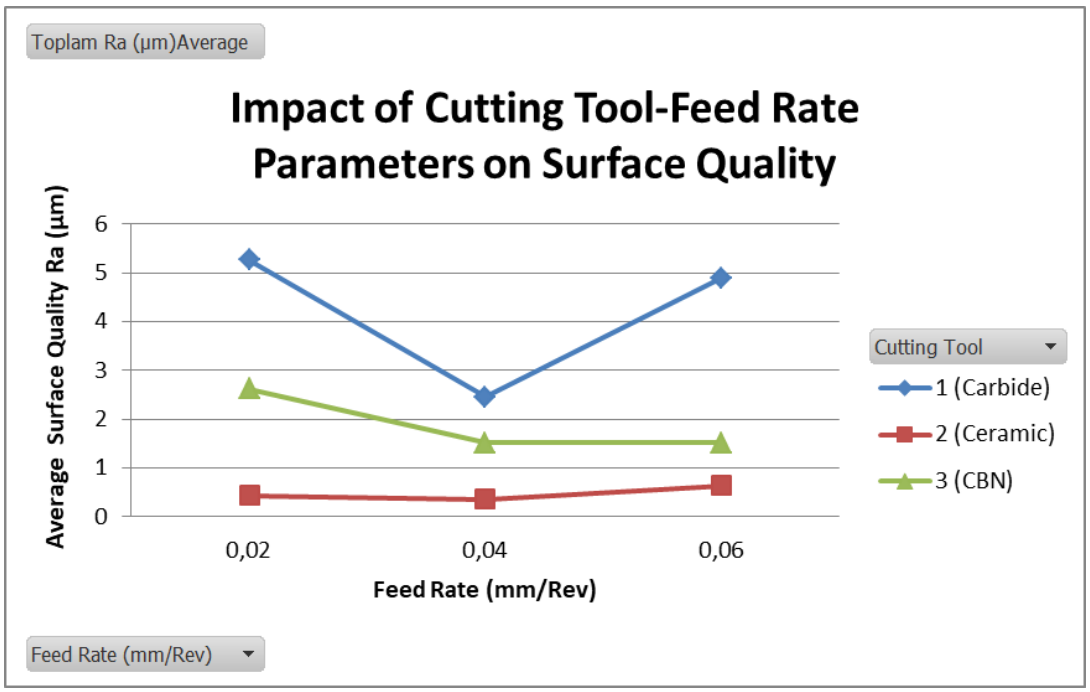

Figure 5. Change of surface roughness depending on cutting tool and feed rate in turning ERDEMIR 5035 Quality Steel

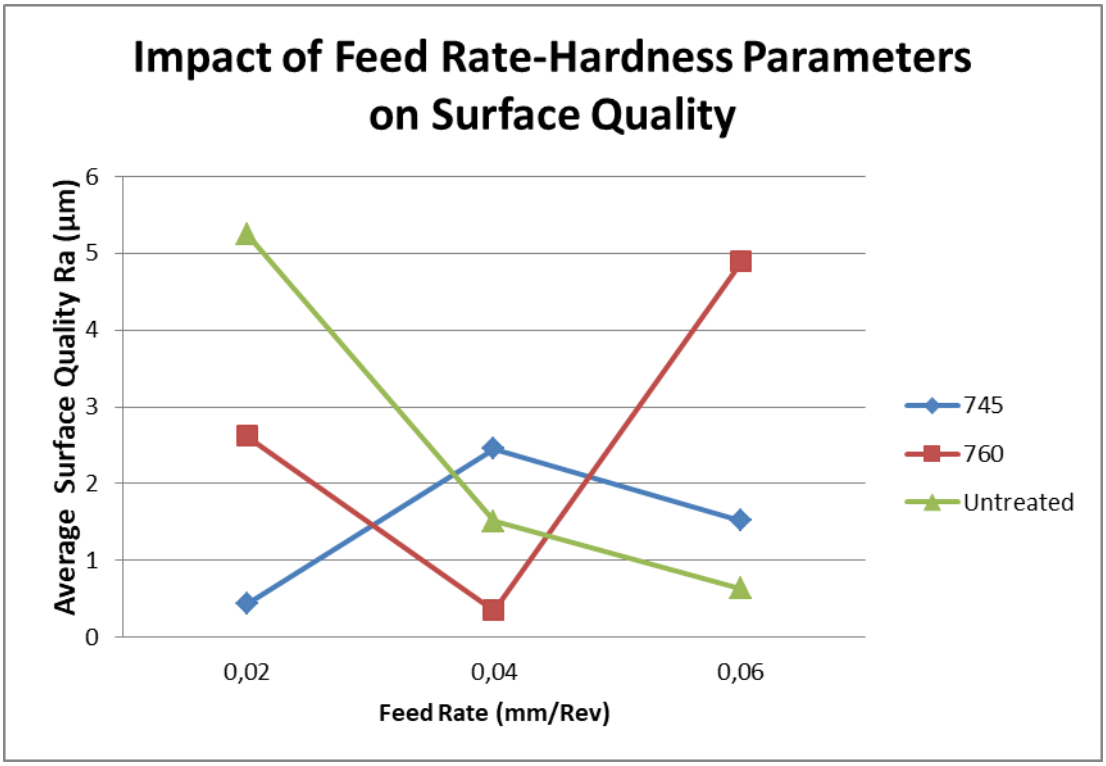

Figure 6. Change of surface roughness depending on hardness and feed rate in turning ERDEMIR 5035 Quality Steel

Change of surface roughness depending on hardness of workpiec and feed rate of cutting tool was explained in Figure 6. Lowest surface roughness in 0,04 mm/cyc feed rate was obtained from steel heat treated at 760 C^{O}. A decrease in surface roughness with an increase feed rate was observed in non-processed specimen, and average the best surface roughness value was seen at steel heat treated at 745 C^{o}

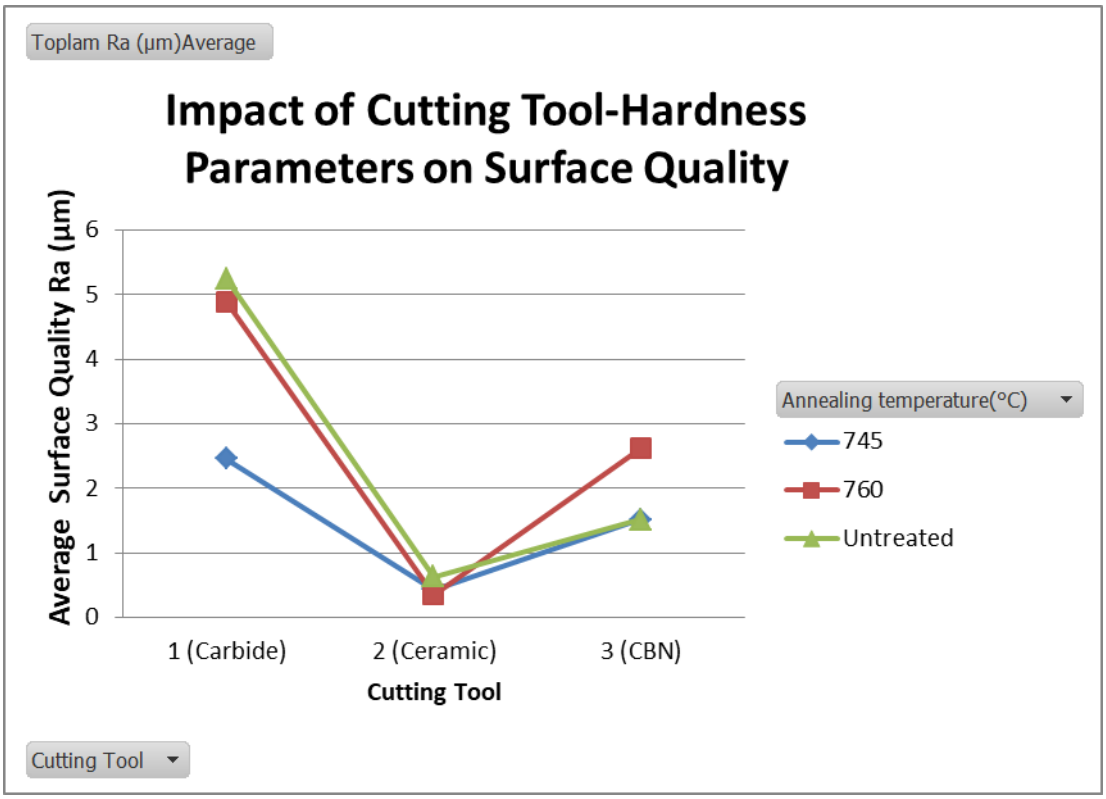

Figure 7. Change of surface roguhness depending on cutting tool and heat treatment (hardness) in turning ERDEMİR 5035 Quality Steel

Change in surface roughness depending on cutting tool and hardness level is explained in Figure 7. While Ceramic cutters exhibits the best performance for every three hardness, surface roughness value in carbide cutters is higher than other ceramic and CBN cutters. Better surface quality was obtained with Ceramic cutters when medium steel is used.

Results

In this study, three different paramaters were evaluated and optimized with regards to machinability because Taguchi experiment design has wide usage area, and it enables to obtain results with both less experiments and lower costs compared with traditional experiment design.

Optimisation of cutting parameters affecting surface roughness values obtained from turning of ERDEMIR 5035 Quality steel was performed in this study. A cutter tool (Ceramic-Level 2), B feed rate (0,04 mm/cyc, Level 2), C hardness (745 C° heat treated-Level 2) were specified. However, this result couldn't be measured in L9 Taguchi experiment design. These levels didn't take place in eliminated experiments because experiments number was reduced from 27 in total factorial to 9. According to analyse result, it was seen that the most efficient parameter on surface roughness was cutting tool with 70,98 % content. Micro hardness values increased with martesite increase taking place in micro structure depending on heat treatment of ERDEMIR 5035 Quality steel. This hardness increase has a positive effect to surface roughness values in turning including medium hardness, while has negative effect in high hardness.

References

Asiltürk I, Akkuş H (2011), *Determining the effect of cutting parameters on surface roughness in hard turning using the Taguchi method*, Measurement 44(9):1697–1704

Çeviker, İ., (1991), *Mikroalaşımlı dövme çeliklerde mikroyapısal karakterizasyon ve mikroyapı-mekanik özellikler ilişkisi,* Y. Lisans Tezi, İTÜ Fen Bilimleri Enstitüsü.

Çolak, O., (2006), *CNC Freze Tezgâhı için Kesme Parametrelerinin Akıllı Yöntemlerle Elektronik Ortamda Optimizasyonu*, Doktora Tezi, Süleyman Demirel Üniversitesi, Fen Bilimleri Enstitüsü.

Demir, H., Çiftçi, İ., Türkmen, M., Gündüz, S., (2011), *Orta Karbonlu Alaşımlı ve Alaşımsız Çeliklerde Isıl İşlem Şartlarının ve Sertliğin İşlenebilirliğe Etkisi*, *6th International Advanced Technologies Symposium (IATS'11), Elazığ, Turkey.*

Elbestawi, M. A., Srivastava, A. K., ans El-Wardany, T. I., (1996), *A model for chip formation during machining of hardened steel*, *CIRP Annals Manufacturing Technology,* **45**, 71-76.

Daghini, L. and Nicolescu, C., (2007), I*nfluence of Inserts Coating and Substrate on Toolox 44 Machining*, Swedish Production Symposium

Dewes, R.C., Ng, E., Chua, K.S., Newton, P.G., Aspinwall, D.K. (1999), *Temperature measurement when high speed machining hardened mould/die steel*, Journal of Material Processing Technology, 92-93:293-301.

Karayel, D (2009), *Prediction and control of surface roughness in CNC lathe using artificial neural network*, Journal of Materials Processing Technology. 209. 3125-3137. 10.1016/j.jmatprotec.2008.07.023.

Ren, J., Zhou, J., Wei, J., (2014), *Optimization of Cutter Geometric Parameters in End Milling of Titanium Alloy Using the Grey-Taguchi Method*, Advances in Mechanical Engineering. Article ID 721093

Savaşkan, M., Taptık, Y. Ürgen, M. (2004), *Deney tasarımı yöntemi ile matkap uçlarında performans optimizasyonu*, İtüdergisi/d Mühendislik, 3(6), 117-128.

Şirvancı, M. (1997), *Kalite için deney tasarımı: Taguçi yaklaşimi*, (pp.12-100), İstanbul:Literatür Yayıncılık.

Tayanç M., Toktaş A. (2001), *Dual-faz edilen 3936 kalite Erdemir özel jant çeliğinin mikroyapı mekanik özellik ilişkisinin araştırılması*, 1.Ulusal Demir-Çelik Sempozyumu, E/2001/274-1:715-718.

Thomas, M., Beauchamp, Y., Youssef, A.Y. and Masounave, J., 1996. Effect of tool vibrations on surface roughness during lathe dry turning process. Computers & industrial engineering, 31, 637-644.

Uzkut, M., Özdemir, İ., (2001), *Farklı çeliklere uygulanan değişen ısıtma hızlarının mekanik özelliklere etkisinin incelenmesi*, DEÜ Mühendislik Fakültesi Fen ve Mühendislik Dergisi, Cilt: 3, Sayı: 3, sh. 65-73,.

Yaka, H., Uğur, L., Akkuş, H., (2016), *AISI 1040 Çeliğinin Tornalanmasında Yüzey Pürüzlülüğünün Çoklu Regresyon ile İncelenmesi*, AKÜ FEMÜBİD 16 (2016) 035901 (770-775)

Yurtkuran, H, Korkmaz, M, Günay, M. (2016), *Modelling and optimization of the surface roughness in high speed hard turning with coated and uncoated CBN insert*, Gazi University Journal of Science, 29 (4), 987-995. Retrieved from http://dergipark.gov.tr/gujs/issue/27537/289712

Zhao, T., Zhou, J.M., Bushlya, V., Stahl, J. E., (2017), *Effect of cutting edge radius on surface roughness and tool wear in hard turning of AISI 52100 steel*, The International Journal of Advanced Manufacturing Technology. August 2017, Volume 91, Issue 9–12, pp 3611–3618

IMPROVEMENT OF SELF-LOOSENING PREVENTION EFFECTS OF THREADED FASTENERS THROUGH FINITE ELEMENT ANALYSIS

Atsushi NOMA, Jianmei HE

Kogakuin University, Department of Mechanical Engineering, Tokyo- Japan

e-mail: Am17057@ns.kogakuin.ac.jp

Abstract: Threaded fasteners using screws/bolts are used not only in industrial field but also in various fields such as precision instruments and medical field. Many accidents caused by the loosening of the screw/bolt threaded fasteners are actually reported. As one countermeasure, nut with spring washer is used, but there remains the problem that effective loosening prevention effects cannot be obtained in the case of increasing in the parts number or no-using of such nuts etc. Then further improvement on loosening prevention effects of screw/bolt threaded fasteners are desired. In this research, new screw/bolt structures having self-loosening prevention effects are designed by applying the spring characteristic swelling effects in loosening direction of springs. 3D CAD modeling and finite element analyses are carried out to evaluate the spring characteristic effects and self-loosening prevention effects of new designed screw/bolt structures. Analytical results indicated that self-loosening prevention effects can be affected by the shape/size design variables of applied helical cuttings introduced for new screw/bolt structures.

Keywords: Threaded fasteners, Screws/Bolts, Spring characteristic effect, Self-loosening prevention effects, 3D CAD modeling, Finite elements analysis

Introduction

There are various kinds of fastening methods using screws/bolts for threaded fasteners, such as using bolts and nuts together or tapping screws. Designers can select different products or fastening methods assuming to different environments. Many of analytical and experimental investigations on self-loosening bolt fasteners problems [1]-[3], however, loosening problems of threaded fasteners are still unavoidable through the screws/bolts tightening methods under cyclic vibrations or external compact loadings. In our previous research [4], spring characteristic effects as shown in Figure1 are interested as applied to new designed screw/bolt structures, which can result to self-loosening preventive effects on threaded fasteners. The spring characteristic effect means that spring structure as shown in Figure 1(a) has the swelling effect under rotating counterclockwise (loosening direction) as shown in Figure 1(b).

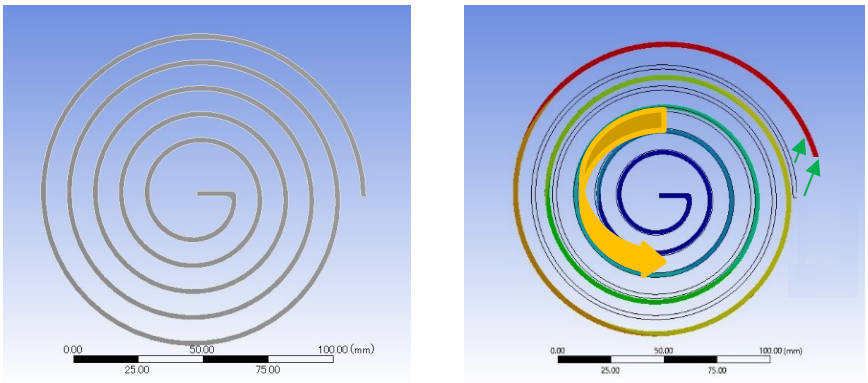

(a) Spring structure (b) Swelling effect in loosening direction

Figure1. Conceptual diagram of spring characteristic effect

Concept structural designs on conventional M6 hexagon bolt for obtaining self-loosening preventable threaded fastener purposes were carried out by using 3D CAD software SolidWorks [4]. Helical cutting with cross-sectional shape and cross thread turning in reverse direction to thread rotation direction were introduced to general hexagon bolts as shown in Figure 2(a) and (b). As the result, new bolt structures provided by plurality of springs cross each other are designed with spring characteristic effects supposed to be imparted as shown in Figure 2(c). Spring characteristic effects of the helical-cutting applied bolts were firstly confirmed by analytical approaches under counterclockwise rotating loading.

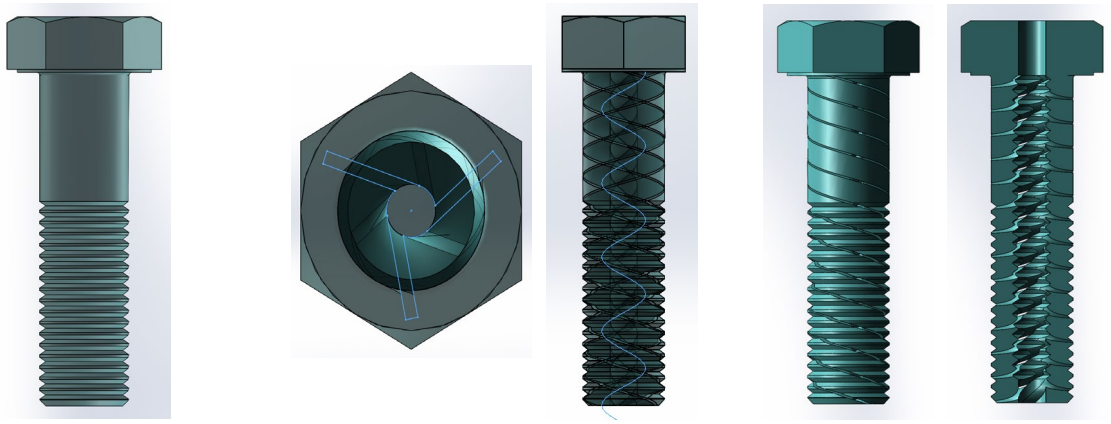

(a) Conventional bolt (b) Cross-sectional cutting shape & thread turning (c) New designed bolt

Figure2. Helical-cutting applied bolt for self-loosening preventable threaded fasteners

In this research, parametrical studies are executed to evaluate the affections of different design variables, such as line width of cross-sectional cutting shape and helical pitch applied to screw structures, on the self-loosening preventive effects of threaded fasteners.

Parametrical investigation of helical cutting process on self-loosening prevention effects

Self-loosening preventable effects of threaded fasteners using the helical-cutting applied bolts can be confirmed through finite element analysis modeling on Junker vibration test, which is based on ISO 16130 standard including new designed bolt, nut, fixed plate and vibration plate as shown in Figure3. The friction generated on the contact surfaces between the stationary plate and the diaphragm and nut are considered not negligible and the friction coefficient are set to 0.17 obtained from experimental result [1]. The contacts between each surfaces are modeled as contact elements based on the penalty method. Table1 shows the constraint conditions used for analytical modeling of Junker vibration test. C45 and X12Cr13 materials are applied for designed bolts, nuts, and testing fixtures of Junker vibration test. Detail material properties are as shown in Table2 for self-loosening prevention effect evaluations.

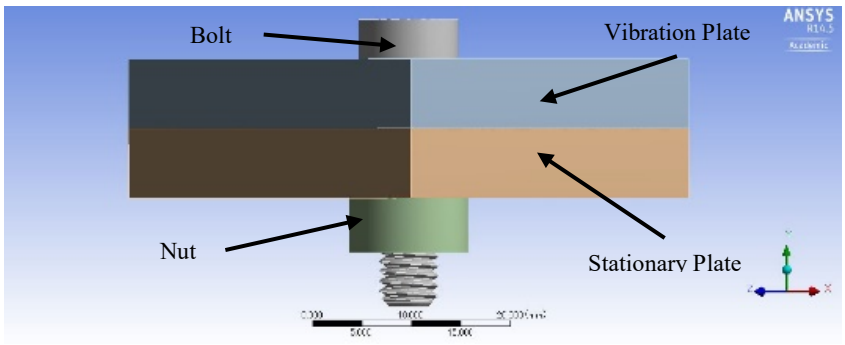

Figure3. Analytical model of Junker vibration test

Table1. Restraint conditions for analytical modeling of Junker vibration test

Test Type	ISO 16130 Junker Vibration Test
Number of Vibrations	1000
Direction of Vibrations	x Direction : $\pm$0.3mm
Fixed	Side of Fixed Plate
	Bolt End : x and z Directions
Fastening Axial Force	4330N

Table2. Material properties used for analytical modeling of Junker vibration test

Material	C45	X12Cr13
Young's Modulus	205GPa	200GPa
Poisson's Ratio	0.3	0.3
Density	7800 kg/m^3	7800 kg/m^3
Applied Parts	Bolt, Nut	Vibration Plate, Stationary Plate

Three dimensional modeling on Junker vibration test of threaded fasteners are executed using new designed M6 screw/bolt structures with different design variables based on the analytical method mentioned above. The design variable of line width of cross-sectional cutting shape as shown in Figure4 are changed from 0.5 mm to 0.9 mm with every 0.1 mm based on conventional M6 bolt. Design variable of helical cutting pitch as shown in Figure5 are changed from 11.0 mm to 19.0 mm with every 2.0 mm for numerical studied. 25 cases combined between line width of cross-sectional cutting shape and helical cutting pitch are considered in the analytical evaluations as shown in Table3.

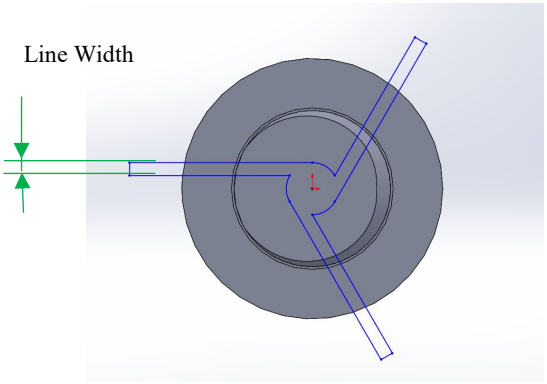

Figure4. Design variable of line width of cross-sectional shape for helical cutting process on M6 bolt

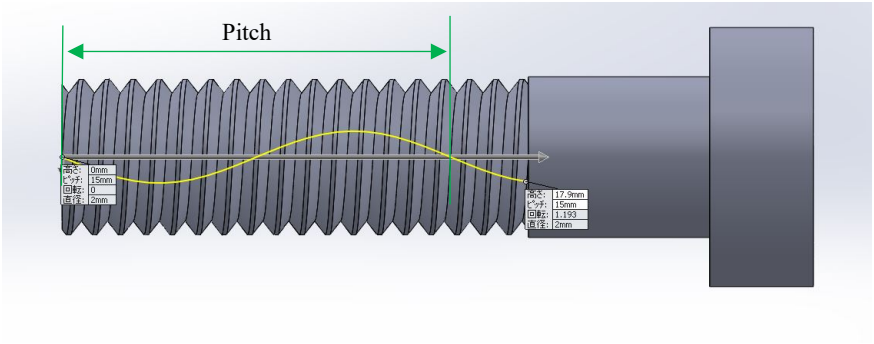

Figure5. Design variable of helical pitch for helical cutting process on M6 bolt

Table3. Design variables for analytical evaluation of Junker vibration test

Helical cutting pitch, mm	Line width of cross-sectional cutting shape, mm				
11	0.5	0.6	0.7	0.8	0.9
13					
15					
17					
19					

Analytical results on self-loosening prevention effect evaluation of threaded fasteners using new designed bolts with helical cutting

Analytical results of the self-loosening prevention effects using the designed new bolt structures with different design variables are shown in Figure6 to Figure15 based on the analysis method above mentioned. Horizontal axis shows the iteration number of vibrations and vertical axis shows the axial forces of threaded fasteners representing the loosening conditions.

Figure6 to Figure10 show the analytical results for each helical cutting pitch with different line widths. From these results, it can be seen firstly that for small helical cutting pitch like 11.0 mm and 13.0 mm, self-loosening preventive functions are observed for most cases of different cross-sectional cutting line width. Secondly, the falling of axial forces due to the iterated vibrations becomes gentle with thicker line width of cross-sectional cutting shape in the cases of helical cutting pitch large than 15.0 mm. These results conclude that utilization of new designed screw/bolt structures with small helical cutting pitch are available to obtain self-loosening preventive threaded fasteners.

Figure11 to Figure15 show the analytical results for each line widths with different helical cutting pitch. From these results, it can be seen that for thicker line width more than 0.7 mm, self-loosening preventive functions can be obtained for more cases of different helical cutting pitch. Secondly, combination between helical cutting pitch

and line width of cross-sectional cutting shape are very important for the self-loosening preventive effect of threaded fasteners.

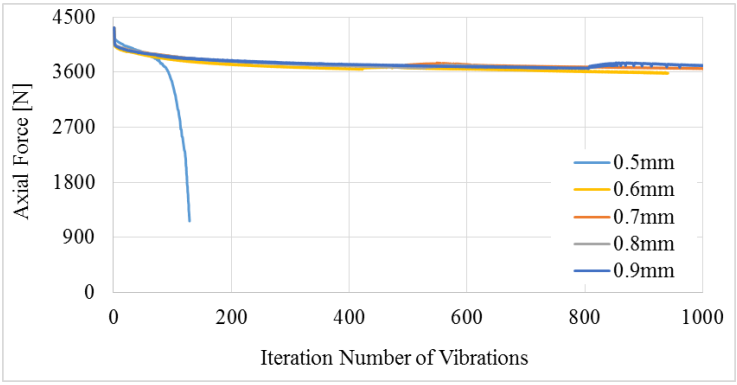

Figure6. Changes on axial forces for pitch of introduced helical cutting process: 11mm

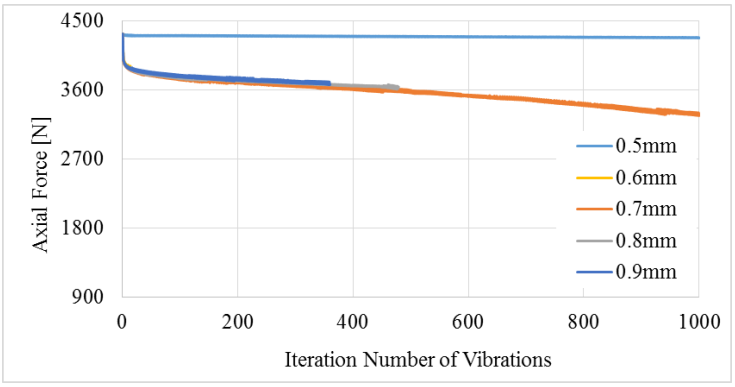

Figure7. Changes on axial forces for pitch of introduced helical cutting process: 13mm

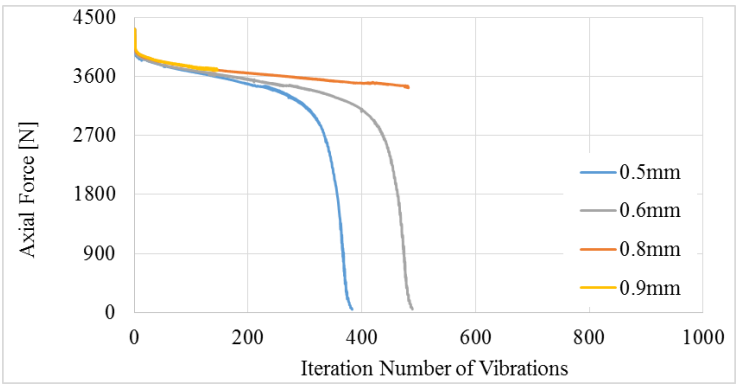

Figure8. Changes on axial forces for pitch of introduced helical cutting process: 15mm

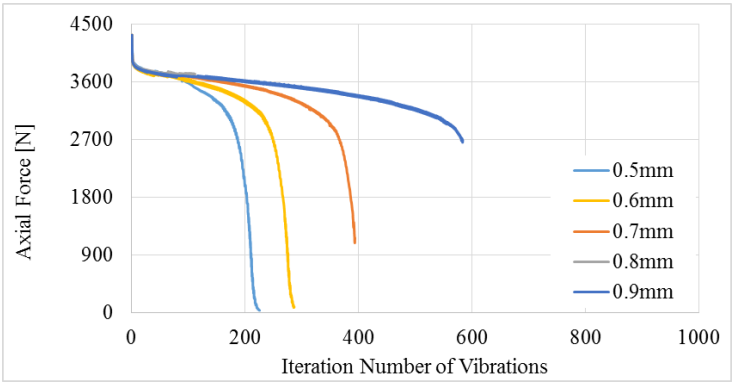

Figure9. Cahnges on axial forces for pitch of introduced helical cutting process: 17mm

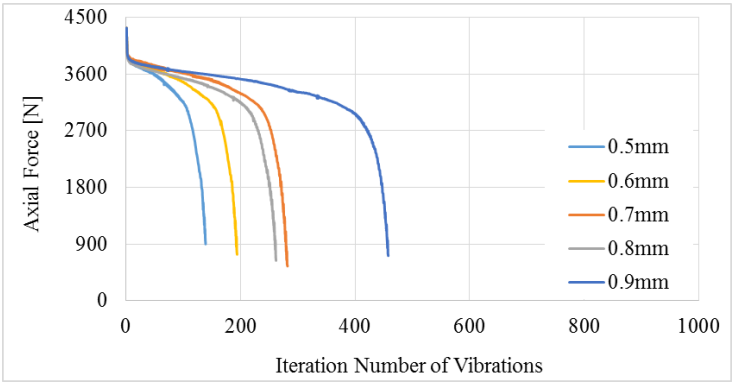

Figure10. Changes on axial forces for pitch of introduced helical cutting process: 19mm

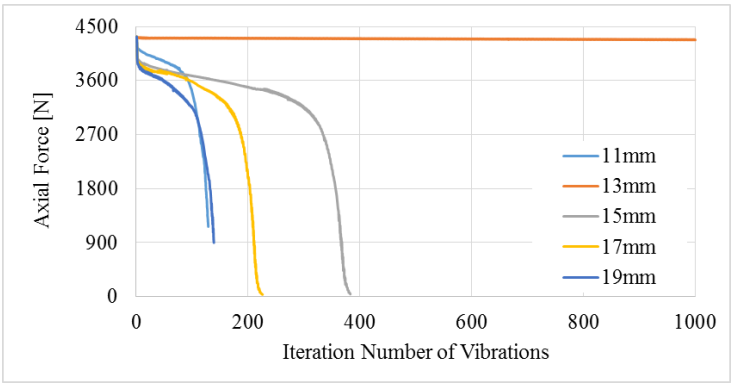

Figure11. Changes on axial forces for line width of cross-sectional cutting shape: 0.5mm

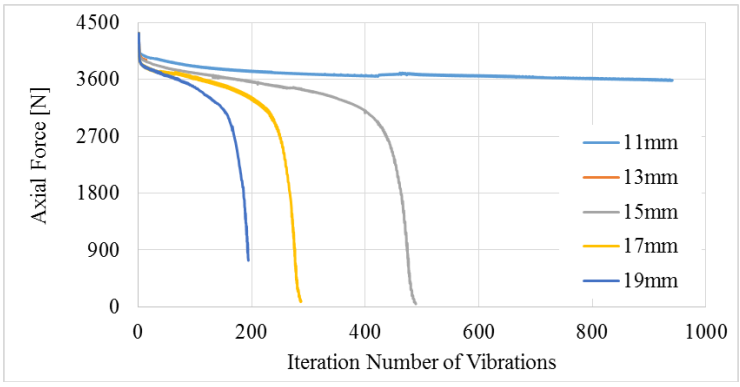

Figure12. Changes on axial forces for line width of cross-sectional cutting shape: 0.6mm

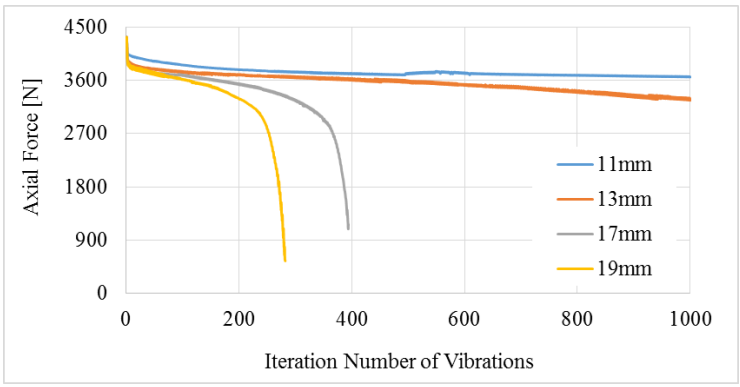

Figure13. Changes on axial forces for line width of cross-sectional cutting shape: 0.7mm

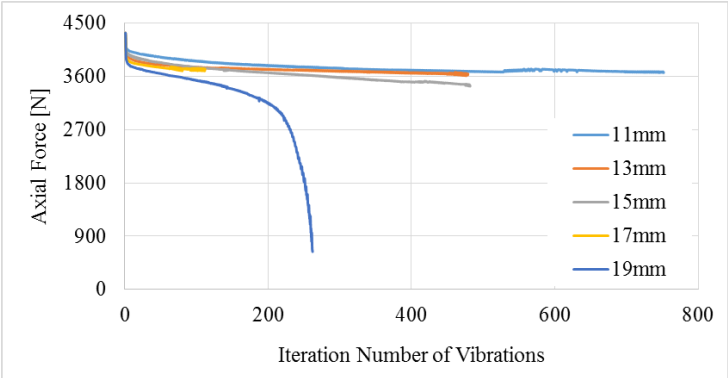

Figure14. Changes on axial forces for line width of cross-sectional cutting shape: 0.8mm

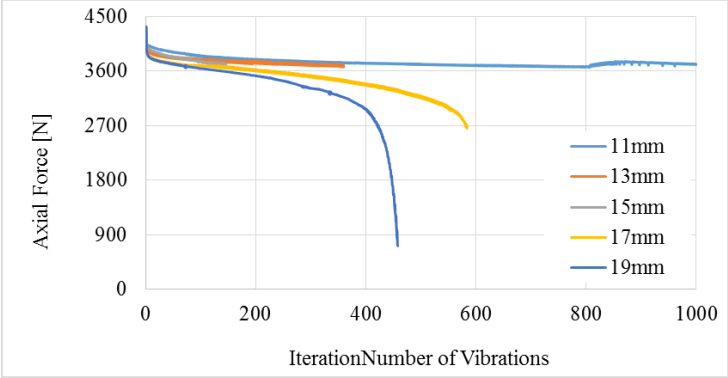

Figure15. Changes on axial forces for line width of cross-sectional cutting shape: 0.9mm

Conclusion

In this study, parametrical studies are executed to evaluate the affections of different design variables, such as line width of cross-sectional cutting shape and helical pitch applied to screw structures, on the self-loosening preventive effects of threaded fasteners. From analytical results, the following conclusions are obtained.

1. Utilization of new designed screw/bolt structures with small helical cutting pitch are very effective to obtain self-loosening preventive threaded fasteners.
2. For cross-sectional cutting shape with thicker line width, self-loosening preventive functions can be obtained for more cases of different helical cutting pitch.
3. Combination between helical cutting pitch and line width are very important for the self-loosening preventive effect of threaded fasteners using different screw/bolt structures.

Because the deterioration on strengths of bolts caused by the helical cutting processing on screw structures, strength evaluation should be carried out for threaded fasteners using the new designed screw/bolt structures in the future study.

References

Yamamoto A., Kasei S., *Investigations on the Self-loosening of Fasteners under Transverse Vibration*, Journal of the Japan Society for Precision Engineering, Vol.43, No4, (1977), pp.470~475.

Izumi S., Yokoyama T., Iwasaki A., Sakai S., *Three-dimensional Finite Element Analysis on Tightening and Loosening Mechanism of Bolted Joint*, Transactions of the Japan Society of Mechanical Engineers, Series(A), Vol.71, No.702, (2005), pp204~212.

Kamiya S., Izumi S., Sakai S., Yamada Y., *Loosening Analysis for Swing Circle Tightening Body of Excavator Subjected to Impact Loading,* Explicit Finite Element Approach, Transactions of the Japan Society of Mechanical Engineers, Series(A), Vol.78, No.795, (2012), pp99~107.

Atsushi Noma, Jianmei He, *Conceptual Design Study on Bolts for Self-Loosening Preventable Threaded Fasteners*, Materials Science and Engineering 269, (2017), doi:10.1088/1757-899X/269/1/012076

IMPROVEMENT ON TENSILE STRENGTH AND FATIGUE PERFORMANCES OF MESHED GUM METAL PLATES FOR BONE GRAFT APPLICATIONS

Koki SEKIGUCHI, Jianmei HE

Kogakuin University, Department of Mechanical Engineering, Tokyo, Japan
e-mail: Am16040@ns.kogakuin.ac.jp

Abstract: Degenerative intervertebral discs have a sign of epidemic as one of diseases caused by aging and lifestyle habits. Currently practiced treatments called spinal fusion surgery using pure titanium or titanium alloy implant products have the problems like overloading on healthy nature bones caused by the extra stiffness and heavy weight of such metal implants. Therefore, creation of implant products that meets mechanism like density, elasticity/rigidity of nature bones are required to reduce the burden on patient's health bones. Meshed titanium plates for bone graft applications have improved with excellent three-dimensional (3D) flexibility, lower elastic modulus and higher strength in previous studies. In this study, mesh structures as applied on Gum Metal plates with high biocompatibility are interested and their tensile strength/fatigue performance are investigated through analytical and experimental approaches for implant application on intervertebral disc defections. Based on different basic mesh shapes designed in this study, sample meshed Gum Metal plates were fabricated by laser cutting process and tensile fatigue experiments were executed. It concluded that high strength and fatigue performance of meshed Gum Metal plates can be obtained by using with some kind of designed basic mesh shapes.

Keywords: Tensile Strength, Fatigue Performance, Mesh Structure, Gum Metal Plates, Analytical and Experimental Approaches

Introduction

Recently in Japan, degenerative intervertebral discs have a sign of epidemic as one of diseases caused by aging and lifestyle habits. Degenerative intervertebral discs include lumber disc herniation, intervertebral disc herniation and cervical disc herniation. Table 1 shows the comparison of annual case numbers of these patients with/without surgeries having been increased year by year.

Table 1: Comparison of annual case number of surgeries for hernia of intervertebral discs

Individual surgeries	Total case number		Average days in hospital	
Accumulation period	2014.4～2015.3	2016.4～2017.3	2014.4～2015.3	2016.4～2017.3
Surgical removal	7,152	8,216	11.5	10.6
Other surgeries	17,187	17,156	18.0	17.3
No surgeries	16,590	17,246	9.8	9.9
Total throughout the year	40,929	42,618	13.5	13.0

In this study, disc herniation as one type of disc defects is interested. Disc herniation means that the intervertebral disc protrudes beyond the normal intervertebral space to compress the nerve and cause pain as shown in Fig.1. The treatment for disc herniation varies depending on different conditions. One of the currently practiced treatments is called spinal fusion surgery using metallic implants as also shown in Fig. 1. In this treatment, the upper and lower spinal cords of the defective disc are fixed using pure titanium or titanium alloy implant products. However, there is a problem that the loads caused by the titanium metal implants on the nature bones of the human body are large and will cause overloading on healthy nature bones[1]. Therefore, in order to reduce the loads on patient's health bones, creation of flexible implant products matching the mechanism such as the elasticity and rigidity of natural bones are desired as much as possible.

Mesh structure[2] applications are then considered for Gum Metal plates as applied on spine for hernia of intervertebral discs. Basic mesh shapes are designed and applied for Gum Metal plates and mechanical performances such as bending stiffness, tensile strength and fatigue performances of such meshed Gum Metal plates are experimentally and analytically evaluated[3]~[6]. The purpose of this study is to improve the tensile strength and fatigue performances of meshed Gum Metal plates as applied for hernia of intervertebral discs.

Fig. 1 MRI image of disc herniation (left) and metallic implant installation examples (right)

Design of Basic Mesh Shapes for Meshed Gum Metal Plates

Mechanical characteristics of Gum Metal plates

As shown in Fig. 2, Gum Metal material shows characteristics like relatively low elasticity rigidity, high strength, large elastic deformability and high biocompatibility compared with other metals and metal alloys.

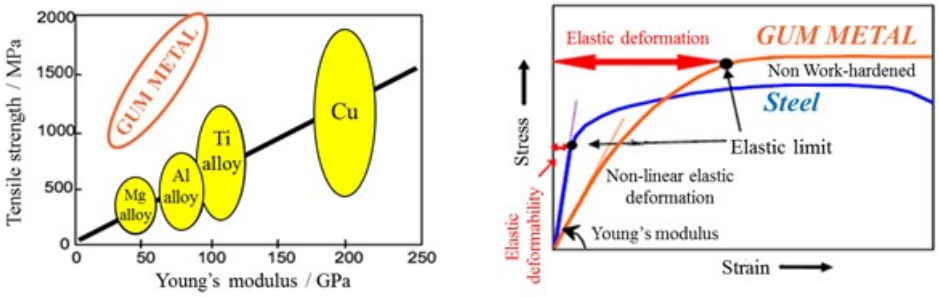

Fig. 2 Comparison of mechanical properties between GUM METAL and other metals

Designed basic mesh shapes and model of meshed Gum Metal plates

Basic mesh shapes are designed under the following design conceptions.

(1) Single fundamental mesh shape construction for simplification of manufacturing processing and cost-down purpose
(2) Higher three-dimensional flexibilities including expansion/contraction, bending and torsion for possibility of handily shape changes during surgery
(3) Easy-controllable mechanical properties like elastic modulus, bending stiffness etc. for approachability to natural-bone's mechanical properties

Fig. 3 shows an example of the meshed structure with S curves obtained by patterning the basic mesh shape following the above design concepts.

Fig. 3 Example of meshed structure with S curves from basic mesh shape pattern

Two types of basic mesh shapes are designed based from regular tetragon and regular hexagon, 90° and 60° axisymmetric mesh shapes, following the above mentioned design concepts using 3D CAD software SolidWorks

as shown in Fig. 4. The radius *R* and diameter *D* of the circles shown in Fig. 4 are taken as design variables of basic mesh shapes for parametric studies. For each types, basic mesh shapes are introduced for analytical and experimental approaches having different design variables and including the improved mesh designs of 90° axisymmetric 90°-④ and 90°-⑤ as shown in Fig. 5. Using these basic mesh shapes, prototype meshed plate models of meshed plates are then created and also shown in Fig. 5. Meshed Gum Metal plate specimens are then manufactured by laser-cutting processing as shown in Fig. 6. These meshed plate specimens are subjected to tensile fatigue experiments to evaluate their tensile fatigue characteristics and shape models are used for stress analysis. The influence on the stress concentration of the meshed plate specimens by different design parameters are evaluated by finite element analysis through ANSYS Workbench.

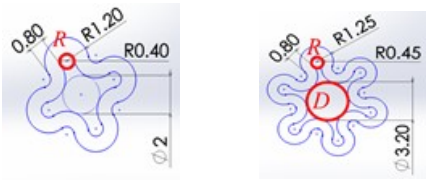

Fig. 4 Design variables of basic mesh shapes (left: 90° axisymmetric type, right: 60° axisymmetric type)

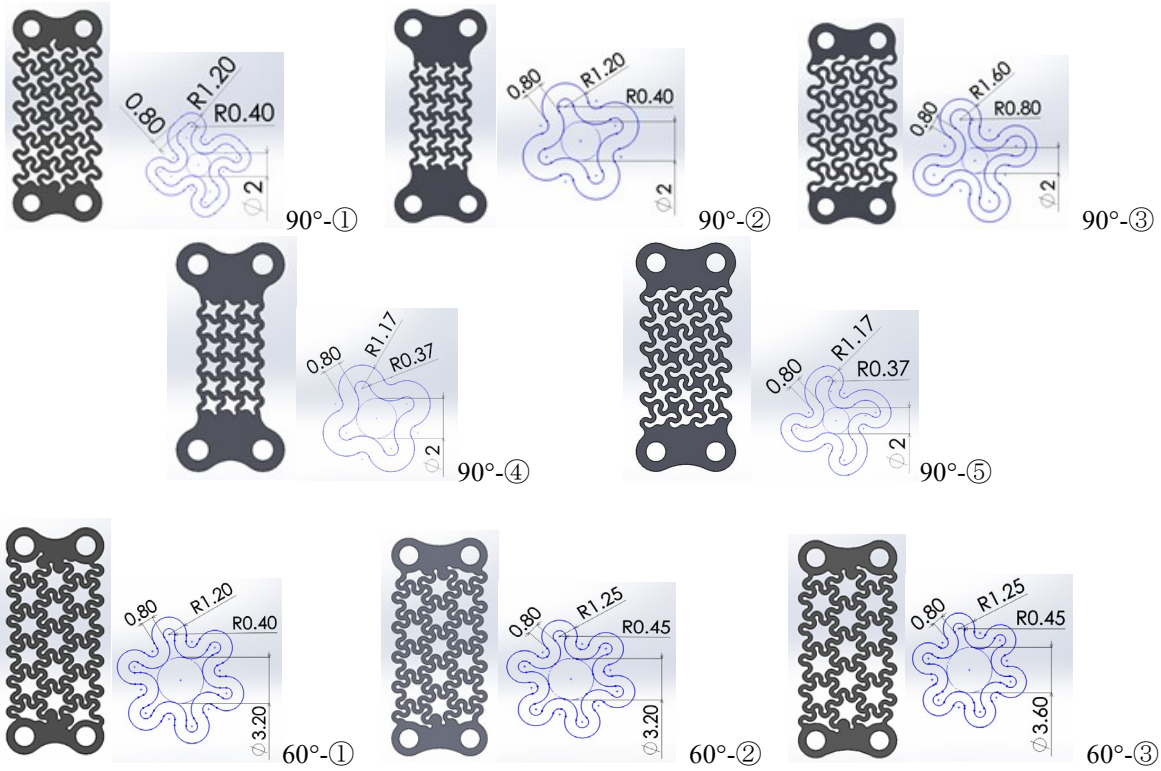

Fig. 5 Basic mesh shapes and meshed plate models for meshed Gum Metal plate specimens (90° axisymmetric shapes: ①-⑤, 60° axisymmetric shapes: ①-③)

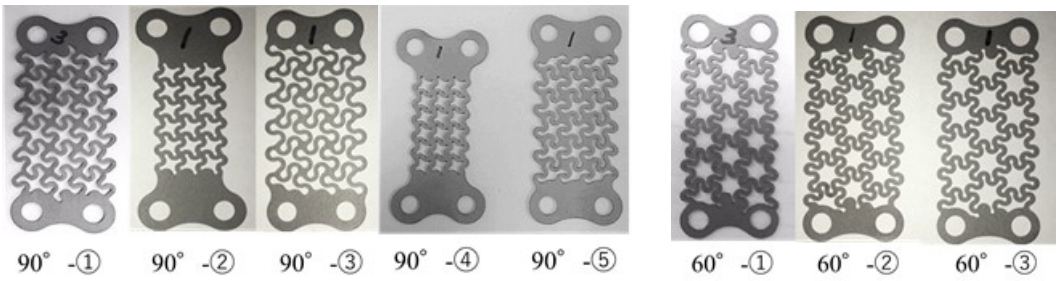

Fig. 6 Sample meshed Gum Metal plate specimens for tensile fatigue tests (left: 90° axisymmetric shapes ①-⑤, right: 60° axisymmetric shapes ①-③)

Tensile Fatigue Characteristics of Meshed Gum Metal Plates

Tensile fatigue experiment on meshed Gum Metal plates

Tensile fatigue tests of meshed Gum Metal plate specimens were conducted based on JIS standard Z 2273 using special fixtures necessary for thin plates. Total 36 specimens of 6 types of meshed plates were tested with testing machine (Asahi Seisakusho FRS-20) and specimen installation as shown in Fig. 7. The amplitude of iterated tensile loads were ranged from 20N to 90N with 10N amplify and 5N minimum tensile loading as shown in Table 1. The frequency of tensile load iteration was set at 10Hz.

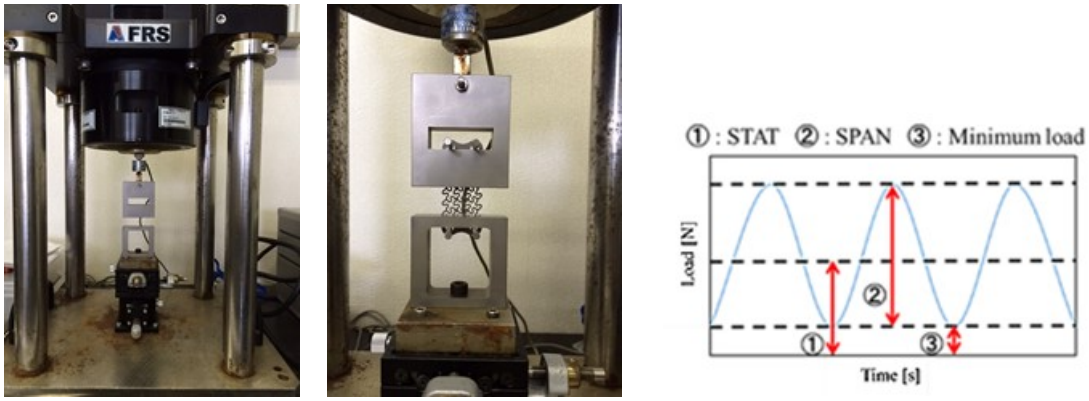

Fig. 7 Tensile fatigue experiment and meshed Gum Metal plate specimens with machine, fixtures and settings

Table 1 Tensile fatigue test tensile loads (90° and 60° axisymmetric specimens)

No. of specimen	No.1~No.6
SPAN [Np-p]	20N~90N
STAT [N]	25N~95N
FREQ [Hz]	10.0

Stress analysis for meshed Gum Metal plates under fatigue tensile loading

It is difficult to use the effective cross-sectional area of the meshed plate specimens for stress calculations because of the complex meshed shapes. Then stress analyses using finite element analysis software ANSYS Workbench were carried out in order to grasp the maximum Von Mises stresses under iterated tensile loading of the tensile fatigue tests. Fig. 8 shows the image of finite element mesh for sample meshed plate specimen models and Table 2 shows the finite element mesh information for all types of meshed plate specimen models. Material properties of Gum Metal shown in Fig. 2 are used for analytical approach.

From the obtained stress contour plots of sample 90° and 60° axisymmetric specimens also shown in Fig. 8, it can be confirmed that the stress concentrations occurred at the same locations and didn't change so much for different specimen types under different tensile loading. Maximum Von Mises stresses with respect to tensile loads obtained from these analytical results are shown in Fig. 9 of sample meshed plate specimen models with different design variables.

Table 2 Analytical conditions for each meshed GUM METAL plates (90° and 60° axisymmetric models)

Analytical conditions	90°-①	60°-①	90°-②	60°-②	90°-③	60°-③	90°-④	90°-⑤
Element size [mm]	0.124	0.125	0.122	0.125	0.128	0.122	0.129	0.129
Number of elements	179,235	187,380	202,740	187,380	188,995	194,304	163,476	201,246
Number of nodes	232,962	240,695	249,774	240,695	245,046	247,303	201,306	252,679

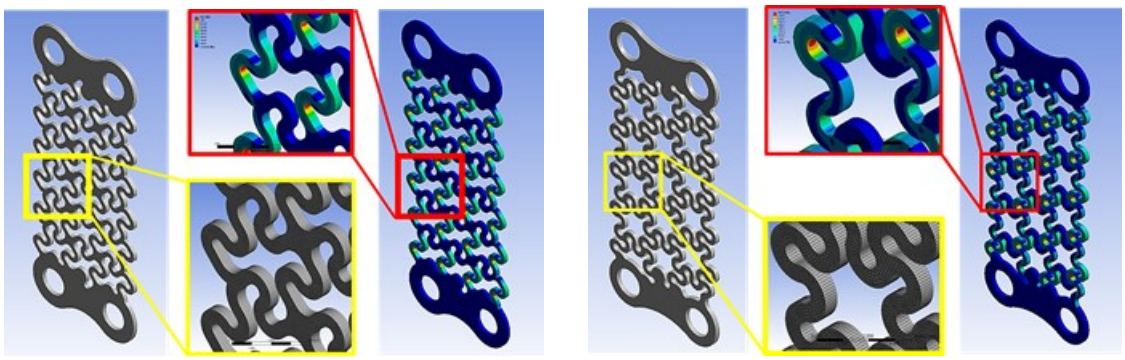

Fig. 8 Finite element mesh and tensile stress results of sample meshed plate models (left: 90°-①, right: 60°-③)

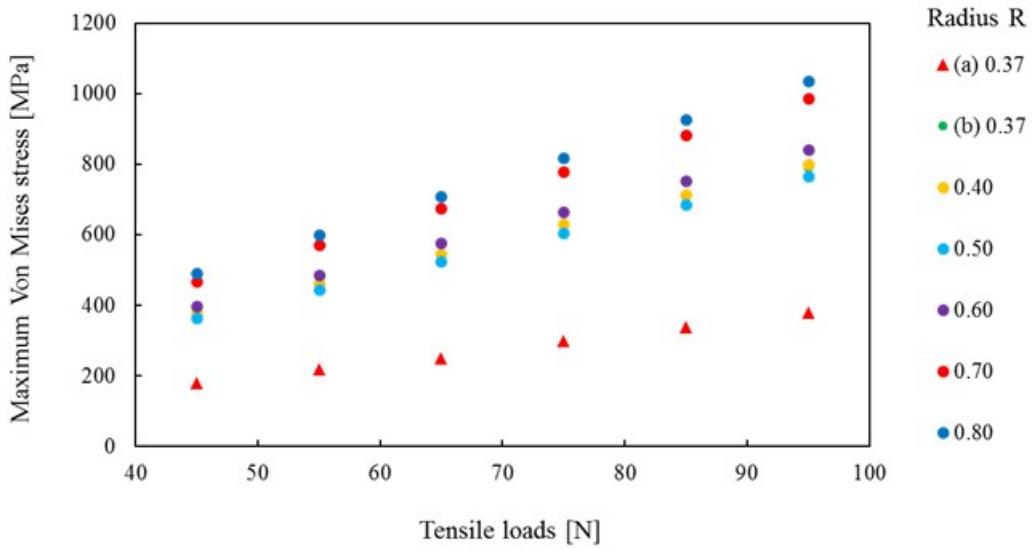

Fig. 9 Maximum Von Mises stress results with respect to tensile loading (90°: circle, 60°: triangle)

Results and Discussion

Tenisle fatigue characteristics of sample meshed Gum Metal plate specimens

Firstly, Fig. 10 and Fig. 11 show the fractured photographs of sample 90° and 60° axisymmetric meshed Gum Metal plate specimens after tensile fatigue tests. Compared with the stress contour diagram of the tensile stress analysis results as shown in Fig. 8, it can be seen that meshed plate specimens fractured at the same location with the stress concentration occurred.

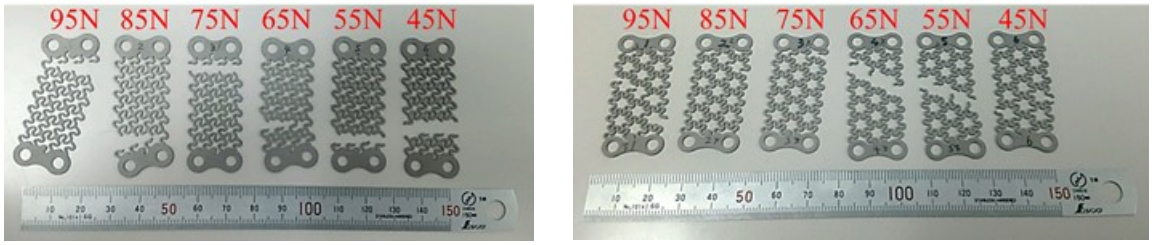

Fig. 10 Meshed Gum Metal plate specimens after tensile fatigue tests
(left: 90° axisymmetric specimen ①, right: 60° axisymmetric specimen ③)

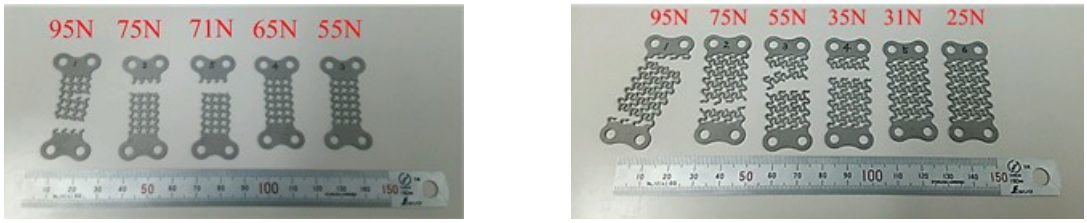

Fig. 11 Improved meshed Gum Metal plate specimens after tensile fatigue tests (left: 90°-④, right: 90°-⑤)

Secondly, the maximum Von Mises stress results are shown in Fig. 12 with respect to maximum iteration number of tensile loading until specimen fractured, combined with experimental and analytical results on the tensile fatigue tests of sample meshed Gum Metal plate specimens. Vertical axis represents the maximum Von Mises stresses under different tensile loads from finite element analysis, and horizontal axis represents the maximum iteration number of tensile loads obtained from the tensile fatigue experiments.

From these results shown in Fig. 12, durability of meshed Gum Metal plate specimens changed little with 60° axisymmetric type specimens under different design variables, which was different with the type of 90° axisymmetric specimens.

On the other hand, the maximum Von Mises stress results of improved meshed Gum Metal plate specimen 90°-④ and 90°-⑤ are also plotted on Fig.12 with respect to maximum iteration number of tensile loading until specimen fractured. From these results shown in Fig. 11 and 12, it can be seen that the improved 90° axisymmetric specimen ④ and ⑤ have both reached the fatigue limit at 10^7 iteration number with lower maximum Von Mises stress value and without specimen fractured. Both improved meshed Gum Metal plate specimens 90°-④ and 90°-⑤ show the same maximum Von Mises stress value approximately 200MPa as the tensile fatigue limit of meshed Gum Metal plates, although under different amplitude of tensile loads.

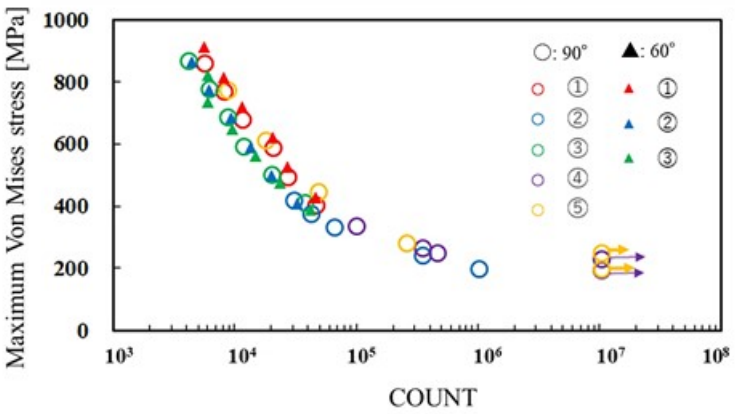

Fig. 12 Combined results of tensile fatigue tests for all sample meshed Gum Metal plate specimens (90°: circle, 60°: triangle)

Improved basic mesh shapes for 90° axisymmetric meshed plate specimens ④ and ⑤ have the following characteristics compared with original 90° and 60° axisymmetric specimens.

(1) Gentle curvatures of S curves caused by the basic mesh shapes
(2) Small S curves with minimum value of radius R of basic mesh shapes
(3) Smaller projected area per basic mesh shape with enough strength to withstand fatigue tensile loads

As the curvature degree of S curve decreases in the improved basic mesh shapes ④ and ⑤, the tensile loads are dispersed and caused lower maximum Von Mises stresses on meshed plate models. It was found that maximum Von Mises stress of the obtained meshed plate specimens can be suppressed and then it's effective to increase the iteration number of fatigue tensile test. It can be concluded that changing the S curves caused by design parameters like radius *R* in basic mesh shapes will affect the stress concentration, and as the results, greatly affect the tensile fatigue characteristics of meshed plate models.

Totally, from the experimental and analytical results obtained in this study, tensile fatigue characteristics of meshed Gum Metal plates are influenced by the stress concentrations mainly caused by S curves of basic mesh shapes. It is considered that for each type of meshed plate specimens, different tensile loads should be determined from finite element analysis to obtain lower than 200MPa maximum Von Mises stresses for meshed Gum Metal plates to reach the tensile fatigue limit at 10^7 iterations.

Conclusion

Experimental and analytical evaluation on tensile fatigue characteristics of meshed Gum Metal plates were executed. From the experimental and analytical results,

(1) Fractures were occurred at the inflectional locations with large curvatures for both type of the specimens, and coincident with the stress concentration locations obtained from analytical results.
(2) The change in curvatures of basic mesh shapes was found to greatly affect maximum tensile stress results. It was also found to effect on experimental results of sample meshed plate specimens, such as the number of cycles at final fractures under different tensile fatigue loads. On the other hand, it was found that changing the central circle diameter D of basic mesh shape would hardly affect the tensile fatigue characteristics of sample meshed plate specimens.
(3) By broadening the tensile load ranges of tensile fatigue tests for different sample specimens, it was confirmed that maximum Von Mises stresses from the sample meshed plate models with different basic mesh shapes can be grasped analytically and then to reach the tensile fatigue limits of meshed plate specimens.

Therefore, design change on meshed structures such as adjustment of the curvature of S curves caused by the pattern of basic mesh shape are effective for improving the fatigue resistance characteristics of meshed plates under tensile loading.

References

Mayfield Brain & Spine Q&A, http://www.mayfieldclinic.com/QA_ArtificialCervicalDisc.htm (Reference Date July 10, 2018)

Jianmei HE, Shigeki Suzuki, Ung-il Chung, Developments of 3D free form titanium mesh plates for implantation (Design of mesh structures for titanium mesh plates), Transactions of the JSME (in Japanese), 2014, pp.1-15 Vol. 80, No 809.

Hitoshi OHARA, Kazutomo Imai, Jianmei He, Evaluation on Mechanical Properties of 3D Flexible Meshed Gum Metal Plate Implants, 2016, The 24th International Congress of Theoretical and Applied Mechanics (ICTAM2016)

Yuki Hamashita, Jianmei He, Investigations on Fatigue Properties of Meshed Gum Metal Plates for Bone Graft Applications, 2016, The 24th International Congress of Theoretical and Applied Mechanics (ICTAM2016)

Hiromichi SUZUKI, Jianmei HE, Evaluation on Bending Properties of Biomaterial Gum Metal Meshed Plates for Bone Graft Applications, 2017, The International Conference on Material, Mechanical, and Manufacturing Engineering (ICMMME 2017)

Koki SEKIGUCHI, Jianmei He, Investigation on Tensile Fatigue Characterization of Meshed Gum Metal Plates as Applied for Bone Graft Applications, 2017, The International Conference on Material, Mechanical, and Manufacturing Engineering (ICMMME 2017)

Introduction of Gunmetal, http://www.nissey-sabae.co.jp/wp/wp-content/uploads/GUMMETAL.pdf (Reference Date July 10, 2018)

INVESTIGATION ON DEVELOPMENT OF HIGH PERFORMANCE MEDICAL STENTS AS APPLIED WITH MESH STRUCTURES

Shoji ASANO, Kazuki HIRAYAMA and Jianmei HE

Kogakuin University, Department of Mechanical Engineering, Tokyo- Japan

e-mail:am17001@ns.kogakuin.ac.jp

Abstract: There are concerns about the occurrence of fatigue fractures caused by stress concentrations due to different shape structures and manufacturing methods in conventional stents, and then new stents having high strength and high flexibility are required. Applicable mesh structures for medical stent applications based on the design concepts of high strength and flexibility are designed to solve various problems of conventional stents in this research. The influence of introduced design variables of basic mesh shapes on compression characteristics of meshed stent models are evaluated through finite element analysis using ANSYS Workbench. From analytical results, compressive stiffness of meshed stent models are found to be changed periodically with compressive directions due to the designed basic mesh shapes. Secondly, compressive flexibility of meshed stent models mostly depends on arm's number and shapes of basic mesh shapes. It concluded that the compressive performance of designed meshed stent models in this study can be easily controlled by increase some design variables like angle proportional to the arm length of designed basic mesh shapes and get closed to conventional medical stents with higher strength performances.

Keywords: Medical Stents, Mesh Structure, Finite Elements Analysis, Compressive Stiffness

Introduction

In recent years, stenosis and occlsion have occurred in body lumen such as blood vessels, bile ducts, trachea and other like indispensable for maintenance of human life as in the superficial femoral artery (SFA) occlusion caused by disease. As an effective treatment for such stenosis and occlusion, indwelling of medical stents is performed. The inside of the living body lumen where the stents are placed is a corrosive environment with complicated structures and severe movements. The difficult environment may cause rejection reactions when foreign matter intrudes. Therefore, it is required that medical stent devices applied for the living body lumen have high flexibility, excellent biocompatibility, high strength and durability etc.

However, ready-made conventional medical stents have concerns that the design and manufacturing methods for stent shape structures have caused stress concentrations and then lead to fatigue fractures due to pulsation, or caused neointimal hyperplasia due to strong radial forces generated on the inner wall of the stents [1]~[9]. Therefore, there are needs for medical stents having high strength and high flexibility capable of following severe movements combined with bending, torsion, expansion and contraction in SFA.

Therefore, the purpose of this research is to design applicable mesh structures [10] for medical stent applications to solve the above mentioned problems. Meshed stent models with higher strength and higher flexibility with integral molding are designed and investigated analytically using finite element analysis code ANSYS. The compression characteristics of meshed stent models are examined through finite element analysis and reported in this paper.

Design of Meshed Stent Model with Mesh Structures

Based on the design concepts of mesh structures with high strength and high flexibility [10], six types of mesh basic shape are designed in this study and applied for meshed stent models as shown in Figure 1. For these mesh basic shape applied stent models shown in Figure 1, the number of basic mesh shape arranged in stent circumferential direction (hereinafter called "N") is changed from 6 to 8, and the angle affecting to arm length (hereinafter called "θ") is changed from 0° to 60°. Three design variables, such as mesh line width (hereinafter called "w"), the angle affecting to arm length "θ" and number of basic mesh shape "N" as shown in Figure 2, are introduced for easy understanding. Then meshed stent models are designed for all combinations of N and θ. In addition, hexagonal based meshed stent models [11] are also introduced in this research for comparison. The diameter of stent cylinder model is set at 6.0mm, the strut thickness is set at 0.18mm and w is set at 0.1mm as layout sizes of meshed stent models for analytical approaches. These stent model sizes are same as the medical stents used in SFA.

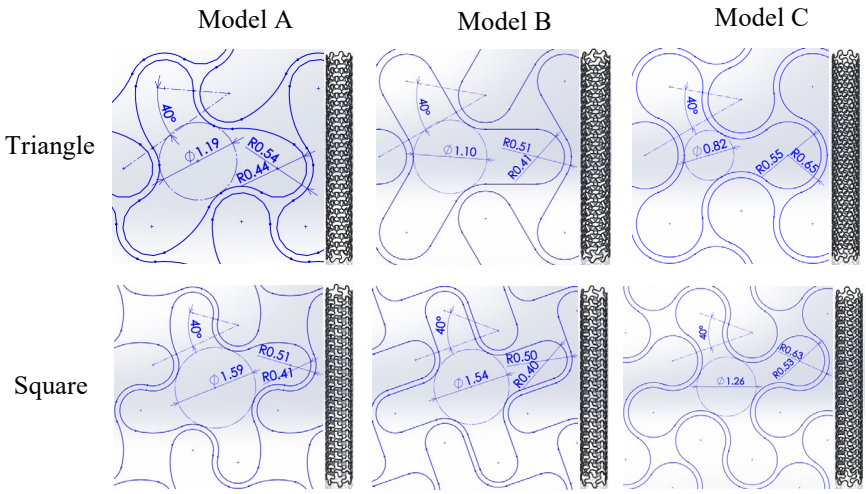

Figure 1. Basic mesh shapes with applied meshed stent models (Triangle and Square)

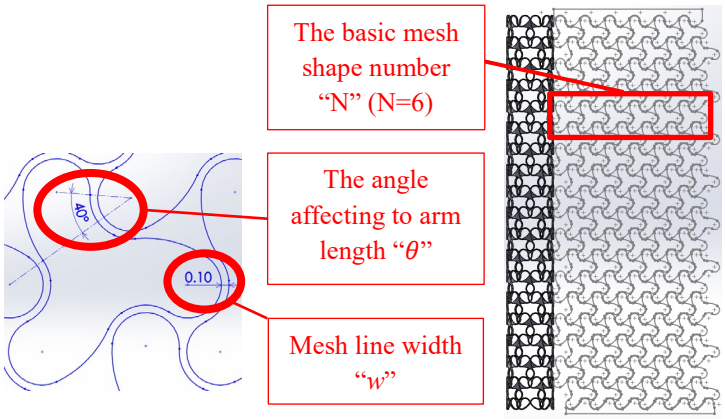

Figure 2. Design variables introduced for analytical approach: mesh line width "w", the angle affecting to arm length "θ" and the number of basic mesh shape arranged in the stent circumferential direction "N"

Evaluation of Compression Characteristics in the Vertical Direction to Cylindrical Axis of Meshed Stent Models

Compression characteristics in the vertical direction to cylindrical axis of meshed stent models were analyzed and evaluated using finite element analysis software ANSYS Workbench. Meshed stent models are sandwiched between flat jigs and applied with compressive load of 10 N in the direction perpendicular to stent cylinder axis as shown in Figure 3. Table 1 shows the material properties and finite element mesh settings for meshed stent modeling. Figure 3 also shows the image of typical finite element mesh of meshed stent model including compressive fixtures.

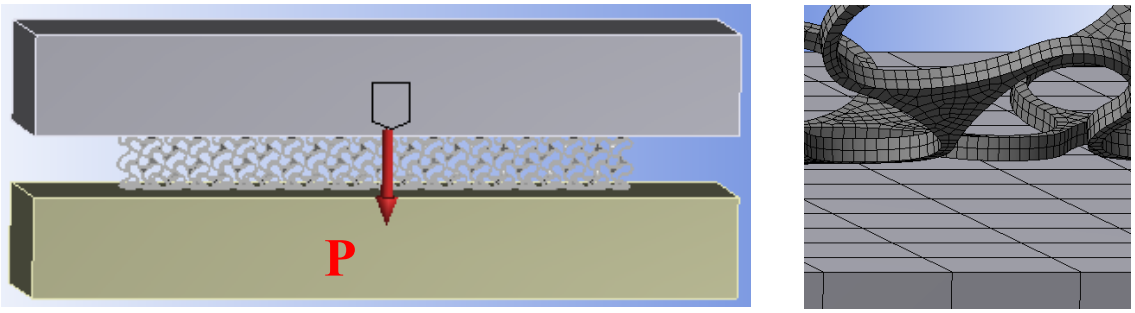

Figure 3. Compression of meshed stent model with flat jigs and typical finite element mesh for meshed stent modeling

Table 1: Material properties of nickel-titanium, and finite element mesh settings

Material properties	Material	Nickel-titanium alloy
	Poisson's ratio	0.3
	Modulus of longitudinal elasticity [GPa]	75
Finite element mesh setting	Size of elements [mm]	0.09～0.10
	Number of element in thickness direction	2～3

In this research, compression characteristics of meshed stent models are evaluated by calculation of compressive stiffness. Compressive stiffness can be calculated by equation (1) and represents the supporting ability of the meshed stent to blood vessel. Compressive stiffness k is then calculated by fitting the deformation δ with compressive load P applied to the meshed stent model as following.

$$k=\frac{P}{\delta} \quad (1)$$

where k : Compressive stiffness [N/mm]
P : Compressive load [N]
δ : Displacement [mm]

Compressive stiffness characteristics of meshed stent models using regular triangle, square and hexagon based mesh shapes

In this section, compressive stiffness of meshed stent models using regular triangle, square and hexagon based mesh shapes are evaluated with fixed w at 0.1 mm and different N and θ. Analyses are carried out to examine the periodicities of meshed stent models due to different basic mesh shapes by rotating the compressive directions round the cylindrical axis from 0° to an angle obtained by dividing 360° by N. Typical compressive stiffness results of different meshed stent models are shown in Figure 4.

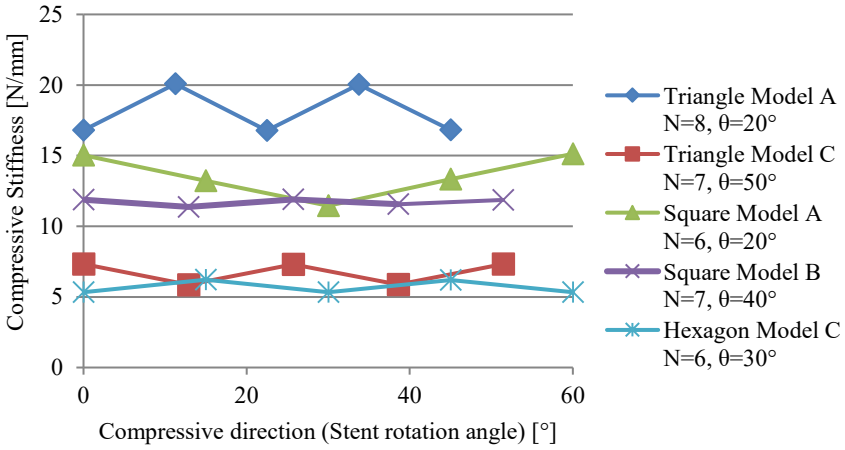

Figure 4. Compressive stiffness of meshed stent models with respect to compressive direction

From these results, it can be seen that the compressive stiffness shows periodicity with the change of the compressive direction. It is considered that the major factors for the periodicity are the axisymmetric basic mesh shapes combined with their numbers used for the meshed stent models.

Maximum deviation in compressive stiffness caused by changing the compressive directions for meshed stent models is found as 7.45 N/mm, which is obtained from Square based Model A with N=8 and θ=40° meshed stent model. On the other hand, minimum deviation in compressive stiffness caused by changing the compressive directions for meshed stent models is found as 0.01 N/mm obtained from Square based Model C with N=7 and θ=50° meshed stent model. In the results of this research, it was found that square based models showed most small deviation in compressive stiffness caused by changing the compressive directions, but it was found that the deviation in compressive stiffness is less likely to occur in the hexagon than the triangle and square. For triangle and square based models, there are many models showing deviation more than 3.0 N/mm in compressive stiffness caused by changing the compressive directions, while for hexagon based models showing less than 2.0 N/mm deviations.

In addition, as a tendency of the changes in compressive stiffness of different compressive direction of the meshed

stent model, in the case of square based models, it was found that the deviation in compressive stiffness becomes sensitive with the even number of mesh shape N. On the other hand, in the case of triangle based model, the deviation in compressive stiffness was not greatly influenced by the number of mesh shape N. It is conceivable that the arrangement of basic mesh shapes on the side of meshed stent models affects these kinds of tendency.

In the case of square based mesh shapes, when the mesh shape boundary shown in Figure 5 is arranged on the side furthest from the compressive surface lines, the stress caused by compressive force is well dispersed and lead to lower compressive stiffness. On the other hand, when the mesh shape center shown in Figure 5 is arranged on the side furthest from the compressive surface lines, stress concentrations tend to be occurred and lead to higher compressive stiffness. When N is an odd number, the mesh shape center appears on one side furthest from the compression surface lines, and a mesh shape border appears on the other side of meshed stent model. However, when N is an even number, it is clearly distinguished ether the mesh shape center or mesh shape boundary appears on both sides furthest from the compressive surface lines. Therefore, in the case of square based models, when N is an even number, the deviation between highest and lowest value of compressive stiffness caused by changing the compressive directions tends to be large.

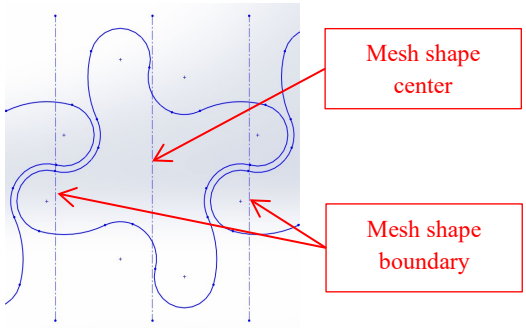

Figure 5."Mesh shape center" and "Mesh shape boundary" in mesh basic shape

From the above discussion, it is necessary to analyze the compressive stiffness of meshed stent models by changing the compressive direction. Then, it is necessary to introduce the average value of compressive stiffness due to the periodicity to evaluate the compression characteristics of meshed stent model. From these results one can see that there is a concern that the blood vessel wall can't be evenly supported using the meshed stent models, and it is necessary to reduce the periodic changes in their compressive stiffness.

Influence of the angle affecting to arm length θ on the compressive stiffness of meshed stent models in direction perpendicular to the cylindrical axis

In this section, effects of the angle affecting arm length to the compressive property of meshed stent models using triangle, square and hexagon based mesh shapes are to be evaluated with basic mesh shape number N setting at 6, 7 and 8, and fixed w of 0.1 mm. Analyses are carried out with changing θ between 0° and 60°. Obtained typical results are shown in Figure 6.

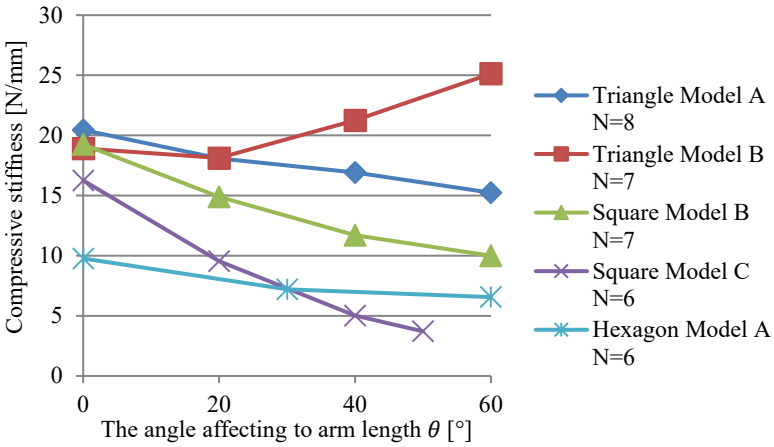

Figure 6. Influence of the angle affecting to arm length θ on the compressive stiffness of meshed stent models

From analytical results, except for triangle Model B, it was found that compressive stiffness is reduced by enlarging θ of all kind of meshed stent models. In particular, in three kind of Model C, the compressive stiffness can be greatly reduced by increasing the design variable "θ". In the triangle based models, Model C N8 showed the most reduced compressive stiffness with a large deviation of 12.61 N/mm created when the arm angles change from 0 ° to50 °. Even with the square based models, Model C N8 showed the most reduced compressive stiffness with a large deviation of 14.66 N/mm created when the arm angles change from 0° to 50°. On the contrary, the compressive stiffness of Model A is hardly to be reduced, like in triangle based Model A within 2.35 N/mm deviations, and like in square based Model A within 4.19 N/mm when the arm angles change from 0° to 60°. By making θ larger for Model C than Model A, it is easier to deepen the curvature of the basic mesh shape, and then improve the flexibility of meshed stent model and lead to different responding.

For triangle Model B, as θ increased, the constant mesh line width portion becomes shorter and then the compressive stiffness of meshed stent model can be considered becoming higher. As shown in Figure 7, in the 20° model, the entire mesh shape is configured with a large constant mesh line width area surrounded in the frame. However, in the 60° model, there are considerably few places where the mesh line width is constant. This is the considered main reason to cause the increase in compressive stiffness of meshed stent model as θ increased.

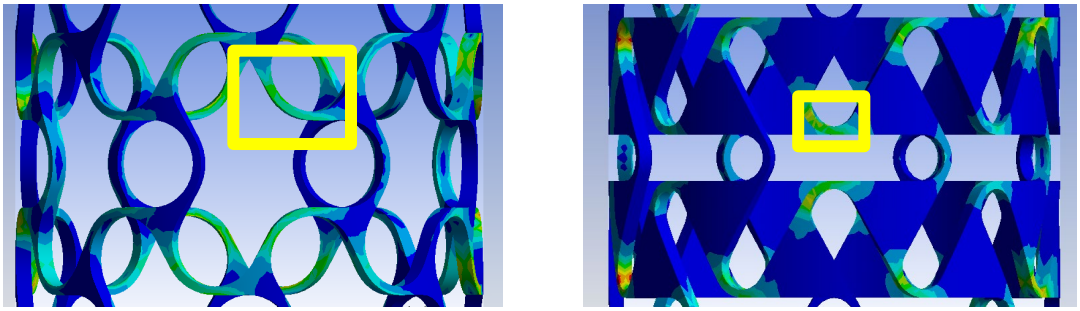

θ = 20° θ = 60°

Figure 7. Equivalent stress diagram accompanying with change in the angle affecting to arm length θ (Triangle, Model B, N8)

Also in both triangle and square based models, if θ was the same, the compressive stiffness tended to be smaller in the model with smaller N. On the contrary, with the fixed mesh shape based stent models, the ratio of reduction in compressive stiffness caused by extension of arms is roughly the same regardless of N. For example, in the square based Model C, regardless of N, compressive stiffness decreased by about 40% at 20° model, about 65% at 40° model, about 75% at 60° model compared with 0° model. A similar tendency can also be seen in the ratio of increase for triangle based Model B in which the compressive stiffness increased with θ increased. Even in the other models, with the fixed mesh shape based stent models, the compressive stiffness decreases almost similarly.

From all the analytical results, it can be seen, as a general trend, the triangle based stent models tend to have lower compressive stiffness than square based models. Furthermore, it can also be found that the compressive stiffness tends to be smaller with the hexagon based models than the triangle based models. The hexagon based stent models have overwhelmingly low compressive stiffness with small value of θ, while with θ increased, the triangle based or square based Model C would show lower compressive stiffness.

Evaluation of Compression Characteristics in the Radial Direction of Meshed Stent Models

In this chapter, compression characteristics in the radial direction of meshed stent models are analyzed and evaluated using finite element analysis software ANSYS Workbench. Assuming equally pressure from blood vessel toward to the stent cylindrical center axis is applied on the stent surface, a displacement of 2.0 mm is caused at the surface of the meshed stent model along the pressure direction. Then, from the analyzed reaction force generated on the surface of the meshed stent model, the compressive stiffness of the designed meshed stent model can be calculated. Figure 8 shows the 3D shape of the meshed stent model before/after deformation and the state of finite element mesh for analysis. In addition, the material properties shown in Table 1 are used in analysis, and the setting of finite elements mesh for meshed stent models are shown in Table 2.

In the radial compression analysis, as well as the evaluation of compression analysis in vertical direction to cylindrical axis, compressive stiffness of meshed stent model can be introduced as an evaluation index. Compressive stiffness of meshed stent models by radial compression analysis then can be calculated by equation (2) based on equation (1).

$$k = \frac{P}{\delta} = \frac{Q}{\Delta D} \tag{2}$$

where k : Compressive stiffness [N/mm]
Q : Reaction force generated on the stent surface [N]
ΔD : Stent diameter deformation amount [mm]

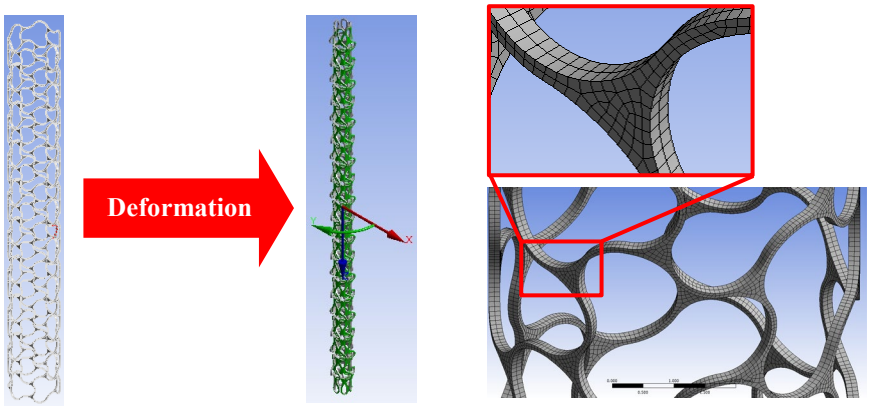

Figure 8. Radial compression analysis of meshed stent models with finite element mesh

Table 2: Finite element mesh setting for radial compression analysis of meshed stent model

Size of elements [mm]	0.08
Number of element in thickness direction	2

Influence of the angle affecting to arm length θ on radial compressive stiffness of meshed stent models
In this section, the influence of the angle of the arm affecting to arm length "θ" relative to the radial compression characteristics of different meshed stent models with number of mesh shape N at 6, 7, 8, and fixed mesh line width w at 0.1 mm are evaluated. Analyses are carried out with changing θ from 0° to 60°. Some of typical obtained results are shown in Figure 9.

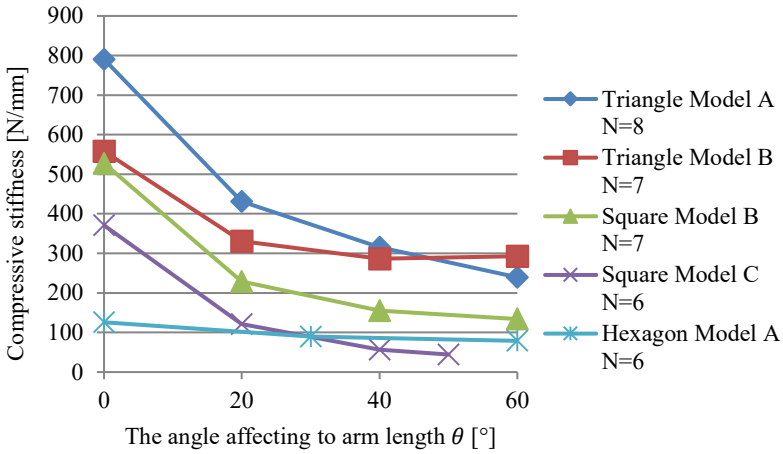

Figure 9. Influence of the angle affecting to arm length θ on the radial compressive stiffness

From the analytical results, it was found that the radial compressive stiffness is reduced by increasing design variable θ in all meshed stent models. In addition, with same number of mesh shape N, radial compressive stiffness of meshed stent models can be most reduced by increasing θ of the Model C. In the triangle based

models, the decrease in radial compressive stiffness of Model C N8 was the largest of more than 700 N/mm with angle θ changes from 0° to 50°, which affects the mesh arm length. Even with the square based models, the radial compressive stiffness of Model C N8 decreased largely close to 700 N/mm with same angle changes from 0° to 50°.

Regarding the Model B, it was found that in the case of square based models, the effects of reducing radial compressive stiffness by extending the arm are larger than that of the Model A. While in the case of triangle based models, the reduction effects are reduced. The radial compressive stiffness of triangle and square based Model B at N = 8 and θ = 50° produced a difference of nearly 200 N/mm. The difference in radial compressive stiffness between triangle and square based other models are shown within 100 N/mm as the largest.

The hexagon based models show smaller radial compressive stiffness than the triangle and triangle based models with smaller "θ", but the effect of reducing the radial compressive stiffness by extending θ tends to be less. Therefore, when θ is smaller, the radial compressive stiffness of the hexagon based models may be lower than that of the triangle or square based models.

Relationship between vertical compression characteristics to cylindrical axis and radial compression characteristics of meshed stent models

In this section, the relationship between the cylindrical axis vertical compression characteristic and the radial compression characteristic will be examined. Based on the above mentioned analytical results, comparison on square based stent models are shown in Figure 10, in which the horizontal axis shows the vertical compressive stiffness and the vertical axis shows the radial compressive stiffness.

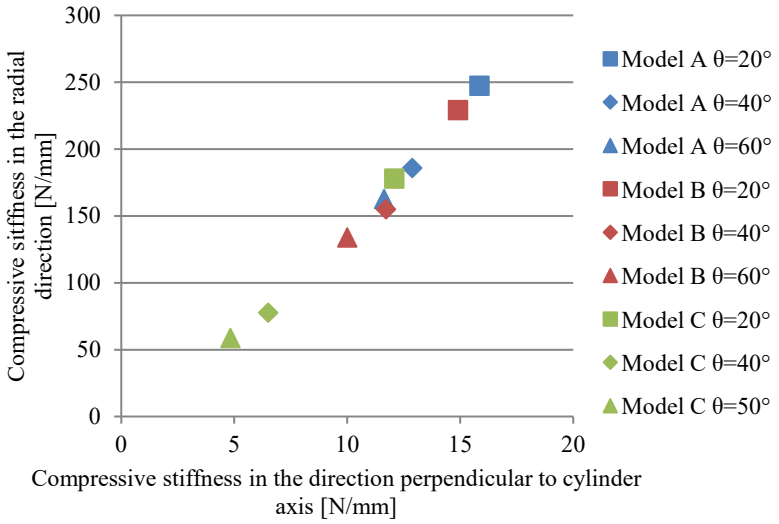

Figure 10. Comparison on cylindrical axis vertical compressive stiffness and radial compressive stiffness of square based N8 stent models

From Figure 10 one can see that radial compressive stiffness is higher than that in cylindrical axis vertical direction. In the case of vertical compression to the cylinder axis, meshed stent models are compressed from one direction, whereas in the case of radial compression, meshed stent models are compressed evenly from all directions, and then lead to higher radial compressive stiffness.

In addition, it was found that for both vertical compression to cylindrical axis and radial compression, the compressive stiffness decreases greatly with θ increased. It means that compression characteristics is very susceptible to the angle affecting to arm length θ of basic mesh shape. It is most effective way to reduce the compressive stiffness of meshed stent models by increasing design variable θ.

Further, strong correlations between vertical compression to cylindrical axis and radial compression can be found from these results shown in Figure 10, The correlation coefficients for different meshed stent Model A, Model B and Model C were found as 0.99, 0.98 and 0.99. These results shown in Figure 10 are from square based N8 stent models, similar tendencies can be observed for all other meshed stent models including hexagonal based models.

Conclusion

Based on the design concepts for mesh structures, meshed stent models are designed for SFA treatment stent application. Different design variables such as basic mesh shape type, number of mesh shape N and the angle affecting to arm length on the compression characteristics of meshed stent models are investigated using finite element analysis. From analytical results, the following conclusions are obtained.

(1) Since the compressive stiffness in the direction perpendicular to cylinder axis of meshed stent models vary periodically according to different compressive directions, it is necessary to introduce an average value for the compressive stiffness of meshed stent models.

(2) Combined with basic mesh shape and design variable of the angle affecting to arm length, the length with constant mesh line width might be extremely short even with large value of the angle affecting to arm length, then cause the increased compressive stiffness in the direction perpendicular to cylinder axis.

(3) Strong correlations between vertical compression to cylindrical axis and radial compression are found in the meshed stent models.

(4) Although there are some exceptions, it is possible to reduce the compressive stiffness of meshed stent models by increasing the design variable of the angle affecting to arm length.

(5) Hexagon based stent models have overwhelmingly low compressive stiffness with small angle affecting to arm length θ, but if θ becomes large, they would have about the same compressive stiffness as triangle or square based stent models.

References

Jaff M, Dake M, Pompa J, Ansel G, Yoder T. Standardized evaluation and reporting of stent fractures in clinical trials of noncoronary devices. Catheter Cardiovasc Interv 2007; 70: 460-2.

Kralj I, Boos I, Müller-Bühl U. Three year results of endovascular therapy with a new generation nitinol stent for femoro-popliteal artery lesionsda single-center outcome analysis of a subcohort of MISAGO 2 study. Vasa 2013; 42: 340-9.

Müller-Hülsbeck S, Schäfer PJ, Charalambous N, Yagi H, Heller M, Jahnke T. Comparison of second-generation stents for application in the superficial femoral artery: an in vitro evaluation focusing on stent design. J Endovasc Ther 2010; 17: 767-76.

Scheinert D, Scheinert S, Sax J, Piorkowski C, Bräunlich S Ulrich M, et al. Prevalence and clinical impact of stent fractures after femoropopliteal stenting. J Am Coll Cardiol 2005; 45: 312-5.

Schlager O, Dick P, Sabeti S, Amighi J, Mlekusch W, Minar E, et al. Long-segment SFA stenting-the dark sides: in-stent restenosis, clinical deterioration, and stent fractures. J Endovasc Ther 2005; 12: 676-84.

Schulte KL, Kralj I, Gissler HM, Bagnaschino LA, Buschmann I, Pernès JM, et al. MISAGO 2: one-year outcomes after implantation of the Misago self-expanding nitinol stent in the superficial femoral and popliteal arteries of 744 patients. J Endovasc Ther 2012; 19: 774-84.

Schulte KL, Müller-Hülsbeck S, Cao P, Becquemin JP, Langhoff R, Charalambous N, et al. MISAGO 1: first-in-man clinical trial with Misago nitinol stent. EuroIntervention 2010; 5: 687-91.

Yazdani SK, Berry JL. Development of an in vitro system to assess stent-induced smooth muscle cell proliferation: a feasibility study. J Vasc Interv Radiol 2009; 20: 101-6.

Zhao HQ, Nikanorov A, Virmani R, Jones R, Pacheco E, Schwartz LB. Late stent expansion and neointimal proliferation of oversized nitinol stents in peripheral arteries. Cardiovasc Intervent Radiol 2009; 32: 720-6.

He J, Suzuki S and Chung UI. Developments of 3D free form titanium mesh plates for implantation (Design of mesh structures for titanium mesh plates). Transactions of the JSME (in Japanese), Vol.80, No.809(2014), DOI:10.1299/taransjsme.2014smm0003.

Hirayama K, He J. Evaluation on Compressive Characteristics of Medical Stents Applied by Mesh Structures. IOP Conf. Series: Materialls Science and Engineering 2017; 269; 012075.

IS TURKEY REALLY A GLOBAL COMPETITOR IN YACHT BUILDING INDUSTRY?

Murat AYDIN[1], Tuğba Yılmaz AYDIN[2]

[1]Isparta University of Applied Sciences, Department of Material and Material Processing, Isparta-Turkey
murataydin@sdu.edu.tr

[2]Isparta University of Applied Sciences, Department of Forest Industry Engineering, Isparta-Turkey
tubayilmaz@sdu.edu.tr

Abstract: As it is well known, Turkey took place near the top of 24m or longer yacht building countries. In the world there are a few leading countries which dominate both production and other processes. In recent years, Turkey is one of the yacht building centers in the world and attracts not only key players' interest but also tourists' with long and beautiful coastal lines and long sunny season. From this point of view, Turkish yacht building industry investigated in terms of design and engineering, yards locations, yacht types, project length, installed engine, transmission or propulsion systems, navigation and telecommunication systems, generator, hull and superstructure materials and classification in this study. According to the results, it can be said that Turkey has lots of advantages to compete with the leading players of this industry but must be focused on added value activities to increase its share from the market.

Keywords: Yacht, Super or Mega Yacht, Turkish Yacht Building Industry

Introduction

Shipbuilding is one of the essential industries of the industrialized countries and it can be classified as commercial and pleasure in terms of type of vessels such as container ship or yacht, respectively. Both building activities are important due to provided added values. Moreover, shipbuilding industry can be assumed as strategic when high tech buildings such as battleship taken into consideration. This strategic industry not only provides military contributions to national security but also to all partners such as suppliers that established in the regions or countries. Therefore shipbuilding is an industry that creates added value. In the world, there are some long-established firms that manufacture or produce shipbuilding related products, tools, and etc. Therefore shipbuilding is an industry that has inter-linkages. For example design and building activities of projects can be done in different locations. Installations can be supplied from different countries. And, finally projects can be finished in a yard.

Term of yacht explained by Aydın (2015), Göksel (2006, 2003), Dear and Kemp (2005), Atmaca (2007), Akyürek (2013), Simpson and Weiner (2001). Yacht building is sub-branch of shipbuilding industry. But it is utterly different from this industry due to some properties such as added value, building duration, investment, and etc. (Turkish Chamber of Shipping, 2015). Yachts are much more emotional than other types of vessels due to perceptions of the potential user or owner. Also, building processes requires more attention and skill because of the exterior and interior designs, expectations, requirements, etc. Seaworthiness, large cabin accommodations, beauty, and high speed are the general characteristics of yacht design (Skene, 1904). According to Aydın (2015) design phase of the yacht projects has important effects on building processes. And building processes starts with the conceptual designs that performed to reveal demands or requirements. Then following steps take place till the delivery.

- Research and development phase (design detailing and engineering)
- Perfecting or purification phase (layout improvement, 3D modeling and detailed construction drawings)
- Building and installations (hull, superstructure, mock-ups and installations)
- Launch and delivery phase

Because of lots of factor such as limited space, function, environmental and climate conditions, and etc. taken into consideration, interior design of yachts has influences on furniture as construction, functionality and aesthetic shape (Stancu et al. 2006). According to Altın (2014) boats became more qualified and functional when furniture became qualified and yachts have been fitted by fixed or movable unique furniture.

According to Duman (2015) yacht interiors, indeed, did not reflect the architectural design codes to ensure physical and psychological comfort of human on-board. Comfort on board also depends on noise and vibration. Pais et al.

(2017) and Aydin et al. (2015) stated the importance of noise and vibration damping not only to fulfill the class requirements but also ensure comfortable interiors.

Gurler (2013) stated that owner of a yacht has perception or feeling that he or she is the member of a certain social group. Also, showing interest to yachts or taking sea journeys may indicate wealth in social sphere (Ryan, 2006). Boats, historically, are indicators of wealth and social status. And, yachting started in 17th century and divided into two; first period till 1815 and second period from 1815 to 1903 (Clark, 1903). From this date, technological developments alter the yachts as everything. Nowadays, yachting industry has been incomparable expanded and evaluated (Nicolantonio, et al, 2015). Then, bigger, more luxury, faster, more comfortable yachts built thanks to developments. This situation was well-explained by Naujok (2002) as boats which are longer than 11m require lots of technologies. And as Payne and Siohan (2008) stated, customers or potential users demanded or wished comfortable, functional, and aesthetic yachts. Therefore these were resulted increase in costs. According to Newing (2013) building smaller yachts without sacrificing quality is the simplest way to decrease costs and design phase is the beginning of cost control. But, this means limited interior or exterior for everyone and everything. Therefore, wealthy people demand everything larger even if the yacht can accommodate a few instead of tens of guests (Newing, 2013). Another way to reduce the cost of a yacht is chartering but lots of owners do not charter their yachts (Newing, 2013).

Khufu, 4500 years old boat, buried in the Keops pyramid (Göksel, 2006) and Azzam yacht, built by Lürssen in Germany, confirms this wealth and social status case from past to present, respectively. Yachts are vessels associated with wealth and luxury (Tokol, 2010, 2013). Yachts, especially luxury ones, represent the status and high social value (Nicolantonio et al. 2015). According to Göksel (2003, 2004) yachts are getting similar to each other in terms of paint, hull and superstructure due to conservative approach and un-scrutinizing. Customers or builders should reflect their authentications to the projects to eliminate this formation. And, as it is well known custom yachts are the best examples of this. For semi-custom or mass-production yachts, this can be somewhat achieved by individualization of interiors by offering some alternatives.

Turkey is one of the twenty countries which are able to design and build different types of vessels with high quality (Ozturk, 2014). General Directorate of Exports (2016) stated that Turkish yards took a great step in yacht building but especially in mega-yacht. According to Aydin and Yilmaz Aydin (2016) Turkey has achievement on yacht building industry but same was not valid for design activities especially for interior design. There can be lots of factors which result this issue but one of the main ones might be the lack of education in this area. But, in recent years a few universities in Turkey focused on this issue to increase share of design projects. When leading yacht builder countries reviewed, it's seen that they far-back started technical education on engineering and design of yachts as Griffiths (1988) mentioned. And, sufficient and developed yacht building industry and sub-industry were already established in these countries. But regarding Turkey, progress started from 90s and this must be taken into consideration.

In Turkish yacht building industry, share of material and labor force in total cost are 60% and 40%, respectively (BAKA, 2012). According to BAKA (2012) domestic share in yacht production in Turkey was around 30%. But, Aydın (2012, 2015) stated that lots of things are import especially for luxury yacht projects. So, can Turkey be assumed as a global competitor in yacht building when value added components of yacht are imported. From this point of view, the aim of this study is figuring out this issue in terms of design, yard, length over all (LOA), yacht type, engine, hull and superstructure materials.

According to Merendino (2014) Turkey has low-cost labor force to thank for being in competition with the leading yacht builder countries such as Italy, Germany and Holland. When, Global Order Book data evaluated, Turkey took place near the top in terms of total length of yachts which longer than 24m. When location and four season climate of Turkey taken into consideration, this achievement not only be related with only low-cost labor cost but also quality of the craftsmanship. Four season climate and famous long coastline with world-ranking touristic facilities provide opportunities to yacht building industry in Turkey. Tandoğan (1998), Turkish Chamber of Shipping (2015), National Marine Manufacturers Association (2016), Yilmaz and Yetgin (2016), Sevinc and Guzel (2016), Nicolantonio et al. (2015), and Sariisik et al. (2011) mentioned the importance of yacht tourism. Martinez (2009) compared yachts in terms of minimal-space space tourism. Cerveira et al. (2012) draw attention to take into consideration of disabled people in designing of sailing yacht.

According to Balance Technology Consulting GmbH (2014) European builders are still forefront partners in terms of developers of special vessel types such as yachts. And, they presented the key partners of European shipbuilding industry which produces from paintings to complete solutions. According to Balance Technology Consulting GmbH (2014) cost savings are one of the important competitive factors and numerous European firms, supply

shipbuilding industry, has moved to Asia to have advantages of cost savings. Merendino (2014) stated that Azimut-Benetti, one of the Italian leading yacht builders, strengthened the production lines which established in Turkey to overcome crisis or provide cost advantage. Aydin (2015) stated that yacht building is a labor-intensive activity and developed countries dislocating their production activities to the countries that provide low labor-cost. Lots of firms started to produce in Turkey because of not only low labor-cost but also high quality production (National Marine Manufacturers Association, 2016). But, they supply the production with value added activities such as design, electronic tools or equipment, and advanced technologies. Therefore, they gain not only competitive advantages but also dependent partners. Another important issue that must not be ignored is regulations to protect environment. Severe sanctions force lots of builders dislocate their production activities to countries that have no or scarcely any environmental regulations. Celebi et al. (2010) expressed that not only environmental protections should be provided by Turkish yards but also safety and health requirements. Occupational health and safety (OHS) in production period is an important issue and according to firms it is a cost increasing factor. But, this industry poses lots of dangers such as contacting with or inhalation of hazardous fiber reinforced plastic (Frassine et al. 2014). Insufficient and improper working environments also threaten the OHS (Tekin, 2013). Aydin and Koc (2015) investigated yacht interior production in Turkey in terms of compliance with OHS regulations and they stated that it's not a pretty sight.

Builders, designers, suppliers or providers, owners, and operators are the parties on the market but builders act as a node that link all the parties together in yacht market (Johansson et al. 2014). Yan (2008) reviewed Taiwan's yacht industry on the basis of two firms and stated that it is a global competitor in the market since the millennium without receiving insignificant subvention. Boote et al. (2012) mentioned challenging growth of Turkey in the yacht building industry. And, this is true when market share of 24m or longer yachts were taken into consideration. But, yachts, especially big ones and long-running custom projects, attract attention but they take a small share of the whole yacht market (GOB 2014). So, taking place near the top does not prove success on the whole yacht market.

From this point of view, this study tried to investigate Turkish yacht building industry on the basis of built yacht projects which were 24m or longer.

Materials and Methods

This study was conducted as a survey using list of yachts (24 meters and longer) which were ordered from Turkeys' yards and started to build. In this study, the term of "yacht" is used to denote a vessel used for pleasure purpose and smaller than 24m yachts were not taken in consideration. List prepared by comprehensive and accurate data of The Global Order Book (GOB) includes the years of 2011 to 2017. According to GOB, data obtained by yards also cross-referenced with other sources. Then, all data was cross-checked before analysis. Obtained data classified by the following topics;

- Design and engineering (Naval Architecture, Exterior and Interior Designs)
- Yards locations
- Yacht types
- Project length
- Engine
- Transmission or propulsion systems
- Navigation systems
- Telecommunication systems
- Generator
- Hull and superstructure materials
- Classification firm and origin

Results and Discussion

Total of 225 projects, built by 57 different builders, were evaluated in this study. 148(66%) and 54(24%) of them are motor yacht (MY) and sailing yacht (SY) respectively. Average LOA (Length Overall) of these projects was 42.75mt and maximum and minimum LOA were 24 and 141m respectively. But as seen in Table 1, when 141m projects neglected max and average LOA values were 87m and 42.32m, respectively. Also distribution of the projects length according to design and engineering origin is seen in this table. Projects lengths, exterior and interior design done by domestic designers, were smaller than foreigners. According to results, 115(51%), 123 (55%) and 124 (55%) of 225 projects belongs to foreigners in terms of Naval Architecture, exterior and interior design respectively. Beside data was not available (N/A) for 33(15%), 25(11%), and 32(14%) of 225 yacht projects in terms of naval architecture, exterior and interior design, respectively. According to Cain et al. (2013:10) Turkey

was not listed in top 5 in terms of yacht designs completed in 2012. But according to Mee et al. (2011) Turkey listed as 5th in terms of yacht designs completed in 2010.

Table 1: LOA values according to design and engineering origin.

	Naval Architecture		Exterior Design		Interior Design		Total (225p)
LOA (m)	Foreign (115p)	Domestic (77p)	Foreign (123p)	Domestic (77p)	Foreign (124p)	Domestic (69p)	
Avrg.	43.36	43.8	46.93	37.75	46.95	36.72	42.75*
Min	24.68	24	24.68	24	24.68	24	24
Max	141*	81	141**	67.4	141*	63	141**

*p: projects, *42,32m when 141m project neglected, **87m when 141m project neglected*

Number of yards, just builder of the evaluated projects, in Antalya, İstanbul, Muğla, Kocaeli, Yalova and Zonguldak are 20, 16, 15, 2, 2 and 1 respectively. According to results seen in Table 2, İstanbul, Antalya and Muğla can be assumed as heart of the yacht building industry in Turkey. This may be explained by being an attractive tourism destination, reachability and strong industrial composition. Yachts built in Istanbul are bigger than others when compared with other location and 141m project not taken into consideration. It can be related to length of yards too.

Table 2: Cross tabulation between yard location and LOA values.

	Yard Locations						Total (225p)
LOA (m)	Antalya (77p)	İstanbul (84p)	İzmit (12p)	Muğla (36p)	Yalova (13p)	Zonguldak (1p)	
Avrg.	38.63	46.32	39.97	44.37*	42.9	41.4	42.75***
Min	24.5	25.3	25.2	24	30	41.4	24
Max	70	81	87	141**	58	41.4	141****

*p: projects, *41.61m when 141m project neglected, **77m when 141m project neglected, ***42.32m when 141m project neglected, ****87m when 141m project neglected.*

148 (65.8%), 54 (24%) and 16 (7.1%) of the 225 yacht projects are MY (Motor Yacth), SY (Sailing Yacht) and EX (Explorer) respectively. A great majority of the 224 projects were engineered and designed by foreigners. Engineering and design origin of these projects were classified by yacht types in Table 3. According to this, foreigners have an important impact on yacht building industry in Turkey.

Table 3: Yacht types and their design and engineering properties.

	Naval Architecture			Exterior Designer			Interior Designer		
Yacht Type	Foreign	Domestic	N/A	Foreign	Domestic	N/A	Foreign	Domestic	N/A
Ex	8	6	2	10	5	1	9	4	3
MY	79	48	21	83	49	16	87	43	18
CT	1	1	0	1	1	0	1	1	0
SF	4	0	0	4	0	0	4	0	0
SY	23	22	9	25	21	8	23	20	11
Total	115 (51%)	77 (35%)	32 (14%)	123 (55%)	76 (34%)	25 (11%)	124 (55%)	68 (31%)	32 (14%)

CAT, MTU and MAN are the most preferred engine brands for 159 (71%) yacht projects as seen in Table 4. And, 85.3% of 225 yacht projects' engines are imported and there was no data for 14.7% of them. When marine engine industry of Turkey is taken into consideration, it can be said that probably 100% of them could be imported. This is a global fact because these are the leading engine supplier for lots of vehicle types. According to Global Order

Book (2015) around 50.7%, 33.9% and 8.4% of 513 (24m or longer) yachts' engines are MTU, CAT, and MAN, respectively.

Table 4: Cross-tabulation of yacht type and engine brands.

	Engine Brand										
Yacht Type	CAT	Cummins	Iveco	MAN	Mitsubishi	MTU	Scania	Volvo	Yanmar	N/A	Total
Ex	7	0	0	2	0	2	0	0	1	4	16
MY	60	1	0	16	1	47	0	0	5	18	148
CT	1	0	0	1	0	0	0	0	0	0	2
SF	2	0	0	0	0	0	0	2	0	0	4
SY	14	9	2	6	1	1	7	4	0	10	54
Total	84	10	2	25	2	50	7	6	6	32	224*

**1 missing value*

Diesel engines are one of the primary sources of power needed to move vessels. Total power of engine varies according to displacement and hull form. In addition, speed of the vessels not only depends on these parameters but also size, diameter and location of propeller, curve and number of blades.

There are lots of yacht building materials which are differ each other by their advantages and disadvantages such as weigh, usability, bondability, weldability and etc. Wood is one of them and according to Aydın (2015) its importance for building material is reducing day by day while increasing for interior or decorative purpose. Classification of used materials according to yacht type for 224 yacht projects is seen in Table 5. Steel and Aluminum are the most common used material for hull and superstructure not only in general but also for MY and EX yacht projects. Wood is most common used superstructure material for SY.

Table 5: Hull and Superstructure materials of yachts.

	Hull Material					Total	Superstructure Material					Total
Yacht Type	Al	C	S	W	N/A		Al	C	S	W	N/A	
Ex	0	2	13	0	1	16	9	5	1	0	1	16
MY	1	41	82	24	0	148	60	45	17	26	0	148
CT	0	1	1	0	0	2	1	1	0	0	0	2
SF	1	2	0	1	0	4	1	2	0	1	0	4
SY	5	7	23	19	0	54	13	7	12	22	0	54
Total	7	53	119	44	1	224*	84	60	30	49	1	224*

**1 missing value, Al: Aluminum, C: Composite, S: Steel, W: Wood*

Geographical location has some influences to both tourism and yacht building industry in Turkey. Muğla and Antalya is one of the coastlines constitute the Turkish Riviera or Turquoise Coast. Blue voyage along the Turkish Riviera, Aegean and Mediterranean seas, is carried out for decades with local gullet schooners. Gulets are traditional sailing vessels that have two or three mast and in general built by wood. This situation is clearly seen in Table 6. Almost half of Sailing Yachts (SY) built or are being built in Muğla. But great majority of these sailing yachts are constructed by steel and aluminum instead of wood as seen in Table 7.

Wood is one of the earliest construction material that human being used but advancing technology provides an opportunity to use different materials that have some better properties than wood. Aluminum, Composites (FRP, GRP, etc.), Steel and wood are the most common used materials for yacht construction. Hull and superstructure material of a yacht can be the same or not. Steel and aluminum are the most preferred construction materials for Hull and Superstructure as seen in Table 5 and 7.

Table 6: Yacht types classified by yard location.

	Yard Location							Total
Yacht Type	Antalya	İstanbul	Kocaeli	Muğla	Yalova	Zonguldak	N/A	
Ex	7	6	1	2	0	0	0	16
MY	55	60	11	10	11	1	0	148
CT	0	2	0	0	0	0	0	2
SF	3	1	0	0	0	0	0	4
SY	12	14	0	24	2	0	2	54
Total	77	83	12	36	13	1	2	224*

**1 missing value*

Table 7: Construction material by yard location.

	Hull Material					Superstructure Material					Total
Yard Location	Al	C	S	W	N/A	Al	C	S	W	N/A	
Antalya	5	33	27	11	1	24	37	2	13	1	77
İstanbul	0	9	51	23	0	45	12	1	25	0	83
Kocaeli	0	10	2	0	0	2	10	0	0	0	12
Muğla	2	0	25	9	0	13	0	13	10	0	36
Yalova	0	1	12	0	0	0	1	12	0	0	13
Zonguldak	0	0	1	0	0	0	0	1	0	0	1
Total	7	53	118	43	1	84	60	29	48	1	222*

**3 missing value, Al: Aluminum, C: Composite, S: Steel, W: Wood*

Yacht projects must be surveyed by some classification societies to verify conformance with the regulatory standards. These standards, composed by members of Societies, govern the design, construction, maintenance and operation of vessels. There are 12 classification societies According to International Association of Classification Societies Ltd. Some of these members, expect Türk Loydu (TL), is seen in Table 8. Türk Loydu (TL) is an authorized classification institute by EU and according to 94/25/EC directive it is able to evaluate of conformity of manufactured vessels to labeling them with CE sign. There is no data available for 69 (31%) yacht projects and it may seriously affect the share. However, RINA is the most preferred classification societies for yachts built or are being built in Turkey. And, only 7 (3%) of 224 projects are classified by Turkish authorities.

Table 8: Classification properties of yachts.

	Classification										Total
Yacht Type	ABS	BV	CE	CE/RINA	GL	LR	RINA	RINA/TL	TL	N/A	
Ex	3	2	0	0	0	1	4	0	0	6	16
MY	12	11	2	2	4	11	60	0	0	46	148
CT	0	0	0	0	0	0	2	0	0	0	2
SF	0	0	0	0	2	0	0	0	0	2	4
SY	0	0	1	0	0	5	28	1	4	15	54
Total	15	13	3	2	6	17	94	1	4	69	224*

**1 missing value, ABS: American Bureau of Shipping, BV: Bureau Veritas, CE: Conformite Europeenne, RINA: Registro Italiano Navale, GL: Germanischer Lloyd, LR: Lloyd's Register, TL: Türk Loydu*

Share of labor and material cost for yachts built in Antalya Freezone in 2011 are 40% and 60%, respectively. And engine (25%), furniture (20%), electric & wiring (18%), structural parts (15%), paint and varnish (12%) and deck parts (10%) are shares of material cost of a yacht (BAKA, 2012). Yacht building industry in Turkey is import-weighted in terms of high value added product, material, equipment or machinery usage. And, when compared with the competitors, world class but relatively low-cost labor is the strongest side of the industry (Aydın, 2015). Also Aydın (2012) stated that yards that build luxury yachts prefers to work with world-famous designers or firms

to increase perception of their firm image and quality.

Almost all yachts propulsion and navigation systems were imported and fitted. There are lots of paint or varnish types for yacht painting such as PU, epoxy, synthetic and etc., and almost all projects painted or varnished with imported coating materials.

According to Turkish Chamber of Shipping (2015) followings are advantages of Turkish yacht or boat building industry.

- Educated and skilled labor force
- World class production quality
- Acceptable costs
- Qualified and sufficient sub-industry
- Modern and technologic foundations
- Easy access to worldwide markets
- Favorable climate

It can be mentioned that there is skilled, educated and relatively low-cost labor force but According to Aydin (2012) industry face with the deficiency of enough skilled labor force when new yards or builders take place or business volume increase. This situation is so clear especially at locations that have non-clustered yacht builders and suppliers.

Except qualified and sufficient sub-industry, almost all captions listed above were confirmed by the reviewed literature. Lack or under qualified, interrupted or insufficient supplier is the primary concern of any type of production and as seen in the tables Turkish yacht building industry has this problem and has been fighting with this issue. And, according to National Marine Manufacturers Association (2016) Turkey is one of the boat exporter countries to US boat market and tries to get share in expensive markets with improving its engineering know-how instead of using cheap labor force advantage. Keep in mind that, subsidiary or partners of international companies take position in Turkish yacht building industry that located at Tuzla, Antalya Free Zone and etc. From this point of view, lots of important actor of this industry is in close connection to each other.

Conclusion

Some of the tables clearly express that yacht building sector in Turkey is dependent to the imported raw material, end products or components that required for building process. But, industry exports pretty much of the builds as a final product. Besides, according to results lots of core activities such as design and engineering are being done by foreigners. And value added parts or technical equipment such as engine, communication devices and etc., are being imported while constructing a yacht in Turkey. Maybe it's due to lack of powerful sub-industry of marine industry. And, import based production increase the costs even if Turkey still has low-labor cost advantage. Therefore industry and related sub-industries must be supported by the government to provide much more added value.

Shipbuilding industry of Turkey provided contributions to economy and it looks like it will continue to do this (Anon, 2014). But, from this point of view, it can be said that results presented in this study confirm that yacht building industry in Turkey is a bit foreign dependent about lots of value added things. Thus, economic impact of this industry may not be well understood and it would be unsatisfactory for the local economy.

So, there is an ironic situation for Turkey, when a great majority of value added things are being exported from competitors such as Italy, Holland, Germany, United States, United Kingdom, then can it be said that Turkey is a global competitor in yacht building industry? It makes little sense but we can say yes when industry and sub-industries run with domestic goods, tools, equipment and etc.

In yacht building industry, there are some exceptional cases such as using tropical wood species and it cannot be supplied by the domestic way due to their rarity and endemism. Therefore such materials must be export oriented for lots of leading yacht builder as Turkey.

Consequently, it is obvious that Turkey is one of the center and leading yacht builders in the world in terms of some criteria such as total project length. But, Turkey must be focused on high added value activities.

Concerning with only 24m or longer yacht projects and aforementioned investigation topics are the limitations of

this study. And, it can be though that result of this study may not reflect the whole industry. Therefore, a comprehensive study should be conducted to figure out an extensive structural analysis of industry.

References

Altın, E. (2014). Examining The context of floating outdoor furniture, custom yacht design of spatial and partial sample study, Ph.D. Thesis, Mimar Sinan Fine Arts University, Istanbul, 262p.

Anonymous, (2014). Turkish Shipbuilding Industry shows optimism at SMM Istanbul Fair Audience highly pleased with new event concept, The International Maritime Conference and Exhibiton, 26-27 Feb. Istanbul.

Aydın, M. (2012). The structural analysis of Turkish yacht furniture manufacturing sector in marmara region, MSc Thesis, İstanbul University, 163p.

Aydın, M. (2015). Effects of yacht interior design on material selection in Turkey. In C. Saçlı, M. Kısa, S. Neşeli, L. Civcik, M.S. Muslu, & Ç. Saçlı (Eds.), *Proceedings of the 3rd National Furniture Congress* (pp.347-357). Konya, Turkey.

Aydın, M., & Koç, K.H. (2015). A study on compliance with occupational health and safety rules in yacht interior production. In H. Çınar, C. Söğütlü, N. Döngel & H.Ö. İmirzi (EDs.), *Proceedings of the 27th International Conference Research for Furniture Industry* (pp.369-376). Ankara, Turkey.

Aydın, M., Yılmaz Aydın, T., & Guentekin, E. (2015). Noise and vibration damping for yacht interior, *Mugla Journal of Science and Technology*, 2(2):166-170.

Aydin, M. & Yilmaz Aydin, T. (2016). Türkiye'de inşa edilen yatların iç mekan tasarımı üzerine bir araştırma, *Tasarım Kuram*, 21:61-77.

Balance Technology Consulting GmbH. (2014). Competitive position and future opportunities of the european marine supplies industry, european commission, Final Report to Contract N° SI2.630862.

Boote, D., Beck, R., Blake, J., Flay, R. et al. (2012). Yacht design. In W. Fricke & R. Bronsart (Eds.), *Proceedings of the 18th Int. Ship and Offshore Structures Congress* (pp.331-396).Schiffbautechnische Gesellschaft, Hamburg.

Cain, M., Dixon, M., Ziriakus, D., Waard, M. & Janssen, M. (2013). The superyacht industry. *The (Super) Yachting Index*, 5th Edition, pp. 7-55

Celebi, U.B., Ekinci, S., Alarcin, F, & Unsalan, D. (2010). The risk of occupational safety and health in shipbuilding industry in Turkey. In C.G. Soares & T.A. Santos (Eds.), *Proceedings of the 3rd International Conference on Maritime and Naval Science and Engineering* (pp.178-185). Constantza , Romania

Cerveira, F., Fonseca, N & Sutjerland L. (2012. Considering disabled people in sailing yacht design. In C.G. Soares, Y. Garbatov, S. Sutulo & T.A. Santos (Eds.) *Maritime Engineering and Technology* (pp.53-62). NY, USA: Taylor & Francis.

Clark, A.H. (1903). *The history of yachting*. London: G.P. Putnam's Sons.

Duman, İ.I. (2015). Human comfort in yacht spaces, *British Journal of Arts and Social Sciences*, 19(2):68-75.

Frassine, R., Fusaro, C. & Ratti, A. (2014). Chemical hazard in FRP pleasure boats manufacturing. In N. Stanton, S. Landry, G.D. Bucchianico & A. Vallicelli (Eds.) *Advances in Human Aspects of Transportation Part I*, (pp.171-182). Danvers, MA, USA: AHFE Conference publishing.

General Directorate of Exports (2016). *Shipbuilding industry*, Ankara: Republic of Turkey-Ministry of Economy.

Guler, A. (2013). *A comparative study on the yacht building industry:The role of desıgn strategy and management in the development of the yacht buildıng industry in the World and Turkey*, Msc. Thesis, Istanbul TechnİcaI Unıversıty, Istanbul.

Griffiths, M. (1988). *Sixty years a yacht designer*. London: Conway Maritime Press,.

Johansson, S., Hall, LJ. & Jutbakc, A. (2014). Market and *Network Analysis of the 60-100 feet Yacht Industry.* MSc.Thesis, Chalmers University of Technology, Gothenburg.

Martinez, V. (2009). Architectural design for space tourism. *Acta Astronautica* 64;382-390.

Mee, T., Waard, d.M. & Janssen M. (2011). The superyacht industry. *The (Super) Yachting Index 4th Edition*. pp, 7-54

Merendino, A. (2014). Mega yacht, Italian leadership and financial crisis. empirical evidence on how Italian leading companies in mega yacht sector overcome the crisis, *European Scientific Journal*, 10(28): 9-35.

National Marine Manufacturers Association. (2016). *Pleasure boat international resource guide a reference for U.S. exporters*, Washington, DC, USA: U.S. Department of Commerce.

Naujok, M. (2002). *Boat interior construction- a bestselling guide to DIY interior boatbulding*. London: Adlard Coles Nautical.

Newing, R. (2013). Yacht designs balance cost and luxury. *Finacial Times*, June 19.

Nicolantonio, M.D., Bucchianico, G.D., Camplone, S. & Vallicelli, A. (2015). The visual pleasantness in yacht design: natural lighting, views and interior colours. *Theoretical Issues in Ergonomics Science*, 16(4):399-

411.
Nicolantonio, M.D., Lagatta, J .& Vallicelli, A. (2015). 80 feet sustainable motoryacht: Technological solutions concept of the living spaces on board. *Procedia Manufacturing* 3:2698-2705
Ozturk, H. (2014). Turkish Maritime & Naval Industry proven quality and power. *Marine and Commerce* September;33-40.
Pais, T., Moro, L., Boote, D. & Biot, M. (2017). Vibration analysis for the comfort assessment of superyachts. *J. Marine Sci. Appl*. 16:323-333.
Payne, R. & Siohan, N. (2008). Comfortable structure, In *Proceedings of the 3rd High Performance Yacht Design Conference*, (pp.1-10). Auckland, New Zealand.
Ryan, J.R. (2006). Our home on the ocean: Lady Brassey and the voyages of the Sunbeam, 1874-1887. *Journal of Historical Geography* 32:579-604.
Sariisik, M., Turkay, O. & Akova, O. (2011). How to manage yacht tourism in Turkey: A swot analysis and related strategies. *Procedia Social and Behavioral Sciences* 24:1014-1025.
Sevinc, F.& Guzel, T. (2016). Competitive strategies in marina enterprises; Implementations in Turkey. *Journal of Travel and Hospitality Management* 13(1):60-76
Skene, N.L. (1904). *Elements of yacht design*. New York, USA: The Rudder Publishing.
Stancu, M., Curtu, I., Ciofoaia, V. & Baba, M. (2006). Functional and construction particularities of the ships furniture. In S. Ekinovic (Ed.), *Proceedings of the 10th International Research Expert Conference on Trends in the Development of Machinery and Associated Technology* (pp.1552). Barcelona, Spain.
Tandoğan, V.U. (1998). Dünya turizm talebi eğilimleri işiğinda türkiyeye yönelik yat turizm talebinin değerlendirilmesi, *Balıkesir University, J. of Social Sci. Inst*. 1(1):145-155.
Tekin, E. (2013). *Tekne ve yat üretim sektöründe iş sağlığı ve güvenliği, iş müfettişi yardımcılığı etüdü*. İzmir, Turkiye: T.C. Çalışma Ve Sosyal Güvenlik Bakanlığı - İş Teftiş Kurulu Başkanlığı.
Tokol, H.T. (2010). Yat iç mekan tasarımı, *TMMOB İçmimarlar Odası Yayını İçmimar Dergisi*, s.98.
Tokol, H.T. (2013). Life, space and equipment relation in transoceanic long-distance cruising sailing yachts, Thesis, Mimar Sinan Fine Arts University, İstanbul.
Turkish Chamber of Shipping, (2015). *2014 maritime sector report*. Istanbul, Turkey: Turkish Chamber of Shipping.
Yan, H.D. (2008). Taiwan's yacht industry: A tale of two entrepreneurial firms. *Global Economic Review* 37(4):469-486
Yilmaz, A. & Yetgin, D. (2016). Product life cycle of the blue cruise in Turkey. *The Social Sci.* 11(20): 4865-4870.

LINEAR MULTISECRET-SHARING SCHEMES

Selda Çalkavur

Math Dept, Kocaeli University, Kocaeli, Turkey
selda.calkavur@kocaeli.edu.tr

Abstract: Cyclic codes form an important class of linear codes. These codes have a rich algebraic structure. Secret sharing is a major topic of cryptography. In this paper, we present a multisecret-sharing scheme based on cyclic codes. This scheme is linear in the sense of that form of each secret. Its security improves on that of multisecret-sharing schemes.

Keywords: Secret sharing, linear multisecret sharing scheme, cyclic code.

Introduction

Secret sharing schemes were examined by Blakley (Blakley, 1979) and Shamir (Shamir, 1997) in 1979. Shamir's scheme is a (t, n)-threshold secret sharing scheme and this scheme was based on polynomial interpolation. A (t, n)-secret sharing scheme is a method of distribution of information among n participants such that $t > 1$ can reconstruct the secret but $(t - 1)$ cannot.

In a secret sharing scheme there are some participants and a dealer. The dealer has a secret and distributes it the other participants. In a minimal t-subset of participants recover the secret while combining their shares. These subsets are called the minimal access sets.

Another secret sharing scheme is the multisecret-sharing scheme. This scheme was proposed in (Horn, 1995), (He, 1994), (Li, 2016), (Pang, 2005), (Yang, 2004), (Çalkavur et al, 2017). In the multisecret-sharing schemes (Li, 2016), (Pang, 2005), (Bai, 1993) there is a set of p secrets can be shared at once and each participant needs to keep one share is called secret share. In these schemes all p secrets are recovered at once or all p secrets cannot reconstruct. To recover the secret the participants need to submit a $pseudo - share$ computed from their secret share instead of the secret share itself.

In this work we propose a new multisecret-sharing scheme based on cyclic codes. We give a secret reconstruction algorithm based on generator polynomial of the code. We analyse the security and performance of the scheme by means of cyclic code theory. We calculate the number of minimal coalitions in this scheme. We introduce the access structure of this scheme and define its accessibility degree and explain its linearity.

We conclude by a comparison between our scheme and the three main other code-based schemes in the literature: Massey's scheme (Massey, 1993), Ding et al (Ding, 1997) and (Çalkavur et al, 2017) multisecret scheme.

The rest of this paper is organized as follows. The next section gives the basic preliminaries used in the paper. Section III presents the proposed scheme, analyses its security and defines the accessibility degree of the scheme. Section IV contains the said comparison and against cheating. Section V collects concluding remarks.

Background and Preliminaries

In this section we give the basic preliminaries and some necessary mathematical information used in this work.

A. Linear Codes

Let q be a prime power and denote the finite field of order q by F_q. An $[n, k]$-code C over F_q is a subspace in $(F_q)^n$, where n is length of the code C and k is dimension of C. The dual code of C is defined to be the set of those vectors $(F_q)^n$ which are orthogonal to every codeword of C. It is denoted by $C^{\perp}$. The code $C^{\perp}$ is an $[n, n - k]$-code. A generator matrix G for a linear code C is a $k \times n$ matrix for which the rows are a basis of C. A parity-check matrix for a linear code C is a generator matrix for its dual code $C^{\perp}$. It is denoted by H.

Let C be an $[n, k]$-code over F_q with generator matrix G. C contains q^k codewords and can be used to communicate any one of q^k distinct messages. We encode the message vector $x = x_1 x_2 \cdots x_k$ as the codeword xG.

If G is a generator matrix for C, then $C = \{ uG \mid u \in (F_q)^k \}$. The map $u \rightarrow uG$ maps the vector space q^k onto a

k-dimensional subspace of $(F_q)^n$.

B. Cyclic codes

A code C is cyclic if

1. C is a linear code,
2. any cyclic shift of a codeword is also a codeword, whenever $a_0a_1\cdots a_{n-1}$ in C, then so is $a_{n-1}a_0a_1\cdots a_{n-2}$ (Hill, 1986).

Theorem 1. Let C be a non-zero cyclic code. Then,

1. there exists a unique polynomial $g(x)$ of smallest degree in C,
2. $C = < g(x) >$,
3. $g(x)$ is a factor of $x^n - 1$ (Hill, 1986).

Definition 1. In a non-zero cyclic code C the monic polynomial of least degree, given by Theorem 1, is called the generator polynomial of C (Hill, 1986).

Lemma 1. Let $g(x) = g_0 + g_1x + \cdots + g_{n-k}x^{n-k}$ be the generator polynomial of a cyclic code. Then g_0 is non-zero (Hill, 1986).

Theorem 2. Suppose C is a cyclic code with generator polynomial $g(x) = g_0 + g_1x + \cdots + g_{n-k}x^{n-k}$ of degree $n-k$. Then $dim(C) = k$ and a generator matrix for C is

$$G = \begin{pmatrix} g_0 & g_1 & g_2 & \cdots & g_{n-k} & 0 & 0 & \cdots & 0 \\ 0 & g_0 & g_1 & \cdots & g_{n-k-1} & g_{n-k} & 0 & \cdots & 0 \\ \vdots & \vdots & \vdots & \cdots & \vdots & \vdots & \vdots & \cdots & \vdots \\ 0 & 0 & 0 & \cdots & 0 & g_0 & g_1 & \cdots & g_{n-k} \end{pmatrix}.$$

This means $aG = (a_0 + a_1x + \cdots + a_{k-1}x^{k-1})g(x)$, where $a = (a_0, a_1, \cdots, a_{k-1}) \in (F_q)^k$ (Hill, 1986).

C. Secret Sharing Schemes

In this section we should think about a case of some malicious behaviors lying among participants which are called cheaters. They modify their shares in order to cheat.

If a group of participants can recover the secret by combining their shares, then any group of participants containing this group can also recover the secret.

Definition 2. An access group is a subset of a set of participants that can recover the secret from its shares. A collection Γ of access groups of participants is called an access structure of the scheme. An element $A \in \Gamma$ is called a minimal access element. Hence a set is a minimal access group if it can recover the secret but no proper subset can recover the secret. Let $\bar{\Gamma}$ be the set of all minimal access elements. We call $\bar{\Gamma}$ the minimal access structure (Kim, 2016). Determining the minimal access structure is a hard problem (Ding, 2000).

Now let us consider the accessibility of an access structure of secret sharing scheme based on binary linear code. Let $P = \{P_1, P_2, \cdots, P_m\}$ be a set of m participants and let A_p be the set of all access elements on P.

Definition 3. The accessibility index on P is the map $\delta_p(\Gamma)$: $A_p \to \mathbb{R}$ given by

$$\delta_p(\Gamma) = \frac{|\Gamma|}{2^m}$$

for $\Gamma \in A_p$, where $m = |P|$. The number $\delta_p(\Gamma)$ will be called the accessibility degree of structure Γ (Carreras, 2006).

Multisecret-Sharing Schemes and Cyclic Codes

A. Scheme Description

In this section, we examine a new multisecret-sharing scheme based on cyclic codes.

Consider an $[n, k]$-cyclic code C over F_q. We construct now a multisecret-sharing scheme based on C.

Let $(F_q)^k$ be the secret space and $(F_q)^n$ be the share space. In the multisecret-sharing scheme the dealer uses a share function $f: (F_q)^k \to (F_q)^n$ to compute the shares among the n participants. The sharing function is chosen as $f(s) = sG$, where $s = (s_0, s_1, \cdots, s_{k-1}) \in (F_q)^k$ is the secret and G is a $k \times n$ matrix over $(F_q)^n$ with rank k. Assume for convenience $s \neq 0$. Thus $c = sG$ is a nonzero codeword of the code C.

In this scheme, the n participants recover the secret by combining their shares as follows.

1. get the generator polynomials and matrices of cyclic code,
2. choose the polynomial for each generator polynomial such that
   $sG = (s_0 + s_1 x + \cdots + s_{k-1} x^{k-1}) g(x)$, (1)
   where $deg(g(x)) = n - k$.
3. get s by solving the linear system (1) of rank k.

Proposition 1. The motivation for condition 2 above is the following inequality: $2 \leq k < n$.

Proof. With the above notation it is clear that $k \neq 0$.
Assume that $k = 1$. In this case the secret consists one entry and then the scheme cannot be multisecret.
If $k = n$, then $deg(g(x)) = n - k = 0$. This means the generator polynomial is 1. Since $k = n$, the secret has size of n.

Corollary 1. If $deg(g(x)) = n - k \geq 2$, then the multisecret-sharing scheme can be constructed based on $[n, k]$-cyclic code.

Proof. By Proposition 1, while $n - k \geq 2$ it can be mentioned about multisecret-sharing. Otherwise it will be single secret-sharing.

An immediate corollary is the following.

Corollary 2. The multisecret-sharing scheme satisfied the hypothesis of the above theorems is also a (k, n)-threshold secret sharing scheme, where k is dimension and n is length of cyclic code C.

Proof. In this scheme, there are n participants and the secret has size of k. So, the result follows.

Now we have to remind an important theorem about linearity of the multisecret-sharing scheme in (Ding, 1997).

Theorem 3. A multisecret-sharing scheme defined over the above secret and share spaces is linear if and only if its share function is of the form

$$f(s) = sG,$$

where $s = (s_0, s_1, \cdots, s_{k-1}) \in (F_q)^k$ and G is a $k \times n$ matrix over $(F_q)^n$ with rank k.

Corollary 3. The multisecret-sharing scheme based on the cyclic code with generator matrix G is a linear (k, n)-threshold scheme.

Proof. It is easily seen from Theorem 3.

B. Statistics on Coalitions

Theorem 4. Let C be a q-ary $[n,k]$-cyclic code with generator matrix G. In a multisecret-sharing scheme based on C while $n-k \geq 2$, the number of minimal coalitions is $\binom{n}{k}$.

Proof. Recall that our scheme is a (k,n)-threshold secret sharing scheme. This means k out of n participants can recover the secret. These k participants consist of minimal access sets. So the number of minimal coalitions is $\binom{n}{k}$.

C. Accessibility Degree

The accessibility degree for multisecret-sharing scheme based on cyclic codes can be defined as follows.

Definition 4. Let $P = \{P_1, P_2, \cdots, P_m\}$ be a set of m participants and let A_p be the set of all access elements on P. The accessibility index on P is the map $\delta_p(\Gamma)$: $A_p \rightarrow \mathbb{R}$ given by

$$\delta_p(\Gamma) = \frac{|\Gamma|}{q^m}$$

for $\Gamma \in A_p$, where $m = |P|$. The number $\delta_p(\Gamma)$ will be called the accessibility degree of structure .

Example 1. Lets find all the ternary cyclic codes of length 4 and write down a generator matrix for each of them.

Over $GF(3)$, the factorization of x^4-1 into irreducible polynomials is

$$x^4-1 = (x-1)(x^3+x^2+x+1) = (x-1)(x+1)(x^2+1).$$

So there are $2^3 = 8$ divisors of x^4-1 in $F_3[x]$ each of which generates a cyclic code. By Theorem 1, these are the only ternary cyclic codes of length 4. The codes are specified below by their generator matrices

Generator Poynomial	Generator Matrix
11	(I_4)
$x-1$	$\begin{pmatrix} -1 & 1 & 0 & 0 \\ 0 & -1 & 1 & 0 \\ 0 & 0 & -1 & 1 \end{pmatrix}$
$x+1$	$\begin{pmatrix} 1 & 1 & 0 & 0 \\ 0 & 1 & 1 & 0 \\ 0 & 0 & 1 & 1 \end{pmatrix}$
x^2+1	$\begin{pmatrix} 1 & 0 & 1 & 0 \\ 0 & 1 & 0 & 1 \end{pmatrix}$
$(x-1)(x+1) = x^2-1$	$\begin{pmatrix} -1 & 0 & 1 & 0 \\ 0 & -1 & 0 & 1 \end{pmatrix}$
$(x-1)(x^2+1) = x^3-x^2+x-1$	$(-1 \quad 1 \quad -1 \quad 1)$
$(x+1)(x^2+1) = x^3+x^2+x+1$	$(1 \quad 1 \quad 1 \quad 1)$
x^4-1	$(0 \quad 0 \quad 0 \quad 0)$

Now we construct a linear multisecret-sharing scheme based on this cyclic code. First we consider the generator polynomial $g(x) = x+1$. Since $deg(g(x)) = 1$ that is $n-k = 1$, $k = 3$. Let the secret vector be $s = (s_0, s_1, s_2)$, where $s_i \in F_3$, $i = 0,1,2$. We can encode s as follows.

$$(s_0 + s_1 x + s_2 x^2) g(x).$$

Let $s_0 = 1, s_1 = 0, s_2 = 1$. Therefore we write

$$(1+x^2)(1+x).$$

We know that this product is equal to sG, where G is the generator matrix. So

$$(1+x^2)(1+x) = (s_0, s_1, s_2)\begin{pmatrix} 1 & 1 & 0 & 0 \\ 0 & 1 & 1 & 0 \\ 0 & 0 & 1 & 1 \end{pmatrix}.$$

We obtain $s_0 = 1, s_1 = 0, s_2 = 1$ by solving the linear system: $s = (101)$. The generator polynomial $(1 + x)$ gives a $(3, 4)$-threshold scheme for multisecret-sharing. The accessibility degree for this scheme is

$$\frac{3}{3^4} = 0{,}037 .$$

Second we consider the generator polynomial $g(x) = x^2 + 1$. Since $deg(g(x)) = 2, k = 2$. Let the secret vector be $s = (s_0, s_1)$ and consider $(s_0 + s_1 x)g(x)$.

Let $s_0 = 1, s_1 = 0$.

$$1.(1 + x^2) = (s_0, s_1)\begin{pmatrix} 1 & 0 & 1 & 0 \\ 0 & 1 & 0 & 1 \end{pmatrix}.$$

By solving the linear system we find $s_0 = 1, s_1 = 0$: $s = (10)$.

The generator polynomial $(1 + x^2)$ gives a $(2, 4)$-threshold scheme for multisecret-sharing. The generator polynomial $(1 + x)$ gives a $(2, 4)$-threshold scheme for multisecret-sharing. The accessibility degree for this scheme is

$$\frac{2}{3^4} = 0{,}024.$$

Note that the multisecret-sharing scheme cannot construct by using the generator polynomials $x^3 - x^2 + x - 1, x^3 + x^2 + x + 1, x^4 - 1$.

Comparison with Other Schemes

We summarize the comparison with other code-based secret sharing schemes in the following table, where we denote by A, B, C the number of participants, the size of a secret, the number of coalitions for an $[n, k]$-code over F_q.

System	Massey	Ding et al.	Çalkavur-Solè	This paper
A	$n - 1$	n	n	n
B	q	q^k	q^k	$q^k - 1$
C	$\binom{n}{k}$	$\binom{n}{k}$	$\geq \binom{n}{d - t}$	$\binom{n}{k}$

t is the error-correcting capacity of code.

A. Against Cheating

In single-secret sharing schemes some participants may present a falsified share for cheating. This problem is the same as for single-secret sharing in multisecret-sharing. By the connection between linear multisecret-sharing schemes and linear codes established by Theorem 3.

Our scheme has been constructed based on cyclic codes. Cyclic codes have a rich algebraic structure. They are splitted the classes by the generator polynomials. This means the codewords are generated by their generator polynomial. We need the genarator polynomial to recover the secret. The polynomial which is multipled by the generator polynomial consists the pieces of secret. Thus, recovering the secret depend on the choice of generator polynomial. So the secret cannot be recovered by any polynomial.

The linear multisecret-sharing scheme based on cyclic codes is attractive in against cheating. This scheme is more resilient to algebraic attacks due to the reconstruction algorithm.

Concluding Remarks

In the present article, we have constructed a new linear multisecret-sharing scheme based on cyclic codes. The reconstruction algorithm is based on generator polynomial of code. Moreover, in this study we introduce the access structure of this scheme and define its accessibility degree.

We refer to approach considered in the paper as the coding approach since

1) in single-secret sharing the secret is a component of the codeword corresponding to the information vector and the shares form all components of the codeword corresponding to the information vector,
2) in multisecret-sharing the multisecret is exactly the information vector and shares form the exact codeword corresponding to the information vector.

The advantage of the coding approach is that a cyclic code has the exclusive generator polynomials and matrices. So each share vector is a codeword of the codes generated by this generator matrix. It is important that choice of generator polynomial has some special properties, this scheme stands well, in particular in terms of security.

References

Bai, L. (1993). *A Reliable (k,n)-Image Secret Sharing Scheme*, Proc. of the 2nd International Symposium on Dependable, Autonomic and Secure Computing DASC' 06, pp. 1-6.

Blakley, G.R. (1979). *Safeguarding Cryptographic Keys*, in Proc. 1979 National Computer Conf., New York, Jun., pp. 313-317.

Carreras, F., Magana, A. & Munuera, C. (2006). *The accessibility of an access structure*, RAIRO-Theoretical Informatics and Applications, 40.04, pp. 559-567.

Çalkavur, S. & Solè, P (2017). *Multisecret sharing schemes and bounded distance decoding of linear codes*, International Journal of Computer Mathematics, vol. 94, issue. 1, pp.107-114.

Ding, C., Laihonen, T. & Renvall, A. (1997). *Linear Multisecret-Sharing Schemes and Error Correcting Codes*, Journal of Computer Science, vol. 3, no. 9, pp. 1023-1036.

Ding, C., Kohel, D. & Ling, S. (2000). *Secret Sharing with a Class of Ternary Codes*, Theor. Comp. Sci., vol. 246, pp. 285-298.

Horn, L. (1995). Comment: Multistage secret sharing based on one-way function, Electronics Letters, vol.31 (4), pp. 262.

He, J. & Dawson, E. (1994). *Multistage secret sharing based on one-way function*, Electronics Letters, vol.30 (19), pp. 1591-1592.

Hill, R. (1986). *A First Course in Coding Theory*, Oxford: Oxford University.

Kim, J. L. & Lee, N. (2016). *Secret sharing schemes based on additive codes over $GF(4)$*, Applicable Algebra in Engineeering, Communication and Computing, pp. 1-19.

Li, H. -X., Cheng, C. -T. & Pang, L. -J. (2005). *A New (t,n) Threshold Multisecret Sharing Scheme*, CIS 2005, vol. 3802, pp. 421-426.

Massey, J. L. (1993). *Minimal codewords and secret sharing*,in Proc. 6th Joint Swedish-Russian Workshop on Information Theory, Mölle, Sweden, pp.276-279.

Pang, L. -J. & Wang, Y. -M. (2005). *A New (t,n) multi-secret sharing scheme based on Shamir's secret sharing*, Applied Math, vol. 167, pp. 840-848.

Shamir, A. (1979). *How to share a secret*, Comm. of the ACM 22 pp. 612--613.

Yang, C. -C., Chang, T. -Y. & Hwang, M. -S. (2004). *A (t,n) multisecret sharing scheme*, Applied Mathematics and Computation, vol. 151, pp. 483-490.

